JSCSEN 80(6)731–838(2015)

ISSN 1820-7421(Online)

# Journal of the Serbian Chemical Society

Electronic version

Volume 80 : : 2015 : : 85 Years of the Journal

1930 Glasnik Hemijskog Društva Kraljevine Jugoslavije
Journal of the Chemical Society of the Kingdom of Yugoslavia

1947 Glasnik hemijskog društva Beograd
Journal of the Chemical Society of Belgrade

1985 Journal of the Serbian Chemical Society

VOLUME 80

No 6

BELGRADE 2015

Available on line at

www.shd.org.rs/JSCS/

The full search of JSCS is available through

DOAJ DIRECTORY OF OPEN ACCESS JOURNALS

www.doaj.org

Journal of the Serbian Chemical Society
JSCS-info@shd.org.rs • www.shd.org.rs/JSCS

*J. Serb. Chem. Soc.* Vol. 80, No. 6 (2015)

CONTENTS



Published by the Serbian Chemical Society
Karnegijeva 4/III, P.O. Box 36, 11120 Belgrade, Serbia
Printed by the Faculty of Technology and Metallurgy
Karnegijeva 4, P.O. Box 35-03, 11120 Belgrade, Serbia

Journal of the Serbian Chemical Society
JSCS-info@shd.org.rs • www.shd.org.rs/JSCS
*J. Serb. Chem. Soc. 80* (6) 731–738 (2015)
*JSCS–4752*
UDC 547.836.3+547.412.11:544.433.21+547–304.2+547.752+547.567
*Original scientific paper*

# An investigation of nucleophilic substitution reactions of 2,3-dichloro-1,4-naphthoquinone with various nucleophilic reagents

CEMIL IBIS*, AHMED HASSEN SHNTAIF, HAKAN BAHAR and SIBEL SAHINLER AYLA

*Department of Chemistry, Faculty of Engineering, Istanbul University, 34320, Avcilar, Istanbul, Turkey*

(Received 24 November 2014, revised 26 February, accepted 1 March 2015)

*Abstract*: Novel *N*-, *N*,*S*- and *N*,*O*-substituted naphthoquinone compounds were prepared by the reactions of 2,3-dichloro-1,4-naphthoquinone (**1**) and the corresponding nucleophiles in the presence of chloroform and triethylamine or an ethanolic solution of $Na_2CO_3$. The structures of the novel naphthoquinone compounds were characterized by microanalysis, FT-IR, $^1$H-NMR, $^{13}$C-NMR, MS and cyclic voltammetry.

*Keywords*: 1,4-naphthoquinone; thioethers; amine; indolylquinones.

## INTRODUCTION

The synthesis of novel quinone derivatives have been receiving great attention because of the bright colors and pharmaceutical properties of quinones.[1–3] Quinone-type drugs systems are also being developed and many of the clinically approved drugs are quinone related compounds.[4–7] Antibacterial and antifungal activities of some novel naphthoquinone derivatives were reported previously in the literature.[8–10]

2,3-Dichloro-1,4-naphthoquinone (**1**) was selected as the starting material because it is reasonably stable, readily available and is known as a key synthetic intermediate in organic, medicinal and industrial chemistry. The aim of this study was the synthesis of derivatives of the quinone and their characterization with spectral methods.

* Corresponding author. E-mail: ibiscml@istanbul.edu.tr
doi: 10.2298/JSC141124021I

## RESULTS AND DISCUSSION

### *Chemistry*

The reactions of 2,3-dichloro-1,4-naphthoquinone (**1**) with various N- or S-nucleophiles resulted in the substitution of one or both of the chlorine atoms.[11,12] The reaction occurs according to the addition–elimination mechanism.[13] Some novel indolylquinones were also synthesized using 3-substituated indole derivatives and *N*-substituted quinonyl derivatives were obtained. These substitution reactions of *p*-chloranil are known from the literature.[14,15]

Compound **3**[16] was obtained by reaction of **1** with **2** in chloroform with triethylamine ($Et_3N$). The novel *N*-, *S*-substituted naphthoquinones **5a**–**e** were obtained by the reactions of compound **3**[16] and various thiols **4a**–**e**. The synthetic strategy for the novel compounds is illustrated in Scheme 1. The $^{13}$C-NMR spectrum of compound **5a** gave two carbon signals for C=O groups at 179.6 and 179.7 ppm due to the naphthoquinone unit. In the IR spectra of compound **5b**, the lactone carbonyl group was seen at 1734 $cm^{-1}$, while the quinone carbonyl group appeared at 1666 $cm^{-1}$. In the mass spectrum of compounds **5c** and **5d**, the accurate mass measurements of the molecular ion peaks were registered at *m*/*z* 395 and 409 $[M+H]^+$, respectively. The S–$CH_2$ protons of **5e** appeared in the $^1$H-NMR spectrum as triplets at 2.50 ppm.

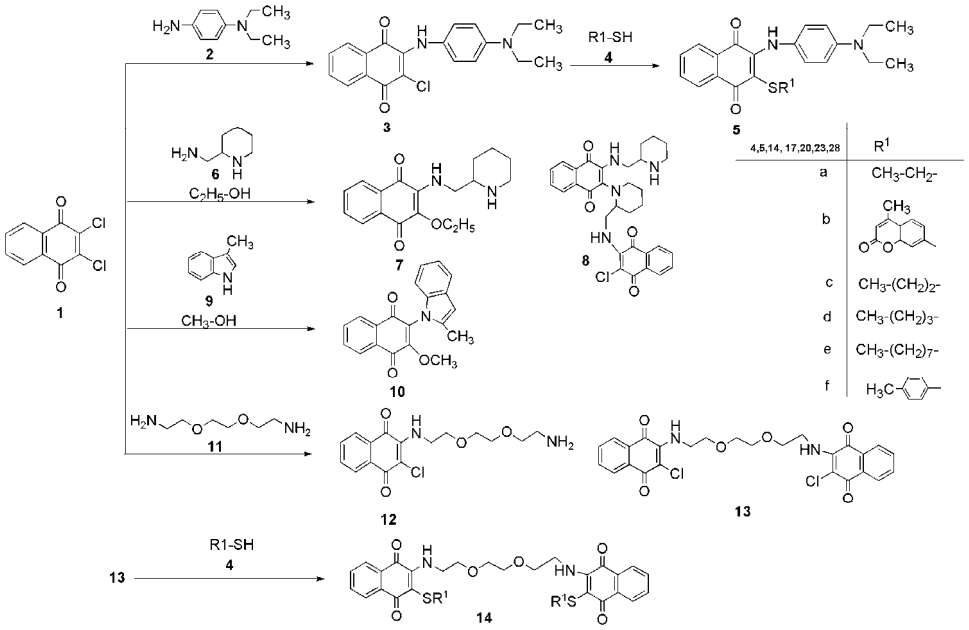


Scheme 1. Synthetic pathway for the synthesis of the novel substituted naphthoquinone derivatives.

*N*- and ethoxy-substituted naphthoquinone **7** was obtained by reaction of **1** and an equivalent number of moles of **6** in an ethanolic solution of $Na_2CO_3$. The $–OCH_2$ protons of **7** appeared in the low-field region of the $^1$H-NMR spectrum as multiplets at 4.57–4.60 ppm. The interesting *N*,*N*-substituted dinaphthoquinone derivative **8** was synthesized by the reaction of **1** and the equivalent number of moles of **6** in chloroform with triethylamine. The derivative **8** was obtained as a stable brown solid in good yield. In the mass spectrum of compound **8**, the accurate mass of the molecular ion peak as the sodium adduct ion was observed at *m*/*z* 595 $[M+Na]^+$.

The reaction of **1** with indole **9** in methanol resulted in the *N*- and methoxy--substituted compound **10**. The $–OCH_3$ protons of compound **10** appeared in the $^1$H-NMR spectrum as singlet at 4.10 ppm. In this reaction, methanol behaved as a nucleophile and attacked the naphthoquinone to give the addition reaction. The indole-substituted quinone derivatives were colored stable compounds.

The known compound **13**[17] and the novel compound **12** were obtained by reaction of **1** with diamine **11**. The mass spectrum of compound **12** in the positive ion mode of the ESI technique confirmed the proposed structure; the protonated molecular ion peak was identified at *m*/z 339 $[M+Na]^+$. The reactions of **13**[17] with thiols **4d** and **e** gave the interesting *N*,*S*-substituted dinaphthoquinone derivatives **14d** and **14e**, which were obtained in high yields. In the $^{13}$C-NMR spectrum of compound **14d**, two carbonyl carbon signals were observed at 179.1 and 180.3 ppm. In the mass spectrum of compound **14e**, the accurate mass of the molecular ion peak was registered at *m*/*z* 749 $[M+H]^+$. The known compound **16**[18] was obtained by reaction of naphthoquinone **1** with amine **15** in chloroform in the presence of $Et_3N$. The reaction of compound **16**[18] with thiols **4d**–**f** gave the novel *N*,*S*-naphthoquinone derivatives **17d**–**f**. In the $^1$H-NMR spectrum of compound **17d**, the $–SCH_2$ protons gave a triplet at 2.96 ppm and the $C–CH_3$ for compound **17f** gave multiplets at 1.40–1.45 ppm (Scheme 2).

The *N*-substituted naphthoquinone **19** was synthesized by reaction of **1** with **18** in chloroform in the presence of $Et_3N$. The $^1$H-NMR spectrum of compound **19** showed the $–NCH_2$ protons as a singlet at 3.37 ppm. The compound **20d** was obtained by the reaction of compound **19** with **4d** in ethanol with $Na_2CO_3$. In the $^{13}$C-NMR spectrum of the *N*,*S*-substituted compound **20d**, two carbonyl carbon signals were observed at 179.4 and 180.5 ppm. The novel compound **22** was obtained by reaction of **1** with amine **21**. The IR spectrum of compound **22** showed a characteristic amine band (–NH) at 3365 $cm^{-1}$. The *N*,*S*-naphthoquinone substituted **23c** and **d** were obtained by reaction of **22** with **4c** and **d** in ethanol containing $Na_2CO_3$. In the mass spectrum of compounds **23c** and **d**, the accurate mass measurements of the molecular ion peaks were registered at *m*/*z* 366 $[M+H]^+$ and 354 $[M–H]^–$, respectively. The *N*-substituted naphthoquinone **25** was obtained in the reaction of **1** with *N*-(2-hydroxyethyl)aniline **24** in chloro-

form in the presence of $Et_3N$. The $–NCH_2$ protons of **25** appeared in the low-field region of the $^1$H-NMR spectrum as triplets at 3.80 ppm.

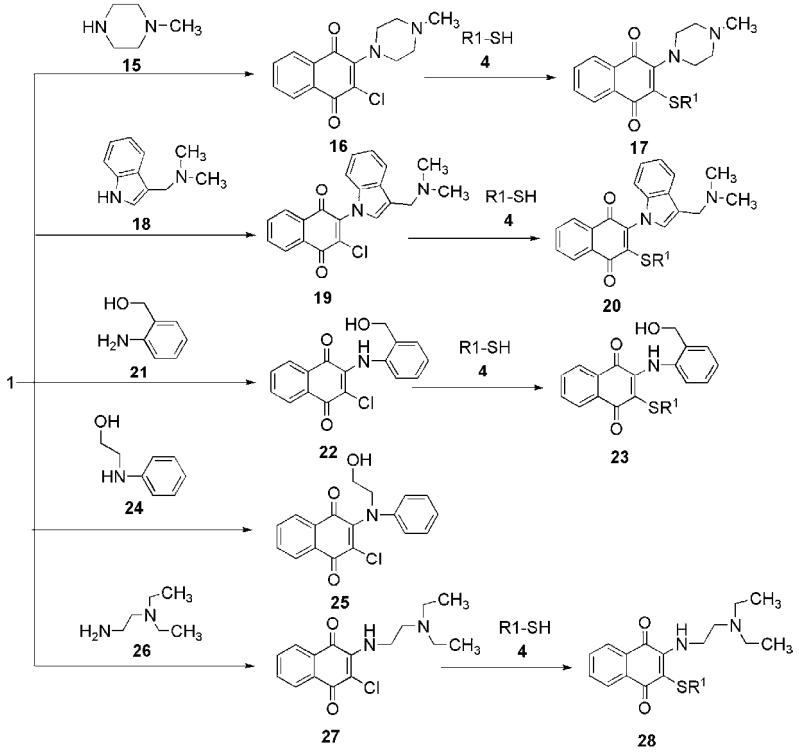


Scheme 2. Synthesis of novel *N*- and *N*,*S*-substituted naphthoquinone derivatives.

The reaction of the known compound **27**[19] with **4d** and **e** gave the *N*,*S*-substituted naphthoquinones **28d** and **e**. The mass spectrum of compounds **28d** and **e** gave molecular ion peaks at *m*/*z* 361 $[M]^+$ and 417 $[M+H]^+$, respectively.

*Electrochemical assay*

Some of the novel naphthoquinone derivatives were studied by cyclic voltammetry in aprotic media (DMF) using tetrabutylammonium perchlorate (0.10 M) as the supporting electrolyte at 100 mV $s^{-1}$ on a glassy carbon electrode. The electrochemical parameters, including cathodic peak potentials ($Epc_1$ and $Epc_2$), the half-wave peak potentials ($E_{1,½}$) and the difference between the first oxidation and reduction processes ($\Delta Ep$) are given in Table I.

The cyclic voltammogram of 2,3-dichloro-1,4-naphthoquinone (**1**) gave two monoelectronic waves. The first ($c_1$) and second ($c_2$) cathodic peaks corresponded to the semiquinone ($Q/Q^-$) and dianion ($Q^-/Q^{2-}$) pairs, respectively.

TABLE I. Half-wave potentials (for the 1st wave) and electrochemical data for some of the naphthoquinone derivatives ($c$ = 1.0×10$^{-3}$ M) in 0.1 M DMF/TBAP; $\Delta Ep_1 = Epa_1 - Epc_1$; $E_{1,1/2} = (Epa_1 + Epc_1)/2$

| Compound | $Epc_1$ / V | $Epc_2$ / V | $\Delta Ep_1$ / mV | $E_{1,1/2}$ / V |
|---|---|---|---|---|
| 2,3-Dichloro-1,4-naphthoquinone (**1**) | –0.4038 | –1.1620 | 235 | –0.2862 |
| **3**[16] | 0.3133 | –0.6661 | 265 | 0.4459 |
| **5a** | 0.2483 | –0.7499 | 300 | 0.3984 |
| **5c** | –0.3043 | –0.7171 | 252 | 0.1262 |
| **5d** | 0.2953 | –0.7361 | 133 | 0.1337 |
| **5e** | 0.2444 | –0.7530 | 303 | 0.3960 |
| **8** | – | –0.9873 | – | – |
| **14d** | –0.2203 | –0.7709 | 102 | –0.2712 |
| **14e** | –0.2774 | –0.7980 | – | – |
| **19** | –0.6961 | –1.235 | 128 | –0.6323 |
| **20d** | –0.7550 | –1.3580 | 88 | 0.7112 |
| **22** | –0.5286 | –0.7391 | – | – |
| **27**[19] | –0.4737 | –0.7410 | – | – |
| **28d** | –0.7839 | –0.7201 | 84 | –0.7520 |
| **28e** | –0.7988 | – | 99 | –0.7494 |

The reduction mechanism changed when 2,3-dichloro-1,4-naphthoquinone (**1**) was substituted with *N*-nucleophiles. Additional cathodic and anodic peaks were detected in the voltammograms because of the various type of substituents.[20] During the electrochemical study of the *N*-substituted compound **3** and the *N*,*S*-substituted compounds **5a**, **5c**–**5e**, **14d** and **14e**, the CV displayed a different profile that did not follow the typical two monoelectronic reversible charge transfer process occurring for 2,3-dichloro-1,4-naphthoquinone (**1**). Three peaks were observed in both cathodic and anodic regions of the CV. The potential in the first reduction step for compound **5a** was seen at $Ep(c_1)$ = 0.2483 V. This could be related the acidity level of the proton settled on the nitrogen atom.[21] The first cathodic peak was not observed in the CV for the dinaphthoquinone compound **8**. The resulting voltammogram of compound **19** showed two typical successive one-electron reduction processes that could be observed for quinones in aprotic media. This can be related to the absence of a proton in the molecule. The *N*-substituted compound **27** gave three cathodic peaks in the CV. The resulting voltammogram of the *N*,*S*-substituted compounds **28d** and **e** showed a decrement in the peak intensities.

## EXPERIMENTAL

### *Chemistry*

The melting points were measured on a Buchi B-540 melting point apparatus. The elemental analyses were realized on a Thermo Finnigan Flash EA 1112 Elemental Analyser. The infrared (IR) spectra were recorded in KBr pellets on a Perkin Elmer Precisely Spectrum One FTIR spectrometer. $^1$H- and $^{13}$C-NMR spectra were recorded on a Varian UNITYINOVA

instrument operating at 500 MHz for $^{1}$H-NMR and 126 MHz for $^{13}$C-NMR spectra. The mass spectra were obtained on a Thermo Finnigan LCQ Advantage MAX LC/MS/MS spectrometer according to ESI probe. The products were isolated by column chromatography on silica gel (Merck Silica gel 60, particle size 63–200 μm). TLC plates silica 60$F_{254}$ (Merck, Darmstadt), detection with ultraviolet light (254 nm). All chemicals were of reagent grade and used without further purification.

The analytical and spectral data of the synthesized compounds are given in Supplementary material to this paper.

Cyclic voltammetry measurements were performed in a conventional three-electrode cell using a computer-controlled Gamry Reference 600 Model potentiostat/galvanostat. A glassy carbon disc was used as the working electrode. The surface of the working electrode was polished with alumina before each run. A platinum wire served as the counter electrode. The reference electrode was an Ag/AgCl electrode. Electrochemical grade tetrabutylammonium perchlorate (TBAP) in extra pure DMF was employed as the supporting electrolyte at a concentration of 0.10 M. Prior to each run, the solutions were purged with nitrogen. Measurements were made over a potential range between 1.0 and –2.0 V with a step rate of 0.1 V $s^{-1}$.

*General procedures*

*Procedure 1.* 1.0 g (4.4 mmol) 2,3-dichloro-1,4-naphthoquinone (**1**) and the corresponding nucleophile were stirred in $CHCl_3$ (30 mL) with triethylamine (3 mL) solution for 2–3 h at room temperature. The color of the solution quickly changed and the reaction was monitored by TLC. Chloroform (30 mL) was added to the reaction mixture. The organic layer was washed with water (4×30 mL), and dried over $Na_2SO_4$. After evaporation of the solvent, the residue was purified by column chromatography on silica gel.

*Procedure 2.* 1.0 g (4.4 mmol) 2,3-dichloro-1,4-naphthoquinone (**1**) and the corresponding nucleophile were stirred in EtOH (65 mL) solution of $Na_2CO_3$ (1.52 g) for 2 to 3 h at room temperature. The color of the solution quickly changed and the reaction was monitored by TLC. Chloroform (30 mL) was added to the reaction mixture. The organic layer was washed with water (4×30 mL), and dried over $Na_2SO_4$. After evaporation of the solvent, the residue was purified by column chromatography on silica gel.

*Procedure 3.* 1.0 g (4.4 mmol) 2,3-dichloro-1,4-naphthoquinone (**1**) and 8.86 mmol nucleophile were stirred in a methanolic (65 mL) solution of $Na_2CO_3$ (1.52 g) for 2 to 3 h at room temperature. The color of the solution quickly changed and the reaction was monitored by TLC. Chloroform (30 mL) was added to the reaction mixture. The organic layer was washed with water (4×30 mL), and dried over $Na_2SO_4$. After evaporation of the solvent, the residue was purified by column chromatography on silica gel.

## CONCLUSIONS

Novel substituted naphthoquinone compounds were synthesized from the reactions of **1** and related nucleophiles in different reaction media. The structures of novel compounds were characterized by microanalysis, FT-IR, $^{1}$H-NMR, $^{13}$C-NMR, MS and cyclic voltammetry.

## SUPPLEMENTARY MATERIAL

The analytical and spectral data of the synthesized compounds are available electronically from http://www.shd.org.rs/ JSCS/, or from the corresponding author on request.

*Acknowledgment.* We gratefully thank the Research Fund of the University of Istanbul for the financial support of this work.

ИЗВОД

## ИСПИТИВАЊЕ РЕАКЦИЈЕ НУКЛЕОФИЛНЕ СУПСТИТУЦИЈЕ 2,3-ДИХЛОР-1,4-НАФТОХИНОНА СА РАЗЛИЧИТИМ НУКЛЕОФИЛИМА

CEMIL IBIS, AHMED HASSEN SHNTAIF, HAKAN BAHAR и SIBEL SAHINLER AYLA

*Department of Chemistry, Faculty of Engineering, Istanbul University, 34320, Avcilar, Istanbul, Turkey*

Синтетисани су нови *N*-, *N*,*S*- и *N*,*O*-супституисани деривати нафтохинона реакцијом 2,3-дихлор-1,4-нафтохинона (**1**) са одговарајућим нуклеофилима у хлороформу у присуству триетиламина или у етанолу у присуству $Na_2CO_3$. Структуре нових једињења одређене су микро-анализом, FT-IR, $^1$H-NMR, $^{13}$C-NMR, MS и цикличном волтаметријом.

(Примљено 24. новембра 2014, ревидирано 26. фебруара, прихваћено 1. марта 2015)

## REFERENCES

1. L. Jiao, H. Lu, H. Zhou, J. J. Wang, *J. Environ. Sci.* **21** (2009) 503
2. K. Venkataraman, *The Chemistry of Synthetic Dyes*, Academic Press, London, 1971, p. 29
3. N. Orban, I. Boldizsar, Z. Szucs, B. Danos, *Dyes Pigm.* **77** (2007) 249
4. M. C. Celli, N. Tran, R. Knox, A. K. Jaiswal, *Biochem. Pharmacol.* **72** (2006) 366
5. F. Prati, M. Bartolini, E. Simoni, A. De Simoni, A. Pinto, V. Andrisano, M. L. Bolognesi, *Bioorg. Med. Chem. Lett.* **23** (2013) 6254
6. T. Takeya, H. Kondo, T. Otsuka, K. Tomita, I. Okamoto, O. Tamura, *Org. Lett.* **9** (2007) 2807
7. E. B. T. Diogo, G. G. Dias, B. L. Rodrigues, T. T. Guimaraes, W. O. Valença, C. A. Camara, R. N. Oliveira, M. G. Da Silva, V. F. Ferreira, Y. G. De Paiva, M. O. F. Goulart, R. F. S. Menna-Barreto, S. L. De Castro, E. N. J. Da Silva, *Bioorg. Med. Chem.* **21** (2013) 6337
8. C. Ibis, A. F. Tuyun, H. Bahar, S. Sahinlar Ayla, M. V. Stasevych, R. Y. Musyanovych, O. Komarovska-Porokhnyavets, V. Novikov, *Med. Chem. Res.* **22** (2013) 2879
9. C. Ibis, A. F. Tuyun, Z. Ozsoy-Gunes, H. Bahar, M. V. Stasevych, R. Y. Musyanovych, O. Komarovska-Porokhnyavets, V. Novikov, *Eur. J. Med. Chem.* **46** (2011) 5861
10. C. Ibis, A. F. Tuyun, Z. Ozsoy-Gunes, S. Sahinler Ayla, M. V. Stasevych, R. Y. Musyanovych, O. Komarovska-Porokhnyavets, V. Novikov, *Phosphorus Sulfur Silicon Relat. Elem.* **188** (2013) 955
11. C. Ibis, S. Sahinler Ayla, H. Asar, *Synth. Commun.* **44** (2014) 121
12. M. Makosza, S. Nizamov, *Tetrahedron* **47** (2001) 9615
13. S. Castellano, A. Bertamino, I. Gomez-Monterrey, M. Santoriello, P. Grieco, P. Camiglia, G. Sbardella, E. Novellino, *Tetrahedron Lett.* **49** (2008) 583
14. X. Li, S.-L. Zheng, X. Li, J. L. Li, O. Qiang, R. Liu, L. He, *Eur. J. Med. Chem.* **54** (2012) 42
15. M. C. Lozada, O. Soria-Arteche, M. T. R. Apan, A. Nieto-Camacho, R. G. Enriquez, T. Izquierdo, A. Jimenez-Corona, *Bioorg. Med. Chem.* **20** (2012) 5077
16. N. P. Buu-Hoi, P. Jacquigenon, N. D. Xuong, V. T. Suu, *J. Chem. Soc.* (1958) 2815
17. A. P. Kartoflitskaya, N. R. Gladun, L. D. Bolibruk, G. I. Zokhnyk, *Zh. Organicheskoi Khimii* **32** (1996) 1429

18. B. Prescott, *J. Med. Chem.* **12** (1969) 181
19. R. K. Y. Zee-Cheng, E. G. Podrebarac, C. S. Menon, C. C. Cheng, *J. Med. Chem.* **22** (1979) 501
20. F. C. Abreau, A. C. O. Lopes, M. O. F. Goulart, *J. Electroanal. Chem.* **562** (2004) 53
21. E. O. Costa, M. T. Molina, F. C. Abreu, F. A. S. Silva, C. O. Costa, W. Pinho, I. B. Valentim, B. Aguilera-Venegas, F. Perez-Cruz, E. Norambuena, C. Olea-Azar, *Int. J. Electrochem. Sci.* **7** (2012) 6524.

Journal of the Serbian Chemical Society
JSCS@tmf.bg.ac.rs • www.shd.org.rs/JSCS
*J. Serb. Chem. Soc. 80* (6) S189–S197 (2015) *Supplementary material*

SUPPLEMENTARY MATERIAL TO

# An investigation of nucleophilic substitution reactions of 2,3-dichloro-1,4-naphthoquinone with various nucleophilic reagents

CEMIL IBIS*, AHMED HASSEN SHNTAIF, HAKAN BAHAR and SIBEL SAHINLER AYLA

[1]*Department of Chemistry, Faculty of Engineering, Istanbul University, 34320, Avcilar, Istanbul, Turkey*

*J. Serb. Chem. Soc.* 80 (6) (2015) 731–738

ANALYTICAL AND SPECTRAL DATA OF THE SYNTHESIZED COMPOUNDS

*2-Chloro-3-((4-(diethylamino)phenyl)amino)naphthalene-1,4-dione* ***(3)***. Compound **3** was synthesized in the reaction of **1** (0.5 g, 2.20 mmol) with **2** (0.36 g, 2.20 mmol) according to general procedure 1.

Yield: 67.53 % (0.52 g); blue solid; m.p.: 159–160 °C (Lit. 159 °C[1]); Anal. Calcd. for $C_{20}H_{19}ClN_2O_2$ (*FW*: 354.113): C, 67.70; H, 5.40; N, 7.89 %. Found: C, 67.65; H, 5.32; N, 7.81 %; $R_f$ ($CHCl_3$): 0.34; IR (KBr, $cm^{-1}$): 3304 (N–H), 2965–2926 (CH aliphatic), 1672–1638 (C=O), 1524–1506 (C=C); $^1$H-NMR (500 MHz, $CDCl_3$, $\delta$ / ppm): 0.98 (3H, *t*, *J* = 7.32 Hz, $CH_3$), 3.24–3.36 (2H, *m*, $NCH_2$), 6.53–6.92 (4H, *m*, CH arom), 7.56–8.09 (4H, *m*, CH arom); $^{13}$C-NMR (125.66 MHz, $CDCl_3$, $\delta$ / ppm) 11.5 ($CH_3$), 43.4 ($NCH_2$), 111.4, 133.9, 124.4, 140.8, 125.2, 125.8, 125.9, 128.8, 131.5, 131.9, 145.2, (C arom, CH arom), 179.7, 176.2 (C=O); MS (*m*/*z* (relative abundance, %)): 381 (100) $[M+H]^+$.

*2-((4-(Diethylamino)phenyl)amino)-3-(ethylthio)naphthalene-1,4-dione* ***(5a)***. Compound **5a** was synthesized in the reaction of **3** (0.1 g, 0.28 mmol) with **4a** (0.017 g, 0.27 mmol) according to general procedure 2.

Yield: 93.45 % (0.1 g); gray oil; $R_f$ ($CH_2Cl_2$): 0.25; Anal. Calcd. for $C_{22}H_{24}N_2O_2S$ (*FW*: 380.50): C, 69.44; H, 6.36; N, 7.36; S, 8.43 %. Found: C, 69.64; H, 6.48; N, 7.12; S, 8.74 %; IR (KBr, $cm^{-1}$): 3330 (N–H), 3018 (C–H arom), 2975–2929 (C–H aliphatic), 1664–1631 (C=O), 1593–1549 (C=C); $^1$H--NMR (500 MHz, $CDCl_3$, $\delta$ / ppm): 0.98 (3H, *t*, *J* =7.5 Hz, $CH_3$), 1.08 (6H, *t*, *J* =7.5 Hz, $NCH_2C\mathbf{H}_3$), 2.53–2.57 (2H, *m*, $SCH_2$), 3.26–3.30 (4H, *m*, $NCH_2$), 7.77 (1H, *s*, NH), 6.55 (2H, *d*, *J* = 7.3 Hz, CH arom), 6.86 (2H, *d*, *J* = 7.3 Hz, CH

* Corresponding author. E-mail: ibiscml@istanbul.edu.tr

arom), 7.95–8.07 (4H, *m*, CH naphtho); $^{13}$C-NMR (125.66 MHz, $CDCl_3$, $\delta$ / ppm) 11.5 ($CH_3$), 13.3 (**C**$H_2CH_3$), 28.6 ($SCH_2$), 43.4 ($NCH_2$),110.3, 112.5, 123.8, 125.4, 125.6, 125.8, 125.9, 129.7, 131.2, 132.8, 133.4, 144.7, 145.4, (CH arom, C arom), 179.6, 179.7 (C=O); MS (*m*/*z* (relative abundance, %)): 381 (100) $[M+H]^+$.

*2-(4-((Diethylamino)phenyl)amino)-3-((4-methyl-2-oxo-2*H*-chromen-7-yl)-thio)naphthalene-1,4-dione (**5b**)*. Compound **5b** was synthesized in the reaction of **3** (0.1 g, 0.28 mmol) with **4b** (0.05 g, 0.26 mmol) according to general procedure 2.

Yield: 64.28 % (0.09 g); blue oil; $R_f$ ($CHCl_3$): 0.45; Anal. Calcd. for $C_{30}H_{26}N_2O_4S$ (*FW*: 510.60): C, 70.57; H, 5.13; N, 5.49; S, 6.28 %. Found: C, 70.33; H, 4.89; N, 5.26; S, 6.03 %; IR (KBr, $cm^{-1}$): 3253 (N–H), 3053 (C–H arom), 2962, 2923, 2852 (C–H aliphatic), 1734 (C=O lactone), 1666 (C=O quinone), 1597, 1537 (C=C),; $^1$H-NMR (500 MHz, $CDCl_3$, $\delta$ / ppm): 1.07 (6H, *t*, *J* = 5.0 Hz, $NCH_2C\mathbf{H}_3$), 1.48 (3H, *s*, $CH_3$), 6.01 (1H, *s*, CH vin), 3.24–3.26 (4H, *m*, $NCH_2$), 6.26–8.13 (11H, *m*, CH arom); $^{13}$C-NMR (125.66 MHz, $CDCl_3$, $\delta$ / / ppm) 11.4, 17.5 ($CH_3$), 43.5 ($NCH_2$), 123.0, 123.2, 124.4, 125.3, 125.9, 126.4, 127.4, 129.2, 131.6, 131.8, 132.8, 134.2, 140.8, 144.7, 145.2, 151.0, 152.5 (CH arom, C arom), 159.6 (C=O coumarin) 179.2, 179.8 (C=O); MS (*m*/*z* (relative abundance, %)): 511 (100) $[M+H]^+$.

*2-((4-(Diethylamino)phenyl)amino)-3-(propylthio)naphthalene-1,4-dione (**5c**)*. Compound **5c** was synthesized in the reaction of **3** (0.1 g, 0.282 mmol) with **4c** (0.02 g, 0.26 mmol) according to general procedure 2.

Yield: 62.72% (0.06 g); gray oil; $R_f$ ($CHCl_3$): 0.40; Anal. Calcd. for $C_{23}H_{26}N_2O_2S$ (*FW*: 394.53): C, 70.02; H, 6.64; N, 7.10; S, 8.13 %. Found: C, 69.89; H, 6.31; N, 7.05; S, 8.21 %; IR (KBr, $cm^{-1}$): 3311 (N–H), 3071 (C–H arom), 2966, 2929, 2870 (C–H aliphatic), 1663 (C=O), 1591, 1562 (C=C); $^1$H--NMR (500 MHz, $CDCl_3$, $\delta$ / ppm): 0.74 (3H, *t*, *J* = 7.5 Hz, $CH_3$), 1.08 (6H, *t*, *J* = 7.5 Hz, $NCH_2C\mathbf{H}_3$), 1.30–1.35 (2H, *m*, $SCH_2C\mathbf{H}_2$), 2.50 (2H, *t*, *J* = 7.5 Hz, $SCH_2$), 3.25–3.29 (4H, *m*, $NCH_2$), 6.54 (1H, *bs*, NH), 6.57–6.87 (4H, *m*, CH arom), 7.94–8.06 (4H, *m*, CH naphtho); $^{13}$C-NMR (125.66 MHz, $CDCl_3$, $\delta$ / ppm): 12.3, 13.0 ($CH_3$), 35.1 ($CH_2$), 40.15 ($SCH_2$), 43.5 ($NCH_2$), 112.8, 121.2, 123.2, 123.8, 125.4, 125.5, 125.6, 126.0, 129.7, 132.8, 133.3, 144.7, 145.3, (CH arom, C arom), 179.5, 179.7 (C=O); MS (*m*/*z* (relative abundance, %)): 395 (100) $[M+H]^+$.

*2-(Butylthio)-3-((4-(diethylamino)phenyl)amino)naphthalene-1,4-dione (**5d**)*. Compound **5d** was synthesized in the reaction of **3** (0.1 g, 0.28 mmol) with **4d** (0.025 g, 0.27 mmol) according to general procedure 2.

Yield: 69.52 % (0.08 g); gray oil; $R_f$ ($CHCl_3$): 0.52; Anal. Calcd. for $C_{24}H_{28}N_2O_2S$ (*FW*: 408.56): C, 70.55; H, 6.91; N, 6.86; S, 7.85 %. Found: C, 70.32; H, 6.78; N, 6.61; S, 7.52 %; IR (KBr, $cm^{-1}$): 3307 (N–H), 3065 (C–H

arom), 2965, 2928, 2870 (C–H aliphatic), 1662, 1610 (C=O), 1591, 1544 (C=C),; $^1$H-NMR (500 MHz, $CDCl_3$, $\delta$ / ppm): 0.78 (3H, *t*, *J* = 7.5 Hz, $CH_3$), 1.10 (6H, *t*, *J* = 15.0 Hz $NCH_2C\mathbf{H}_3$), 1.14–1.18 (2H, *m*, $C\mathbf{H}_2CH_3$), 1.24–1.29 (2H, *m*, $SCH_2C\mathbf{H}_2$), 2.50 (2H, *t*, *J* = 7.5 Hz, $SCH_2$), 3.25–3.29 (4H, *m*, $NCH_2$), 7.77 (1H, *bs*, NH), 6.52–6.87 (4H, *m*, CH arom), 7.94–8.06 (4H, *m*, CH naphtho); $^{13}$C--NMR (125.66 MHz, $CDCl_3$, $\delta$ / ppm): 11.5, 12.6 ($CH_3$), 30.4, 32.8 ($CH_2$), 37.8 ($SCH_2$), 43.4 ($NCH_2$ ), 110.3, 112.9, 123.8, 125.5, 125.6, 125.9, 129.7, 131.2, 132.8, 133.3, 145.2, 144.7 (CH arom, C arom), 179.5, 179.7 (C=O); MS (*m*/*z* (relative abundance, %)): 409 (100). $[M+H]^+$.

*2-((4-(Diethylamino)phenyl)amino)-3-(octylthio)naphthalene-1,4-dione (**5e**)*. Compound **5e** was synthesized in the reaction of **3** (0.1 g, 0.28 mmol) with **4e** (0.041 g, 0.28 mmol) according to general procedure 2.

Yield: 83.20 % (0.109 g); blue oil; $R_f$ ($CHCl_3$:ethyl acetate 3:1): 0.85; Anal. Calcd. for $C_{28}H_{36}N_2O_2S$ (*FW*: 464.66): C, 72.38; H, 7.81; N, 6.03; S, 6.90 %. Found: C, 72.19; H, 7.61; N, 5.81; S, 6.68 %; IR (KBr, $cm^{-1}$): 3318 (N–H), 3071 (C–H arom), 2964, 2926, 2853 (CH aliphatic), 1663, 1633 (C=O), 1592, 1548 (C=C),; $^1$H-NMR (500 MHz, $CDCl_3$, $\delta$ / ppm): 0.77 (3H, *t*, *J* = 5.0 Hz, $CH_2C\mathbf{H}_3$), 1.08–1.11 (6H, *m*, $NCH_2C\mathbf{H}_3$), 1.14–1.18 (10H, *m*, $((CH_2)_5)$), 1.26––1.31 (2H, *m*, $SCH_2C\mathbf{H}_2$), 2.50 (2H, *t*, *J* = 7.5 Hz, $SCH_2$), 3.26–3.31 (4H, *m*, $NCH_2$), 7.77 (H, *s*, NH), 6.53 (2H, *d*, *J* = 5.0 Hz, CH arom), 6.87 (2H, *d*, *J* = 5.0 Hz, CH arom), 8.02 (2H, *dd*, *J* = 5.0 and 6.3 Hz, CH naphtho) 7.59 (2H, *t*, *J* = 7.5 Hz, CH naphtho); $^{13}$C-NMR (125.66 MHz, $CDCl_3$, $\delta$ / ppm) 11.5 ($CH_3$), 13.0 ($CH_3$) thio, 30.7, 28.6, 28.4, 28.1, 28.0, 27.7 ($CH_2$), 33.1 ($SCH_2$), 43.5 ($NCH_2$), 110.3, 113.0, 123.8, 125.4, 125.7, 125.9, 129.7, 131.2, 132.8, 133.4, 144.7, 145.2 (CH arom, C arom), 179.6, 179.8 (C=O); MS (*m*/*z* (relative abundance, %)): 465 (100) $[M+H]^+$.

*3-Ethoxy-3-(((piperidin-2-yl)methyl)amino)naphthalene-1,4-dione (**7**)*. Compound **7** was synthesized in the reaction of **1** (0.50 g, 2.20 mmol) with **6** (0.25 g, 2.19 mmol) according to general procedure 2.

Yield: 34.73 % (0.33 g); blue oil; $R_f$ ($CHCl_3$): 0.31; Anal. Calcd. for $C_{18}H_{22}N_2O_{43}$ (*FW*: 414.38): C, 68.77; H, 7.05; N, 8.91 %. Found: C, 68.52; H, 6.88; N, 8.58 %; IR (KBr, $cm^{-1}$): 3385 (N–H), 3010 (C–H arom), 2926, 2850 (C–H aliphatic), 1703, 1613 (C=O), 1594, 1505 (C=C); $^1$H-NMR (500 MHz, $CDCl_3$, $\delta$ / ppm): 0.76–0.82 (3H, *m*, $CH_3$), 1.17–1.26 (6H, *m*, $CH_2$ piper.), 1.50 (2H, *bs*, NH), 2.20–2.25 (4H, *m*, $NCH_2$), 2.78–2.81 (H, *m*, NCH), 4.57–4.60 (2H, *m*, $OCH_2$), 7.69–8.71 (4H, *m*, CH arom); $^{13}$C-NMR (125.66 MHz, $CDCl_3$, $\delta$ / / ppm) 20.7 ($CH_3$), 28.3, 28.6, 28.9 ($CH_2$), 30.9, 35.2 ($NCH_2$), 52.3 ($OCH_2$), 124.6, 124.7, 127.3, 128.9, 130.1, 131.5, 131.7, 136.2 (CH arom, C arom), 174.7, 178.8 (C=O); MS (*m*/*z* (relative abundance, %)): 314 (100) $[M+H]^+$.

*2-(2-(((3-Chloro-1,4-dioxonaphthalen-2-yl)amino)methyl)piperidin-1-yl)-3--(((piperidin-2-yl)methyl)amino)naphthalene-1,4-dione (**8**)*. Compound **8** was

synthesized in the reaction of **1** (0.5g, 2.20 mmol) with **6** (0.25 g, 2.19 mmol) according to general procedure 1.

Yield: 50.79 % (0.64 g); brown solid; m.p.: 155–156 °C; $R_f$ ($CH_2Cl_2$:petroleum ether 2:1, 40–60 °C): 0.41; Anal. Calcd. for $C_{32}H_{33}ClN_4O_4$ (*FW*: 573.08): C, 67.07; H, 5.80; N, 9.78 %. Found: C, 66.85; H, 5.56; N, 9.63 %; IR (KBr, $cm^{-1}$ ): 3400 (N–H), 3048 (C–H arom), 2938–2855 (C–H aliphatic), 1633––1614 (C=O), 1593 (C=C),; $^1$H-NMR (500 MHz, $CDCl_3$, $\delta$ / ppm): 1.37–1.90 (12H, *m*, $CH_2$ piper.), 3.49 (4H, *t*, *J* = 7.3 Hz, $NCH_2$), 4.18 (4H, *t*, *J* = 7.3 Hz, $NCH_2$), 2.60–3.10 (2H, *m*, NCH), 7.77 (3H, m, NH), 7.45–8.06 (8H, *m*, CH arom); $^{13}$C-NMR (125.66 MHz, $CDCl_3$, $\delta$ / ppm) 28.6, 24.2, 22.5 ($CH_2$), 52.68, 52.74 ($NCH_2$), 108.9, 122.7, 125.2, 129.9, 130.9, 130.1, 131.8, 144.7, 157.5 (CH aromatic, C aromatic), 176.9 (C=O); MS (*m*/*z* (relative abundance, %)): 595 (100) $[M+Na]^+$).

*2-Ethoxy-3-(2-methyl-1*H*-indol-1-yl)naphthalene-1,4-dione (**10**)*. Compound **10** was synthesized in the reaction of **1** (0.50 g, 2.20 mmol) with **9** (0.288 g, 2.19 mmol) according to general procedure 3.

Yield: 9.66 % (0.14 g); blue oil; $R_f$ ($CHCl_3$): 0.72; Anal. Calcd. for $C_{20}H_{15}NO_3$ (*FW*: 317.34): C, 75.70; H, 4.74; N, 4.41 %. Found: C, 75.51; H, 4.85; N, 4.12 5; IR (KBr, $cm^{-1}$ ): 3018 (C–H arom), 2926, 2854 (C–H aliphatic), 1717, 1664 (C=O), 1596, 1459 (C=C); $^1$H-NMR (500 MHz, $CDCl_3$, $\delta$ / ppm): 2.27 (3H, *s*, $CH_3$), 4.10 (3H, *s*, $OCH_3$), 7.01–8.18 (8H, *m*, CH arom); $^{13}$C-NMR (125.66 MHz, $CDCl_3$, $\delta$ / ppm) 12.8 ($CH_3$), 61.0 ($OCH_3$), 104.8, 126.1, 126.2, 126.3, 125.7, 129.8, 130.6, 131.1, 132.7, 132.9, 133.6, 134.3, 140.8 141.8, 146.5 (CH aromatic, C aromatic), 177.3 180.9 (C=O); MS (*m*/*z* (relative abundance, %)): 318 (100) $[M+H]^+$.

*2-((2-(2-(2-Aminoethoxy)ethoxy)ethyl)amino)-3-chloronaphthalene-1,4-dione (**12**)*. Compound **12** was synthesized in the reaction of **1** (0.50 g, 2.20 mmol) with **11** (0.652 g, 4.39 mmol) according to general procedure 1.

Yield: 3.22 % (0.048 g); brown oil; $R_f$ ($CH_3OH$): 0.93; Anal. Calcd. for $C_{16}H_{19}ClN_2O_4$ (*FW*: 338.79): C, 56.72; H, 5.65; N, 8.27 %. Found: C, 56.63; H, 5.77; N, 8.36 %; IR (KBr, $cm^{-1}$ ): 3334 (N–H), 3012 (C–H arom), 2872 (C–H aliphatic), 1678, 1644 (C=O), 1574, 1515 (C=C),; $^1$H-NMR (500 MHz, $CDCl_3$, $\delta$ / ppm): 3.97–4.04 (8H, *m*, $OCH_2$), 3.60–3.70 (4H, *m*, $NCH_2$), 7.47–7.99 (4H, *m*, CH arom); $^{13}$C-NMR (125.66 MHz, $CDCl_3$, $\delta$ / ppm) 43.4 ($NCH_2$), 68.9 ($OCH_2$), 69.4 ($OCH_2$**C**$H_2$NH), 76.2 (**C**$H_2CH_2NH_2$), 125.7, 131.4, 133.8 (CH aromatic, C aromatic), 179.3, 181.3 (C=O); MS (*m*/*z* (relative abundance, %)): 339 (100) $[M+H]^+$.

*2,2'-[1,2-Ethanediylbis(oxy-2,1-ethanediylimino)]bis(3-chloronaphthalene--1,4-dione) (**13**)*. Compound **13** was synthesized in the reaction of **1** (0.50 g, 2.20 mmol) with **11** (0.652 g, 4.39 mmol) according to general procedure 1.

Yield: 64.49% (0.75 g); red solid; m.p.: 150–152 °C (Lit 150–152 °C[2]); $R_f$ ($CHCl_3$:ethyl acetate 1:1): 0.48; Anal. Calcd. for $C_{26}H_{22}ClN_2O_6$ (*FW*: 528.09) C, 58.99; H, 4.19; N, 5.29 %. Found: C, 58.78; H, 4.27; N, 5.16 %; IR (KBr, $cm^{-1}$): 3053 (C–H arom), 2900–2863 (C–H aliphatic), 1679–1636 (C=O), 1579–1513 (C=C), 3334 (N–H); $^1$H-NMR (500 MHz, $CDCl_3$, $\delta$ / ppm): 3.72 (4H, *t*, *J* = 6.8 Hz, $NCH_2$), 4.0–4.04 (8H, *m*, $OCH_2$), 7.60–7.98 (8H, *m*, CH arom); $^{13}$C-NMR (125.66 MHz, $CDCl_3$, $\delta$ / ppm) 43.41 ($NCH_2$), 68.9, 69.4 ($OCH_2$), 125.7, 128.6, 131.5, 131.4, 133.8, 143.1, (CH arom, C arom), 179.3, 175.7 (C=O); MS (*m*/*z* (relative abundance, %)): 529 (38) $[M+H]^+$.

*2,2'-[1,2-Ethanediylbis(oxy-2,1-ethanediylimino)]bis[3-(buthylthio)naphthalene-1,4-dione] (**14d**)*. Compound **14d** was synthesized in the reaction of **13** (0.25 g, 0.47 mmol) with **4d** (0.061 g, 0.67 mmol) according to general procedure 2.

Yield: 57.76 % (0.17 g); red oil; $R_f$ ($CHCl_3$): 0.35; Anal. Calcd. for $C_{34}H_{40}N_2O_6S_2$ (*FW*: 636.82): C, 64.13; H, 6.33; N, 4.40; S, 10.07 %. Found: C, 64.22; H, 6.46; N, 4.72; S, 10.25 %; IR (KBr, $cm^{-1}$ ): 3066 (C–H arom), 2956, 2927, 2870 (C–H aliphatic), 1674, 1629 (C=O), 1592, 1550 (C=C); $^1$H-NMR (500 MHz, $CDCl_3$, $\delta$ / ppm): 0.80 (6H, *t*, *J* = 7.5 Hz, $CH_3$), 1.29–1.34 (4H, *m*, $CH_2$), 1.45–1.51 (4H, *m*, $SCH_2C\mathbf{H}_2$), 2.72 (4H, *t*, *J* = 7.5 Hz, $SCH_2$), 3.69 (2H, *t*, *J* = 7.5 Hz, $NCH_2$), 4.08 (8H, *t*, *J* = 7.5 Hz, $OCH_2$), 7.47–8.02 (8H, *m*, C–H arom); $^{13}$C-NMR (125.66 MHz, $CDCl_3$, $\delta$ / ppm) 12.6 ($CH_2\mathbf{C}H_3$), 21.0 ($\mathbf{C}H_2CH_3$), 30.9 ($CH_2S$), 33.7 ($\mathbf{C}H_2CH_2$–S), 44.4 ($NHCH_2$), 69.0 (O–$\mathbf{C}H_2CH_2NH$), 69.5 ($OCH_2$), 125.5, 125.7, 130.9, 132.7, 133.4 (CH arom, C arom), 179.1, 180.3 (C=O); MS (*m*/*z* (relative abundance, %)): 659 (100) $[M+Na]^+$.

*2,2'-[1,2-Ethanediylbis(oxy-2,1-ethanediylimino)]bis[3-(buthylthio)naphthalene-1,4-dione] (**14e**)*. Compound **14e** was synthesized in the reaction of **13** (0.3 g, 0.56 mmol) with **4e** (0.082 g, 0.56 mmol) according to general procedure 2.

Yield: 58.80 % (0.25 g); red oil; $R_f$ ($CHCl_3$:ethyl acetate 2:3): 0.82; Anal. Calcd. for $C_{42}H_{56}N_2O_6S_2$ (*FW*: 749.03): C, 67.35; H, 7.54; N, 3.74; S, 8.56 %. Found: C, 66.98; H, 7.76; N, 3.45; S, 8.23 %; IR (KBr, $cm^{-1}$): 3066 (C–H arom), 2956, 2927, 2870 (C–H aliphatic), 1674, 1629 (C=O), 1592, 1550 (C=C); $^1$H-NMR (500 MHz, $CDCl_3$, $\delta$ / ppm): 0.80 (6H, *t*, *J* = 7.3 Hz, $CH_3$), 1.15–1.19 (12H, *m*, $CH_2$), 1.46–1.51 (12H, *m*, $CH_2$), 2.72 (4H, *t*, *J* = 7.3 Hz, $SCH_2$), 3.69 (4H, *t*, *J* = 6.8 Hz, $NCH_2$), 4.08 (8H, *t*, *J* = 6.8 Hz, $OCH_2$), 7.46–8.02 (8H, *m*, CH arom); $^{13}$C-NMR (125.66 MHz, $CDCl_3$, $\delta$ / ppm) 13.0 ($CH_3$), 34.0, 30.7, 28.9, 28.6, 28.1, 28.1 ($CH_2$), 38.2 ($SCH_2$), 44.4 ($NHCH_2$), 69.0 (O–$\mathbf{C}H_2CH_2NH$), 69.5 ($OCH_2$), 125.3, 125.5, 130.9, 132.7, 133.4 (CH arom, C arom), 179.0, 180.3 (C=O); MS (*m*/*z* (relative abundance, %)): 749 (100) $[M+H]^+$.

*2-Chloro-3-(4-methylpiperazin-1-yl)naphthalene-1,4-dione (**16**)*. Compound **16** was synthesized in the reaction of **1** (0.50 g, 2.20 mmol) with **15** (0.22 g, 2.19 mmol) according to general procedure 1.

Yield: 65 % (0.33 g); brown solid; m.p.: 105–106 °C (Lit. for **16**·HCl: 220––225 °C[3]); $R_f$ (ethyl acetate): 0.73; Anal. Calcd. for $C_{15}H_{15}ClN_2O_2$ (*FW*: 290.74): C, 61.97; H, 5.20; N, 9.64 %. Found: C, 61.73; H, 5.11; N, 9.56 %; IR (KBr, $cm^{-1}$): 3072 (C–H arom), 2929, 2855 (C–H aliphatic), 1682, 1614 (C=O), 1592, 1562 (C=C); $^1$H-NMR (500 MHz, $CDCl_3$, $\delta$ / ppm): 1.18 (3H, *s*, $NCH_3$), 2.89–3.02 (8H, *m*, $NCH_2$), 7.99–8.88 (4H, *m*, CH arom); $^{13}$C-NMR (125.66 MHz, $CDCl_3$, $\delta$ / ppm) 28.6 ($NCH_3$), 44.7, 44.02 ($NCH_2$), 125.6, 125.9, 127.7, 127.9, 128.5, 128.8, 140.4 (CH arom, C arom), 175.4, 177.5 (C=O); MS (*m*/*z* (relative abundance, %)): 291 (100) $[M+H]^+$.

*2-(Butylthio)-3-(4-methylpiperazin-1-yl)naphthalene-1,4-dione (**17d**)*. Compound **17d** was synthesized in the reaction of **16** (0.50 g, 1.72 mmol) with **4d** (0.15 g, 1.66 mmol) according to general procedure 2.

Yield: 18.15 % (0.071 g); violet oil; $R_f$ (ethyl acetate): 0.73; Anal. Calcd. for $C_{19}H_{24}N_2O_2S$ (*FW*: 344.47): C, 66.25; H, 7.02; N, 8.13; S, 9.31 %. Found: C, 65.96; H, 7.20; N, 7.82; S, 9.21 %; IR (KBr, $cm^{-1}$): 3005 (C–H arom), 2928, 2793 (C–H aliphatic), 1667, 1640 (C=O), 1591, 1563 (C=C); $^1$H-NMR (500 MHz, $CDCl_3$, $\delta$ / ppm): 0.84 (3H, *t*, $J$ = 7.3 Hz, $CH_3$), 1.21–1.24 (4H, *m*, $NCH_2$), 1.32–1.36 (4H, *m*, $NCH_2$), 2.96 (2H, *t*, $J$ = 7.3 Hz, $SCH_2$), 7.63–7.97 (4H, *m*, CH arom); $^{13}$C-NMR (125.66 MHz, $CDCl_3$, $\delta$ / ppm) 17.39 ($CH_3$), 27.52–29.84 ($CH_2$), 39.39 ($SCH_2$), 43.53 ($NCH_3$), 49.61 ($NCH_2$), 122.16, 127.25, 128.24, 128.9, 129.40, 146.51 (CH arom, C arom), 176.5, 177.5 (C=O); MS (*m*/*z* (relative abundance, %)): 345 (100) $[M+H]^+$.

*2-(4-Methylpiperazin-1-yl)-3-(*p*-tolylthio)naphthalene-1,4-dione (**17f**)*. Compound **17f** was synthesized in the reaction of **16** (0.50 g, 1.72 mmol) with **4f** (0.15 g, 0.39 mmol) according to general procedure 2.

Yield: 18.15 % (0.071 g); brown solid; m.p.: 278–279 °C, $R_f$ ($CHCl_3$:ethyl acetate 2:1): 0.73; Anal. Calcd. for $C_{22}H_{22}N_2O_2S$ (*FW*: 378.49): C, 69.81; H, 5.86; N, 7.40; S, 8.47 %. Found: C, 69.29; H, 5.03; N, 7.26; S, 7.36 %; IR (KBr, $cm^{-1}$): 3000 (C–H arom), 2927, 2855 (C–H aliphatic), 1718, 1654 (C=O), 1593, 1491 (C=C); $^1$H-NMR (500 MHz, $CDCl_3$, $\delta$ / ppm): 1.40–1.45 (3H, *m*, $CH_3$), 1.18–2.26 (8H, *m*, $NCH_2$), 7.04–8.01 (4H, *m*, CH arom); $^{13}$C-NMR (125.66 MHz, $CDCl_3$, $\delta$ / ppm) 27.91 (C arom-$CH_3$), 42.8 ($CH_3$), 52.9, 53.21 ($NCH_2$), (C arom-S), 125.78, 126.17, 127.78, 128.24, 128.7, 128.76, 129.1, 129.8, 130.6, 131.2, 132.5, 133.3, 136.8 (CH arom, C arom), 175.3, 176.5 (C=O); MS (*m*/*z* (relative abundance, %)): 379 (100) $[M+H]^+$.

*2-Chloro-3-(3-((dimethylamino)methyl)-1*H*-indol-1-yl)naphthalene-1,4-dione (**19**)*. Compound **19** was synthesized in the reaction of **1** (0.50 g, 2.20 mmol) with **18** (0.38 g, 2.23 mmol) according to general procedure 1.

Yield: 54.82% (0.44 g); red solid; m.p.: 67–68 °C. $R_f$ ($CHCl_3$:petroleum ether 1:1, 40–60 °C): 0.35; Anal. Calcd. for $C_{21}H_{17}N_2O_2$ (*FW*: 364.82): C, 69.14; H, 4.70; N, 8.77 %. Found: C, 68.84; H, 4.62; N, 8.49 %; IR (KBr, $cm^{-1}$):

3020 (C–H arom), 2961, 2926 (C–H aliphatic), 1676, 1643 (C=O), 1593, 1519 (C=C); $^1$H-NMR (500 MHz, $CDCl_3$, $\delta$ / ppm): 3.17 (6H, *s*, $NCH_3$), 3.37 (2H, *s*, $NCH_2$), 7.18 (1H, *s*, CH vin), 7.52–8.07 (8H, *m*, CH arom); $^{13}$C-NMR (125.66 MHz, $CDCl_3$, $\delta$ / ppm) 44.6 ($NCH_3$), 47.05 ($NCH_2$), 120.4, 126.7, 127.8, 129.3, 129.9 131.6, 131.9, 133.1, 133.9, 134.1, 134.4, 135.1, 135.6, 151.1 (CH arom, C arom), 178.1, 182.4 (C=O); MS (*m*/*z* (relative abundance, %)): 366 (100) $[M+H]^+$.

*2-(Butylthio)-3-(3-((dimethylamino)methyl)-1*H*-indol-1-yl)naphthalene-1,4--dione (**20d**)*. Compound **20d** was synthesized in the reaction of **19** (0.050 g, 0.13 mmol) with **4d** (0.012 g, 0.013 mmol) according to general procedure 2.

Yield: 52.24 % (0.03 g); red solid; m.p.: 134–135 °C; $R_f$ ($CHCl_3$): 0.43; Anal. Calcd. for $C_{25}H_{26}N_2O_2S$ (*FW*: 418.55): C, 71.74; H, 6.26; N, 6.69; S, 7.66 %. Found: C,71.58; H, 6.13; N, 6.48; S, 7.46 %; IR (KBr, $cm^{-1}$): 3015 (C–H arom), 2961, 2926, 2871 (C–H aliphatic), 1655, 1592 (C=O), 1459, 1377 (C=C); $^1$H-NMR (500 MHz, $CDCl_3$, $\delta$ / ppm): 0.89 (3H, *t*, *J* = 7.2 Hz, $CH_3$), 1.18–1.55 (4H, *m*, $CH_2$), 2.70 (2H, *t*, *J* = 7.2 Hz, $SCH_2$), 3.37 (6H, *s*, $NCH_3$), 3.40 (2H, *s*, $NCH_2$), 7.19 (H, *s*, CH vin), 7.51–8.08 (8H, *m*, CH arom); $^{13}$C-NMR (125.66 MHz, $CDCl_3$, $\delta$ / ppm) 12.4 ($CH_3$), 22.2 ($\mathbf{C}H_2CH_3$), 30.9 ($SCH_2\mathbf{C}H_2$), 31.5 ($SCH_2$), 32.8 ($NCH_3$), 36.1 ($NCH_2$), 125.3, 125.5, 125.7, 125.8, 125.9, 128.7, 129.6, 130.9, 131.3, 131.7, 132.8, 133.5, 133.9, 143.8 (CH arom, C arom), 179.4, 180.5 (C=O); MS (*m*/*z* (relative abundance, %): 441 (12) $[M+H]^+$.

*2-Chloro-3-((2-(hydroxymethyl)phenyl)amino)naphthalene-1,4-dione (**22**)*. Compound **22** was synthesized in the reaction of **1** (0.50 g, 2.20 mmol) with **21** (0.27 g, 2.19 mmol) according to general procedure 1.

Yield: 58 % (0.4 g); red oil; $R_f$ ($CHCl_3$): 0.32; Anal. Calcd. for $C_{17}H_{12}ClNO_3$ (*FW*: 313.74): C, 65.08; H, 3.86; N, 4.46 %. Found: C, 65.25; H, 4.08; N, 4.29 %; IR (KBr, $cm^{-1}$): 3010 (C–H arom), 3365 (N–H), 2910–2871 (C–H aliphatic), 1674–1606 (C=O), 1568–1505 (C=C); $^1$H-NMR (500 MHz, $CDCl_3$, $\delta$ / ppm): 3.81–3.87 (2H, *m*, $OCH_2$), 4.20 (1H, *m*, OH), 7.01 (1H, *s*, NH), 7.46–8.09 (8H, *m*, CH arom); $^{13}$C-NMR (125.66 MHz, $CDCl_3$, $\delta$ / ppm) 68.4 ($CH_2O$), 108.5, 110, 127, 127.1, 129.1, 132.1, 135.2, 138.5, 143.2, 167.3 (CH arom, C arom), 175.2, 180.8 (C=O); MS (*m*/*z* (relative abundance, %)): 314 (100) $[M+H]^+$.

*2-(2-((Hydroxymethyl)phenyl)amino)-3-(propylthio)naphthalene-1,4-dione (**23c**)*. Compound **23c** was synthesized in the reaction of **22** (0.1 g, 0.31 mmol) with **4c** (0.02 g, 0.026 mmol) according to general procedure 2.

Yield: 81.80 % (0.09 g); pink oil; $R_f$ ($CHCl_3$:Ethyl acetate 3:1): 0.66; Anal. Calcd. for $C_{20}H_{19}NO_3S$ (*FW*: 353.43): C, 67.97; H, 5.42; N, 3.96; S, 9.07 %. Found: C, 67.74; H, 5.28; N, 3.84; S, 8.77 %; IR (KBr, $cm^{-1}$): 3439 (O–H), 3289 (N–H), 3010 (C–H arom), 2962, 2929, 2871 (C–H aliphatic), 1667, 1636 (C=O), 1585, 1548 (C=C); $^1$H-NMR 500 MHz, $CDCl_3$, $\delta$ / ppm): 0.70 (3H, *t*, *J* = 7.3 Hz,

$CH_3$), 1.44 (1H, *bs*, OH), 1.12–1.28 (2H, *m*, $CH_2$), 2.50 (2H, *t*, *J* = 7.3 Hz, $SCH_2$), 4.73 (2H, *s*, $OCH_2$), 6.80 (1H, *s*, NH), 7.57–8.08 (8H, *m*, CH arom); $^{13}$C-NMR (125.66 MHz, $CDCl_3$, $\delta$ / ppm) 21.9 ($CH_3$), 28.6 ($SCH_2$**C**$H_2$), 34.5 ($SCH_2$), 63.0 ($CH_2O$), 121.8, 123.3, 125.6, 125.8, 126.5, 127.1, 127.8, 129.8, 130.5, 131.7, 132.5, 133.4, 137.4, 144.8 (CH arom, C arom), 179.4, 180.0 (C=O); MS (*m*/*z* (relative abundance, %)): 354 (100) $[M+H]^+$.

*2-(Butylthio)-3-((2-(hydroxymethyl)phenyl)amino)naphthalene-1,4-dione (**23d**)*. Compound **23d** was synthesized in the reaction of **22** (0.10 g, 0.31 mmol) with **4d** (0.020 g, 0.022 mmol) according to general procedure 2.

Yield: 81.80 % (0.09 g); pink oil; $R_f$ ($CHCl_3$:ethyl acetate 3:1): 0.36; Anal. Calcd. for $C_{21}H_{21}NO_3S$ (*FW*: 367.46): C, 68.64; H, 5.76; N, 3.81, S, 8.73 %. Found: C, 68.52; H, 5.94; N, 3.97, S, 8.52 %; IR (KBr, $cm^{-1}$): 3293 (N–H), 3011 (C–H arom), 2958, 2929, 2872 (C–H aliphatic), 1667, 1636 (C=O), 1586, 1548 (C=C); $^1$H-NMR (500 MHz, $CDCl_3$, $\delta$ / ppm): 0.74 (3H, *t*, *J* = 7.3 Hz, $CH_3$), 1.44 (1H, *bs*, OH), 1.18–1.24 (4H, *m*, $CH_2$), 2.49 (2H, *t*, *J* = 7.3 Hz, $SCH_2$), 4.74 (2H, *s*, $OCH_2$), 6.85 (1H, *s*, NH), 7.57–8.08 (8H, *m*, CH arom); $^{13}$C-NMR (125.66 MHz, $CDCl_3$, $\delta$ / ppm) 20.7 ($CH_3$), 28.6 ($SCH_2CH_2$**C**$H_2$), 30.6 ($SCH_2$**C**$H_2$), 32.2 ($SCH_2$), 63.0 ($CH_2O$), 117.7 121.8, 123.2, 125.6, 125.8, 127, 127.7, 128.7, 129.8, 130.5, 132.5, 133.3, 144.7 (CH arom, C arom), 179.4, 180.0 (C=O); MS (*m*/*z* (relative abundance, %)): 366 (100) $[M+H]^+$.

*2-Chloro-3-(*N*-(2-hydroxyethyl)-*N*-phenylamino)naphthalene-1,4-dione (**25**)*. Compound **25** was synthesized in the reaction of **1** (1 g, 4.404 mmol) with **24** (0.64 g, 4.40 mmol) according to general procedure 1.

Yield: 45.18% (0.65 g); violet oil; $R_f$ ($CHCl_3$): 0.45; Anal. Calcd. for $C_{18}H_{14}ClNO_3$ (*FW*: 327.76): C, 65.96; H, 4.31; N, 4.27 %. Found: C, 65.68; H, 4.62; N, 4.44 %; IR (KBr, $cm^{-1}$): 3330 (OH), 3067 (C–H arom), 2940, 2880 (C–H aliphatic), 1731, 1674 (C=O), 1593, 1557 (C=C); $^1$H-NMR (500 MHz, $CDCl_3$, $\delta$ / ppm): 1.20 (1H, *s*, OH), 3.80 (2H, *t*, *J* = 6.8 Hz, $NCH_2$), 4.01(2H, *t*, *J* = 6.8 Hz, $OCH_2$), 7.25–8.14 (9H, *m*, CH arom); $^{13}$C-NMR (125.66 MHz, $CDCl_3$, $\delta$ / / ppm) 52.5 ($NCH_2$), 60.1 ($CH_2O$), 116.8, 126.6, 127.9, 128, 128.1, 128.3, 130.6, 132.7, 133, 133.1, 133.4, 144.8, 147.2 (CH arom, C arom), 177.0, 181.1 (C=O); MS (*m*/*z* (relative abundance, %)): 327 (100) $[M]^+$.

*2-Chloro-3-((2-(diethylamino)ethyl)amino)naphthalene-1,4-dione (**27**)*. Compound **27** was synthesized in the reaction of **1** (1 g, 4.40 mmol) with **26** (0.51 g, 4.38 mmol) according to general procedure 1.

Yield: 70% (0.95 g); yellow solid; m.p.: 86–87 °C (Lit. for **27**·HCl m.p.: 242 °C[4]); $R_f$ ($CHCl_3$): 0.44; Anal. Calcd. for $C_{16}H_{19}ClN_2O_2$ (*FW*: 306.11): C, 62.64; H, 6.24; N, 9.13 %. Found: C, 62.82; H, 6.36; N, 9.23 %; IR (KBr, $cm^{-1}$): 3267 (N–H), 3002 (C–H arom), 2966, 2931, 2887 (C–H aliphatic), 1682, 1639 (C=O), 1594, 1576 (C=C),; $^1$H-NMR (500 MHz, $CDCl_3$, $\delta$ / ppm): 0.81–0.84 (6H, *m*, $CH_3$), 3.75–3.79 (8H, *m*, $NHCH_2$), 7.53–8.09 (4H, *m*, CH arom); $^{13}$C-

-NMR (125.66 MHz, $CDCl_3$, $\delta$ / ppm) 10.9 ($CH_3$), 40.8 (NH–$CH_2$), 50.5 (N**C**$H_2CH_3$), 65.9 ($NCH_2$), 108.7, 158.4, 125.6, 131.2, 133.6 (CH arom, C arom), 183.6, 179.8 (C=O); MS (*m*/*z* (relative abundance, %)): 309 (100) $[M+H]^+$.

*2-(Butylthio)-3-((2-(diethylamino)ethyl)amino)naphthalene-1,4-dione (**28d**)*. Compound **28d** was synthesized in the reaction of **27** (0.1 g, 0.24 mmol) with **4d** (0.021 g, 0.058 mmol) according to general procedure 1.

Yield: 75 % (0.06 g); red oil; $R_f$ (methanol): 0.56; Anal. Calcd. for $C_{20}H_{28}N_2O_2S$ (*FW*: 360.51): C, 66.63; H, 7.83; N, 7.77; S, 8.89 %. Found: C, 66.87; H, 7.92; N, 7.69; S, 8.76 %; IR (KBr, $cm^{-1}$): 3266 (N–H), 3096 (C–H arom), 2959, 2927, 2871 (C–H aliphatic), 1673, 1628 (C=O), 1592, 1557 (C=C); $^1$H-NMR (500 MHz, $CDCl_3$, $\delta$ / ppm): 0.80 (3H, *t*, *J* = 7.3 Hz, $CH_3$), 0.86 (6H, *t*, *J* = 7.3 Hz, $CH_3$), 1.00–1.29 (4H, *m*, $CH_2$), 1.30–1.37 (1H, *m*, NH), 2.64 (2H, *t*, *J* = 7.3 Hz, $SCH_2$), 2.72 (6H, *t*, $NCH_2$), 3.90 (1H, *bs*, NH), 7.64–8.07 (4H, *m*, CH arom); $^{13}$C-NMR (125.66 MHz, $CDCl_3$, δ / ppm) 12.6, 13.1 ($CH_3$), 31.0, 21.6 ($CH_2$), 37.8 ($SCH_2$), 42.0 ($NHCH_2$), 45.4, 50.6 ($NCH_2$), 125.2, 125.5, 130.8, 132.9, 133 (CH arom, C arom), 179.2, 180.7 (C=O); MS (*m*/*z* (relative abundance, %)): 361 (100)) $[M+H]^+$.

*2-(2-((Diethylamino)ethyl)amino)-3-(octylthio)naphthalene-1,4-dione (**28e**)*. Compound **28e** was synthesized in the reaction of **27** (0.50 g, 1.62 mmol) with **4e** (0.23 g, 1.57 mmol) according to general procedure 1.

Yield: 65 % (0.44 g); red oil; $R_f$ ($CHCl_3$): 0.87; Anal. Calcd. for $C_{24}H_{36}N_2O_2S$ (*FW*: 416.62): C, 69.19; H, 8.71; N, 6.72; S, 7.70 %. Found: C, 68.98; H, 9.02; N, 6.51; S, 7.54 %; IR (KBr, $cm^{-1}$): 3258 (N–H), 3065 (C–H arom), 2956, 2925, 2853 (C–H aliphatic), 1673, 1630 (C=O), 1592, 1552 (C=C); $^1$H-NMR (500 MHz, $CDCl_3$, $\delta$ / ppm): 0.77–0.87 (9H, *m*, $CH_3$), 1.01–1.20 (12H, *m*, ($CH_2$), 2.61 (2H, *t*, *J* = 7.2 Hz, $SCH_2$), 2.72 (6H, *t*, *J* = 7.2 Hz, $NCH_2$), 3.90 (1H, *bs*, NH), 7.63–8.07 (4H, *m*, CH arom); $^{13}$C-NMR (125.66 MHz, $CDCl_3$, $\delta$ / / ppm) 13.05, 13.07 ($CH_3$), 21.6, 28.2, 28.6, 28.9, 30.3, 30.7 ($CH_2$), 38.2 ($SCH_2$), 42.0 ($NHCH_2$), 45.4, 50.6, (N**C**$H_2$), 125.2, 125.5, 129.8, 130.8, 132.2, 132.9, 133.3, 137.1 (CH arom, C arom), 179.1, 180.6 (C=O); MS (*m*/*z* (relative abundance, %)): 417 (100) $[M+H]^+$.

## REFERENCES


1. N. P. Buu-Hoi, P. Jacquigenon, N. D. Xuong, V. T. Suu, *J. Chem. Soc.* (1958) 2815
2. A. P. Kartoflitskaya, N. R. Gladun, L. D. Bolibruk, G. I. Zokhnyk, *Zh. Org. Khim.* **32** (1996) 1429
3. B. Prescott, *J. Med. Chem.* **12** (1969) 181
4. R. K. Y. Zee-Cheng, E. G. Podrebarac, C. S. Menon, C. C. Cheng, *J. Med. Chem.* **22** (1979) 501.

Journal of the Serbian Chemical Society
JSCS-info@shd.org.rs • www.shd.org.rs/JSCS
*J. Serb. Chem. Soc. 80* (6) 739–747 (2015)
*JSCS–4753*
UDC 547.821–116+547.828–116+542.913+547.587.51:615.28–188
*Original scientific paper*

# Synthesis of modified pyridine and bipyridine substituted coumarins as potent antimicrobial agents

HEMALI B. LAD, RAKESH R. GIRI, YOGITA L. CHOVATIYA and DINKAR I. BRAHMBHATT*

*Department of Chemistry, Sardar Patel University, Vallabh Vidyanagar 388120, Gujarat, India*

(Received 4 August 2014, revised 8 January, accepted 11 January 2015)

*Abstract*: In the search for new antimicrobial agents, a series of new modified pyridine and bipyridine substituted coumarins **5a**–**y** was designed and synthesized by adopting a molecular hybridization strategy. All the synthesized compounds were evaluated for their *in vitro* antimicrobial activity using the broth dilution method against selected bacterial (Gram-positive and Gram-negative) and fungal strains. Compounds **5a**, **5f**, **5g**, **5n**, **5r**, **5t**, **5w**, **5x** and **5y** demonstrated promising antibacterial activity, while the other derivatives showed comparable activity to those of the standard drugs used as references.

*Keywords*: coumarins; bipyridines; Krohnke reaction; antimicrobial activity; broth dilution method.

## INTRODUCTION

In recent years, the mounting threat of bacterial resistance has heightened the urgency to discover and develop effective agents with novel mechanisms of action and enhanced activity profiles. Considerable research efforts have been directed to the discovery of high potency local antimicrobial agents with reduced or without systemic adverse effects. The development of potent and effective antimicrobial agents is of utmost importance to overcome the emerging multi-drug resistance strains of bacteria and fungi.

A large number of heterocyclic substituted and heterocyclic fused coumarin derivatives has drawn immense attention among medicinal chemists as they exhibit several significant biological activities, such as anti-alzheimer,[1] antimalarial,[2] anticancer,[3] antioxidant,[4] antitumor,[5] anti-inflammatory,[6] antipyretic,[7] analgesic,[7] antimicrobial,[8] *etc*. Among the heterocyclic-substituted coumarins, pyridine-substituted coumarins constitute an elite class of compounds as they exhibit important biological activities, such as CNS depressant,[9] antifungal,[10] antibacterial,[11] antitubercular,[12] *etc*. During a literature survey, some modified

* Corresponding author. E-mail: drdib317@gmail.com
doi: 10.2298/JSC140804004L

pyridine nuclei emerged, such as cyclopenta[*b*]pyridine, 5,6,7,8-tetrahydroquinoline and indeno[1,2-*b*]pyridine, which are endowed with antiproliferative,[13] anti-inflammatory,[14,15] antimicrobial,[16,17] anticancer,[18] antidiabetic,[19] antiplasmodial,[20] anti-alzheimer,[21] cytotoxic,[22] calcium antagonistic,[23] and bovine liver glutathione-*S*-transferase inhibitory activities.[24] Certain bipyridinyl moieties are reported to possess important biological properties, such as antimicrobial,[25] antioxidant,[25] cardiotonic,[26] DNA interacting[27] and cytotoxic[27]. In a literature search, it was observed that hitherto no significant efforts have been made to synthesize coumarin derivatives incorporating such modified pyridine nuclei (cyclopenta[*b*]pyridine, 5,6,7,8-tetrahydroquinoline and indeno[1,2-*b*]pyridine) and to study their biological properties. Encouraged by potential biological activities of modified pyridines and in continuation of previous investigation on biopotent coumarin derivatives,[28] the present efforts were focused on the design and synthesis of biologically potent heterocyclic system *via* the combination of the therapeutically active moieties coumarin and modified pyridine nuclei together in a single scaffold.

## RESULTS AND DISCUSSION

### *Chemistry*

The strategy adopted for the synthesis of the key precursors **3a**–**e** and the target compounds is depicted in Scheme 1. The coumarin chalcones **3a**–**e** were synthesized by reacting 8-acetyl-7-hydroxy-4-methylcoumarin **1** with various benzaldehydes **2a**–**e** in ethanol containing piperidine in a catalytic amount.

The synthesis of title compounds **5a**–**y** was realized by reacting coumarin chalcones **3a**–**e** with cyclopentanone **4a**, cyclohexanone **4b**, indanone **4c** and (pyridinecarbonylmethyl)pyridinium iodide salts **4d** and **4e** under Krohnke reaction condition.[29] The reaction proceeded *via* a Michael addition by the nucleophilic addition of active methylene group in **4a**–**e** to the $\alpha,\beta$-unsaturated carbonyl functionality in **3a**–**e** to afford the 1,5-dicarbonyl intermediates. The corresponding intermediate undergoes cyclization in presence of ammonia and subsequent loss of water afforded target compounds **5a**–**y**.

The analytic and spectroscopic data of all the synthesized compounds are given in the Supplementary material to this paper.

### *Evaluation of antimicrobial activity*

The antimicrobial activity of the synthesized compounds **5a**–**y** was determined by the broth dilution method as described by NCCLS.[30] The antibacterial activity was screened against two Gram-positive (*Staphylococcus aureus* MTCC 96 and *Bacillus subtilis* MTCC 441) and two Gram-negative (*Escherichia coli* MTCC 443 and *Salmonella enterica* subsp. *enterica* serovar typhi MTCC 98) bacteria using ampicillin, ciprofloxacin and chloramphenicol as standard antibacterial drugs. Antifungal activity was screened against two fungal species

(*Candida albicans* MTCC 227 and *Aspergillus niger* MTCC 282) where griseofulvin and nystatin were used as the standard antifungal drugs. The antimicrobial activity data are presented in Table I.

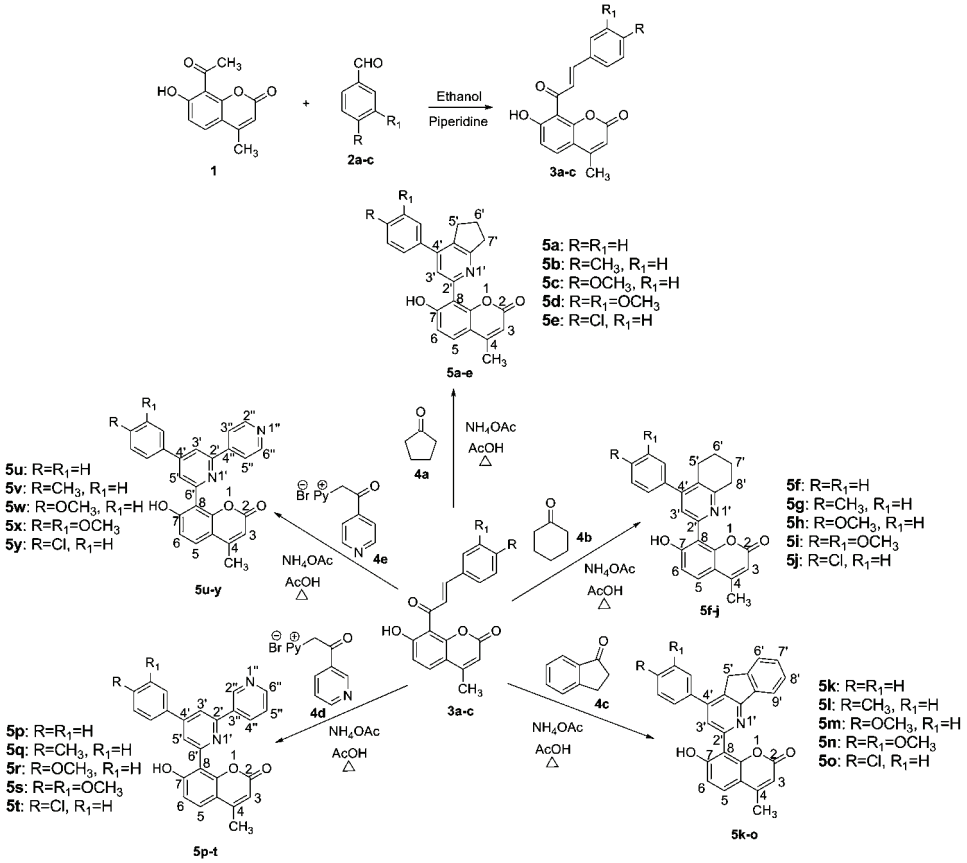


Scheme 1. Strategy adopted for the synthesis of the precursors **3a**–**e** and the target compounds **5a**–**y**.

All the newly synthesized compounds **5a**–**y** exerted significant inhibitory activity against all the employed strains. The antimicrobial assessment data of compounds **5a**–**y** revealed that compounds **5n** and **5w** (*MIC* = 50 μg mL$^{-1}$); compounds **5a** and **5x** (*MIC* = 62.5 μg mL$^{-1}$) exhibited excellent activity against *S. aureus* compared to ampicillin (*MIC* = 250 μg mL$^{-1}$) and comparable activity to chloramphenicol and ciprofloxacin (*MIC* = 50 μg mL$^{-1}$). In addition, compounds **5d**, **5f**, **5g**, **5i** and **5r** (*MIC* = 100 μg/mL) also showed significant activity against *S. aureus* compared to ampicillin (*MIC* = 250 μg mL$^{-1}$). Against *B. subtilis*, compound **5f** (*MIC* = 50 μg mL$^{-1}$) demonstrated remarkable activity compared to ampicillin (*MIC* = 250 μg mL$^{-1}$) and was equipotent to chloramphenicol

and ciprofloxacin (*MIC* = 50 μg $mL^{-1}$). Compounds **5a**, **5j** and **5n** (*MIC* = 100 μg $mL^{-1}$) also showed superior activity to ampicillin (*MIC* = 250 μg $mL^{-1}$) against *B. subtilis*. Compound **5r** (*MIC* = 12.5 μg $mL^{-1}$) depicted excellent activity against *E. coli* compared to all the drugs used as standards. Compounds **5t**, **5y** (*MIC* = 50 μg $mL^{-1}$) and **5g** (*MIC* = 62.5 μg $mL^{-1}$) showed excellent activity compared to ampicillin (*MIC* = 100 μg $mL^{-1}$) and comparable activity to chloramphenicol and ciprofloxacin (*MIC* = 50 μg $mL^{-1}$) against *E. coli*. Against *S. typhi*, compound **5r** (*MIC* = 50 μg $mL^{-1}$) and **5g** (*MIC* = 62.5 μg $mL^{-1}$) showed significant activity compared to ampicillin (*MIC* = 100 μg $mL^{-1}$) and comparable activity to chloramphenicol (*MIC* = 50 μg $mL^{-1}$).

TABLE I. Antimicrobial activity (*MIC* / μg $mL^{-1}$) of compounds **5a–y**; AMP: ampicillin, CHL: chloramphenicol, CIP: ciprofloxacin, GRIS: griseofulvin, NYT: nystatin. –: not tested

| Compd. | Gram-positive bacteria | | Gram-negative bacteria | | Fungi | |
|---|---|---|---|---|---|---|
| | *S. aureus* MTCC 96 | *B. subtilis* MTCC 441 | *E. coli* MTCC 443 | *S. enterica* MTCC 98 | *C. albicans* MTCC 227 | *A. niger* MTCC 282 |
| **5a** | 62.5 | 100 | 100 | 200 | 1000 | 1000 |
| **5b** | 500 | 500 | 500 | 500 | 500 | 1000 |
| **5c** | 500 | 250 | 250 | 250 | 1000 | 500 |
| **5d** | 100 | 250 | 100 | 200 | 250 | >1000 |
| **5e** | 250 | 500 | 500 | 500 | 500 | 1000 |
| **5f** | 100 | 50 | 200 | 200 | >1000 | >1000 |
| **5g** | 100 | 250 | 62.5 | 62.5 | 1000 | 1000 |
| **5h** | 250 | 250 | 250 | 500 | 500 | 1000 |
| **5i** | 100 | 200 | 250 | 100 | >1000 | >1000 |
| **5j** | 250 | 100 | 500 | 500 | 500 | 500 |
| **5k** | 250 | 250 | 100 | 200 | >1000 | 500 |
| **5l** | 250 | 500 | 100 | 250 | 500 | 500 |
| **5m** | 200 | 500 | 100 | 100 | 1000 | >1000 |
| **5n** | 50 | 100 | 250 | 250 | 250 | 250 |
| **5o** | 250 | 200 | 250 | 500 | >1000 | 250 |
| **5p** | 500 | 250 | 100 | 200 | 250 | 1000 |
| **5q** | 250 | 250 | 250 | 250 | 1000 | >1000 |
| **5r** | 100 | 200 | 12.5 | 50 | 500 | 1000 |
| **5s** | 500 | 200 | 100 | 100 | >1000 | 200 |
| **5t** | 250 | 200 | 50 | 200 | 1000 | >1000 |
| **5u** | 250 | 500 | 250 | 200 | 1000 | 500 |
| **5v** | 500 | 250 | 100 | 250 | 500 | 1000 |
| **5w** | 50 | 500 | 200 | 500 | 1000 | >1000 |
| **5x** | 62.5 | 250 | 200 | 100 | 500 | 1000 |
| **5y** | 200 | 250 | 50 | 100 | 1000 | 1000 |
| AMP | 250 | 250 | 100 | 100 | – | – |
| CHL | 50 | 50 | 50 | 50 | – | – |
| CIP | 50 | 50 | 25 | 25 | – | – |
| GRIS | – | – | – | – | 100 | 100 |
| NYT | – | – | – | – | 500 | 100 |

Compounds **5m** and **5y** (*MIC* = 200 μg $mL^{-1}$) showed better activity, while compounds **5e**, **5h**, **5j**, **5k**, **5l**, **5o**, **5q**, **5t** and **5u** (*MIC* = 250 μg $mL^{-1}$) were found equipotent compared to ampicillin (*MIC* = 250 μg $mL^{-1}$) against *S. aureus*. Compounds **5i**, **5o**, **5r**, **5s** and **5t** (*MIC* = 200 μg $mL^{-1}$) exhibited better activity and compounds **5c**, **5d**, **5g**, **5h**, **5k**, **5p**, **5q**, **5v**, **5x** and **5y** (*MIC* = 250 μg $mL^{-1}$) were found equipotent to ampicillin (*MIC* = 250 μg $mL^{-1}$) against *B. subtilis*. Compounds **5a**, **5d**, **5k**, **5l**, **5m**, **5p**, **5s** and **5v** (*MIC* = 100 μg $mL^{-1}$) against *E. coli* and compounds **5i**, **5m**, **5s**, **5x** and **5y** (*MIC* = 100 μg $mL^{-1}$) against *S. enterica* subsp. *enterica* serovar typhi were found equipotent to ampicillin (*MIC* = 100 μg $mL^{-1}$).

A close look at the SAR (structure–activity relationship) of these compounds clearly indicated the influence of peripheral substituents on the aryl ring (*i.e.*, R and $R_1$) and the nature of the pyridine moiety on antimicrobial potency. It is interesting to note that almost all the compounds **5a**–**y** possessed promising antibacterial activity against Gram-positive bacteria *B. subtilis* and *S. aureus*. In the case of compounds **5a**–**e** bearing cyclopenta[*b*]pyridine moiety, introduction of electron donating group, *i.e.*, compounds **5b** (R = $CH_3$) and **5c** (R = $OCH_3$), reduced the antibacterial activity significantly. Upon introduction of a second methoxyl group, *i.e.*, compound **5d** (R = $R_1$= $OCH_3$), enhanced the antibacterial activity against *S. aureus*. Replacement of cyclopenta[*b*]pyridine moiety with 5,6,7,8-tetrahydroquinoline moiety boosts the antibacterial potency against all the bacterial strains. The enhancement in the antibacterial activity of the compounds **5f**–**j** may be attributed to the increased lipophilicity due to insertion of an additional –$CH_2$– group in the modified pyridine moiety than those of compounds **5a**–**e**. In compounds **5f**–**j**, altering the substitution on the appended aryl ring did not affect the activity against *S. aureus* but it reduced the activity against *B. subtilis*. Introduction of methyl group, *i.e.*, compound **5g** (R = $CH_3$), remarkably intensified the antibacterial potency against Gram-positive bacterial strains, which may be credited to further enhancement in lipophilicity. A marked reduction in the antibacterial potency against the Gram-positive bacteria *B. subtilis* was observed when the pyridine moiety was modified to indeno[1,2-*b*]pyridine, *i.e.*, compounds **5k**–**o**, but the antibacterial potency was appreciably enhanced against *E. coli*.

Surprisingly, upon replacement of the modified pyridine moiety with bipyridine, *i.e.*, compounds **5p**–**y**, the antibacterial effectiveness increased significantly. In fact, compound **5r** (*MIC* = 12.5 μg $mL^{-1}$) emerged as the most potent derivative of the series. In addition, compounds **5t**, **5w**, **5x** and **5y** exhibited appreciable antibacterial activity. The compounds bearing a bipyridine moiety with a 2-3′ linkage (compounds **5p**–**t**) depicted better antibacterial potency than compounds with a 2-4′ linkage (compounds **5u–y**). Among the compounds **5p–y**, derivatives bearing two methoxyl group or a chlorine group, *i.e.*, compounds **5s**,

**5x** (R = $R_1$ = $OCH_3$), **5t** and **5y** (R = Cl) showed better activity than the other analogs. The compounds **5p**–**y** bearing a bipyridine moiety, exhibited enhanced antibacterial activity compared to compounds **5a**–**o** bearing a modified pyridine moiety.

The antifungal screening data (Table I) revealed that compounds **5d**, **5n** and **5p** (*MIC* = 250 μg $mL^{-1}$); compounds **5b**, **5e**, **5h**, **5j**, **5l**, **5r**, **5v** and **5x** (*MIC* = = 500 μg $mL^{-1}$) showed comparable activity to griseofulvin against *C. albicans*. None of the compounds showed promising antifungal activity against *A. niger*.

## EXPERIMENTAL

All reactions were performed with commercially available reagents and they were used without further purification. Organic solvents were purified by standard methods and stored over molecular sieves. All reactions were monitored by thin-layer chromatography (TLC, on aluminum plates coated with silica gel 60 $F_{254}$, 0.25 mm thickness, Merck) and detection of the components was made by exposure to UV light. The compounds were purified by column chromatography using silica gel (60–120 mesh). Melting points were determined in open capillaries and are uncorrected. IR spectra were recorded on a Shimadzu FTIR 8401 spectrophotometer using potassium bromide pellets in the range 4000–400 $cm^{-1}$ and frequencies of only characteristic peaks are expressed in $cm^{-1}$. $^1$H- and $^{13}$C-NMR spectra were recorded on a Bruker Avance 400 (MHz) spectrometer (Bruker Scientific Corporation Ltd., Switzerland) operating at 400 MHz and 100 MHz, respectively. Chemical shifts are reported in parts per million (ppm) using $CDCl_3$ as solvent and calibrated with the standard solvent signal. The coupling constants (*J*) are given in Hertz (Hz). Mass spectra of representative compounds were scanned on a Shimadzu QP 2010 spectrometer (Shimadzu, Tokyo, Japan). The precursors 8-acetyl-7-hydroxy-4-methylcoumarin **1**,[31] 8-(3-arylacryloyl)-7-hydroxy-4-methyl--chromen-2-ones **3a**, **3c** and **3d**,[32] (pyridinecarbonylmethyl)pyridinium iodide salts **4d** and **4e**[33] were prepared using reported procedures.

### *General procedure for the synthesis of **5a**–**y***

In a 100-mL round bottom flask equipped with a condenser, guard tube and magnetic needle, an appropriate active methylene compound **4a**–**e** (*i.e.*, cyclopentanone **4a**, cyclohexanone **4b**, 1-indanone **4c**, (pyridinecarbonylmethyl)pyridinium iodide salts **4d** and **4e** (0.003 mol) in glacial acetic acid (15mL) was taken. To this, ammonium acetate (0.03 mol) was added under stirring at room temperature. Then a solution of an appropriate 8-(3-arylacryloyl)-7-hydroxy-4-methyl-chromen-2-ones **3a**–**e** (0.003 mol) in glacial acetic acid (15 mL) was added under stirring and the reaction mixture was further stirred for 1 h at room temperature and then refluxed for 8 h at 140 °C. The mixture was then allowed to cool to room temperature and then poured into ice-cold water (75 mL). The crude solid obtained was extracted with chloroform (3×30 mL). The organic layer was washed with 5 % sodium bicarbonate solution (3×20 mL) and water (2×20 mL), and dried over anhydrous sodium sulfate. The removal of chloroform under reduced pressure gave a crude material that was subjected to column chromatography using silica gel and chloroform–petroleum ether (60–80, 1:4) as the eluent to give the targeted compounds **5a**–**y**.

### *Biological assay*

The *in vitro* antimicrobial activities of all the compounds and standard drugs were assessed against Gram-positive bacteria, *viz. Staphylococcus aureus* (MTCC 96) and *Bacillus*

*subtilis* (MTCC 441), Gram-negative bacteria, *viz.*, *Salmonella enterica* subsp. *enterica* serovar typhi (MTCC 98) and *Escherichia coli* (MTCC 443) and two fungi, *viz.*, *Aspergillus niger* (MTCC 282) and *Candida albicans* (MTCC 227) by the broth microdilution *MIC* (Minimum inhibitory concentration) method according to NCCLS (National Committee for Clinical Laboratory Standards). The employed strains were procured from (MTCC – micro type culture collection) Institute of Microbial Technology, Chandigarh. Mueller–Hinton Broth was used as the nutrient medium to grow and dilute the compound suspension for the test bacteria and Sabouraud dextrose broth was used for fungal nutrition. Ampicillin, chloramphenicol and ciprofloxacin were used as standard antibacterial drugs, while griseofulvin and nystatin were used as standard antifungal drugs. The bacterial strains were primarily inoculated into Mueller–Hinton agar and, after overnight growth, a number of colonies were directly suspended in saline solution until the turbidity matched the turbidity of the McFarland standard (approximately $10^8$ CFU $mL^{-1}$). *i.e.*, the inoculum size for test strain was adjusted to $10^8$ CFU $mL^{-1}$ (colony forming unit) per milliliter well by comparing the turbidity (turbidimetric method). Similarly, the fungi were inoculated on Sabouraud dextrose broth; the procedures of inoculum standardization were also similar. DMSO was used as diluent to obtain the desired concentration of the synthesized compounds and the standard drugs for the test upon the standard microbial strains, *i.e.*, the compounds were dissolved in DMSO and the solutions were diluted with a culture medium. Each compound and standard drug was diluted to obtain 2000 μg $mL^{-1}$ stock solutions. By further progressive dilutions with the test medium, the required concentrations were obtained for primary and secondary screening. In primary screening, 1000, 500, and 250 μg $mL^{-1}$ concentrations of the synthesized compounds were taken. The active compounds found in this primary screening were further diluted to obtain 200, 100, 62.5, 50, 25, 12.5 and 6.25 μg $mL^{-1}$ concentrations for secondary screening to test in a second set of dilution against all microorganisms. Briefly, the control tube containing no antibiotic was immediately sub-cultured (before inoculation) by spreading a loopful evenly over a quarter of a plate of medium suitable for the growth of the test organism. The tubes were then incubated at 37 °C for 24 h for the bacteria and 48 h for the fungi. Growth or a lack of growth in the tubes containing the antimicrobial agent was determined by comparison with the growth control, indicated by turbidity. The lowest concentration that completely inhibited visible growth of the organism was recorded as the minimum inhibitory concentration (*MIC* / μg $mL^{-1}$), *i.e.*, the amount of growth from the control tube before incubation (which represents the original inoculum) was compared. A set of tubes containing only seeded broth and the solvent controls were maintained under identical conditions to ensure that the solvent had no influence on strain growth. The protocols are summarized in Table I as the minimum inhibitory concentration (*MIC* / μg $mL^{-1}$).

## CONCLUSIONS

In conclusion, a series of modified pyridine and bipyridine substituted coumarins, which emerged as a new and important class of antimicrobial agents, was successfully designed and synthesized. The results revealed the positive contribution of methoxyl substituents at the *meta* and *para* positions of the phenyl ring to the observed antimicrobial activity. The results also indicated that coumarins bearing the bipyridine moiety showed marked enhancement in their antibacterial activity than those bearing a modified pyridine moiety. It is believed that the

observed results may be useful in guiding future global efforts to discover new compounds with improved antimicrobial activity.

## SUPPLEMENTARY MATERIAL

General procedure for the synthesis of **3a**–**e** and physical, analytical and spectral data of the synthesized compounds **5a**–**y** are available electronically from http://www.shd.org.rs/JSCS/, or from the corresponding author on request.

*Acknowledgements*. The authors are thankful to the Head of Department of Chemistry, Sardar Patel University, for providing research amenities. Financial assistance to the authors from the University Grants Commission, New Delhi, India, is highly acknowledged.

## ИЗВОД

## СИНТЕЗА ДЕРИВАТА КУМАРИНА СУПСТИТУИСАНИХ МОДИФИКОВАНИМ ПИРИДИНИМА И БИПИРИДИНИМА КАО ПОТЕНЦИЈАЛНИХ АНТИМИКРОБНИХ АГЕНАСА

HEMALI B. LAD, RAKESH R. GIRI, YOGITA L. CHOVATIYA и DINKAR I. BRAHMBHATT

*Department of Chemistry, Sardar Patel University, Vallabh Vidyanagar 388120, Gujarat, India*

Током истраживања нових антимикробних агенаса синтетисана је серија деривата кумарина **5a**–**y** супституисаних модификованим пиридинима и бипиридинима. Свим синтетисаним дериватима испитана је антимикробна активност применом методе разблаживања у бујону (*broth dilution method*) према одабраним сојевима бактерија (грам-позитивне и грам-негативне) и гљива. Једињења **5a**, **5f**, **5g**, **5n**, **5r**, **5t**, **5w**, **5x** и **5y** показују значајне антибактеријске активности, док преостали деривати имају активности блиске стандардним лековима.

(Примљено 4. августа 2014, ревидирано 8. јануара, прихваћено 11. јануара 2015)

## REFERENCES

1. P. Anand, B. Singh, N. Singh, *Bioorg. Med. Chem.* **20** (2012) 1175
2. K. V. Sashidhara, A. Kumar, R. Dodda, N. Krishna, P. Agarwal, K. Srivastava, S. K. Puri, *Bioorg. Med. Chem. Lett.* **22** (2012) 3926
3. J. T. Konc, E. Hejchman, H. Kruszewska, I. Wolska, D. Maciejewska, *Eur. J. Med. Chem.* **46** (2011) 2252
4. N. S. Radulović, G. A. Bogdanović, P. D. Blagojević, V. S. Dekić, R. D. Vukićević, *J. Chem. Crystallogr.* **41** (2011) 545
5. S. Cosconati, A. Rizzo, R. Trotta, B. Pagano, S. Iachettini, S. De Tito, I. Lauri, I. Fotticchia, M. Giustiniano, L. Marinelli, C. Giancola, E. Novellino, A. Biroccio, A. Randazzo, *J. Med. Chem.* **55** (2012) 9785
6. K. V. Sashidhara, M. Kumar, R. Modukuria, R. Sonkar, G. Bhatia, A. K. Khanna, S. Rai, R. Shukla, *Bioorg. Med. Chem. Lett.* **21** (2011) 4480
7. S. Khode, V. Maddi, P. Aragade, M. Palkar, P. K. Ronad, S. Mamledesai, A. Thippeswamy, D. Satyanarayana, *Eur. J. Med. Chem.* **44** (2009) 1682
8. N. M. Sabry, H. M. Mohamed, A. E. H. Khattab, S. S. Motlaq, A. M. El-Agrody, *Eur. J. Med. Chem.* **46** (2011) 765
9. R. B. Moffett, *J. Med. Chem.* **7** (1964) 446
10. S. Sardari, Y. Mori, K. Horita, R. G. Micetich, S. Nishibe, M. Daneshtalab, *Bioorg. Med. Chem.* **7** (1999) 1933

11. J. N. Modranka, E. Nawrot, J. Graczyk, *Eur. J. Med. Chem.* **41** (2006) 1301
12. V. G. Bhila, C. V. Patel, N. H. Patel, D. I. Brahmbhatt, *Med. Chem. Res.* **22** (2013) 4346
13. M. M. Ghorab, F. A. Ragab, M. M. Hamed, *Eur. J. Med. Chem.* **44** (2009) 4211
14. K. L. Kees, T. M. Smith, M. L. McCaleb, D. H. Prozialeck, R. S. Cheeseman, T. E. Christos, W. C. Patt, K. E. Steiner, *J. Med. Chem.* **35** (1992) 944
15. M. Yu. Gavrilov, L. G. Mardanova, V. E. Kolla, M. E. Konshin, *Pharm. Chem. J.* **22** (1988) 554
16. A. Altundas, S. Ayvaz, E. Logoglu, *Med. Chem. Res.* **20** (2011) 1
17. M. A. Patel, V. G. Bhila, N. H. Patel, A. K. Patel, D. I. Brahmbhatt, *Med. Chem. Res.* **21** (2012) 4381
18. I. Jacquemond-Collet, F. Benoit-Vical, A. Valentin, E. Stanislas, M. Mallié, I. Fourasté, *Planta Med.* **68** (2002) 68
19. S. Rizzo, A. Bisi, M. Bartolini, F. Mancini, F. Belluti, S. Gobbi, V. Andrisano, A. Rampa, *Eur. J. Med. Chem.* **46** (2011) 4336
20. R. Miri, K. Javidnia, B. Hemmateenejad, A. Azarpirab, Z. Amirghofranc, *Bioorg. Med. Chem.* **12** (2004) 2529
21. S. Kolb, M. Goddard, A. Loukaci, O. Mondesert, B. Ducommunc, E. Braud, C. Garbay, *Eur. J. Med. Chem.* **45** (2012) 896
22. R. Crossley, A. Opalko, R. G. Shepherd, U.S. patent, 5,112,832 (1992)
23. C. Safak, R. Simsek, Y. Altas, S. Boydag, K. Erol, *Boll. Chim. Farm.* **136** (1997) 665
24. T. Dace, T. Gunars, V. Brigita, B. Gunars, *Biochem. Pharmacol.* **46** (1993) 773
25. M. N. Patel, B. S. Bhatt, P. A. Dosi, V. R. L. A. Narsimhacharya, H. P. Movaliya, *Appl. Organomet. Chem.* **26** (2012) 217
26. D. W. Robertson, E. E. Beedle, J. K. Swartzendruber, *J. Med. Chem.* **29** (1986) 635
27. M. N. Patel, P. A. Dosi, B. S. Bhatt, *J. Coord. Chem.* **65** (2012) 3833
28. a) H. B. Lad, A. A. Patel, K. R. Pandya, C. V. Patel, D. I. Brahmbhatt, *Med. Chem. Res.* **22** (2013) 4745; b) H. B. Lad, R. R. Giri, D. I. Brahmbhatt, *Chin. Chem. Lett.* **24** (2013) 227; c) A. K. Kaneria, R. R. Giri, V. G. Bhila, H. J. Prajapati, D. I. Brahmbhatt, *Arabian J. Chem*., doi: 10.1016/j.arabjc.2013.01.017; d) D. I. Brahmbhatt, N. H. Patel, A. K. Patel, M. A. Patel, V. G. Patel, *J. Heterocycl. Chem.* **48** (2011) 840; e) A. K. Patel, N. H. Patel, M. A. Patel, D. I. Brahmbhatt, *J. Heterocycl. Chem.* **49** (2012) 504
29. F. Krohnke, *Synthesis* **1** (1976) 1
30. National Committee for Clinical Laboratory Standards (NCCLS), Performance Standards for Antimicrobial Susceptibility Testing; Twelfth Informational Supplement (ISBN 1--56238-454-6), 2002, M100-S12 (M7)
31. S. Gummudavelly, Y. Sri Ranganath, S. Bhasker, N. Rajkumar, *Asian J. Res. Chem.* **2** (2009) 46
32. M. S. Y. Khan, P. Sharma, *Indian J. Chem*., *B* **32** (1993) 374
33. A. Basnet, P. Thapa, R. Karki, Y. Na, Y. Jahng, B.-S. Jeong, T. C. Jeong, C.-S. Lee, E.-S. Lee, *Bioorg. Med. Chem.* **15** (2007) 4351.

Journal of the Serbian Chemical Society
JSCS-info@shd.org.rs • www.shd.org.rs/JSCS
*J. Serb. Chem. Soc. 80* (6) S198–S207 (2015) *Supplementary material*

SUPPLEMENTARY MATERIAL TO

# Synthesis of modified pyridine and bipyridine substituted coumarins as potent antimicrobial agents

HEMALI B. LAD, RAKESH R. GIRI, YOGITA L. CHOVATIYA and DINKAR I. BRAHMBHATT*

*Department of Chemistry, Sardar Patel University, Vallabh Vidyanagar 388120, Gujarat, India*

*J. Serb. Chem. Soc.* 80 (6) (2015) 739–747

## GENERAL PROCEDURE FOR THE SYNTHESIS OF **3a–e**

The derivatives **3a**, **3c** and **3d** were prepared according to a literature procedure.[1] The preparation of derivatives **3b** and **3e** is given below.

A mixture of 8-acetyl-7-hydroxy-4-methylcoumarin (0.01 mol) and appropriate aromatic aldehyde (0.012 mol) in ethanol (20–25 mL) containing a catalytic amount of piperidine was refluxed for half an hour to two hours. On concentrating the reaction mixture to a small volume, the chalcone separated out and was filtered and crystallized from chloroform–hexane.

*7-Hydroxy-4-methyl-8-(3-*p*-tolylacryloyl)chromen-2-one (**3b**)*. Yield: 71 %; m.p.: 156 °C; Anal. Calcd. for $C_{20}H_{16}O_4$: C, 74.99; H, 5.03 %. Found: C, 74.76; H, 5.05 %; IR (KBr, $cm^{-1}$): 3425 (O–H stretching), 3062 (aromatic C–H stretching), 1723 (C=O *δ*-lactone stretching), 1655 (C=O *α*,*β*-unsaturated carbonyl group), 1612 (aromatic C=C stretchings), 838 (C–H bending for *p*-di-substituted benzene ring); $^1$H-NMR (400 MHz, $CDCl_3$, *δ* / ppm): 2.45 (6H, *s*, 2×$CH_3$), 6.21 (1H, *s*, $C_3$–H), 6.96–8.26 (8H, *m*, 6 Ar-H + 2 olefinic protons), 13.89 (1H, *s*, OH).

*7-Hydroxy-4-methyl-8-[3-(4-chlorophenyl)acryloyl]chromen-2-one (**3e**)*. Yield: 75 %; m.p.: 197–198 °C; Anal. Calcd. for $C_{19}H_{13}ClO_4$: C, 66.97; H, 3.85 %. Found: C, 66.72; H, 3.84 %; IR (KBr, $cm^{-1}$): 3419 (O–H stretching), 3061 (aromatic C–H stretching), 1720 (C=O *δ*-lactone stretching), 1657 (C=O *α*,*β*-unsaturated carbonyl group), 1610 (aromatic C=C stretchings), 836 (C–H bending for *p*-disubstituted benzene ring); $^1$H-NMR (400 MHz, $CDCl_3$, *δ* / ppm): 2.46 (3H, *s*, $CH_3$), 6.22 (1H, *s*, $C_3$–H), 6.97–8.26 (8H, *m*, 6 Ar-H + 2 olefinic protons), 13.75 (1H, *s*, OH).

* Corresponding author. E-mail: drdib317@gmail.com

ANALYTICAL AND SPECTRAL DATA FOR THE TARGET COMPOUNDS **5a**–**y**

*7-Hydroxy-4-methyl-8-(4-phenyl-6,7-dihydro-5*H*-cyclopenta[*b*]pyridin-2-yl)-chromen-2-one (**5a**)*. Yield: 66 %; m.p.: 181–182 °C; Anal. Calcd. for $C_{24}H_{19}NO_3$: C, 78.03; H, 5.18; N, 3.79 %. Found: C, 78.21; H, 5.12; N, 3.73 %; IR (KBr, $cm^{-1}$): 3417 (O–H stretching), 3056 (aromatic C–H stretching), 2989 (aliphatic C–H stretching), 1725 (C=O $\delta$-lactone stretching), 1600 and 1555 (aromatic C=C and C=N stretchings), 705 and 723 (C–H out of plane bending for mono substituted benzene ring); $^1$H-NMR (400 MHz, $CDCl_3$, $\delta$ / ppm): 2.22 (2H, *m*, $C_6'$–H), 2.45 (3H, *s*, $CH_3$), 3.17 (4H, *m*, $C_5'$–H and $C_7'$–H), 6.16 (1H, *s*, $C_3$–H), 6.99–7.70 (8H, *m*, 7 Ar-H + OH), 8.64 (1H, *s*, $C_3'$–H); $^{13}$C-NMR (100 MHz, $CDCl_3$, $\delta$ / ppm): 19.23 ($CH_3$), 23.48 ($CH_2$), 31.02 ($CH_2$), 34.09 ($CH_2$), 108.42 (C), 110.37 (CH), 112.17 (C), 115.25 (CH), 123.00 (CH), 125.91 (CH), 128.43 (CH), 128.72 (CH), 128.83 (CH), 134.16 (C), 138.37 (C), 147.60 (C), 151.97 (C), 153.15 (C), 153.45 (C), 160.53 (C), 162.22 (C) and 163.90 (CO of coumarin).

*7-Hydroxy-4-methyl-8-(4-*p*-tolyl-6,7-dihydro-5*H*-cyclopenta[*b*]pyridin-2-yl)-chromen-2-one (**5b**)*. Yield: 72 %; m.p.: 201 °C; Anal. Calcd. for $C_{25}H_{21}NO_3$: C, 78.31; H, 5.52; N, 3.65 %. Found: C, 78.11; H, 5.56; N, 3.63 %; IR (KBr, $cm^{-1}$): 3422 (O–H stretching), 3022 (aromatic C–H stretching), 2953 (aliphatic C–H stretching), 1723 (C=O $\delta$-lactone stretching), 1598 and 1550 (aromatic C=C and C=N stretchings), 818 (C–H bending of *p*-disubstituted benzene ring); $^1$H-NMR (400 MHz, $CDCl_3$, $\delta$ / ppm): 2.22 (2H, *m*, $C_6'$–H), 2.45 (6H, *s*, 2 × $CH_3$), 3.16 (4H, *m*, $C_5'$–H and $C_7'$–H), 6.14 (1H, *s*, $C_3$–H), 6.99–7.58 (7H, *m*, 6 Ar-H + OH), 8.65 (1H, *s*, $C_3'$–H); $^{13}$C-NMR (100 MHz, $CDCl_3$, $\delta$ / ppm): 19.26 ($CH_3$), 21.31 ($CH_3$), 23.55 ($CH_2$), 31.12 ($CH_2$), 34.10 ($CH_2$), 108.37 (C), 110.37 (CH), 112.17 (C), 115.31 (CH), 122.91 (CH), 125.89 (CH), 128.35 (CH), 129.58 (CH), 134.06 (C), 135.48 (C), 138.84 (C), 147.69 (C), 151.87 (C), 153.49 (C), 158.13 (C), 160.59 (C), 162.07 (C), 164.09 (CO of coumarin).

*7-Hydroxy-8-[4-(4-methoxyphenyl)-6,7-dihydro-5*H*-cyclopenta[*b*]pyridin-2--yl]-4-methyl-chromen-2-one (**5c**)*. Yield: 68 %; m.p.: 203 °C; Anal. Calcd. for $C_{25}H_{21}NO_4$: C, 75.17; H, 5.30; N, 3.51 %. Found: C, 75.32; H, 5.24; N, 3.54 %; IR (KBr, $cm^{-1}$): 3422 (O–H stretching), 3053 (aromatic C–H stretching), 2957 (aliphatic C–H stretching), 1716 (C=O $\delta$-lactone stretching), 1597 and 1552 (aromatic C=C and C=N stretchings), 836 (C–H bending of *p*-disubstituted benzene ring); $^1$H-NMR (400 MHz, $CDCl_3$, $\delta$ / ppm): 2.32 (2H, *m*, $C_6'$–H), 2.44 (3H, *s*, $CH_3$), 3.22 (2H, *t*, $J$ = 7.2 Hz, $C_5'$–H), 3.50 (2H, *t*, poorly resolved triplet, $C_7'$–H), 3.90 (3H, *s*, $OCH_3$), 6.14 (1H, *s*, $C_3$–H), 7.06–7.86 (8H, *m*, 7 Ar-H + OH); $^{13}$C-NMR (100 MHz, $CDCl_3$, $\delta$ / ppm): 19.22 ($CH_3$), 23.67 ($CH_2$), 31.23 ($CH_2$), 33.39 ($CH_2$), 55.43 ($OCH_3$), 110.64 (CH), 114.46 (CH), 115.41 (CH), 121.73 (C), 123.76 (CH), 126.44 (C), 127.47 (CH), 128.53 (C), 128.97

(C), 129.80 (C), 130.04 (CH), 135.11 (C), 149.06 (C), 152.92 (C), 153.34 (C), 160.46 (C), 160.62 (C), 161.43 (CO of coumarin).

*8-[4-(3,4-Dimethoxyphenyl)-6,7-dihydro-5*H*-cyclopenta[*b*]pyridine-2-yl]-7--hydroxy-4-methyl-chromen-2-one (**5d**)*. Yield: 70 %; m.p.: 164 °C; Anal. Calcd. for $C_{26}H_{23}NO_5$: C, 72.71; H, 5.40; N, 3.26 %. Found: C, 72.90; H, 5.34; N, 3.27 %; IR (KBr, $cm^{-1}$): 3422 (O–H stretching), 3076 (aromatic C–H stretching), 2962 (aliphatic C–H stretching), 1723 (C=O $\delta$-lactone stretching), 1600 and 1552 (aromatic C=C and C=N stretchings); $^1$H-NMR (400 MHz, $CDCl_3$, $\delta$ / ppm): 2.23 (2H, *m*, $C_6'$–H), 2.46 (3H, *s*, $CH_3$), 3.18 (4H, *m*, $C_5'$–H and $C_7'$–H), 3.97 and 4.07 (6H, 2 × *s*, 2 × $OCH_3$), 6.14 (1H, *s*, $C_3$–H), 6.99–7.54 (6H, *m*, 5 Ar-H + 1 OH), 8.72 (1H, *s*, $C_3'$–H); $^{13}$C-NMR (100 MHz, $CDCl_3$, $\delta$ / ppm): 19.20 ($CH_3$), 23.36 ($CH_2$), 31.01 ($CH_2$), 34.15 ($CH_2$), 55.96 ($OCH_3$), 56.11 ($OCH_3$), 110.26 (CH), 112.21 (C), 115.35 (CH), 123.01 (CH), 125.62 (CH), 128.31 (CH), 128.72 (CH), 128.83 (CH), 134.06 (C), 138.23 (C), 147.50 (C), 151.76 (C), 153.15 (C), 153.37 (C), 154.26 (C), 158.76 (C), 160.52 (C), 162.22 (C), 163.70 (CO of coumarin).

*8-[4-(4-Chlorophenyl)-6,7-dihydro-5*H*-cyclopenta[*b*]pyridin-2-yl]-7-hyd-roxy-4-methyl-chromen-2-one (**5e**)*. Yield: 70 %; m.p.: 198–199 °C; Anal. Calcd. for $C_{24}H_{18}ClNO_3$: C, 71.38; H, 4.49; N, 3.47 %. Found: C, 71.19; H, 4.52; N, 3.51 %; IR (KBr, $cm^{-1}$): 3433 (O–H stretching), 3068 (aromatic C–H stretching), 2961 (aliphatic C–H stretching), 1727 (C=O $\delta$-lactone stretching), 1599 and 1549 (aromatic C=C and C=N stretchings), 837 (C–H bending of *p*-disubstituted benzene ring); $^1$H-NMR (400 MHz, $CDCl_3$, $\delta$ / ppm): 2.23 (2H, *m*, $C_6'$–H), 2.45 (3H, *s*, $CH_3$), 3.15 (4H, *m*, $C_5'$–H and $C_7'$–H), 6.15 (1H, *s*, $C_3$–H), 6.99–7.61 (7H, *m*, 6 Ar-H + OH), 8.62 (1H, *s*, $C_3'$–H); $^{13}$C-NMR (100 MHz, $CDCl_3$, $\delta$ / ppm): 19.24 ($CH_3$), 23.52 ($CH_2$), 31.11 ($CH_2$), 34.15 ($C_7'$), 108.19 (C), 110.17 (CH), 112.10 (C), 115.15 (CH), 122.71 (CH), 125.89 (CH), 128.53 (CH), 129.85 (CH), 134.06 (C), 135.38 (C), 138.94 (C), 147.39 (C), 151.78 (C), 153.94 (C), 158.31 (C), 160.45 (C), 162.07 (C), 164.12 (CO of coumarin).

*7-Hydroxy-4-methyl-8-(4-phenyl-5,6,7,8-tetrahydroquinolin-2-yl)chromen--2-one (**5f**)*. Yield: 67 %; m.p.: 200 °C; Anal. Calcd. for $C_{25}H_{21}NO_3$: C, 78.31; H, 5.52; N, 3.65 %. Found: C, 78.20; H, 5.55; N, 3.61 %; IR (KBr, $cm^{-1}$): 3405 (O–H stretching), 3059 (aromatic C–H stretching), 2929 (aliphatic C–H stretching), 1717 (C=O $\delta$-lactone stretching), 1600 and 1539 (aromatic C=C and C=N stretchings), 704 and 725 (C–H out of plane bending for mono substituted benzene ring); $^1$H-NMR (400 MHz, $CDCl_3$, $\delta$ / ppm): 1.80 (2H, *m*, $C_6'$–H), 1.99 (2H, *m*, $C_7'$–H), 2.43 (3H, *s*, $CH_3$), 2.73 (2H, *m*, $C_5'$–H), 3.08 (2H, *t*, $J$ = 6.4 Hz, $C_8'$–H), 6.10 (1H, *s*, $C_3$–H), 6.97–7.53 (8H, *m*, 7 Ar-H + OH), 8.50 (1H, *s*, $C_3'$–H); $^{13}$C-NMR (100 MHz, $CDCl_3$, $\delta$ / ppm): 19.22 ($CH_3$), 22.55 ($CH_2$), 22.79 ($CH_2$), 27.27 ($CH_2$), 31.84 ($CH_2$), 107.44 (C), 110.15 (CH), 111.83 (C), 115.45 (CH), 124.08 (CH), 126.09 (CH), 128.23 (CH), 128.55 (CH), 128.66

(CH), 129.57 (C), 131.91 (C), 138.88 (C), 150.70 (C), 152.20 (C), 153.14 (C), 153.46 (C), 160.52 (C), 164.90 (CO of coumarin).

*7-Hydroxy-4-methyl-8-(4-*p*-tolyl-5,6,7,8-tetrahydroquinolin-2-yl)chromen--2-one (**5g**)*. Yield: 62 %; m.p.: 218 °C; Anal. Calcd. for $C_{26}H_{23}NO_3$: C, 78.57; H, 5.83; N, 3.52 %. Found: C, 78.69; H, 5.85; N, 3.48 %; IR (KBr, $cm^{-1}$): 3433 (O–H stretching), 3045 (aromatic C–H stretching), 2936 (aliphatic C–H stretching), 1731 (C=O $\delta$-lactone stretching), 1603 and 1538 (aromatic C=C and C=N stretchings), 837 (C–H bending of *p*-disubstituted benzene ring); $^1$H-NMR (400 MHz, $CDCl_3$, $\delta$ / ppm): 1.82 (2H, *m*, $C_6'$–H), 1.97 (2H, *m*, $C_7'$–H), 2.44 (6H, *s*, 2×$CH_3$), 2.75 (2H, *t*, *J* = 6.4 Hz, $C_5'$–H), 3.08 (2H, *t*, *J* = 7.2 Hz, $C_8'$–H), 6.10 (1H, *s*, $C_3$–H), 6.97–7.53 (7H, *m*, 6 Ar-H + OH), 8.50 (1H, *s*, $C_3'$–H); $^{13}$C-NMR (100 MHz, $CDCl_3$, $\delta$ / ppm): 19.24 ($CH_3$), 21.25 ($CH_3$), 22.53 ($CH_2$), 22.82 ($CH_2$), 27.34 ($CH_2$), 31.79 ($CH_2$), 107.43 (C), 110.14 (CH), 111.82 (C), 115.48 (CH), 124.19 (CH), 126.04 (CH), 128.60 (CH), 129.24 (CH), 129.65 (C), 135.89 (C), 138.11 (C), 150.54 (C), 152.30 (C), 153.00 (C), 153.44 (C), 153.47 (C), 160.51 (C), 164.93 (CO of coumarin).

*7-Hydroxy-4-methyl-8-[4-(4-methoxyphenyl)-5,6,7,8-tetrahydroquinolin-2-yl]--4-methyl-chromen-2-one (**5h**)*. Yield: 69 %; m.p.: 192–193 °C; Anal. Calcd. for $C_{26}H_{23}NO_4$: C, 75.53; H, 5.61; N, 3.39 %. Found: C, 75.30; H, 5.63; N, 3.34 %; IR (KBr, $cm^{-1}$): 3420 (O–H stretching), 3050 (aromatic C–H stretching), 2927 (aliphatic C–H stretching), 1720 (C=O $\delta$-lactone stretching), 1594 and 1538 (aromatic C=C and C=N stretchings), 835 (C–H bending of *p*-disubstituted benzene ring); $^1$H-NMR (400 MHz, $CDCl_3$, $\delta$ / ppm): 1.81 (2H, *m*, $C_6'$–H), 1.98 (2H, *m*, $C_7'$–H), 2.44 (3H, *s*, $CH_3$), 2.76 (2H, *t*, *J* = 6.4 Hz, $C_5'$–H), 3.07 (2H, *t*, *J* = 7.2 Hz, $C_8'$–H), 3.89 (3H, *s*, $OCH_3$) 6.11 (1H, *s*, $C_3$–H), 6.97–7.53 (7H, *m*, 6 Ar-H + OH), 8.51 (1H, *s*, $C_3'$–H); $^{13}$C-NMR (100 MHz, $CDCl_3$, $\delta$ / ppm): 19.29 ($CH_3$), 22.61 ($CH_2$), 22.91 ($CH_2$), 27.48 ($CH_2$), 31.84 ($CH_2$), 55.36 ($OCH_3$), 107.47 (C), 110.12 (CH), 111.79 (C), 114.05 (CH), 115.48 (CH), 124.19 (CH), 126.05 (CH), 129.62 (C), 130.11 (CH), 131.17 (C), 150.70 (C), 151.83 (C), 152.81 (C), 153.08 (C), 153.48 (C), 159.69 (C), 160.61 (C), 165.06 (CO of coumarin).

*8-[4-(3,4-Dimethoxyphenyl)-5,6,7,8-tetrahydroquinolin-2-yl]-7-hydroxy-4--methyl-chromen-2-one (**5i**)*. Yield: 70 %; m.p.: 221 °C; Anal. Calcd. for $C_{27}H_{25}NO_5$: C, 73.12; H, 5.68; N, 3.16 %. Found: C, 73.29; H, 5.62; N, 3.12 %; IR (KBr, $cm^{-1}$): 3415 (O–H stretching), 3068 (aromatic C–H stretching), 2932 (aliphatic C–H stretching), 1719 (C=O $\delta$-lactone stretching), 1598 and 1539 (aromatic C=C and C=N stretchings); $^1$H-NMR (400 MHz, $CDCl_3$, $\delta$ / ppm): 1.82 (2H, *m*, $C_6'$–H), 1.99 (2H, *m*, $C_7'$–H), 2.44 (3H, *s*, $CH_3$), 2.82 (2H, *t*, *J* = 6.4 Hz, $C_5'$–H), 3.08 (2H, *t*, *J* = 6.4 Hz, $C_8'$–H), 3.96 and 4.01 (6H, 2 × *s*, 2 × $OCH_3$), 6.10 (1H, *s*, $C_3$–H), 6.97–7.53 (6H, *m*, 5 Ar-H + OH), 8.54 (1H, *s*, $C_3'$–H); $^{13}$C-NMR (100 MHz, $CDCl_3$, $\delta$ / ppm): 19.26 ($CH_3$), 22.58 ($CH_2$), 22.95 ($CH_2$), 27.59

($CH_2$), 31.92 ($CH_2$), 55.99 ($OCH_3$), 56.14 ($OCH_3$), 110.12 (CH), 110.98 (CH), 111.84 (C), 112.53 (CH), 115.43 (CH), 121.32 (CH), 124.30 (CH), 126.07 (CH), 129.46 (C), 131.40 (C), 149.14 (C), 149.31 (C), 150.66 (C), 151.30 (C), 151.67 (C), 153.29 (C), 153.41 (C), 153.56 (C), 160.54 (C), 164.84 (CO of coumarin).

*8-[4-(4-Chlorophenyl)-5,6,7,8-tetrahydroquinolin-2-yl]-7-hydroxy-4-methyl--chromen-2-one (**5j**)*. Yield: 68 %; m.p.: 251–252 °C; Anal. Calcd. for $C_{25}H_{20}ClNO_3$: C, 71.85; H, 4.82; N, 3.35 %. Found: C, 71.98; H, 4.84; N, 3.30 %; IR (KBr, $cm^{-1}$): 3423 (O–H stretching), 3058 (aromatic C–H stretching), 2928 (aliphatic C–H stretching), 1732 (C=O $\delta$-lactone stretching), 1602 and 1538 (aromatic C=C and C=N stretchings), 830 (C–H bending of *p*-disubstituted benzene ring); $^1$H-NMR (400 MHz, $CDCl_3$, $\delta$ / ppm): 1.81 (2H, *m*, $C_6'$–H), 1.98 (2H, *m*, $C_7'$–H), 2.43 (3H, *s*, $CH_3$), 2.70 (2H, *t*, $J$ = 6.4 Hz, $C_5'$–H), 3.07 (2H, *t*, $J$ = 6.4 Hz, $C_8'$–H), 6.11 (1H, *s*, $C_3$–H), 6.96–7.53 (7H, *m*, 6 Ar-H + OH), 8.48 (1H, *s*, $C_3'$–H); $^{13}$C-NMR (100 MHz, $CDCl_3$, $\delta$ / ppm): 19.24 ($CH_3$), 22.50 ($CH_2$), 22.74 ($CH_2$), 27.25 ($CH_2$), 31.90 ($CH_2$), 107.31 (C), 110.17 (CH), 111.85 (C), 115.43 (CH), 123.91 (CH), 126.18 (CH), 128.84 (CH), 129.37 (C), 130.06 (CH), 134.44 (C), 137.26 (C), 150.82 (C), 150.89 (C), 153.43 (C), 153.50 (C), 160.47 (C), 164.79 (CO of coumarin).

*7-Hydroxy-4-methyl-8-(4-phenyl-5*H*-indeno[1,2-*b*]pyridin-2-yl)chromen-2--one (**5k**)*. Yield: 72 %; m.p.: 264–265 °C; Anal. Calcd. for $C_{28}H_{19}NO_3$: C, 80.56; H, 4.59; N, 3.36 %. Found: C, 80.77; H, 4.53; N, 3.40 %; IR (KBr, $cm^{-1}$): 3423 (O–H stretching), 3057 (aromatic C–H stretching), 2986 (aliphatic C–H stretching), 1729 (C=O $\delta$-lactone stretching), 1599 and 1551 (aromatic C=C and C=N stretchings), 694 and 722 (C–H out of plane bending for mono substituted benzene ring); $^1$H-NMR (400 MHz, $CDCl_3$, $\delta$ / ppm): 2.45 (3H, *s*, $CH_3$), 4.09 (2H, *s*, $C_5'$–H), 6.14 (1H, *s*, $C_3$–H), 7.03–8.07 (11H, *m*, Ar-H), 8.73 (1H, *s*, $C_3'$–H), 15.90 (1H, *bs*, OH); $^{13}$C-NMR (100 MHz, $CDCl_3$, $\delta$ / ppm): 19.25 ($CH_3$), 34.96 ($CH_2$), 108.55 (C), 110.46 (CH), 112.26 (C), 115.30 (CH), 120.97 (CH), 123.18 (CH), 125.21 (CH), 126.20 (CH), 127.51 (CH), 128.50 (CH), 129.03 (CH), 129.07 (CH), 129.48 (CH), 133.37 (C), 138.12 (C), 139.12 (C), 144.16 (C), 147.99 (C), 152.80 (C), 153.25 (C), 153.44 (C), 157.03 (C), 160.46 (C), 163.89 (CO of coumarin).

*7-Hydroxy-4-methyl-8-(4-*p*-tolyl-5*H*-indeno[1,2-*b*]pyridin-2-yl)chromen-2--one (**5l**)*. Yield: 75 %; m.p.: 280 °C; Anal. Calcd. for $C_{29}H_{21}NO_3$: C, 80.72; H, 4.91; N, 3.25 %. Found: C, 80.90; H, 4.96; N, 3.24 %; IR (KBr, $cm^{-1}$): 3410 (O–H stretching), 3042 (aromatic C–H stretching), 2920 (aliphatic C–H stretching), 1716 (C=O $\delta$-lactone stretching), 1600 and 1553 (aromatic C=C and C=N stretchings), 834 (C–H bending of *p*-disubstituted benzene ring); $^1$H-NMR (400 MHz, $CDCl_3$, $\delta$ / ppm): 2.46 and 2.47 (6H, 2×*s*, 2×$CH_3$), 4.11 (2H, *s*, $C_5'$–H), 6.16 (1H, *s*, $C_3$–H), 7.05–8.09 (10H, *m*, Ar-H), 8.75 (1H, *s*, $C_3'$–H), 15.97 (1H, *bs*, OH); $^{13}$C-NMR (100 MHz, $CDCl_3$, $\delta$ /ppm): 19.28 ($CH_3$), 21.35 ($CH_3$),

35.06 ($CH_2$), 108.65 (C), 110.48 (CH), 112.30 (C), 115.30 (CH), 120.98 (CH), 123.13 (CH), 125.21 (CH), 126.20 (CH), 127.52 (CH), 128.40 (CH), 129.42 (CH), 129.79 (CH), 133.28 (C), 135.27 (C), 139.15 (C), 139.22 (C), 144.22 (C), 148.06 (C), 152.75 (C), 153.47 (C), 157.07 (C), 160.52 (C), 163.92 (C), 169.77 (CO of coumarin).

*7-Hydroxy-8-[4-(4-methoxyphenyl)-5*H*-indeno[1,2-*b*]pyridin-2-yl]-4-methyl--chromen-2-one (**5m**)*. Yield: 71 %; m.p.: 246 °C; Anal. Calcd. for $C_{29}H_{21}NO_4$: C, 77.84; H, 4.73; N, 3.13 %. Found: C, 77.70; H, 4.75; N, 3.16 %; IR (KBr, $cm^{-1}$): 3418 (O–H stretching), 3054 (aromatic C–H stretching), 2920 (aliphatic C–H stretching), 1721 (C=O $\delta$-lactone stretching), 1598 and 1552 (aromatic C=C and C=N stretchings), 841 (C–H bending of *p*-disubstituted benzene ring); $^1$H--NMR (400 MHz, $CDCl_3$, $\delta$ / ppm): 3.60 (3H, *s*, $CH_3$), 5.05 (3H, *s*, $OCH_3$), 5.25 (2H, *s*, $C_5'$–H), 7.29 (1H, *s*, $C_3$–H), 8.18–9.22 (10H, *m*, Ar-H), 9.88 (1H, *s*, $C_3'$–H), 17.15 (1H, *bs*, OH); $^{13}$C-NMR (100 MHz, $CDCl_3$, $\delta$ / ppm): 19.28 ($CH_3$), 33.18 ($CH_2$), 55.42 ($OCH_3$), 108.59 (C), 110.44 (CH), 112.26 (C), 114.56 (CH), 115.33 (CH), 120.95 (CH), 122.85 (CH), 125.20 (CH), 126.15 (CH), 127.50 (CH), 129.40 (CH), 129.89 (CH), 130.43 (C), 132.96 (C), 139.21 (C), 144.14 (C), 147.53 (C), 152.68 (C), 153.26 (C), 153.51 (C), 156.96 (C), 160.36 (C), 160.53 (C), 163.96 (CO of coumarin).

*8-[4-(3,4-Dimethoxyphenyl)-5*H*-indeno[1,2-*b*]pyridin-2-yl]-7-hydroxy-4--methyl-chromen-2-one (**5n**)*. Yield: 73 %; m.p.: 257–258 °C; Anal. Calcd. for $C_{30}H_{23}NO_5$: C, 75.46; H, 4.85; N, 2.93 %. Found: C, 75.63; H, 4.89; N, 2.95 %; IR (KBr, $cm^{-1}$): 3425 (O–H stretching), 3083 (aromatic C–H stretching), 2918 (aliphatic C–H stretching), 1724 (C=O $\delta$-lactone stretching), 1601 and 1553 (aromatic C=C and C=N stretchings); $^1$H-NMR (400 MHz, $CDCl_3$, $\delta$ / ppm): 2.45 (3H, *s*, $CH_3$), 3.99 and 4.10 (6H, 2×*s*, 2×$OCH_3$), 4.12 (2H, *s*, $C_5'$–H), 6.13 (1H, *s*, $C_3$–H), 7.02–8.06 (9H, *m*, Ar-H), 8.78 (1H, *s*, $C_3'$–H), 15.98 (1H, *bs*, OH ); $^{13}$C-NMR (100 MHz, $CDCl_3$, $\delta$ / ppm): 19.31 ($CH_3$), 35.27 ($CH_2$), 55.92 ($OCH_3$), 56.34 ($OCH_3$), 104.01 (C), 108.47 (C), 110.31 (CH), 111.23 (CH), 111.84 (CH), 112.27 (C), 115.38 (CH), 117.98 (C), 120.86 (CH), 122.86 (CH), 125.20 (CH), 126.20 (CH), 127.47 (CH), 129.42 (CH), 130.61 (C), 132.80 (C), 139.09 (C), 144.16 (C), 147.39 (C), 149.53 (C), 149.92 (C), 152.76 (C), 153.60 (C), 157.06 (C), 160.59 (CO of coumarin).

*8-[4-(4-Chlorophenyl)-5*H*-indeno[1,2-b]pyridin-2-y])-7-hydroxy-4-methyl--chromen-2-one (**5o**)*. Yield: 70 %; m.p.: 285 °C; Anal. Calcd. for $C_{28}H_{18}ClNO_3$: C, 74.42; H, 4.01; N, 3.10 %. Found: C, 74.63; H, 4.05; N, 3.08 %; IR (KBr, $cm^{-1}$): 3405 (O–H stretching), 3055 (aromatic C–H stretching), 2920 (aliphatic C–H stretching), 1716 (C=O $\delta$-lactone stretching), 1598 and 1551 (aromatic C=C and C=N stretchings), 839 (C–H bending of *p*-disubstituted benzene ring); $^1$H--NMR (400 MHz, $CDCl_3$, $\delta$ / ppm): 2.48 (3H, *s*, $CH_3$), 4.10 (2H, *s*, $C_5'$–H), 6.18 (1H, *s*, $C_3$–H), 7.07–8.12 (10H, *m*, Ar-H), 8.73 (1H, *s*, $C_3'$–H), 15.72 (1H, *bs*,

OH); $^{13}$C-NMR (100 MHz, $CDCl_3$, $\delta$ / ppm): 19.34 ($CH_3$), 35.28 ($CH_2$), 108.68 (C), 110.47 (CH), 112.33 (C), 114.66 (CH), 115.39 (CH), 121.08 (CH), 122.96 (CH), 125.36 (CH), 126.21 (CH), 127.53 (CH), 129.51 (CH), 130.06 (CH), 130.58 (C), 133.02 (C), 139.33 (C), 144.22 (C), 147.63 (C), 152.78 (C), 153.36 (C), 153.60 (C), 157.08 (C), 160.44 (C), 160.53 (C), 164.05 (CO of coumarin).

*7-Hydroxy-4-methyl-8-(4-phenyl-[2,3′-bipyridin]-6′-yl)chromen-2-one* ***(5p)***. Yield: 75 %; m.p.: 261 °C; Anal. Calcd. for $C_{26}H_{18}N_2O_3$: C, 76.83; H, 4.46; N, 6.89 %. Found: C, 76.62; H, 4.44; N, 6.91 %; IR (KBr, $cm^{-1}$): 3435 (O–H stretching), 3035 (aromatic C–H stretching), 2961 (aliphatic C–H stretching), 1732 (C=O $\delta$-lactone stretching), 1608 and 1547 (aromatic C=C and C=N stretchings), 707 and 760 (C–H out of plane bending for mono-substituted benzene ring); $^1$H-NMR (400 MHz, $CDCl_3$, $\delta$ / ppm): 2.48 (3H, *s*, $CH_3$), 6.20 (1H, *s*, $C_3$–H), 7.03–9.00 (12H, *m*, Ar-H ), 9.25 (1H, poorly resolved doublet, $C_2''$–H), 15.48 (1H, *bs*, OH); $^{13}$C-NMR (100 MHz, $CDCl_3$, $\delta$ / ppm): 19.29 ($CH_3$), 108.11 (C), 110.66 (CH), 112.42 (C), 115.24 (CH), 117.82 (CH), 123.34 (CH), 123.95 (CH), 126.92 (CH), 127.45 (CH), 129.46 (CH), 129.83 (CH), 133.70 (C), 134.33 (CH), 137.71 (C), 148.26 (CH), 150.69 (CH), 151.85 (C), 152.19 (C), 153.43 (C), 153.52(C), 154.77(C), 160.29(C) and 163.70 (CO of coumarin).

*7-Hydroxy-8-(4-*p*-tolyl-[2,3′-bipyridin]-6-yl)-4-methyl-chromen-2-one* ***(5q)***. Yield: 68 %; m.p.: 250 °C; Anal. Calcd. for $C_{27}H_{20}N_2O_3$: C, 77.13; H, 4.79; N, 6.66 %. Found: C, 77.40; H, 4.82; N, 6.62 %; IR (KBr, $cm^{-1}$): 3412 (O–H stretching), 3041 (aromatic C–H stretching), 2968 (aliphatic C–H stretching), 1720 (C=O $\delta$-lactone stretching), 1607 and 1544 (aromatic C=C and C=N stretchings), 814 (C–H bending of *p*-disubstituted benzene ring; $^1$H-NMR (400 MHz, $CDCl_3$, $\delta$ / ppm): 2.47 (6H, *s*, 2×$CH_3$), 6.20 (1H, *s*, $C_3$–H), 7.01–8.98 (11H, *m*, Ar-H ), 9.23 (1H, poorly resolved *d*, $C_2''$–H), 15.58 (1H, *bs*, OH); $^{13}$C-NMR (100 MHz, $CDCl_3$, $\delta$ / ppm): 19.30 ($CH_3$), 21.33 ($CH_3$), 108.10 (C), 110.63 (CH), 112.39 (C), 115.24 (CH), 117.51 (CH), 123.04 (CH), 123.94 (CH), 126.86 (CH), 127.29 (CH), 130.19 (CH), 133.76 (C), 134.33 (CH), 134.75 (C), 140.13 (C), 148.27 (CH), 150.64 (CH), 151.71 (C), 152.07 (C), 153.45 (C), 153.53 (C), 154.71 (C), 160.29 (C), 163.83 (CO of coumarin).

*7-Hydroxy-8-[4-(4-methoxyphenyl)-[2,3′-bipyridin]-6-yl]-4-methyl-chromen--2-one* ***(5r)***. Yield: 70 %; m.p.: 247–248 °C; Anal. Calcd. for $C_{27}H_{20}N_2O_4$: C, 74.30; H, 4.62; N, 6.42 %. Found: C, 74.44; H, 4.60; N, 6.48 %; IR (KBr, $cm^{-1}$): 3418 (O–H stretching), 3044 (aromatic C–H stretching), 2960 (aliphatic C–H stretching), 1727 (C=O $\delta$-lactone stretching), 1605 and 1544 (aromatic C=C and C=N stretchings), 810 (C–H bending of *p*-disubstituted benzene ring; $^1$H-NMR (400 MHz, $CDCl_3$, $\delta$ / ppm): 2.47 (3H, *s*, $CH_3$), 3.90 (3H, *s*, $OCH_3$), 6.19 (1H, *s*, $C_3$–H), 7.0–8.96 (11H, *m*, Ar-H ), 9.22 (1H, poorly resolved *d*, $C_2''$–H), 15.67 (1H, *bs*, OH); $^{13}$C-NMR (100 MHz, $CDCl_3$, $\delta$ / ppm): 19.27 ($CH_3$), 55.45 ($OCH_3$), 108.03 (C), 110.54 (CH), 112.31 (C), 114.90 (CH), 115.26 (CH),

117.03 (CH), 122.55 (CH), 123.91 (CH), 126.80 (CH), 128.70 (CH), 129.82 (C), 133.75 (C), 134.28 (CH), 148.22 (CH), 150.59 (CH), 151.18 (C), 151.95 (C), 153.44 (C), 153.54 (C), 154.59 (C), 160.30 (C), 161.18 (C), 163.89 (CO of coumarin).

*8-[4-(3,4-Dimethoxyphenyl)-[2,3′-bipyridin]-6-yl]-7-hydroxy-4-methyl-chromen-2-one (**5s**)*. Yield: 72 %; m.p.: 245 °C; Anal. Calcd. for $C_{28}H_{22}N_2O_5$: C, 72.09; H, 4.75; N, 6.01 %. Found: C, 71.82; H, 4.74; N, 6.03 %; IR (KBr, $cm^{-1}$): 3410 (O–H stretching), 3043 (aromatic C–H stretching), 2948 (aliphatic C–H stretching), 1724 (C=O $\delta$-lactone stretching), 1604 and 1545 (aromatic C=C and C=N stretchings); $^1$H-NMR (400 MHz, $CDCl_3$, $\delta$ / ppm): 2.48 (3H, *s*, $CH_3$), 3.99 and 4.11 (6H, 2×*s*, 2×$OCH_3$), 6.17 (1H, *s*, $C_3$–H), 7.01–9.06 (10H, *m*, Ar-H), 9.23 (1H, poorly resolved *d*, $C_2$″–H), 15.67 (1H, *bs*, OH); $^{13}$C-NMR (100MHz, $CDCl_3$, $\delta$ / ppm): 19.29 ($CH_3$), 56.02 ($OCH_3$), 56.26 ($OCH_3$), 107.66 (C), 110.19 (CH), 110.35 (CH), 111.52 (CH), 112.21 (C), 115.29 (CH), 116.69 (CH), 119.70 (CH), 122.46 (CH), 123.88 (CH), 126.81 (CH), 129.91 (C), 133.60 (C), 134.20 (CH), 148.13 (CH), 149.78 (C), 150.53 (CH), 150.69 (C), 150.96 (C), 151.72 (C), 153.47 (C), 153.61 (C), 154.55 (C), 160.18 (C), 164.12 (CO of coumarin).

*8-[4-(4-Chlorophenyl)-[2,3′-bipyridin]-6-yl]7-hydroxy-4-methyl-chromen-2--one (**5t**)*. Yield: 60 %; m.p.: 270–271 °C; Anal. Calcd. for $C_{26}H_{17}ClN_2O_3$: C, 70.83; H, 3.89; N, 6.35 %. Found: C, 70.59; H, 3.86; N, 6.39 %; IR (KBr, $cm^{-1}$): 3440 (O–H stretching), 3059 (aromatic C–H stretching), 2958 (aliphatic C–H stretching), 1725 (C=O $\delta$-lactone stretching), 1608 and 1545 (aromatic C=C and C=N stretchings), 810 (C–H bending of *p*-disubstituted benzene ring); $^1$H-NMR (400 MHz, $CDCl_3$, $\delta$ / ppm): 2.49 (3H, *s*, $CH_3$), 6.21 (1H, *s*, $C_3$–H), 7.04–8.97 (11H, *m*, Ar-H ), 9.24 (1H, poorly resolved *d*, $C_2$″–H), 15.34 (1H, *bs*, OH); $^{13}$C-NMR (100 MHz, $CDCl_3$, $\delta$ / ppm): 19.30 ($CH_3$), 110.69 (CH), 112.41 (C), 115.27 (CH), 115.88 (C), 117.48 (CH), 123.14 (CH), 123.96 (CH), 124.77 (C), 125.49 (C), 126.05 (C), 127.05 (CH), 128.71 (CH), 129.71 (CH), 130.65 (C), 132.61 (C), 134.33 (CH), 136.14 (C), 136.23 (C), 147.19 (C), 148.25 (CH), 150.80 (CH), 153.55 (C), 154.95 (CO of coumarin).

*7-Hydroxy-4-methyl-8-(4-phenyl-[2,4′-bipyridin]-6-yl)chromen-2-one (**5u**)*. Yield: 73 %; m.p.: 248 °C; Anal. Calcd. for $C_{26}H_{18}N_2O_3$: C, 76.83; H, 4.46; N, 6.89 %. Found: C, 76.68; H, 4.43; N, 6.86 %; IR (KBr, $cm^{-1}$): 3417 (O–H stretching), 3064 (aromatic C–H stretching), 2960 (aliphatic C–H stretching), 1722 (C=O $\delta$-lactone stretching), 1606 and 1543 (aromatic C=C and C=N stretchings), 704 and 765 (C–H out of plane bending for mono substituted benzene ring); $^1$H-NMR (400 MHz, $CDCl_3$, $\delta$ / ppm): 2.47 (3H, *s*, $CH_3$), 6.19 (1H, *s*, $C_3$–H), 7.03–8.82 (12H, *m*, Ar-H ), 9.02 (1H, poorly resolved *d*, $C_3$″–H), 15.40 (1H, *bs*, OH); $^{13}$C-NMR (100 MHz, $CDCl_3$, $\delta$ / ppm): 19.29 ($CH_3$), 110.79 (CH), 112.48 (C), 115.69 (CH), 117.81 (CH), 120.86 (CH), 123.85 (CH), 128.76 (CH), 129.79 (CH), 135.91 (CH), 136.44 (CH), 144.85 (C), 150.62 (C),

150.94 (C), 150.96 (CH), 152.23 (C), 153.48 (C), 153.69 (C), 154.99 (C), 160.27 (C), 160.63 (C), 163.64 (CO of coumarin).

*7-Hydroxy-4-methyl-8-(4*-p-*tolyl-[2,4′-bipyridin]-6-yl)chromen-2-one* ***(5v)***. Yield: 65 %; m.p.: 260–261 °C; Anal. Calcd. for $C_{27}H_{20}N_2O_3$: C, 77.13; H, 4.79; N, 6.66 %. Found: C, 77.39; H, 4.81; N, 6.69 %; IR (KBr, $cm^{-1}$): 3415 (O–H stretching), 3030 (aromatic C–H stretching), 2961 (aliphatic C–H stretching), 1726 (C=O $\delta$-lactone stretching), 1598 and 1542 (aromatic C=C and C=N stretchings), 812 (C–H bending of *p*-disubstituted benzene ring); $^1$H-NMR (400 MHz, $CDCl_3$, $\delta$ / ppm): 2.47 (6H, *s*, 2×$CH_3$), 6.19 (1H, *s*, $C_3$–H), 7.02–8.82 (11H, *m*, Ar-H), 9.01 (1H, poorly resolved *d*, $C_3''$–H), 15.48 (1H, *bs*, OH); $^{13}$C-NMR (100 MHz, $CDCl_3$, $\delta$ / ppm): 19.29 ($CH_3$), 21.35 ($CH_3$), 110.66 (CH), 112.43 (CH), 115.22 (CH), 117.68 (CH), 120.99 (CH), 123.87 (CH), 126.96 (CH), 127.25 (C), 130.23 (CH), 134.53 (C), 139.78 (C), 140.26 (C), 145.07 (C), 150.18 (C), 150.83 (CH), 151.81 (C), 151.92 (C), 153.39 (C), 153.53 (C), 154.71 (C), 160.25 (CO of coumarin).

*7-Hydroxy-8-[4-(4-methoxyphenyl)-[2,4′-bipyridin]-6-yl]-4-methyl-chromen--2-one* ***(5w)***. Yield: 78 %; m.p.: 240–241 °C; Anal. Calcd. for $C_{27}H_{20}N_2O_4$: C, 74.30; H, 4.62; N, 6.42 %. Found: C, 74.54; H, 4.58; N, 6.39 %; IR (KBr, $cm^{-1}$): 3417 (O–H stretching), 3032 (aromatic C–H stretching), 2963 (aliphatic C–H stretching), 1730 (C=O $\delta$-lactone stretching), 1602 and 1542 (aromatic C=C and C=N stretchings), 818 (C–H bending of *p*-disubstituted benzene ring); $^1$H--NMR (400 MHz, $CDCl_3$, $\delta$ / ppm): 3.08 (3H, *s*, $CH_3$), 3.91 (3H, *s*, $OCH_3$), 6.21 (1H, *s*, $C_3$–H), 7.04–8.83 (11H, *m*, Ar-H), 9.02 (1H, poorly resolved *d*, $C_3''$–H), 15.59 (1H, *bs*, OH); $^{13}$C-NMR (100 MHz, $CDCl_3$, $\delta$ / ppm): 19.28 ($CH_3$), 55.44 ($OCH_3$), 107.90 (C), 110.56 (CH), 112.33 (C), 114.89 (CH), 115.25 (CH), 117.20 (CH), 120.92 (CH), 123.33 (CH), 126.91 (CH), 128.67 (CH), 129.61 (C), 145.01 (C), 150.82 (CH), 151.23 (C), 151.81 (C), 153.43 (C), 153.56 (C), 154.61 (C), 160.24 (C), 161.22 (C), 163.82 (CO of coumarin).

*8-[4-(3,4-Dimethoxyphenyl)-[2,4′-bipyridin]-6-yl]-7-hydroxy-4-methyl-chromen-2-one* ***(5x)***. Yield: 75 %; m.p.: 236 °C; Anal. Calcd. for $C_{28}H_{22}N_2O_5$: C, 72.09; H, 4.75; N, 6.01 %. Found: C, 71.80; H, 4.73; N, 6.04 %; IR (KBr, $cm^{-1}$): 3418 (O–H stretching), 3040 (aromatic C–H stretching), 2949 (aliphatic C–H stretching), 1736 (C=O $\delta$-lactone stretching), 1598 and 1542 (aromatic C=C and C=N stretchings); $^1$H-NMR (400 MHz, $CDCl_3$, $\delta$ / ppm): 2.47 (3H, *s*, $CH_3$), 3.98 and 4.10 (6H, 2×*s*, 2×$OCH_3$), 6.16 (1H, *s*, $C_3$–H), 7.01–8.81 (10H, *m*, Ar-H), 9.06 (1H, poorly resolved *d*, $C_3''$–H), 15.70 (1H, *bs*, OH); $^{13}$C-NMR (100 MHz, $CDCl_3$, $\delta$ / ppm): 19.29 ($CH_3$), 56.00 ($OCH_3$), 56.25 ($OCH_3$), 107.51 (C), 110.09 (CH), 110.36 (CH), 111.40 (CH), 112.21 (C), 115.27 (CH), 116.86 (CH), 119.65 (CH), 120.82 (CH), 123.24 (CH), 126.92 (CH), 129.66 (C), 144.87 (C), 149.76 (C), 150.72 (CH), 150.99 (C), 151.54 (C), 153.41 (C), 153.66 (C), 154.53 (C), 160.13 (C), 163.99 (CO of coumarin).

*8-[4-(4-Chlorophenyl)-[2,4'-bipyridin]-6-yl]-7-hydroxy-4-methyl-chromen--2-one (**5y**)*. Yield: 70 %; m.p.: 265–267 °C; Anal. Calcd. for $C_{26}H_{17}ClN_2O_3$: C, 70.83; H, 3.89; N, 6.35 %. Found: C, 70.65; H, 3.87; N, 6.32 %; IR (KBr, $cm^{-1}$): 3422 (O–H stretching), 3030 (aromatic C–H stretching), 2960 (aliphatic C–H stretching), 1728 (C=O $\delta$-lactone stretching), 1597 and 1542 (aromatic C=C and C=N stretchings), 819 (C–H bending of *p*-disubstituted benzene ring); $^1$H-NMR (400 MHz, $CDCl_3$, $\delta$ / ppm): 2.47 (3H, *s*, $CH_3$), 6.18 (1H, *s*, $C_3$–H), 7.01–8.81 (11H, *m*, Ar-H ), 8.95 (1H, poorly resolved *d*, $C_3''$–H), 15.25 (1H, *bs*, OH); $^{13}$C-NMR (100 MHz, $CDCl_3$, $\delta$ / ppm): 19.29 ($CH_3$), 107.79 (C), 110.70 (CH), 112.40 (C), 117.72 (CH), 120.81 (CH), 123.80 (CH), 128.71 (CH), 129.69 (CH), 135.86 (CH), 136.33 (CH), 144.76 (C), 150.54 (C), 150.85 (C), 150.91 (CH), 152.19 (C), 153.38 (C), 153.62 (C), 154.94 (C), 160.21 (C), 160.63 (C), 163.54 (CO of coumarin).

## REFERENCES

1. M. S. Y. Khan, P. Sharma, *Indian J. Chem., B* **32** (1993) 374.

Journal of the Serbian Chemical Society
JSCS-info@shd.org.rs • www.shd.org.rs/JSCS
*J. Serb. Chem. Soc. 80* (6) 749–754 (2015)
*JSCS–4754*
UDC 547.657:576.314:541.132.3
*Short communication*

SHORT COMMUNICATION

# The influence of naphthenic acids and their fractions on cell membrane permeability

KSENIJA PAVLOVIĆ[1*#], LJUBICA GRBOVIĆ[1#], BOJANA VASILJEVIĆ[1#], ANDREA ŽUPUNSKI[2], MARINA PUTNIK-DELIĆ[2], IVANA MAKSIMOVIĆ[2] and SLAVKO KEVREŠAN[2**#]

[1]*Department of Chemistry, Biochemistry and Environmental Protection, Faculty of Sciences, University of Novi Sad, Trg Dositeja Obradovića 3, Serbia and* [2]*Faculty of Agriculture, University of Novi Sad, Trg Dositeja Obradovića 8, Serbia*

(Received 1 December 2014, revised 29 January, accepted 3 February 2015)

*Abstract*: The influence of naphthenic acids (NAs) mixture and their narrow fractions (called NA pH 4, pH 8 and pH 10) on the permeability of beetroot cell membrane was examined. The results showed that the effect depends on the treatment duration, concentration and the structures of the NAs. Longer treatment of plant cell membranes with sodium naphthenate (Na-naph) resulted in an increase in the membrane permeability (*e.g.*, a 4-hour treatment with Na-naph ($c$ = 100 μmol $L^{-1}$) increased the membrane permeability by about 3 times, while prolongation of treatment to 24 h resulted in an 18-fold increase in the effect). NAs in the concentration range from 0.1 to 10 μmol $L^{-1}$ did not change membrane permeability, while the membrane permeability increased linearly with increasing concentration from 10–100 μmol $L^{-1}$. The fraction pH 8, where bi- and tricyclic carboxylic acids are the most abundant, expressed the strongest effect. These structures were predominant in the total NAs mixture as well. This could explain the similar, but slightly weaker effect of the mixture, compared to the effect of the NAs present in fraction pH 8. The effect of NAs on beetroot cell membrane was between the effects of the tested anionic (SDS and LS) and non-ionic surfactants (Triton X-100).

*Keywords*: naphthenic acids (NAs); naphthenic acid fractions; physiological activity; cell membranes permeability.

## INTRODUCTION

Crude oil contains 95–98 % of structurally similar hydrocarbon molecules, while the rest consists of oxygen, sulfur and nitrogen compounds. Carboxylic

*,** Corresponding authors. E-mail: (*)ksenija.pavlovic@dh.uns.ac.rs, (**)kevresan@polj.uns.ac.rs
# Serbian Chemical Society active member.
doi: 10.2298/JSC141201012P

acids present in the oil are mostly alkane and cycloalkane compounds, called naphthenic acids (NAs). NAs present chemically stabile compounds, while, depending of the oil source, their relative molecular mass could be in a wide range and the structures quite different. Carboxylic acids are present in all types of oil, occurring in concentrations of 2.5–0.5 % or even less, on average. NAs represent a "finger print" for each type of oil, giving very important data about the genesis and nature of a particular oil.

The NAs isolated from Vojvodina crude oil Velebit[1,2] represent mixtures of alkyl-substituted cycloaliphatic and acyclic monocarboxylic acids, with bi- and tricyclic carboxylic acids being predominant.[3]

Fractionation of the total NAs, based on their different solubilities in water and modification of the solution pH afforded narrow fractions of the acids. The concentrating of the active structures into narrow fractions leads to differences in physiological activity of the fractions, mimicking the activity of certain plant hormones of the auxin and gibberellin type, which could be attributed to the structural differences of the examined NAs, determined based on high-resolution mass spectroscopy.[3]

There are very few data about the influence of NAs on cation uptake.[4,5] There are only data about their influence on the uptake of glucose[6] and phosphate ions[7] of bean plants. Previous results suggested that sodium naphthenate (Na-naph) in low concentrations acted at the level of the root cell membrane, causing subtle modifications of the membrane and changes in its permeability for cadmium ions.[8] Furthermore, low-concentration treatment of young soybean plants with Na-naph ($10^{-7}$ mol $L^{-1}$) affected the accumulation of some essential elements (Mn, Fe, Zn, Ni, K and Na).[5]

Furthermore, being amphiphilic molecules, molecules that have both hydrophilic (carboxylic group) and hydrophobic (hydrocarbon) parts, similarly to detergents, NAs could act as surfactants. It is well known that detergents could cause changes in cell function and transport through the membrane by changing the membrane structures and membrane exchange processes.[9] Thanks to their physicochemical similarities with detergents, it could be assumed that NAs could act as surfactants as well, by specific modification and thus influence the permeability of cell membranes.

The aim of this research was to study the influence of total NAs and their fractions on cell membrane permeability, using beetroot (*Beta vulgaris*) as a model-system,[10,11] and to compare the effects of NAs with the effects of amphiphilic ionic (*N*-lauroylsarcosine, sodium salt, LS and sodium dodecyl sulfate, SDS) and non-ionic (polyethylene glycol, 4-(1,1,3,3-tetramethylbutyl)phenyl-ether, Triton X-100) surfactants.

The study of changes in the permeability of plant cell membrane was performed by measuring the absorbance of samples containing betanin, originating from treated segments of beetroot.[11]

## EXPERIMENTAL

Isolation, fractionalization and characterization of naphthenic acids from Vojvodina crude oil Velebit was described previously.[1-3]

*Determination of the effects of NAs on the beetroot cell membrane permeability*

Comparative tests of the effects of Na-naph, LS, SDS and Triton X-100 were performed with concentration of the tested compounds corresponding to one *CMC* (critical micellar concentration; 1 $CMC_{\text{Na-naph}}$ = 2.4 mmol $L^{-1}$, 1 $CMC_{\text{LS}}$ = 14.6 mmol $L^{-1}$, 1 $CMC_{\text{SDS}}$ = 8.2 mmol $L^{-1}$ and 1 $CMC_{\text{Triton X-100}}$ = 0.23 mmol $L^{-1}$).

For all calculations and solution preparation, the average molar masses of total NAs ($M_{\text{NAs}}$ = 280.8 g $mol^{-1}$) and the corresponding fractions ($M_{\text{NAs pH 4}}$ = 328 g $mol^{-1}$, $M_{\text{NAs pH 8}}$ = = 425 g $mol^{-1}$ and $M_{\text{NAs pH 10}}$ = 285 g $mol^{-1}$) were used.

Stock (1 mmol $L^{-1}$) of solution Na-naph was prepared by dissolving the necessary amount of total NAs in an equimolar solution of sodium hydroxide. The solutions of the Na-naph for test were prepared by dilution with water, as well as the Na salts of the NAs fractions obtained at pH 4, 8 or 10.

Cylinders (diameter of 6 mm) removed from beetroot were cut into discs of 2 mm thickness. The obtained uniform segments were washed with water for 6 h, and then left overnight in water at 4 °C. Twenty beetroot segments were then treated with the required test solution (20 mL; experiments were repeated three times. Standard deviations of the mean results were within ±5%), and the betanin concentrations were estimated by measuring absorbance at betanin-characteristic maximum (538 nm,[11] UV/Vis 6105 Jenway, UK, spectrophotometer) immediately after adding the test solution (zero time) and after 2, 4, 6, 8, 10, 12 and 24 h.

## RESULTS AND DISCUSSION

The results of this study showed that NAs changed permeability of the cell membrane of beetroot. Namely, as can be seen from Fig. 1, the effect of Na-naph on beetroot cell membrane permeability practically laid between the effects of the tested non-ionic (Triton X-100) and ionic (LS and SDS) surfactants.

These comparative studies indicated that NAs at a 1 *CMC* concentration influenced significantly the cell membrane permeability, which prompted a study of the effect of lower concentrations of NAs on the membrane permeability. It was found that there was practically no change in the membrane permeability with increasing concentration from 0.1 to 10 μmol $L^{-1}$, while thereafter, linear increases in permeability were evidenced with further concentration increases. Based on these facts, further tests were performed with Na-naph in the concentration range from 10 to 100 μmol $L^{-1}$. The results presented on Fig. 2, show that the absorbance of the solutions at all tested concentrations increased with prolongation of the treatment. Thus, the membrane permeability had increased by about 3 times after 4 h of treatment with NAs ($c$ = 100 μmol $L^{-1}$) and nearly 18 times after 24-h treatment.

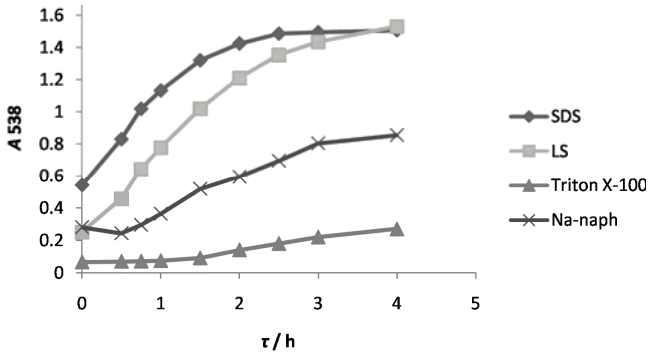


Fig. 1. Time dependencies of the cell permeabilities, estimated by the betaine-characteristic absorbance maximum (538 nm) of 1 *CMC* solutions of non-ionic (Triton X-100) and ionic (LS and SDS) surfactants and Na-naph.

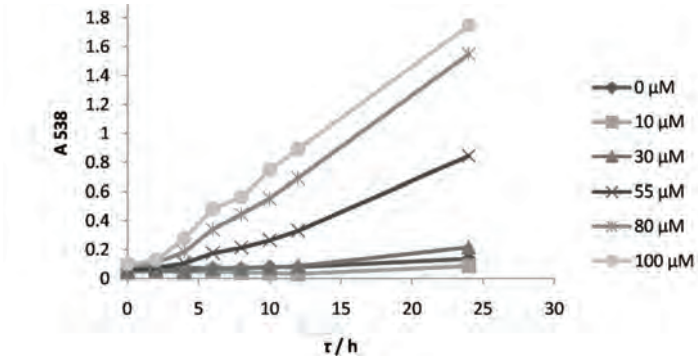


Fig. 2. Time dependency of the cell permeabilities, estimated at the betaine-characteristic absorbance maximum (538 nm) of different concentrations of total NAs salts (Na-naph).

It is evident that the strongest effect on cell membrane permeability showed the most concentrated test solution ($c$ = 100 μmol $L^{-1}$). Comparing to the solution $c$ = 10 μmol $L^{-1}$ during 24 h, this was an about 20 times stronger effect on the membranes.

Similar tendencies of increasing membrane permeability as a function of time and concentration were exhibited by aqueous solutions of Na–naph fractions. By comparing the data obtained after 24-h treatment (Fig. 3), it could be seen that the strongest effect on membrane permeability was expressed by the fraction isolated from total NAs at pH 8, and that this effect was even stronger than the effect of the total NAs. The effects on membrane permeability, based on these results could be correlated to the structures of the tested NAs.[3] Namely, in the fraction of NAs labeled as pH 8, the most common NAs were bi- and tricyclic carboxylic acids, which were also the most common in the mixture of the total NAs. The fraction isolated at pH 4, consisting predominantly of tricyclic carboxylic acids, showed a somewhat lower effect on membrane permeability. Finally,

NAs fraction isolated at pH 10, with acyclic carboxylic acids being predominant, exhibited the lowest effect.

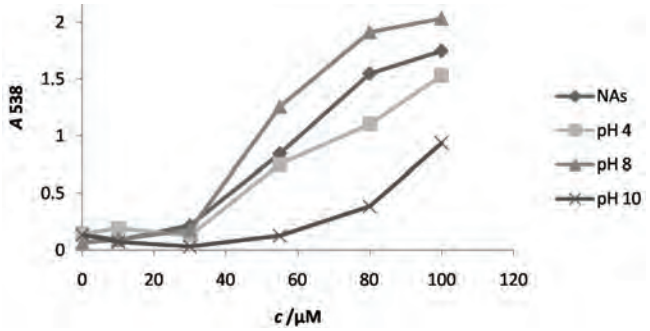


Fig. 3. Estimation of cell permeabilities 24 h after treatment with different concentrations of Na-NAs solutions of total NAs and NAs isolated at pH 4, pH 8 or pH 10, using the betaine-characteristic absorbance maximum (538 nm) as the probe.

Connected with these results, it was observed that the biggest differences in membrane permeability are expressed at $c$ = 80 μmol $L^{-1}$ (Fig. 3), whereby fraction pH 8 showed (by about 24 %) stronger and the fraction pH 4 (by about 29 %) and pH 10 (by about 75 %) lower effects compared to the mixture of total NAs.

Similar effects on membrane permeability were observed in the experiments with Na-naph solutions at $c$ = 55 and 100 μmol $L^{-1}$ (Fig. 3).

## CONCLUSION

Generally, it could be concluded that the effect of total NAs and its fractions on cell membrane permeability increased with increasing concentration and prolongation of treatment. The results showed that some differences in membrane permeability could be correlated with the structures of carboxylic acids present predominantly in the total NAs and its fractions. Namely, the fraction of NAs isolated at pH 8 had the most similar chemical composition to that of the total NAs; hence, it could be concluded that bi- and tricyclic carboxylic acids from this fraction are mostly responsible for increasing cell membrane permeability. However, the effect of the fraction isolated at pH 8 was slightly more expressed compared to the effect of the total NAs. Considering this fact and the fact that fraction pH 4, with tricyclic carboxylic acids as most common, showed something lower effect, comparing to total NAs, the conclusion is that bicyclic carboxylic acids are the mostly responsible for changes in cell membranes. Finally, fraction pH 10, with the lowest influence on cell membrane, consisted predominantly of acyclic carboxylic acids. The obtained results indicated that a possible cause of phytotoxicity of NAs could be their influence on cell membrane permeability.

*Acknowledgements*. This study was supported by the Ministry of Education, Science and Technological Development of the Republic of Serbia, Project No. 172006 and Project No. TR31036.

И З В О Д

## УТИЦАЈ НАФТНИХ КИСЕЛИНА И ЊИХОВИХ ФРАКЦИЈА НА ПРОПУСТЉИВОСТ ЋЕЛИЈСКИХ МЕМБРАНА

КСЕНИЈА ПАВЛОВИЋ[1], ЉУБИЦА ГРБОВИЋ[1], БОЈАНА ВАСИЉЕВИЋ[1], АНДРЕА ЖУПУНСКИ[2], МАРИНА ПУТНИК-ДЕЛИЋ[2], ИВАНА МАКСИМОВИЋ[2] и СЛАВКО КЕВРЕШАН[2]

*[1]Департман за хемију, биохемију и заштиту животне средине, Природно–математички факултет, Универзитет у Новом Саду, Трг Доситеја Обрадовића 3, Нови Сад и [2]Пољопривредни факултет, Универзитет у Новом Саду, Трг Доситеја Обрадовића 8, Нови Сад*

Испитиван је утицај смеше нафтних киселина (naphthenic acids; NAs) и њихових ужих фракција (означених као pH 4, pH 8 и pH 10) на пропустљивост ћелијских мембрана цвекле. Резултати су показали да ефекат зависи од времена деловања, концентрације и структуре NAs. Дужи контакт натријум-нафтената (Na-naph) са биљним мембранама доводи до пораста мембранске пропустљивости (нпр. третман Na-naph ($c$ = 100 μmol $L^{-1}$) за време од 4 сата повећава пропустљивост мембрана око три пута док продужавањем третмана на 24 сата поменути ефекат порасте око осамнаест пута). NAs у опсегу концентрација од 0,1 до 10 μmol $L^{-1}$ не изазивају промене у пропустљивости мембрана а порастом концентрације од 10–100 μmol $L^{-1}$ пропустљивост линеарно расте. Најснажнији ефекат испољила је фракција pH 8 у којој су најзаступљеније би- и трицикличне структуре карбоксилних киселина. Ове структуре су истовремено доминантне и у укупној смеши NAs чиме би се могао објаснити њихов најближи али нешто слабији ефекат у односу на карбоксилне киселине концентрисане у фракцији pH 8. Ефекат NAs на пропустљивост ћелијских мембрана цвекле је између ефекта који имају анјонски сурфактанти и нејонски сурфактант.

(Примљено 1. децембра 2014, ревидирано 29. јануара, прихваћено 3. фебруара 2015)

## REFERENCES

1. V. Ćirin-Novta, K. Kuhajda, S. Kevrešan, J. Kandrač, Lj. Radić, *Acta Period. Technol.* **33** (2002) 135
2. V. S. Ćirin-Novta, S. E. Kevrešan, K. N. Kuhajda, J. E. Kandrač, Lj. M. Radić, P. A. Rodić, *Acta Period. Technol.* **34** (2003) 49
3. Lj. Grbović, K. Pavlović, B. Prekodravac, K. Kuhajda, S. Kevrešan, M. Popsavin, J. Milić, V. Ćirin-Novta, *J. Serb. Chem. Soc.* **77** (2012) 147
4. G. G. Slivinskii, A. F. Artamonov, M. I. Goryaev, *Tsitologiya* **17** (1975) 1283
5. S. Kevrešan, V. Ćirin-Novta, K. Kuhajda, J. Kandrač, N. Petrović, Lj. Grbović, Ž. Kevrešan, *Belg. J. Bot.* **138** (2005) 11
6. J. G. Severson, *Phytochemistry* **11** (1972) 71
7. D. J. Wort, J. G. Severson, D. R. Peirson, *Plant Physiol.* **52** (1973) 162
8. S. Kevrešan, V. Ćirin-Novta, K. Kuhajda, J. Kandrač, N. Petrović, Lj. Grbović, Ž. Kevrešan, *Biol. Plant.* **48** (2004) 453
9. M. H. Mohamed, L. D. Wilson, K. M. Peru, J. V. Headley, *J. Colloid Interface Sci.* **395** (2013) 104
10. C. Grunwald, *Plant Physiol.* **43** (1968) 484
11. D. L. Sutton, C. L. Foy, *Bot. Gaz. (Chicago)* **132** (1971) 299.

Journal of the Serbian Chemical Society
JSCS-info@shd.org.rs • www.shd.org.rs/JSCS
*J. Serb. Chem. Soc. 80* (6) 755–766 (2015)
*JSCS–4755*
UDC 547.1'13+546.814+547.78+
547.367:615.281/.282–188
*Original scientific paper*

# Synthesis and spectroscopic characterization of mononuclear/binuclear organotin(IV) complexes with 1*H*-1,2,4-triazole-3-thiol: Comparative studies of their antibacterial/antifungal potencies

BUSHRA PARVEEN[1]*, IFTIKHAR HUSSAIN BUKHARI[1], SAIRA SHAHZADI[2], SAQIB ALI[2], SHABBIR HUSSAIN[1], KULSOOM GHULAM ALI[1] and MUHAMMAD SHAHID[3]

*[1]Department of Chemistry, GC University, Faisalabad, Pakistan, [2]Department of Chemistry, Quaid-i-Azam University, Islamabad 45320, Pakistan and [3]Department of Chemistry and Biochemistry, University of Agriculture, Faisalabad-38000, Pakistan*

(Received 11 July 2014, revised 30 January, accepted 21 February 2015)

*Abstract*: A series of di- and tri-organotin(IV) complexes of the general formula, $R_2(Cl)SnL$ (**1**: R = Me; **2**: R = Bu) and $R_3SnL$ (**3**: R = Bu; **4**: R = Ph) were synthesized by refluxing equivalent mole ratios of organotin(IV) chlorides ($R_2SnCl_2$/$R_3SnCl$) with 1*H*-1,2,4-triazole-3-thiol (LH) in dry methanol. The synthesized complexes (**1**–**4**) were further treated with $CS_2$ and $R_2SnCl_2$/ /$R_3SnCl$ in 1:1:1 mole ratio to yield homobimetallic complexes of the types $R_2(Cl)SnLCS_2Sn(Cl)R_2$ (**5**: R = Me; **6**: R = Bu) and $R_3SnLCS_2SnR_3$ (**7**: R = = Bu; **8**: R = Ph). The ligand and the complexes were characterized by elemental microanalysis (CHNS), FT-IR and multinuclear NMR ($^1$H- and $^{13}$C-), and electron ionization mass spectrometry. The IR data demonstrated that the dithiocarbamate donor site of the ligand acts in a bidentate manner and that the geometry around Sn(IV) is trigonal bipyramidal in the solid state. The $^1$H- and $^{13}$C-NMR data supported the tetrahedral geometry with thiol donor sites of the ligand while tetra- and penta-coordinated environments around dithiocarboxylate bound tin(IV) in the solution state. Mass spectrometric data supported well the structures of the synthesized complexes. The homobimetallic derivatives were found more active than the mononuclear organotin(IV) compounds and free ligand against various strains of bacteria and fungi.

*Keywords*: homobimetallic complex; organotin chloride; NMR; IR; mass spectra; antimicrobial study; 1*H*-1,2,4-triazole-3-thiol; dithiocarboxylate.

## INTRODUCTION

Organotin(IV) compounds are amongst the most widely used organometallic compounds owing to the variety of their industrial and agricultural applications,

* Corresponding author. E-mail: bushra_nauman@hotmail.com
doi: 10.2298/JSC140711010P

including their use as pesticides, fungicides and anti-fouling agents.[1] Interest in the complexes of main group and transition metals with sulphur donor ligands is owed to their wide variety of structures and biological applications.[2,3] Sulphur--containing organotin compounds are currently under investigations as chemo-protectants in platinum-based chemotherapy.[4] In particular, thiocarbonyl and thiol donors have shown promising properties for chemical use in modulating cisplatin nephrotoxicity.[5]

Metal dithiocarboxylates are widely used in the vulcanization of rubber,[6] as rodent repellents, as pesticides[7] and as synthetic precursors for the formation of SnS nanocrystals by their solvothermal decomposition[8] and are subjected to thermal and chemical vapour deposition (CVD) studies.[9] The chemistry of organotin(IV) derivatives with sulphur ligands has grown with prolific speed on account of multifaceted reasons. One of the important structural consequences of dithiol ligands is the preferential stabilization of a specific stereochemistry in their metal complexes and they are considered as soft donors showing excellent coordination ability. Dithiocarbamate anions are highly effective ligands owing to the stability of the resulting metal dithiocarbamates, due to a significant contribution of the resonance forms, shown in Scheme 1 (structure IV), to the overall electronic structure.[10]

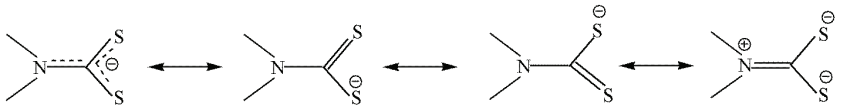


Scheme 1. Resonant forms of the –NCSS$^-$ moiety.

In view of structural importance and biological applications of organotins, a new series of di- and tri-alkyl/aryltin derivatives of 1*H*-1,2,4-triazole-3-thiol ($C_2H_3N_3S$) were synthesized. The choice of the ligand was made based on that after insertion of $CS_2$ it has the simultaneous availability of thiol and dithiocarbamate donor sites, thus enabling its bimetallic complexation with organotin moieties. The products were characterized by elemental analysis, FT-IR, $^1$H- and $^{13}$C-NMR spectroscopy and mass spectrometry. These complexes were screened against various bacteria and fungi to investigate their possible use as antibacterial and antifungal agents.

## EXPERIMENTAL

### *Chemicals and instrumentation*

1*H*-1,2,4-Triazole-3-thiol, triphenyltin chloride, tributyltin chloride, dibutyltin dichloride and dimethyltin dichloride were purchased from Aldrich (USA) and were used without any further purification. $CS_2$ was obtained from Riedel-de-Haën. The organic solvents of analytical grade (chloroform, *n*-hexane, ethanol, methanol, DMSO and acetone) were procured

from Merck (UK). Nutrient agar, nutrient broth, and potato dextrose agar (PDA) were purchased from Oxoid Company (UK). The solvents were dried by standard procedures.[11] Melting points were determined in capillary tubes on an electrothermal melting point apparatus, model Stuart SMP3 (UK), and are uncorrected. The percentage composition of carbon, hydrogen, nitrogen and sulphur were determined using a CHNS-932 Leco (USA). The FT-IR spectra in the range of 4000–250 $cm^{-1}$ were obtained on a Thermo Nicolet-6700 FT-IR spectrophotometer. The NMR spectra were recorded on a Bruker AM-250MHz FT-NMR spectrometer (Germany). Mass spectral data were measured on a JEOL JMS 600-H mass spectrometry in the ionization mode at 70 eV. The antimicrobial activities were determined in an incubator (Sanyo, Germany) and sterilized in an autoclave (Omron, Japan).

Physical, analytical and spectral data of the synthesized compounds are given in Supplementary material to this paper.

*General procedure for the synthesis of the homobimetallic complexes*

*Step-1*. 1*H*-1,2,4-Triazole-3-thiol (1 mmol) and $R_2SnCl_2/R_3SnCl$ (1 mmol) were refluxed together in 20 mL dry methanol for 6 h.[12] The solvent was evaporated under reduced pressure on a rotary evaporator. The formed precipitates were filtered and dried in open air. The product was recrystallized from ethanol.

*Step-2*. The product (1 mmol) obtained in 1st step was dissolved in methanol (15 mL) in a round-bottom two-necked flask with stirring. To the above solution, $CS_2$ (1 mmol) was added dropwise at room temperature and the reaction mixture was stirred for 30 min.[13] Then $R_2SnCl_2/R_3SnCl$ was added in 1:1 mole ratio and the reaction mixture was refluxed for 6–7 h (Scheme 2). The solvent was evaporated slowly at room temperature and the product was dried in air. The product was recrystallized from ethanol.

*Antimicrobial activities*

*Growth medium, culture and inoculum preparation*. The bacterial strains (*Escherichia coli, Bacillus subtilis, Staphylococcus aureus* and *Pasteurella multocida*) were cultured in nutrient agar medium at 37 °C overnight. The pure bacterial cultures obtained were maintained in the medium in slants and Petri plates. For inoculums preparation, 13 g of nutrient broth was added to one litre of distilled water, mixed homogenously and was autoclaved for 15 min at 121 °C. Then 10 μL of pure culture of a bacterial strain was added to this freshly prepared nutrient broth medium (100 mL) and incubated in a shaker (140 rpm) at 37 °C for 24 h. The prepared inocula were stored at 4 °C. Inocula with $1\times10^8$ spores $mL^{-1}$ were used for further analysis.

The fungal strains (*Aspergillus niger, Aspergillus flavus, Rhizoctonia solani* and *Alternaria alternata*) were cultured in potato dextrose agar medium overnight at 28 °C. The pure cultures were maintained in Sabouraud dextrose agar (SDA) medium in slants and Petri plates, which had been pre-sterilized in a hot air oven at 180 °C for 3 h. These cultured slants were incubated at 28 °C for multiplication of fungal strains for 3–4 days.

*Antibacterial/antifungal assay by the disc diffusion method*. The antibacterial and antifungal activities of the ligand and the synthesized complexes were determined by the disc diffusion method.[14] For medium preparation, 2.8 g of nutrient agar (for the antibacterial activities) or 3.9 g of potato dextrose agar (for the antifungal activities) was suspended in 100 mL distilled water and mixed well to distribute homogenously. After this, the medium was sterilized by autoclaving at 121 °C for 15 min, mixed well with 100 μL inoculums and transferred into the sterilized Petri plates. Then small filter paper discs (size, 9 mm) each soaked with 100 μL solution of a test sample were placed flat on the growth medium and the

Petri plates were incubated for 24 h at 37 °C for the bacterial growth and for 48 h at 28 °C for the fungal growth. The biologically active samples inhibited the bacterial/fungal growth to form clear zones. A zone reader was used to measure the zones of inhibition in mm.

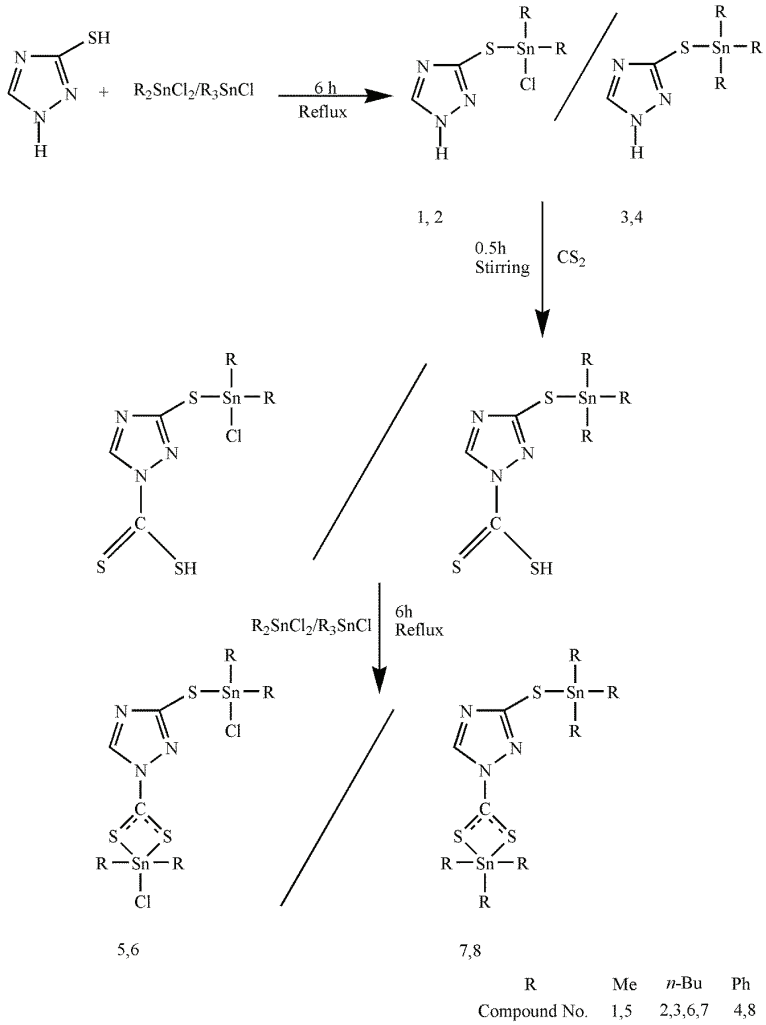


Scheme 2. Synthesis of the homobimetallic complexes.

*Statistical analysis*

The antimicrobial activity data are presented in the tabulation mode along with their mean, standard deviation and the data were tested by one-way ANOVA.[15]

## RESULTS AND DISCUSSION

The synthesized complexes were solid and stable in air. They had sharp melting points and were soluble in common organic solvents. The elemental (C,

H, N and S) analysis data agreed very well with the proposed formulas of the complexes. The physical data of ligand and its complexes are summarized in Table S-I of the Supplementary material to this paper.

*Infrared spectroscopy*

IR spectra of HL and complexes were recorded in the range of 4000 to 250 $cm^{-1}$ and data is given in Table S-II of the Supplementary material. The values related to different functional groups were assigned by comparison of the spectra of the complexes with that of the free ligand. The precursor ligand (LH) exhibited a broad band at 2560 $cm^{-1}$ due to ν(S–H) vibrations. This band was absent in the spectra of complexes **1**–**8** due to sulphur–tin coordination, which was also confirmed by the appearance of ν(Sn–S) bands in the region 437–471 $cm^{-1}$ in the spectra of the complexes.[16] All the complexes displayed a sharp Sn–C peak in the range 535–563 $cm^{-1}$, except for triphenyltin(IV) derivatives, for which a weak vibration appeared at 263–265 $cm^{-1}$ due to Sn–C stretching.[17] The chlordiorganotin derivatives **1**, **2**, **5** and **6** displayed a peak associated with ν(Sn–Cl) in the region 320–336 $cm^{-1}$.[18]

In the free ligand, ν(NH) band appeared at 3148 $cm^{-1}$; the maintenance of this band in almost the same region (3143–3149 $cm^{-1}$) in complexes **1**–**4** evidently described the non-involvement of the imino nitrogen in bonding with tin. However, the ν(NH) stretching vibration was absent in the spectra of complexes **5**–**8** due to insertion of $CS_2$ and the consequent bonding of the dithiocarbamate moiety with tin. Thus, new bands appeared for ν(C–S) and ν(C–N) stretching vibrations that gave valuable information about the coordination behaviour of the dithiocarbamate group (N–CSS) to the tin atom. In the IR spectra of complexes **5**–**8**, the strong peaks at 1034–1051 $cm^{-1}$ and 963–976 $cm^{-1}$ were assigned to the asymmetric absorption $\nu(CS_2)_{asym}$ and the symmetric absorption $\nu(CS_2)_{sym}$ frequencies, respectively. According to the literature,[19] the differences between $\nu(CS_2)_{asym}$ and $\nu(CS_2)_{sym}$ of 68–79 $cm^{-1}$ for complexes **5**–**8** indicated that the 1,1-dithioate moiety was linked to the central tin in a bidentate fashion. The values of ν(N–CSS) stretching vibrations (1456–1505 $cm^{-1}$) fall between those reported for C–N single bond (1250–1360 $cm^{-1}$) and C=N double bond (1640––1690 $cm^{-1}$), which is an indication of the partial double bond character of the C–N bond.[16,20] A partial double bond character for the C–N bond would result in some partial double bond character for the C–S bonds, as a result both the sulphur atoms were involved in coordination with the metal, resulting in bidentate coordination[16] and pentacoordinated geometry.[21] This interaction could be viewed as the coordination of one normal Sn–S bond and one weak Sn–S bond. A weak Sn–S bond is possibly through π overlap of the empty d-orbitals of the tin atom and the p-orbitals of sulphur.

*$^{1}$H-NMR*

The $^{1}$H-NMR spectra were recorded for compounds **1**–**8** in DMSO-$d_6$. The characteristic chemical shifts (Table S-III of the Supplementary material) were recognized by their intensity and multiplicity patterns. The numbers of protons, calculated from the integration curves, were in agreement with the proposed molecular structure theoretically calculated by the incremental method.[22] The singlet resonance at 13.357 ppm for –SH proton of the free ligand (HL) was absent in the spectra of all the complexes **1**–**8** and was taken as verification of thiol––tin coordination.[23] The signal at 11.48 ppm for the imino proton of the free ligand persisted in the spectra of complexes **1**–**4**, indicating its non-involvement in coordination; however, this signal was absent in the spectra of complexes **5**–**8**, due to insertion of –CSS in order to develop the dithiocarbamate–tin linkage. New signals in the expected range for the organotin moieties were evidence for complex formation.[23,24] In the *n*-butyl derivatives **2**, **3**, **6** and **7**, the terminal methyl protons absorb at 0.87–0.80 ppm as a triplet with a $^{3}J(^{1}\text{H}–^{1}\text{H})$ coupling constant of 7.0–7.2 Hz, while the $\alpha$-$CH_2$, $\beta$-$CH_2$ and $\gamma$-$CH_2$ protons appear as multiplets.[25] In the dimethyltin(IV) derivative **5**, the $CH_3$ protons gave a sharp singlet at 1.46 ppm[23,26] with a $^{2}J[^{119}\text{Sn}–^{1}\text{H}]$ coupling constant of 79 Hz, which corresponds to trigonal bipyramidal geometry of tin in the solution state. In the triphenyltin derivatives **4** and **8**, the phenyl group attached to the Sn atom gave complex multiplets in the range of 7.31–7.96 ppm.[27]

*$^{13}$C-NMR*

The characteristic resonance signals in the $^{13}$C-NMR spectra of the selected complexes, recorded in DMSO, are given in Table S-IV of the Supplementary material. The upfield resonance shift of the SH bonded carbon (labelled as 2) from 165.57 ppm in the free ligand to 152.11–154.33 ppm in the complexes, indicates that the ligand acts in the thiolate form and this carbon is deshielded upon complexation of the ligand to the positive Sn center.[23] The –CSS group in the complexes gave a signal in the range 191.36–194.85 ppm, indicating the coordination of sulphur to tin. The methyl group linked to the Sn atom in complex **5** gave a sharp signal at 10.6 ppm.[28] Complexes **6** and **7** showed signals of the *n*-butyl group in the range of 13.5–14.7 ppm (for $CH_3$) and 25.4–29.3 ppm (for $CH_2$).[29] In complex **8**, the phenyl carbons gave signals in the range 129.5––138.1 ppm in the $^{13}$C-NMR spectra, as reported earlier.[30]

In order to gain further information regarding the possible coordination geometries in solution, the $^{1}J[^{119}\text{Sn}–^{13}\text{C}]$ and $^{2}J[^{119}\text{Sn}–^{1}\text{H}]$ coupling constants were examined closely, as structural details, such as the determination of C–Sn–C bond angles, can be obtained by use of the methods reported in the literature.[31,32] The C–Sn–C bond angles, calculated by application of the Lockhart equation[31,32] are given in Table S-V of the Supplementary material; the data strongly supports

the trigonal bipyramidal geometries in the chlorodialkyltin(IV) derivatives **5** and **6**, while a tetrahedrally coordinated metal centre was supported in the tributyltin(IV) complex **7**.

*Mass spectrometry*

The conventional EI mass spectral data at 70 eV for both the ligand and the complexes were recorded along with *m*/*z* and intensity, which are listed in Table S-VI of the Supplementary material. In mass spectral data of the compounds, each fragment ion occurred in a group of peaks as a result of tin isotopes. For simplicity, the mass spectral fragmentation data reported here are related to the principal isotope $^{120}Sn$ or $^{120}Sn^{35}Cl$ peak in each species, and must be regarded as approximate.[33] The molecular ion peaks, $M^+$, are either not observed or if observed have very low intensities in synthesized organotin complexes. The fragmented ions are in good agreement with the expected structure of the compounds and consistent with the literature.[34,35] For the triorganotin compounds, the primary fragmentation from the molecular ion appeared in two ways. The first one was initiated with the loss of R (R = Bu or Ph), whereas the second fragmentation was due to the loss of ligand (L). For complexes **3** and **4**, the former pattern predominated and gave $C_2H_2N_3SSnR_2^+$ species, which could then lose either R–R or R in two successive steps to form further $EE^+$. The $[R_3Sn]^+$, formed by the loss of the ligand part, forms a $[Sn]^+$ fragment by the successive elimination of the R radical. Somewhat different mass fragments were suggested for the diorganotin compounds, but these pathways end up in a similar fashion as suggested for the triorganotin compounds. In addition, the following ions were also observed with reasonable intensities in the mass spectra of all organotin(IV) derivatives, $[C_6H_5]^+$, $[C_4H_9]^+$ and $[CH_3]^+$.

*Antibacterial activity*

The synthesized complexes and free ligand were screened for their *in vitro* antibacterial activities by the disc diffusion method[11] against *S. aureus*, *E. coli*, *B. subtilis* and *P. multocida*, and the results were summarized in Table I. The data revealed that the synthesized complexes had significant antimicrobial activities against the pathogenic bacteria as compared to the ligand, which indicates that metallation increased antibacterial activity in accordance with earlier reports.[36] This higher activity may be ascribed to the Tweedy theory, according to which chelation reduces the polarity of the central metal atom because of partial sharing of its positive charge with the ligand, which favours the permeation of the complex through the lipid layer of the membrane.[37,38]

In general, the triorganotin(IV) complexes were found to be more active than the diorganotin(IV) complexes, a trend consistent with an earlier report.[39] Complex **8** showed strong antibacterial activity against *E. coli*, while complexes **1** and **5** exhibited strong antibacterial activity against *P. multocida.*

TABLE I. Antibacterial activity (bacterial inhibition zone, mm) data of organotin(IV) complexes **1**–**8**; concentration = 10 mg $mL^{-1}$ in DMSO; standard = rifampicin. The antibacterial values are mean±*SD* of three samples analyzed individually in triplicate. Different letters in superscripts indicate significant differences; a = maximum activity, b = intermediate activity, c = minimum activity, ab = activity between maximum and intermediate and bc = activity between intermediate and minimum

| Compd. | Bacterium | | | |
|---|---|---|---|---|
| | *S. aureus* | *E. coli* | *B. subtilis* | *P. multocida* |
| HL | $11.2^{c}$±0.7 | $16.1^{c}$±0.1 | $12.2^{c}$±0.7 | $13.2^{c}$±0.7 |
| **1** | $17^{b}$±0.5 | $24.5^{b}$±0.5 | $19.5^{bc}$±0.1 | $22.5^{ab}$±1.0 |
| **2** | $14.5^{bc}$±0.7 | $19^{bc}$±0.5 | $14^{bc}$±0.2 | $15.1^{bc}$±0.1 |
| **3** | $16^{b}$±0.5 | $25.2^{ab}$±0.7 | $15.5^{bc}$±0.1 | $14.5^{bc}$±0.1 |
| **4** | $19.5^{ab}$±0.1 | $27.8^{ab}$±0.7 | $21^{ab}$±0.1 | $20.2^{ab}$±0.5 |
| **5** | $16^{b}$±0.5 | $26.5^{ab}$±0.5 | $21.5^{b}$±0.5 | $23.8^{ab}$±0.1 |
| **6** | $17^{b}$±0.5 | $21.8^{bc}$±0.1 | $15.5^{bc}$±0.5 | $16.3^{bc}$±0.5 |
| **7** | $17.5^{b}$±0.1 | $26^{ab}$±0.5 | $17^{ab}$±0.5 | $19^{b}$±0.5 |
| **8** | $22^{ab}$±0.5 | $28.3^{ab}$±0.1 | $22.3^{ab}$±0.7 | $15.5^{bc}$±0.1 |
| Standard | $32^{a}$±0.5 | $38^{a}$±0.7 | $30^{a}$±0.5 | $37^{a}$±0.5 |

The variation in the trends for these compounds may be explained based on three possible factors, *i.e.*, lipophilic character, diffusion and on the bacterial strain. The former two factors are associated with complexes. The lipophilic character increased with increasing chain length whereas diffusion has an inverse effect. The enhanced activities of the triorganotin complexes could be well described by the lipophilic character. In some cases, the diorganotin complexes were found more active, *e.g.*, in dimethyltin complexes due to dominating diffusive nature of small methyl group. The reported bimetallic organotin(IV) complexes show enhanced antibacterial activity compared to monometallic organotin(IV) complexes.[40,41] No compound showed better inhibitory action than the standard drug.

*Antifungal activity*

The disc diffusion method was employed to test the antifungal activities of the synthesized compounds against four different strains of fungi, *A. niger*, *A. flavus*, *R. solani* and *A. alternata* and fluconazole was used as the standard drug. The results are shown in Table II. The complexes exhibited greater antifungal potentials than the precursor ligand, which may be due to the chelation and the presence of sulphur atoms.[42] The triorganotin(IV) derivatives were more active than the diorganotin(IV) complexes against the fungal strains and even more than the standard drug. The higher activity of complex **3** may be due to highest lipophilic character of the tributyltin(IV) derivatives.[43] That the homobimetallic complexes showed greater activity might be due to the presence of two Sn atoms.[13,40,41]

TABLE II. Antifungal activity data (fungal inhibition zone, mm) of organotin(IV) complexes **1**–**8**; concentration = 10 mg/mL in DMSO; standard = fluconazole. The antifungal values are mean±*SD* of three samples analyzed individually in triplicate. Different letters in superscripts indicate significant differences; a = maximum activity, b = intermediate activity, c = minimum activity, ab = activity between maximum and intermediate and bc = activity between intermediate and minimum

| Compd. | Fungus | | | |
|---|---|---|---|---|
| | *A. niger* | *A. flavus* | *R. solani* | *A. alternata* |
| HL | $10.2^{c}\pm0.5$ | $13.2^{c}\pm0.8$ | $8.0^{c}\pm1.0$ | $10.0^{c}\pm0.5$ |
| **1** | $11.2^{c}\pm0.3$ | $13.9^{c}\pm0.5$ | $10.2^{c}\pm0.1$ | $19.2^{bc}\pm1.0$ |
| **2** | $21.6^{bc}\pm0.7$ | $10.1^{c}\pm0.4$ | $9.0^{c}\pm0.2$ | $23.2^{bc}\pm0.1$ |
| **3** | $44^{ab}\pm0.5$ | $46.4^{a}\pm0.2$ | $36^{ab}\pm0.5$ | $36.0^{ab}\pm0.5$ |
| **4** | $36^{ab}\pm1.2$ | $32.3^{ab}\pm0.2$ | $31.2^{bc}\pm0.3$ | $35.2^{bc}\pm1.0$ |
| **5** | $11.5^{c}\pm0.3$ | $13.5^{c}\pm0.5$ | $10.1^{c}\pm0.5$ | $22.3^{bc}\pm0.1$ |
| **6** | $21.5^{bc}\pm0.7$ | $10.5^{c}\pm0.7$ | $8.6^{c}\pm0.5$ | $21.3^{bc}\pm0.5$ |
| **7** | $49.2^{a}\pm0.5$ | $48.2^{a}\pm0.1$ | $54^{a}\pm0.7$ | $42.8^{a}\pm0.1$ |
| **8** | $39^{ab}\pm0.5$ | $41.5^{a}\pm0.5$ | $34.3^{ab}\pm0.1$ | $38.8^{ab}\pm0.5$ |
| Standard | $26^{b}\pm0.5$ | $28^{b}\pm0.5$ | $30^{b}\pm0.5$ | $29.2^{b}\pm0.5$ |

## CONCLUSIONS

Homobimetallic complexes of organotin(IV) with a sulphur–sulphur donor ligand (1*H*-1,2,4-triazole-3-thiol) were synthesized under reflux. An IR study confirms the dithiocarbamate donor site of the ligand acts in a bidentate manner and showed trigonal bipyramidal geometry around Sn(IV) in the solid state. NMR data revealed that the tetrahedral geometry with thiol donor sites of the ligand while tetra- and penta-coordinated environments around dithiocarbamate bound tin(IV) in the solution state. Mass spectrometric and elemental analysis data supported the solid and solution spectroscopic results. Antimicrobial results revealed that the activity was enhanced upon coordination with tin. In addition, the triorganotin(IV) derivatives superseded the diorganotin(IV) compounds in their antimicrobial action. Such a study would be helpful in the design of novel metal-based drugs.

## SUPPLEMENTARY MATERIAL

The physical, analytical and spectral data of the synthesized complexes, Tables S-I–S--VI, are available electronically from http://www.shd.org.rs/JSCS/, or from the corresponding author on request.

*Acknowledgment*. Bushra Parveen thanks the Higher Education Commission, Islamabad, Pakistan, for financial support under the PhD Fellowship Scheme Batch-VI (PIN Code: 106--2038-ps6-083).

ИЗВОД

## СИНТЕЗА И СПЕКТРОСКОПСКА КАРАКТЕРИЗАЦИЈА МОНО- И ДИНУКЛЕАРНИХ КОМПЛЕКСА КАЛАЈА(IV) СА 1*H*-1,2,4-ТРИАЗОЛ-3-ТИОЛОМ: УПОРЕДНА ИЗУЧАВАЊА ЊИХОВЕ АНТИБАКТЕРИЈСКЕ И АНТИФУНГАЛНЕ АКТИВНОСТИ

BUSHRA PARVEEN[1], IFTIKHAR HUSSAIN BUKHARI[1], SAIRA SHAHZADI[2], SAQIB ALI[2], SHABBIR HUSSAIN[1], KULSOOM GHULAM ALI[1] и MUHAMMAD SHAHID[3]

*[1]Department of Chemistry, GC University, Faisalabad, Pakistan, [2]Department of Chemistry, Quaid-i-Azam University, Islamabad 45320, Pakistan and [3]Department of Chemistry and Biochemistry, University of Agriculture, Faisalabad-38000, Pakistan*

Синтетисана је серија ди- и триорагано комплекса калаја(IV), опште формуле $R_2(Cl)SnL$ (**1**: R = Me; **2**: R = Bu) и $R_3SnL$ (**3**: R = Bu; **4**: R = Ph). Комплекси су синтетисани рефлуксом еквимоларних количина калај(IV)-хлорида ($R_2SnCl_2$/$R_3SnCl$) и 1*H*-1,2,4-триазол-3-тиола (LH) у сувом метанолу као растварачу. Овако синтетисани комплекси **1**–**4** су након третирања са $CS_2$ и $R_2SnCl_2$/$R_3SnCl$ (у молском односу 1:1:1) наградили полинуклеарне Sn(IV) комплексе, опште формуле $R_2(Cl)SnLCS_2Sn(Cl)R_2$ (**5**: R = = Me; **6**: R = Bu) and $R_3SnLCS_2SnR_3$ (**7**: R = Bu; **8**: R = Ph). Полазни лиганд и комплекси су окарактерисани помоћу елементалне микроанализе, FT-IR и NMR ($^1$H- и $^{13}$C-) спектроскопије, као и масене спектрометрије. На основу IR података закључено је да се испитивани лиганд преко дитиокарбаматног дела молекула бидентатно координује формирајући у чврстом стању тригонално-бипиримидалну геометрију Sn(IV) комплекса. На основу $^1$H- и $^{13}$C-NMR испитивања у раствору нађено је да се испитивани лиганд координује преко тиолног атома сумпора и гради тетраедарску геометрију комплекса, док се у случају дитиокарбоксилатне координације лиганда граде комплекси са тетра- и пентакоординационом сфером око калаја(IV). Резултати добијени на основу масене спектрометрије су у сагласности са спектроскопски претпостављеном геометријом испитиваних комплекса. На основу испитивања активности на различитим сојевима бактерија и гљива закључено је да су полинуклеарни комплекси активнији од одговарајућих мононуклеарних Sn(IV) комплекса.

(Примљено 11. јула 2014, ревидирано 30. јануара, прихваћено 21. фебруара 2015)

## REFERENCES

1. M. Gielen, A. G. Davies, K. Pannell, E. Tiekink, Eds., *Tin Chemistry: Fundamentals, Frontiers and Applications*, Wiley, Chichester, 2008
2. S. Shahzadi, S. Ali, *J. Iran. Chem. Soc.* **5** (2008)16
3. E. R. T. Tiekink, *Appl. Organomet. Chem.* **22** (2008) 533
4. N. Ferrell, *Transition* in *Catalysis by Metal Complexes*, Vol. 11, B. R. James, R. Ugo, Eds., Kluwer, Dordrecht, 1989, p. 44
5. R. T. Dorr, H. M. Pinedo, J. H. Schornagel, *Platinum and Other Metal Coordination Compounds in Cancer Chemotherapy*, Vol. 2, Plenum Press, New York, 1996, p. 131
6. P. J. Nieuwenhuizen, J. Reedijk, M. Van Duin, W. J. McGill, *Rubber Chem. Technol.* **70** (1997) 368
7. M. Cicotti, *Handbook of Residue Analytical Methods for Agrochemicals*, Vol. 2, Wiley, Chichester, 2003
8. D. C. Menezes, G. M. De Lima, A. O. Porto, C. L. Donnici, J. D. Ardisson, A. C. Doriguetto, J. Ellena, *Polyhedron* **23** (2004) 2103
9. A. T. Kana, T. G. Hibbert, M. F. Mahon, K. C. Molloy, I. P. Parkin, L. S. Price, *Polyhedron* **20** (2001) 2989

10. Zia-ur-Rehman, N. Muhammada, S. Shuja, S. Ali, I. S. Butler, A. Meetsma, M. Khan, *Polyhedron* **28** (2009) 3439
11. W. L. F. Armarego, C. L. L. Chai, *Purification of Laboratory Chemicals*, Elsevier, New York, 2003
12. T. R. Fritsche, M. Dermott, T. R. Shryock, R. D. Walker, *J. Clin. Microbiol.* **45** (2007) 2758
13. J. Anwer, S. Ali, S. Shahzadi, M. Shahid, S. K. Sharma, K. Qanungo, *J. Coord. Chem*. **66** (2013) 1142
14. Zia-ur-Rehman, M. M. Barsan, I. Wharf, N. Muhammad, S. Ali, A. Meetsma, I. S. Butler, *Inorg. Chim. Acta* **361** (2008) 3322
15. F. G. D. Steel, J. H. Torrie, D. A. Dikey, *Principles and Procedures of Statistics: a Biometrical Approach*, 3rd ed., McGraw Hill, New York, 1997
16. S. Hussain, S. Ali, S. Shahzadi, S. K. Sharma, K. Qanungo, M. Altaf, H. S. Evans, *Phosphorus Sulfur Silicon Relat. Elem*. **186** (2011) 542
17. M. Rizwan, S. Ali, S. Shahzadi, S. K. Sharma, K. Qanungo, M. Shahid, S. Mahmood, *J. Coord. Chem*. **67** (2014) 341
18. A. A. Soliman, G. G. Mohammed, *Thermochim. Acta* **42** (2004) 151
19. I. Baba, A. F. Abdul-Muthalib, Y. F. Abdul-Aziz, N. S. Weng, *Phosphorus Sulfur Silicon Relat. Elem*. **186** (2011) 1326
20. S. Thirumaran, K. Ramalingam, *Transition Met. Chem.***25** (2000) 60
21. H. L. Singh, A. K. Varshney, *Appl. Organomet. Chem.* **15** (2001) 762
22. H. O. Kalinowski, S. Berger, S. Braun, *$^{13}$C NMR Spektroskopie*, Vol. 56, Thieme, Stuttgart, 1984, p. 133
23. C. Ma, J. Li, R. Zhang, *Heteroatom Chem*. **17** (2006) 353
24. R. Singh, N. K. Kaushik, *Spectrochim. Acta, A* **72** (2009) 691
25. M. Nath, M. Sulaxna, X. Song, G. Eng, *J. Organomet. Chem.* **691** (2006) 1649
26. Q. Wang, Q. C. Ma, G. He, Y. Li, *Heteroatom Chem*. **23**(2012) 531
27. M. Hussain, M. Zaman, M. Hanif, S. Ali, M. Danish, *J. Serb. Chem. Soc.* **73** (2008) 179
28. M. Careri, A. Mangla, G. Predieri, C. Vignali, *J. Organomet. Chem*. **375** (1989) 39
29. S. Shahzadi, S. Ali, M. H. Bhatti, M. Fettouhi, M. Athar, *J. Organomet. Chem*. **691** (2006) 1797
30. Y. F. Win, S. G. Teoh, T. S. T. Muhammad, Y. Sivasothy, S. T. Ha, *Am. J. Appl. Sci*. **301** (2010) 31
31. T. P. Lockhart, W. F. Manders, *Inorg. Chem*. **25** (1986) 892
32. J. Holecek, M. Nadvornik, K. Handlir, A. Lycka, *J. Organomet. Chem.* **315** (1986) 299
33. A. G. Davies, *Organotin Chemistry*, 2nd ed., Wiley–VCH, Weinheim, 2004, pp. 17–22
34. Zia-ur-Rehman, N. Muhammad, S. Ali, I. S. Butler, A. Meetsma, *Inorg. Chim. Acta* **373** (2011) 187
35. A. Tarassoli, T. Sedaghat, B. Neumuller, M. Ghassemzadeh, *Inorg. Chim. Acta* **318** (2001) 15
36. E. R. T. Tiekink, *Appl. Organomet. Chem*. **22** (2008) 533
37. B. G. Tweedy, *Phytopathology* 55 (1964) 910
38. S. S. Konstantinović, B. C. Radovanović, S. P. Sovilj, S. Stanojević, *J. Serb. Chem. Soc*. **73** (2008) 7
39. K. Tahira, S. Ali, S. Shahzadi, S. K. Sharma, K. Qanungo, *J. Coord. Chem*. **64** (2011) 1871
40. M. K. Samota, G. Seth, *Heteroatom Chem.* **21** (2010) 44
41. L. Dostal, R. Jambor, A. Ruzicka, R. Jirasko, J. Taraba, J. Holecek, *J. Organomet. Chem*. **692** (2007) 3750

42. T. R. Fritsche, P. F. McDermott, T. R. Shryock, R. D. Walker, *J. Clin. Microbiol*. **45** (2007) 2758
43. G. J. M. van der Kerk, J. G. A. Luijten, *J. Appl. Chem*. **6** (1956) 56.

Journal of the Serbian Chemical Society
JSCS@tmf.bg.ac.rs • www.shd.org.rs/JSCS
*J. Serb. Chem. Soc. 80* (6) S208–S211 (2015) *Supplementary material*

SUPPLEMENTARY MATERIAL TO

# Synthesis and spectroscopic characterization of mononuclear/binuclear organotin(IV) complexes with 1*H*-1,2,4-triazole-3-thiol: Comparative studies of their antibacterial/antifungal potencies

BUSHRA PARVEEN[1]*, IFTIKHAR HUSSAIN BUKHARI[1], SAIRA SHAHZADI[2], SAQIB ALI[2], SHABBIR HUSSAIN[1], KULSOOM GHULAM ALI[1] and MUHAMMAD SHAHID[3]

[1]*Department of Chemistry, GC University, Faisalabad, Pakistan,* [2]*Department of Chemistry, Quaid-i-Azam University, Islamabad 45320, Pakistan and* [3]*Department of Chemistry and Biochemistry, University of Agriculture, Faisalabad-38000, Pakistan*

*J. Serb. Chem. Soc.* 80 (6) (2015) 755–766

TABLE S-I. Physical data for the organotin(IV) complexes **1**–**8**

| Compd. | Mol. formula | MW g mol$^{-1}$ | M.p. °C | Yield % | Calcd. (found), % | | | |
|---|---|---|---|---|---|---|---|---|
| | | | | | C | H | N | S |
| HL | $C_2H_3N_3S$ | 101 | 232–34 | – | 23.73 (23.27) | 2.96 (2.99) | 41.53 (41.97) | 31.64 (31.56) |
| **1** | $C_4H_8ClN_3SSn$ | 284.5 | 208–11 | 41.8 | 16.87 (16.76) | 2.81 (2.71) | 14.76 (14.68) | 11.24 (11.39) |
| **2** | $C_{10}H_{20}ClN_3SSn$ | 368.5 | 219–22 | 91.2 | 32.56 (32.51) | 5.42 (5.41) | 11.39 (11.49) | 8.68 (8.62) |
| **3** | $C_{14}H_{29}N_3SSn$ | 390 | 122–25 | 60 | 43.96 (42.93) | 7.43 (7.27) | 10.76 (10.63) | 8.20 (8.39) |
| **4** | $C_{20}H_{17}N_3SSn$ | 450 | 197–99 | 93.2 | 53.33 (53.39) | 3.77 (3.49) | 9.33 (9.28) | 7.11(7.20) |
| **5** | $C_7H_{13}Cl_2N_3S_3Sn_2$ | 544 | 202–04 | 58 | 15.44 (15.40) | 2.38 (2.55) | 7.72 (7.75) | 17.64 (17.54) |
| **6** | $C_{19}H_{37}Cl_2N_3S_3Sn_2$ | 712 | 214–15 | 68.3 | 31.97 (31.86) | 5.19 (5.23) | 5.89 (5.73) | 13.48 (13.66) |
| **7** | $C_{27}H_{55}N_3S_3Sn_2$ | 755 | 115–18 | – | 42.91 (42.75) | 7.28 (7.21) | 5.56 (5.51) | 12.71 (12.70) |
| **8** | $C_{39}H_{31}N_3S_3Sn_2$ | 875 | 183–185 | 79.3 | 53.48 (53.22) | 3.54 (3.46) | 4.80 (4.42) | 10.97 (10.80) |

* Corresponding author. E-mail: bushra_nauman@hotmail.com

TABLE S-II. Infrared absorption bands ($cm^{-1}$) of organotin(IV) complexes **1**–**8**

| Compd. | ν(S–H) | ν(N–H) | ν(C–N) | $\nu(CS_2)_{asym}$ | $\nu(CS_2)_{sym}$ | ν(Sn–C) | ν(Sn–S) | ν(Sn–Cl) |
|---|---|---|---|---|---|---|---|---|
| HL | 2560 | 3148 | – | – | – | – | – | – |
| **1** | – | 3148 | – | – | – | 560 | 470 | 335 |
| **2** | – | 3149 | – | – | – | 535 | 447 | 328 |
| **3** | – | 3145 | – | – | – | 545 | 441 | – |
| **4** | – | 3143 | – | – | – | 265 | 437 | – |
| **5** | – | – | 1505 | 1048 | 973 | 563 | 471 | 336 |
| **6** | – | – | 1490 | 1044 | 976 | 539 | 449 | 320 |
| **7** | – | – | 1475 | 1051 | 972 | 556 | 445 | – |
| **8** | – | | 1456 | 1034 | 963 | 263 | 438 | – |

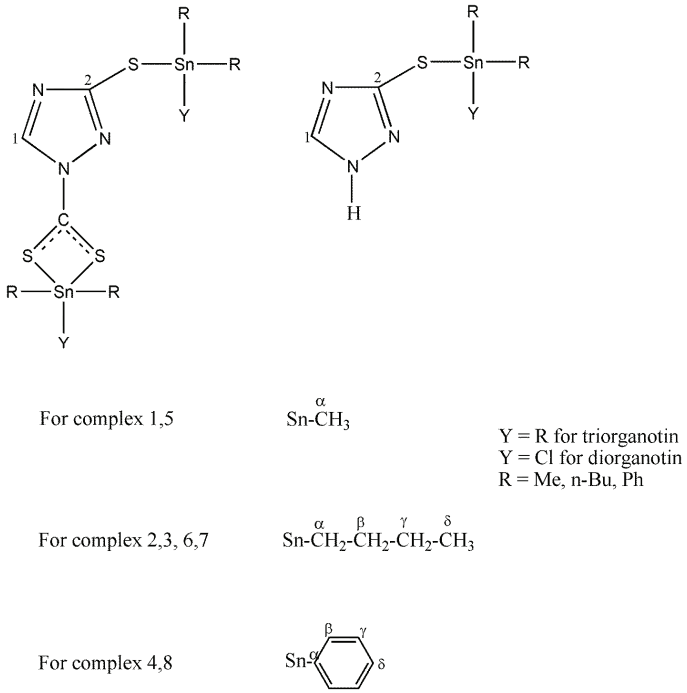


Scheme S-1. Numbering scheme for NMR data.

TABLE S-III. $^1$H-NMR data (ppm) of the organotin(IV) complexes **1**–**8** in DMSO-$d_6$

| Compd. | –CH | –NH | –SH | R |
|---|---|---|---|---|
| HL | 8.21 | 11.48 | 13.357 | – |
| **1** | 8.24 | 11.45 | – | 1.03 (*s*) |
| **2** | 8.24 | 11.48 | – | 1.62–1.58 (*m*, H*α*), 1.40–1.47 (*m*, H*β*), 1.32–1.23 (*m*, H*γ*), 0.87 (*t*, H*δ*), $^3J$ = 7.2 Hz |
| **3** | 8.24 | 11.43 | – | 1.54–1.46 (*m*, H*α*), 1.44–1.39 (*m*, H*β*), 1.27–1.13 (*m*, H*γ*), 0.81 (t, H*δ*), $^3J$ = 7.0 Hz |
| **4** | 8.23 | 11.30 | – | 7.97–7.72 (*m*), 7.52–7.36 (*m*) |

TABLE S-III. Continued

| Compd. | –CH | –NH | –SH | R |
|---|---|---|---|---|
| **5** | 8.20 | – | – | 1.46, *s*, $^2J$ [79/76], H$\alpha$ |
| **6** | 8.21 | – | – | 1.63–1.55 (*m*, H$\alpha$), 1.39–1.47 (*m*, H$\beta$), 1.31–1.25 (*m*, H$\gamma$), 0.87 (*t*, $^3J$ = 7.2 Hz, H$\delta$) |
| **7** | 8.23 | – | – | 1.52–1.48 (*m*, H$\alpha$), 1.44–1.40 (*m*, H$\beta$), 1.26–1.12 (*m*, H$\gamma$), 0.80 (t, $^3J$ = 7.0 Hz, H$\delta$) |
| **8** | 8.23 | – | – | 7.96–7.74 (*m*), 7.48–7.31 (*m*) |

Table S-IV. $^{13}$C-NMR data (ppm) of the organotin(IV) complexes **5**–**8**; Chemical shifts ($\delta$) in ppm and $^nJ[^{119/117}$Sn, $^{13}$C] values in Hz are listed in square brackets

| Compd. | 1C | 2C | –CSS | R |
|---|---|---|---|---|
| HL | 140.44 | 165.57 | – | – |
| **5** | 140.78 | 153.36 | 191.36 | 10.6 (C-$\alpha$, $^1J$[570,545]) |
| **6** | 140.65 | 154.16 | 193.80 | 26.5 (C-$\alpha$, $^1J$[496/479]), 29.3 (C-$\beta$, $^2J$[44]), 28.3 (C-$\gamma$, $^3J$[112/109]), 14.7 (C-$\delta$) |
| **7** | 140.32 | 153.15 | 194.85 | 25.4 (C-$\alpha$, $^1J$[346/332]), 29.2 (C-$\beta$, $^2J$[34]), 27.1 (C-$\gamma$, $^3J$[68/62]), 13.5 (C-$\delta$) |
| **8** | 140.35 | 152.15 | 191.78 | 138.1 (C-$\alpha$), 136.3 (C-$\beta$, $^2J$[47.3/45]), 129.1 (C-$\gamma$, $^3J$[61.5/59.2]), 129.5 (C-$\delta$, $^4J$ [12.8]) |

TABLE S-V. (C–Sn–C) angles based on the NMR parameters of complexes **5**–**7**

| Compd. | $^1J(^{119}$Sn, $^{13}$C) / Hz | $^2J(^{119}$Sn, $^1$H) / Hz | Angle, ° | |
|---|---|---|---|---|
| | | | $^1J$ | $^2J$ |
| **5** | 570 | 79 | 126.75 | 124 |
| **6** | 495 | – | 120.1 | – |
| **7** | 346 | – | 107.1 | – |

Table S-VI. Mass fragments, *m*/*z*, and relative abundance of the organotin(IV) complexes **1**–**8**; n.o. – not observed

| Compd. | Mass fragmentation: *m*/*z* (intensity, %) |
|---|---|
| HL | 101 (100) $[C_2H_3N_3S]^+$, 74 (87.4) $[CH_2N_2S]^+$, 60 (27.4) $[CH_2NS]^+$, 47 (10.8) $[NHS]^+$, 42 (70.5) $[CH_2N_2]^+$ |
| **1** | 285 (1.2) $[(CH_3)_2Sn(–SN_3C_2H_2)Cl]^+$, 270 (4.2) $[(CH_3)Sn(–SN_3C_2H_2)Cl]^+$, 255 (2.0) $[Sn(–SN_3C_2H_2)Cl]^+$, 155 (38.8) $[SnCl]^+$, 100 (100) $[(SN_3C_2H_2)]^+$, 250 (3.0) $[(CH_3)_2Sn(–SN_3C_2H_2)]^+$, 220 (5.0) $[Sn(–SN_3C_2H_2)]^+$, 120 (8.1) $[Sn]^+$, 185 (19.2) $[(CH_3)_2SnCl]^+$, 150 (2.2) $[(CH_3)_2Sn]^+$, 135 (6.1) $[CH_3–Sn]^+$ |
| **2** | 369 (11.1) $[(Bu)_2Sn(–SN_3C_2H_2)Cl]^+$, 334 (97.6) $[(Bu)_2Sn(–SN_3C_2H_2)]^+$, 312 (5.8) $[(Bu)Sn(–SN_3C_2H_2)Cl]^+$, 220 (68.0) $[Sn(–SN_3C_2H_2)]^+$, 100 (11.8) $[(SN_3C_2H_2)]^+$, 120 (9.5) $[Sn]^+$, 269 (20.9) $[Sn–Bu_2Cl]^+$, 212 (13) $[SnBu–Cl]^+$, 155 (16.2) $[SnCl]^+$, 57 (92.5) $[Bu]^+$ |
| **3** | 391 (0.5) $[(Bu)_3Sn(–SN_3C_2H_2)]^+$, 277 (12.3) $[(Bu)Sn(–SN_3C_2H_2)]^+$, 220 (35.6) $[Sn(–SN_3C_2H_2)]^+$, 100 (100) $[(SN_3C_2H_2)]^+$, 120 (8.0) $[Sn]^+$, 291 (15.6) $[(Bu)_3\ Sn]^+$, 234 (20.9) $[(Bu)_2\ Sn]^+$, 177 (21.68) $[Bu(Sn)]^+$ |

TABLE S-VI. Continued

| Compd. | Mass fragmentation: *m*/*z* (intensity, %) |
|---|---|
| **4** | 451 (3.9) $[(Ph)_3Sn(–SN_3C_2H_2)]^+$, 100 (100) $[(SN_3C_2H_2)]^+$, 374 (36.8) $[(Ph)_2Sn(–SN_3C_2H_2)]^+$, 297 (3.5) $[(Ph)Sn(–SN_3C_2H_2)]^+$, 220 (4.2) $[C_2H_3N_3SSn]^+$, 100 (9.5) $[C_2H_3N_3S]^+$, 351 (48.3) $[(Ph)_3Sn]^+$, 274 (2.6) $[(Ph)_2Sn]^+$, 197 (45.6) $[Ph–Sn]^+$, 77 (20.9) $[Ph]^+$, 51 (16.3) $[C_4H_3]^+$, 120 (12.7) $[Sn]^+$ |
| **5** | 545 (<0.5) $[(CH_3)_2ClSn(–S–CS)–NC_2HN_2S(–Sn(CH_3)_2Cl]$, 469 (1.2) $[(CH_3)_2ClSn(–NC_2HN_2S)(–Sn(CH_3)_2Cl]^+$, 285 (4.1) $[(CH_3)_2Sn(–SN_3C_2H_2)Cl]^+$, 185 (6.5) $[(CH_3)_2SnCl]^+$, 100 (100) $[(SN_3C_2H_2)]^+$, 76 (7.1) $[S–CS]^+$, 196 (2.4) $[Sn–(S–CS)]^+$, 143 (2.8) $[CS–NC_2HN_2S]^+$ |
| **6** | 713 (n.o) $[(Bu)_2ClSn(–S–CS)–NC_2HN_2S(–Sn(Bu)_2Cl]$, 637 (<0.5) $[(Bu)_2ClSn(–NC_2HN_2S)(–Sn(Bu)_2Cl]^+$, 369 (4.6) $[(Bu)_2Sn(–SN_3C_2H_2)Cl]^+$, 269 (100) $[(Bu)_2SnCl]^+$, 100 (16) $[(SN_3C_2H_2)]^+$, 76 (7.1) $[S–CS]^+$, 196 (6.4) $[Sn–(S–CS)]^+$ |
| **7** | 757 (n.o.) $[(Bu)_3Sn(–S–CS)–NC_2HN_2S(–Sn(Bu)_3)]^+$, 681 (2.4) $[(Bu)_3Sn–NC_2HN_2S(–Sn(Bu)_3)]^+$, 291 (2.1) $[(Bu)_3\ Sn]^+$, 196 (6.4) $[Sn–(S–CS)]^+$, 76 (10.3) $[S–CS]^+$, 120 (2.0) $[Sn]^+$, 57 (3.3) $[Bu]^+$ |
| **8** | 877 (n.o.) $[(Ph)_3Sn(–S–CS)–NC_2HN_2S(–Sn(Ph)_3)]^+$, 801 (<0.5) $[(Ph)_3Sn–NC_2HN_2S(–Sn(Ph)_3)]^+$, 350 (4.8) $[Ph_2SnC_6H_4]^+$, 723 (1.1) $[(Ph)Sn(–S–CS)–NC_2HN_2S(–Sn(Ph)_3)]^+$, 196 (16.9) $[Sn–C_6H_4]^+$, 154 (83.1) $[Ph–Ph]^+$, 76 (12.3) $[S–CS]^+$, 451 (1.9) $[(Ph)_3Sn(–SN_3C_2H_2)]^+$ |

Journal of the Serbian Chemical Society
JSCS-info@shd.org.rs • www.shd.org.rs/JSCS
*J. Serb. Chem. Soc. 80* (6) 767–777 (2015)
*JSCS–4756*
UDC 519.677+543.637:546.32+547.416+547.233'821:632.954
*Original scientific paper*

# Analysis of the chemical reactivity of aminocyclopyrachlor herbicide through the Fukui function

LUIS HUMBERTO MENDOZA-HUIZAR*

*Universidad Autónoma del Estado de Hidalgo, Área Académica de Química Químicas, Mineral de la Reforma, Hidalgo, C.P. 42186, México*

(Received 25 December 2014, Accepted 25 January 2015)

*Abstract*: The global and local DFT reactivity descriptors were calculated at the MP2/6-311++G (2d,2p) level of theory for aminocyclopyrachlor herbicide in the aqueous phase. Global reactivity descriptors, such as ionization energy, molecular hardness, electrophilicity and total energies, were calculated to evaluate the reactivity of aminocyclopyrachlor. The local reactivity was evaluated through the Fukui function. The obtained results suggest that the cationic and dipolar forms of aminocyclopyrachlor exhibit similar global reactivity and are susceptible to de-amination and decarboxylation. In addition, opening of the ring might become feasible through free radical attacks on the neutral form, while a similar process is caused by nucleophilic attacks on the anionic form.

*Keywords*: aminocyclopyrachlor; reactivity; Fukui; MP2; PCM.

## INTRODUCTION

Rangelands and pastures (RP) are the major source of high quality protein and fat for human beings through the meat obtained from animals that graze thereon.[1–3] However, the incidence of weeds on these RP reduces the grass density, and forage production.[1–3] Weed control on RP is realized with specific herbicides. However, some of these herbicides used to control many forb species in pastures may also injure desirable native grass species.[4,5] In this sense, potassium 6-amino-5-chloro-2-cyclopropylpyrimidine-4-carboxylate (aminocyclopyrachlor), see Fig. 1, is used to control or suppress several broad-leaved weeds and woody plant species in pastures, rangelands and various non-crop sites,[6] with a less injury to the native grasses in comparison to other herbicides.[4] According to EPA, this herbicide poses very low risk to humans, including workers and the general population, due to its low toxicity and low volatility.[7] Moreover, it was reported that an evaluation of the available scientific infor-

* E-mail: hhuizar@uaeh.edu.mx
doi: 10.2298/JSC141224008M

mation found that this herbicide does not present an unacceptable risk to human health or the environment.[8,9] However, the signs of toxicity associated with aminocyclopyrachlor involve decreased body weight, decreased weight gain, decreased food consumption, and decreased food conversion efficiency.[10] The mechanism by which aminocyclopyrachlor causes decreased food conversion efficiency has not yet been clarified.[10] Additionally, it is important to mention that aminocyclopyrachlor is environmentally persistent, soluble in water, non-volatile, and with a low sorption potential. Pesticides with such features tend to move easily through the soil profile into groundwater.[11,12] Hence, extensive application of this herbicide may increase its concentration in the soil and groundwater and thus aminocyclopyrachlor is recognized as having the potential to pollute groundwater.[13–15]

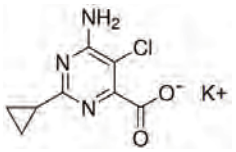


Fig. 1. Potassium 6-amino-5-chloro-2-cyclopropylpyrimidine-4--carboxylate.

Aminocyclopyrachlor slowly degrades by aerobic microbial metabolism with half-lives ranging from 114–433 days in different soils and it is stable to degradation *via* other pathways.[13,16] However, in some cases, this half-life is more related to transport losses from runoff and leaching rather than degradation.[9] Furthermore, the leaching potential of aminocyclopyrachlor is similar to that exhibited by picloram, which is recognized as an emerging water contaminant.[11] Due to its dissociation constant ($pK_a$ = 4.65), aminocyclopyrachlor is in the anionic form at typical soil pH levels.[17] Here, it is important to mention that anionic pesticides are generally weakly retained by most soil and sediment components and potentially could reach and contaminate surface and groundwaters.[18,19]

Unfortunately, information on the degradation and metabolic pathways of aminocyclopyrachlor in water is limited, since the main source of information is related to its absorption in soils. Thus, a good understanding of the reactivity of aminocyclopyrachlor would allow the development of efficient degradation methods for its removal from groundwater. To the best of existing knowledge, the reactivity of aminocyclopyrachlor at the molecular level has not hitherto been analyzed. Therefore, in this work, the molecular reactivity of this herbicide is analyzed through the formulation of chemical reactivity based on the density functional theory (DFT).[20] It is considered that this kind of study would contribute to a better understanding of the chemical behavior of this herbicide in aqueous media.

*Theory*

The formulation of the chemical reactivity theory derived within the framework of the density functional theory has enabled parameters that give information about the general behavior of a molecular system to be defined.[20] These parameters are the electronic chemical potential ($\mu$), the electronegativity ($\chi$) and hardness ($\eta$), which can be evaluated through the following equations:[21–26]

$$\mu = \left(\frac{\partial E}{\partial N}\right)_{v(r)} = -\frac{1}{2}(I - A) \tag{1}$$

$$\chi = -\mu \tag{2}$$

$$\eta = \left(\frac{\partial \mu}{\partial N}\right)_{v(r)} = \left(\frac{\partial^2 E}{\partial N^2}\right)_{v(r)} = (I - A) \tag{3}$$

In these equations, $E$, $N$ and $v(r)$ are the energy, number of electrons and the external potential of the system, respectively. The energy value of the vertical electronic affinity ($A$) can be calculated as $A = E(N) - E(N+1)$, where $E(N)$ and $E(N+1)$ are the total ground-state energies in the neutral $N$ and the singly charged $(N+1)$ configurations. Moreover, the ionization potential ($I$) can be calculated as $I = E(N-1) - E(N)$. The chemical potential measures the escaping tendency of an electron and it can be associated with the molecular electronegativity,[27] while $\eta$ determines the resistance of the chemical species to lose electrons and can be related to the stability and polarizability of the molecular system.[28,29] On the other hand, the global electrophilicity index ($\omega$) is defined as a measurement of the susceptibility of a chemical species to accept electrons and it can be calculated as:[30]

$$\omega = \frac{\mu^2}{2\eta} \tag{4}$$

According to this definition, low values of $\omega$ suggest a good nucleophile while higher values indicate the presence of a good electrophile.[30]

Additionally to the global reactivity parameters, it is possible to define local reactivity parameters, which can be used to analyze the reactivity on different sites within a molecule.[31,32] This local reactivity can be evaluated through the Fukui function $\left(f(\vec{r})\right)$,[33,34] which is defined as:[35]

$$f(\vec{r}) = \left(\frac{\partial \rho(\vec{r})}{\partial N}\right)_{v(r)} = \left(\frac{\partial \mu(\vec{r})}{\partial v(r)}\right) \tag{5}$$

where $\rho(\vec{r})$ is the electronic density. The Fukui function, Eq. (5), can be evaluated by using a finite difference approximation. However, due to the discontinuity of the electron density with respect to the number of electrons ($N$), this

approximation leads to three types of Fukui functions for a system, namely, $f^+(\vec{r})$, $f^-(\vec{r})$, and $f^0(\vec{r})$ for nucleophilic, electrophilic, and free radical attacks respectively. These condensed functions can be evaluated as:[31]

$$f^+(\vec{r}) = \rho_{N+1}(\vec{r}) - \rho_N(\vec{r}) \quad (6)$$

$$f^-(\vec{r}) = \rho_N(\vec{r}) - \rho_{N-1}(\vec{r}) \quad (7)$$

$$f^0(\vec{r}) = \frac{1}{2}\left[\rho_{N+1}(\vec{r}) - \rho_{N-1}(\vec{r})\right] \quad (8)$$

However, for studying the reactivity at the atomic level, a more convenient way of calculating the Fukui function is through the condensed forms of the Fukui function for an atom $j$ in a molecule which are expressed as:[31]

$$f_j^+(\vec{r}) = q_{j(N)} - q_{j(N+1)} \quad (9)$$

$$f_j^-(\vec{r}) = q_{j(N-1)} - q_{j(N)} \quad (10)$$

$$f_j^0(\vec{r}) = \frac{1}{2}\left\{q_{j(N-1)} - q_{j(N+1)}\right\} \quad (11)$$

In these equations, $q_j$ is the atomic charge (evaluated from the Mulliken population, electrostatic-derived charge, *etc*.) at the $j^{th}$ atomic site in the neutral (N), anionic (N+1) or cationic (N–1) chemical species.

## METHODOLOGY

The optimal conformations of aminocyclopyrachlor chemical species were subjected to full geometry optimization in aqueous phase employing the hybrid functional B3LYP,[36-38] the basis set 6-311++G(2d,2p),[39,40] and the PCM solvation model.[41,42] The optimized geometries in the aqueous phase were re-optimized employing the second order Moller Plesset theory[43] and the basis set 6-311++G(2d,2p). The final atomic charges for aminocyclopyrachlor studied in the aqueous phase were obtained within the framework of the MP2 theory. In all calculations of these atomic charges, the Density=MP2 option was used in order to ensure that the charges were calculated at the MP2 level. All the calculations reported here were performed with the package Gaussian 09,[44] and visualized with the GaussView ver. 3.09 packages.[45]

## RESULTS AND DISCUSSION

Aminocyclopyrachlor rapidly dissociates into the acid form (6-amino-5--chloro-2-cyclopropyl-4-pyrimidinecarboxylic acid) with the addition of water at pH 4.65,[46] see Fig. 2a. Furthermore, it is important to consider that in an aqueous environment at pH ≈7, the carboxyl groups are usually deprotonated, meaning they lose an $H^+$ and become negatively charged, see Fig. 2b. Moreover, the nitrogen of the pyrimidine ring can be protonated at pH 1.23 and the protonated and the dipolar forms may exist at acid pH values,[47,48] see Fig. 2c.

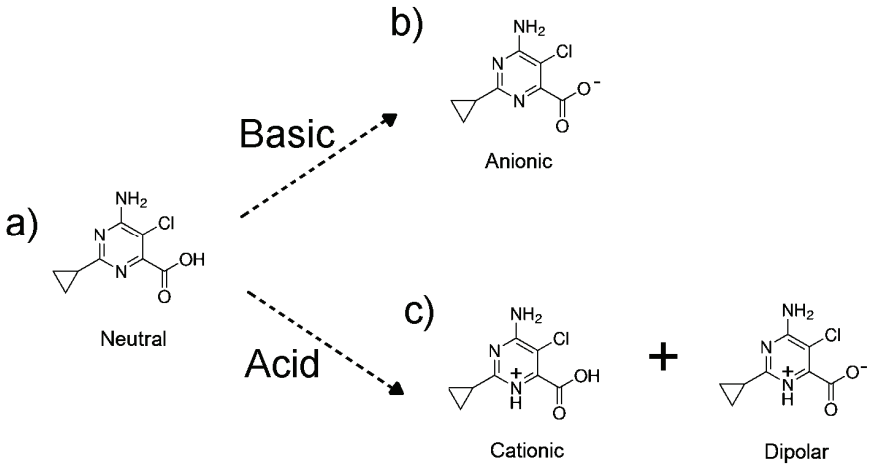


Fig. 2. Chemical species of aminocyclopyrachlor at different pH values.

Under these considerations, the chemical species shown in Fig. 2 were optimized, at the B3LYP/6-311++G (2d,2p) level, in the aqueous phase without any symmetry constraints employing the PCM solvation model. A frequency analysis was applied to the optimized geometries to verify the stability criterion and in all cases, the frequency values were positive and their values were similar to those reported in the literature for pyrimidine.[49] The optimized geometries at the B3LYP/6-311++G (2d,2p) level were re-optimized at the MP2/6-311++G (2d,2p) level. The optimized geometries of the neutral form at the MP2/6--311++G (2d,2p) level are depicted in Fig. 3. Note the existence of two possible conformers for this neutral form in which the cyclopropyl is oriented in a position either *cisoid* (Fig. 3a) or *transoid* (Fig. 3b). The electronic energies for the *cisoid* and *transoid* conformers are –1082.672645 and –1082.672819 hartrees, respectively. Note that there is an energy difference of 0.11 kcal* $mol^{-1}$ between both conformers, which could be expected for two isoenergetic conformers. In addition, the optimized geometries of the anionic, cationic and dipolar forms are reported in Figs. 4–6, respectively. For the anionic, cationic and dipolar forms, the energy differences between the *cisoid* and *transoid* conformers are 0.07, 2.32 and 1.76 kcal $mol^{-1}$, respectively. These results suggest the existence of two isoenergetic conformers for aminocyclopyrachlor chemical species. However, it is important to mention that a conformer may be converted into another *via* an inversion symmetry operation. Thus, under the Born–Oppenheimer approximation, these conformers must have identical electronic structures and energy and the observed differences may be due exclusively to numerical imprecision.[50]

* 1 kcal = 4186 J

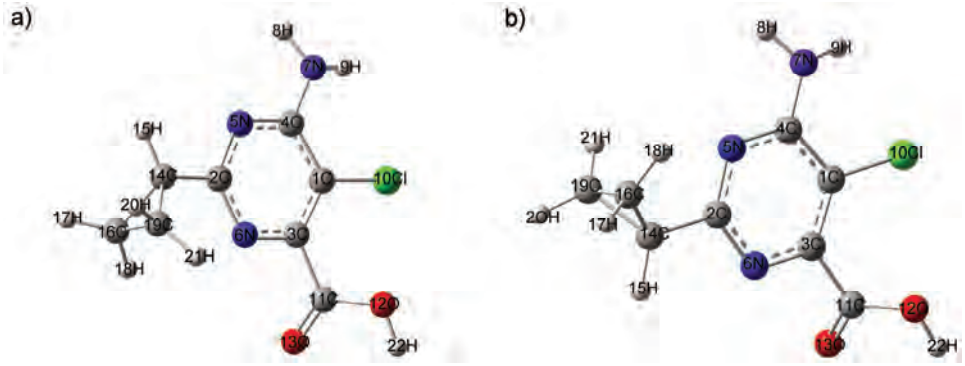


Fig. 3. Neutral aminocyclopyrachlor. a) Bond distances (Å): 1C–10Cl = 1.74, 1C–3C = 1.38 , 3C–11C = 1.50, 3C–6N = 1.34, 11C–13O = 1.21, 11C–12O = 1.34 , 12O–22H = 0.97, 6N–2C = 1.34, 2C–14C = 1.47, 2C–5N = 1.34 , 5N–4C = 1.34 , 4C–7N = 1.36, 7N–8H = 1.01, 7N–9H = 1.01, 14C–15H = 1.08, 14C–16C = 1.52, 14C–19C = 1.52, 16C–19C = 1.50 , 16C–17H = 1.08, 16C–18H = 1.08, 19C–20H = 1.08 and 19C–21H= 1.08, dihedral angles (°): 19C–14C–2C–5N = –145.65 and 6N–3C–11C–13O = 58.43. b) The bond distances were the same as in conformer (a) but the dihedral angles were 19C–14C–2C–5N = –34.80 and 6N–3C–11C–13O = 59.15.

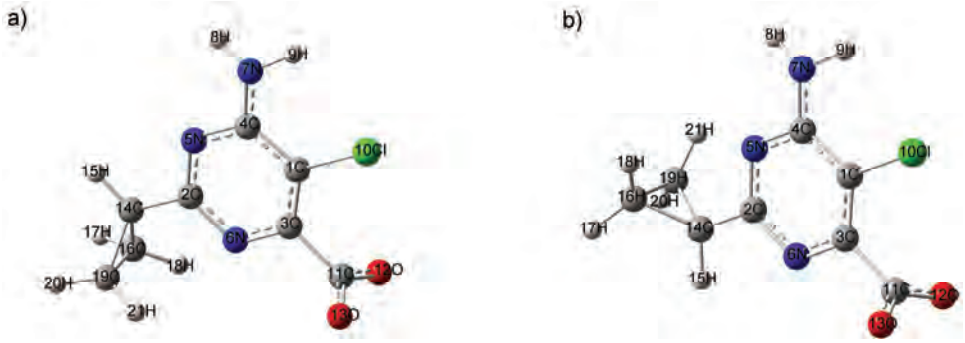


Fig. 4. Anionic aminocyclopyrachlor. a) Bond distances (Å): 1C–10Cl = 1.74, 1C–3C = 1.38 , 3C–11C = 1.52, 3C–6N = 1.35, 11C–13O = 1.26, 11C–12O = 1.26 , 6N–2C = 1.34, 2C–14C = = 1.48, 2C–5N = 1.34, 5N–4C = 1.34 , 4C–7N = 1.37, 7N–8H = 1.01, 7N–9H = 1.01, 14C–15H = 1.08, 14C–16C = 1.52, 14C–19C = 1.52, 16C–19C = 1.50 , 16C–17H = 1.08, 16C–18H = 1.08, 19C–20H = 1.08 and 19C–21H = 1.08, dihedral angles (°): 19C–14C–2C–5N = –145.69 and 6N–3C–11C–13O = 89.76. b) The same bond distances were the same as in conformer (a) but the dihedral angles were 19C–14C–2C–5N = –34.63 and 6N–3C–11C–13O = 89.85.

*Global reactivity descriptors*

The values of the global reactivity descriptors ($\mu$, $\eta$ and $\omega$) were calculated at the MP2/6-311++G(2d,2p) level of theory employing Eqs. (1), (2) and (3), respectively, see Table I. From the results reported in this Table, it may be observed that the global hardness of the aminocyclopyrachlor chemical species

increases with increasing pH value. This result suggests an increment in the stability of aminocyclopyrachlor in the aqueous phase in terms of the pH value. In addition, note that the values of $\mu$ and $\omega$ decrease and increase, respectively. This behavior suggests that the electronegativity and nucleophilic behavior of aminocyclopyrachlor diminishes with increasing pH.

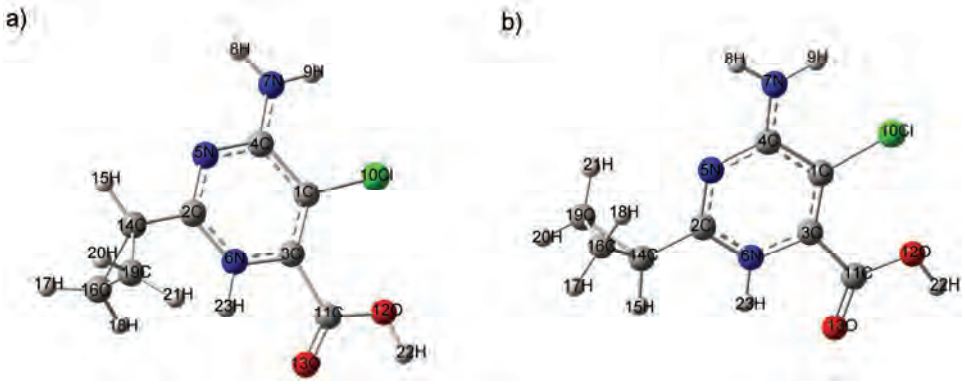


Fig. 5. Cationic aminocyclopyrachlor. a) Bond distances (Å): 1C–10Cl = 1.72, 1C–3C = 1.37 , 3C–11C = 1.50, 3C–6N = 1.36, 6N–23H = 1.02, 11C–13O = 1.22, 11C–12O = 1.33, 12O–22H = 0.97, 6N–2C = 1.35, 2C–14C = 1.46, 2C–5N = 1.32 , 5N–4C = 1.35 , 4C–7N = = 1.32, 7N–8H = 1.01, 7N–9H = 1.01, 14C–15H = 1.08, 14C–16C = 1.52, 14C–19C = 1.52, 16C–19C = 1.50 , 16C–17H = 1.08, 16C–18H = 1.08, 19C–20H = 1.08 and 19C–21H = 1.08, dihedral angles(°): 19C–14C–2C–5N = –145.80 and 6N–3C–11C–13O = –0.004. b) The bond distances were the same as in conformer (a) but the dihedral angles were 19C–14C–2C–5N = –33.42 and 6N–3C–11C–13O = 0.007.

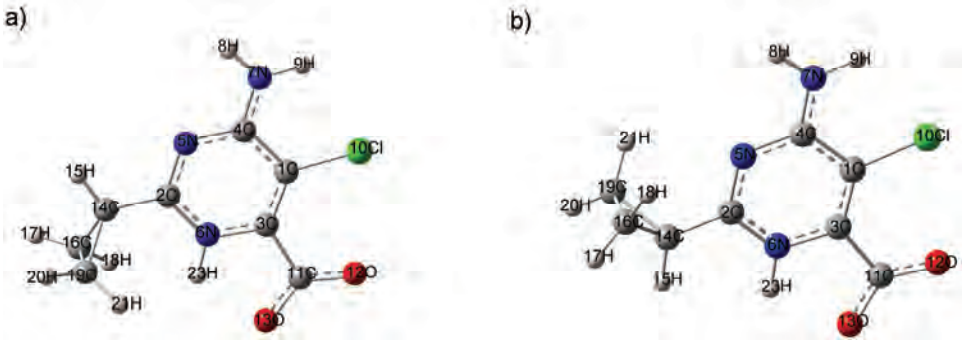


Fig. 6. Dipolar aminocyclopyrachlor. a) Bond distances (Å): 1C–10Cl = 1.72, 1C–3C = 1.37 , 3C–11C = 1.54, 3C–6N = 1.36, 6N–23H = 1.03, 11C–13O = 1.26, 11C–12O = 1.25, 6N–2C = = 1.34, 2C–14C = 1.46, 2C–5N = 1.32 , 5N–4C = 1.35 , 4C–7N = 1.33, 7N–8H = 1.01, 7N–9H = 1.01, 14C–15H = 1.08, 14C–16C = 1.52, 14C–19C = 1.52, 16C–19C = 1.50, 16C–17H = 1.08, 16C–18H = 1.08, 19C–20H = 1.08 and 19C–21H = 1.08, dihedral angles(°): 19C–14C–2C–5N = –145.46 and 6N–3C–11C–13O = –0.008. b) The bond distances were the same as in conformer (a) but the dihedral angles were 19C–14C–2C–5N = –33.69 and 6N–3C–11C–13O = 0.

TABLE I. Global reactivity descriptors for aminocyclopyrachlor chemical species at the MP2/6-311++G(2d,2p) level of theory

| Descriptor | $I$ / eV | $A$ / eV | $\eta$ / eV | $\mu$ / eV | $\omega$ / eV |
|---|---|---|---|---|---|
| Cationic | 9.55 | 3.11 | 6.44 | –3.22 | 0.80 |
| Dipolar | 8.93 | 2.01 | 6.92 | –3.46 | 0.86 |
| Neutral | 8.48 | 1.53 | 6.95 | –3.47 | 0.87 |
| Anionic | 7.96 | 0.51 | 7.45 | –3.73 | 0.93 |

*Local reactivity descriptors*

In order to evaluate the reactivity at atomic resolution, the Fukui function was evaluated through Eqs. (9)–(11). It is well known that the Fukui function allows the determination of the pinpoint distribution of the active sites on a molecule. However, the value of this function is completely dependent on the scheme of charges used. A variety of schemes to evaluate atomic charges has been reported.[42] However, atomic charges derived from the electrostatic potential (*MEP*) have found good acceptance to calculate the condensed Fukui function and good agreement with the experimental results was obtained.[50–52] The values of the Fukui function in terms of *MEP* charges for the *cisoid* and *transoid* conformers of aminocyclopyrachlor in its neutral form are reported in Table S-I of the Supplementary material to this paper. Observe that for neutral *cisoid*-aminocyclopyrachlor, the more reactive sites for electrophilic, nucleophilic and free radical attacks are the 2C, 3C, and 3C atoms, respectively. On the other hand, 7N, 3C, and 6N are the more reactive sites for electrophilic, nucleophilic and free radical attacks respectively in the case of the neutral *transoid*-aminocyclopyrachlor conformer. Note that even though the *cisoid* and *transoid* conformers are isoenergetic, the local reactivity is different when electrophilic and free radical attacks are considered.

The values of the condensed Fukui function for the anionic, cationic and dipolar forms are reported in Tables S-II–S-IV, respectively. The more reactive sites for neutral, anionic, cationic and dipolar forms are summarized in Table II. From these results, observe that the cationic and dipolar forms are susceptible to de-amination (7N) and decarboxylation (3C). In the neutral *cisoid* form, an elec-

TABLE II. The more reactive sites for aminocyclopyrachlor chemical species; 7N (de-amination), 3C (decarboxylation), 2C (electrophilic substitution), 5N (opening of the ring), 1C (dechlorination), 6N (opening of the ring)

| Form | *Cisoid* | | | *Transoid* | | |
|---|---|---|---|---|---|---|
| | Electrophilic | Nucleophilic | Free radical | Electrophilic | Nucleophilic | Free radical |
| Cationic | 7N | 3C | 7N | 7N | 3C | 7N |
| Dipolar | 7N | 3C | 7N | 7N | 3C | 7N |
| Neutral | 2C | 3C | 3C | 7N | 3C | 6N |
| Anionic | 2C | 5N | 1C | 2C | 1C | 1C |

trophilic substitution is expected on 2C and decarboxylation may be caused by either nucleophiles or free radicals by attack on 3C. In the neutral *transoid* form, de-amination, decarboxylation and opening of the ring processes are expected through electrophilic, nucleophilic and free radicals attacks, respectively. At basic pH values, electrophilic, nucleophilic and free radicals attacks on the anionic *cisoid* form would cause electrophilic substitution, opening of the ring and dechlorination, respectively. For the anionic *transoid* form, electrophilic substitution is expected through electrophilic attacks, while dechlorination process may be caused by either nucleophilic or free radicals attacks. These results suggest that a degradation process that involves the opening of the ring might be feasible through free radical attacks to the neutral *transoid* form and nucleophilic attacks on the anionic *cisoid* form. Theoretical analyses of the possibility of more reactive free radicals and nucleophiles to open the pyrimidine ring are beyond of the scope of this paper, however they will be analyzed in future works.

## CONCLUSIONS

In the present work, DFT reactivity descriptors for aminocyclopyrachlor herbicide in the aqueous phase were calculated. The cationic and dipolar forms of aminocyclopyrachlor showed similar values of the global reactivity parameters, which is indicative of equivalent global chemical behavior under acid aqueous conditions. Under these acid conditions, the values of the Fukui function suggest that attacks by free radicals and electrophiles on 7N would cause a de-amination process, while a nucleophilic attack would cause decarboxylation. For the neutral form, nucleophilic and free radical attacks would cause a decarboxylation process, while electrophilic substitution is expected on 2C. The neutral *transoid* form is susceptible to de-amination, decarboxylation and opening of the pyrimidine ring through electrophilic, nucleophilic and free radical attacks, respectively. At basic pH values where the anionic form of aminocyclopyrachlor is predominant, the *cisoid* form is susceptible to electrophilic substitution (2C), opening of the ring (5N) and dechlorination (1C). On the other hand, the *transoid* form would be vulnerable to electrophilic attacks on 2C, and a possible dechlorination through nucleophilic and free radical attacks on 1C.

## SUPPLEMENTARY MATERIAL

Values of the condensed Fukui function, Tables S-I–S-IV, are available electronically from http://www.shd.org.rs/JSCS/ or from the corresponding author on request.

*Acknowledgments*. LHMH gratefully acknowledges financial support from CONACYT (Project INFR-2014-227999) and to the Universidad Autónoma del Estado de Hidalgo through the projects PIFI 2008-13M8U0017T-04-01 and PIFI-2009-13MSU0017T-04-01. LHMH wishes to thank the National Laboratory for the Characterization of Physicochemical Properties and Molecular Structure, (LACAPFEM) for providing supercomputing time.

ИЗВОД

## АНАЛИЗА ХЕМИЈСКЕ РЕАКТИВНОСТИ ХЕРБИЦИДА АМИНОЦИКЛОПИРАХЛОР ПОМОЋУ ФУКУИЈЕВЕ ФУНКЦИЈЕ

LUIS HUMBERTO MENDOZA-HUIZAR

*Universidad Autónoma del Estado de Hidalgo, Área Académica de Química Químicas, Mineral de la Reforma, Hidalgo, C.P. 42186, México*

Израчунати су глобални и локални DFT реакциони дескриптори за хербицид аминоциклопирахлор на MP2/6-311++G (2d,2p) нивоу теорије у воденој фази. Глобални реакциони дескриптори су енергија јонизације, молекулска тврдоћа, електрофилност и укупна енергија. Локална реактивност је процењена помоћу Фукуијеве фунције. Добијени резултати указују на то да катјонске и диполарне форме аминоциклопирахлора имају сличну глобалну реактивност, и подлежу деаминовању и декарбоксилацији.

(Примљено 25. децембра 2014, прихваћено 25. јануара 2015)

## REFERENCES

1. A. Catrileo, R. Morales, C. Rojas, D. Cancino, *Chil. J. Agr. Res.* **74** (2014) 366
2. H. Mut, I. Ayan, Z. Acar, U. Baùaran, Ö. Onal-AùÇi, *Turk. J. Field Crops* **15** (2010) 198
3. D. P. Poppi, S. R. McLennan, *J. Anim. Sci.* **73** (1995) 278.
4. K. R. Harmoney, P. W. Stahlman, P. W. Geier, R. Rupp, *Weed Technol.* **26** (2012) 455
5. M. H. Ralphs, T. D. Whitson, D. N. Ueckert, *Rangelands* **13** (1991) 73
6. S. K. Rick, J. H. Meredith. *Weed Sci. Soc. Am. Abstr.* **51** (2011) 316
7. Maryland Pesticide Network, http://www.mdpestnet.org/resources/news2011/ (December 2014)
8. Aminocyclopyrachlor – Proposed Registration Decision PRD2014-08 – Health Canada Consultation Notice, http://www.hc-sc.gc.ca/cps-spc/pest/part/consultations/_prd2014-08/prd2014-08-eng.php#a7 (December 2014)
9. New York State Department of Environmental Conservation, http://pmep.cce.cornell.edu/profiles/herb-growthreg/24-d-butylate/aminocyclopyrachlor/aminocyclopyrachlor_reg_0313.pdf
10. SERA TR-056-01-03a, Aminocyclopyrachlor Human Health and Ecological Risk Assessment Final Report, http://www.fs.fed.us/foresthealth/pesticide/pdfs/Aminocyclopyrachlor.pdf (December 2014)
11. R. S. Oliveira, D. G. Alonso, W. C. Koskinen, *J. Agric. Food Chem.* **59** (2011) 4045e4050
12. Minimizing Pesticide Contaminated Soil Around the Home and Garden, http://store.msuextension.org/publications/AgandNaturalResources/MT201008AG.pdf (December 2014)
13. J. L. Rittenhouse, P. J. Rice, K. A. Spokas, W. C. Koskinen. *Environ. Pollut.* **189** (2014) 92e97
14. R. S. Oliveira, D. G. Alonso , W. C. Koskinen, S. K. Papiernik, *J. Environ. Sci. Health, Part B* **48** (2013) 1049
15. California Code of Regulations (Title 3. Food and Agriculture), Division 6. Pesticides and Pest Control Operations. http://www.cdpr.ca.gov/docs/legbills/calcode/040101.htm (December 2014)
16. K. L. Conklin, R. G. Lym, *Weed Technol.* **27** (2013) 552
17. A. Cabrera, C. Trigo, L. Cox, R. Celis, M. C. Hermosin, J. Cornejo, W. C. Koskinen, *Eur. J. Soil Sci.* **63** (2012) 694
18. J. A. Goodrich, B. J. Lykins, R. M. Clark. *J. Environ. Qual.* **20** (1991) 707

19. M. C. Hermosín, J. Cornejo. *J. Environ. Qual.* **22** (1993) 325
20. M. H. Cohen, A. Wasserman, *J. Phys. Chem., A* **111** (2007) 2229
21. J. L. Gázquez, *J. Mex. Chem. Soc.* **52** (2008) 3
22. P. Geerlings, F. De Proft, W. Langenaeker, *Chem. Rev.* **103** (2003) 1793
23. H. Chermette, *J. Comput. Chem.* **20** (1999**)** 129
24. P. W. Ayers, J. S. M. Anderson, L. J. Bartolotti, *Int. J. Quantum Chem.* **101** (2005) 520
25. P. K. Chattaraj, U. Sarkar, D. R. Roy, *Chem. Rev.* **106** (2006) 2065
26. S. B. Liu, *Acta Phys. Chim. Sin.* **25** (2009) 590
27. R. G. Parr, R. A. Donnelly, M. Levy, W. E. Palke, *J. Chem. Phys.* **68** (1978) 3801
28. R. G. Parr, R. G. Pearson, *J. Am. Chem. Soc.* **105** (1983) 7512
29. R. G. Pearson, *J. Chem. Educ.* **64** (1987) 561
30. R. G. Parr, L. Szentpaly, S. Liu, *J. Am. Chem. Soc.* **121** (1999) 1922
31. R. G. Parr, W. Yang, *Density Functional Theory of Atoms and Molecules*, Oxford University Press , New York, 1989, p. 99
32. S. B. Liu, *Electrophilicity*, in *Chemical reactivity theory: A density functional view*, P. K. Chattaraj, Ed., Taylor and Francis, Boca Raton, FL, 2009, Ch. 13, p. 179
33. J. L. Gazquez, F. Mendez, *J. Phys. Chem.* **98** (1994) 4591
34. F. Mendez, J. L. Gazquez, *J. Am. Chem. Soc.* **116** (1994) 9298
35. R. G. Parr, W. Yang, *J. Am. Chem. Soc.* **106** *(*1984) 4048
36. A. D. Becke, *J. Chem. Phys.* **98** (1993) 5648
37. A. D. Becke, *Phys. Rev. A* **38** (1988) 3098
38. C. Lee, W. Yang, R. G. Parr, *Phys. Rev., B* **37** (1988) 785
39. R. Krishnan, J. S. Binkley, R. Seeger, J. A. Pople, *J. Chem. Phys.* **72** (1980) 650
40. A. D. McLean, G. S. Chandler, *J. Chem. Phys.* **72** (1980) 5639
41. S. Miertus, J. Tomasi, *J. Chem. Phys.* **65** (1982) 239
42. S. Miertus, E. Scrocco, J. Tomasi, *J. Chem. Phys.* **55** (1981) 117
43. M. Head-Gordon, J. A. Pople, M. Frisch, *J. Chem. Phys. Lett.* **153** (1988) 503
44. Gaussian 09, Revision A.01, Gaussian, Inc., Wallingford, CT, 2009
45. Gaussview Rev. 3.09, Windows version, Gaussian Inc., Pittsburgh, PA, 2003
46. D. Ovalle, E. Posada, EP, WO2014093210 A1 (2014)
47. T. P. Selvam, C. R. James, P. V. Dniandev, S. K. Valzita, *Res. Pharm*. **2** (2012) 1
48. M. W. Cheung, J. W. Biggar, *J. Agric. Food Chem.* **22** (1974) 2
49. S. Breda, I. D. Reva, L. Lapinski, M. J. Nowak, R. Fausto, *J. Mol. Struct.* **786** (2006) 193
50. L. H. Mendoza Huizar, C. H. Rios-Reyes, N. J. Olvera-Maturano, J. Robles, J. A. Rodriguez, *Open Chem.* **13** (2015) 52
51. B. H. Besler, K. M. Merz, P. A. Kollman, *J. Comput. Chem.* **11** (1990) 431
52. L. H. Mendoza-Huizar, C. H. Rios-Reyes. *J. Mex. Chem. Soc.* **55** (2011) 14.

Journal of the Serbian Chemical Society
JSCS@tmf.bg.ac.rs • www.shd.org.rs/JSCS
*J. Serb. Chem. Soc. 80* (6) S212–S214 (2015) *Supplementary material*

SUPPLEMENTARY MATERIAL TO

# Analysis of the chemical reactivity of aminocyclopyrachlor herbicide through the Fukui function

LUIS HUMBERTO MENDOZA-HUIZAR*

*Universidad Autónoma del Estado de Hidalgo, Área Académica de Química Químicas, Mineral de la Reforma, Hidalgo, C.P. 42186, México*

*J. Serb. Chem. Soc.* 80 (6) (2015) 767–777

TABLE S-I. Values of the condensed Fukui function for the neutral aminocyclopyrachlor conformers computed from *MEP* charges according to Eqs. (9)–(11)

| Position | *cisoid* Conformer | | | *transoid* Conformer | | |
|---|---|---|---|---|---|---|
| | $f^-(\vec{r})$ | $f^+(\vec{r})$ | $f^0(\vec{r})$ | $f^-(\vec{r})$ | $f^+(\vec{r})$ | $f^0(\vec{r})$ |
| 1C | 0.091 | 0.067 | 0.079 | 0.084 | 0.031 | 0.058 |
| 2C | ***0.203*** | –0.008 | 0.097 | 0.196 | –0.038 | 0.079 |
| 3C | 0.112 | ***0.237*** | ***0.174*** | 0.083 | ***0.206*** | 0.145 |
| 4C | 0.032 | –0.046 | –0.007 | 0.034 | 0.02 | 0.027 |
| 5N | –0.139 | 0.173 | 0.017 | –0.171 | 0.106 | –0.032 |
| 6N | 0.151 | 0.052 | 0.102 | 0.199 | 0.151 | ***0.175*** |
| 7N | 0.182 | 0.077 | 0.129 | ***0.217*** | 0.1 | 0.159 |
| 8H | 0.039 | 0.014 | 0.026 | 0.036 | 0.016 | 0.026 |
| 9H | –0.001 | –0.007 | –0.004 | –0.007 | –0.007 | –0.007 |
| 10Cl | 0.155 | 0.140 | 0.148 | 0.150 | 0.124 | 0.137 |
| 11C | –0.088 | –0.050 | –0.069 | –0.083 | –0.052 | –0.067 |
| 12° | 0.028 | 0.075 | 0.051 | 0.028 | 0.071 | 0.049 |
| 13° | 0.071 | 0.155 | 0.113 | 0.068 | 0.145 | 0.107 |
| 14C | –0.067 | 0.001 | –0.033 | –0.052 | 0.012 | –0.020 |
| 15H | 0.056 | 0.020 | 0.038 | 0.033 | 0.021 | 0.027 |
| 16C | 0.023 | 0.004 | 0.014 | 0.033 | –0.009 | 0.012 |
| 17H | 0.033 | 0.02 | 0.027 | 0.023 | 0.018 | 0.020 |
| 18H | 0.019 | 0.013 | 0.016 | 0.026 | 0.027 | 0.027 |
| 19C | 0.014 | –0.015 | 0.000 | 0.029 | –0.016 | 0.007 |
| 20H | 0.034 | 0.021 | 0.027 | 0.024 | 0.019 | 0.022 |
| 21H | 0.028 | 0.031 | 0.029 | 0.025 | 0.025 | 0.025 |
| 22H | 0.025 | 0.029 | 0.027 | 0.024 | 0.028 | 0.026 |

* E-mail: hhuizar@uaeh.edu.mx

TABLE S-II. Values of the condensed Fukui function for the anionic aminocyclopyrachlor conformers computed from *MEP* charges according to Eqs. (9)–(11)

| Position | *cisoid* Conformer | | | *transoid* Conformer | | |
|---|---|---|---|---|---|---|
| | $f^-(\vec{r})$ | $f^+(\vec{r})$ | $f^0(\vec{r})$ | $f^-(\vec{r})$ | $f^+(\vec{r})$ | $f^0(\vec{r})$ |
| 1C | 0.279 | 0.169 | ***0.224*** | 0.244 | ***0.221*** | ***0.232*** |
| 2C | ***0.400*** | –0.046 | 0.177 | ***0.362*** | 0.005 | 0.183 |
| 3C | 0.061 | 0.126 | 0.093 | 0.036 | 0.088 | 0.062 |
| 4C | 0.223 | –0.049 | 0.087 | 0.198 | –0.037 | 0.080 |
| 5N | –0.410 | ***0.253*** | –0.078 | –0.416 | 0.154 | –0.131 |
| 6N | 0.154 | 0.141 | 0.147 | 0.209 | 0.166 | 0.188 |
| 7N | –0.346 | 0.115 | –0.116 | –0.225 | 0.049 | –0.088 |
| 8H | 0.108 | 0.025 | 0.066 | 0.099 | 0.029 | 0.064 |
| 9H | 0.038 | –0.011 | 0.013 | 0.027 | –0.014 | 0.006 |
| 10Cl | 0.199 | 0.107 | 0.153 | 0.184 | 0.136 | 0.160 |
| 11C | –0.160 | –0.178 | –0.169 | –0.148 | –0.186 | –0.167 |
| 12O | 0.117 | 0.129 | 0.123 | 0.109 | 0.135 | 0.122 |
| 13O | 0.117 | 0.130 | 0.123 | 0.110 | 0.135 | 0.123 |
| 14C | –0.099 | –0.011 | –0.055 | –0.073 | 0.010 | –0.031 |
| 15H | 0.083 | 0.031 | 0.057 | 0.041 | 0.020 | 0.031 |
| 16C | 0.022 | –0.013 | 0.004 | 0.040 | –0.020 | 0.010 |
| 17H | 0.052 | 0.023 | 0.038 | 0.034 | 0.028 | 0.031 |
| 18H | 0.037 | 0.025 | 0.031 | 0.045 | 0.036 | 0.040 |
| 19C | 0.052 | –0.010 | 0.021 | 0.068 | –0.009 | 0.029 |
| 20H | 0.046 | 0.023 | 0.035 | 0.030 | 0.026 | 0.028 |
| 21H | 0.027 | 0.024 | 0.025 | 0.025 | 0.030 | 0.028 |

TABLE S-III. Values of the condensed Fukui function for the cationic aminocyclopyrachlor conformers computed from *MEP* charges according to Eqs. (9)–(11)

| Position | *cisoid* Conformer | | | *transoid* Conformer | | |
|---|---|---|---|---|---|---|
| | $f^-(\vec{r})$ | $f^+(\vec{r})$ | $f^0(\vec{r})$ | $f^-(\vec{r})$ | $f^+(\vec{r})$ | $f^0(\vec{r})$ |
| 1C | 0.091 | 0.028 | 0.060 | 0.089 | 0.020 | 0.054 |
| 2C | –0.067 | 0.008 | –0.030 | –0.048 | 0.009 | –0.020 |
| 3C | 0.055 | ***0.224*** | 0.140 | 0.048 | ***0.218*** | 0.133 |
| 4C | –0.259 | 0.089 | –0.085 | –0.259 | 0.133 | –0.063 |
| 5N | 0.264 | 0.087 | 0.176 | 0.256 | 0.033 | 0.145 |
| 6N | 0.251 | –0.007 | 0.122 | 0.244 | 0.017 | 0.130 |
| 7N | ***0.646*** | 0.070 | ***0.358*** | ***0.659*** | 0.045 | ***0.352*** |
| 8H | –0.035 | 0.027 | –0.004 | –0.037 | 0.034 | –0.001 |
| 9H | –0.042 | 0.011 | –0.016 | –0.045 | 0.013 | –0.016 |
| 10Cl | 0.092 | 0.139 | 0.115 | 0.089 | 0.143 | 0.116 |
| 11C | –0.077 | 0.088 | 0.005 | –0.077 | 0.083 | 0.003 |
| 12O | 0.011 | 0.003 | 0.007 | 0.012 | 0.007 | 0.010 |
| 13O | 0.049 | 0.114 | 0.082 | 0.046 | 0.117 | 0.081 |
| 14C | –0.046 | –0.005 | –0.025 | –0.067 | 0.004 | –0.032 |
| 15H | 0.019 | 0.022 | 0.021 | 0.030 | 0.013 | 0.021 |
| 16C | –0.001 | –0.002 | –0.001 | 0.001 | –0.005 | –0.002 |
| 17H | 0.014 | 0.013 | 0.013 | 0.015 | 0.014 | 0.015 |

TABLE S-III. Continued

| Position | *cisoid* Conformer | | | *transoid* Conformer | | |
|---|---|---|---|---|---|---|
| | $f^-(\vec{r})$ | $f^+(\vec{r})$ | $f^0(\vec{r})$ | $f^-(\vec{r})$ | $f^+(\vec{r})$ | $f^0(\vec{r})$ |
| 18H | 0.009 | 0.015 | 0.012 | 0.004 | 0.019 | 0.011 |
| 19C | –0.001 | –0.002 | –0.001 | 0.000 | –0.005 | –0.002 |
| 20H | 0.014 | 0.013 | 0.013 | 0.015 | 0.014 | 0.015 |
| 21H | 0.009 | 0.015 | 0.012 | 0.004 | 0.019 | 0.012 |
| 22H | 0.017 | 0.035 | 0.026 | 0.017 | 0.034 | 0.026 |
| 23H | –0.012 | 0.015 | 0.002 | 0.003 | 0.022 | 0.012 |

Table S-IV. Values of the condensed Fukui function for the dipolar aminocyclopyrachlor conformers computed from *MEP* charges according to Eqs. (9)–(11)

| Position | *cisoid* Conformer | | | *transoid* Conformer | | |
|---|---|---|---|---|---|---|
| | $f^-(\vec{r})$ | $f^+(\vec{r})$ | $f^0(\vec{r})$ | $f^-(\vec{r})$ | $f^+(\vec{r})$ | $f^0(\vec{r})$ |
| 1C | 0.147 | –0.055 | 0.046 | 0.145 | –0.037 | 0.054 |
| 2C | –0.082 | 0.030 | –0.026 | –0.065 | 0.014 | –0.026 |
| 3C | –0.007 | ***0.246*** | 0.119 | –0.016 | ***0.228*** | 0.106 |
| 4C | –0.254 | 0.151 | –0.051 | –0.251 | 0.195 | –0.028 |
| 5N | 0.238 | 0.101 | 0.170 | 0.227 | 0.043 | 0.135 |
| 6N | 0.290 | 0.032 | 0.161 | 0.283 | 0.059 | 0.171 |
| 7N | ***0.634*** | 0.126 | ***0.380*** | ***0.646*** | 0.088 | ***0.367*** |
| 8H | –0.026 | 0.025 | 0.000 | –0.027 | 0.034 | 0.004 |
| 9H | –0.037 | 0.022 | –0.008 | –0.040 | 0.021 | –0.009 |
| 10Cl | 0.097 | 0.096 | 0.096 | 0.094 | 0.104 | 0.099 |
| 11C | –0.078 | –0.017 | –0.047 | –0.075 | –0.014 | –0.044 |
| 12° | 0.045 | 0.079 | 0.062 | 0.045 | 0.082 | 0.064 |
| 13° | 0.052 | 0.087 | 0.069 | 0.046 | 0.085 | 0.066 |
| 14C | –0.043 | –0.018 | –0.031 | –0.060 | 0.001 | –0.030 |
| 15H | 0.021 | 0.030 | 0.026 | 0.029 | 0.017 | 0.023 |
| 16C | –0.002 | –0.002 | –0.002 | –0.001 | –0.010 | –0.006 |
| 17H | 0.013 | 0.016 | 0.014 | 0.014 | 0.018 | 0.016 |
| 18H | 0.009 | 0.019 | 0.014 | 0.005 | 0.025 | 0.015 |
| 19C | –0.002 | –0.002 | –0.002 | –0.001 | –0.010 | –0.006 |
| 20H | 0.013 | 0.016 | 0.014 | 0.014 | 0.018 | 0.016 |
| 21H | 0.009 | 0.019 | 0.014 | 0.005 | 0.025 | 0.015 |
| 23H | –0.039 | 0.001 | –0.019 | –0.019 | 0.015 | –0.002 |

Journal of the Serbian Chemical Society
JSCS-info@shd.org.rs • www.shd.org.rs/JSCS
*J. Serb. Chem. Soc. 80* (6) 779–787 (2015)
*JSCS–4757*
UDC 546.57+539.12+549.67:544.726+66.094.2:546.49–71
*Original scientific paper*

# Anisotropic silver nanoparticles deposited on zeolite A for selective $Hg^{2+}$ colorimetric sensing and antibacterial studies

ALIREZA KHORSHIDI*, BEHROOZ HEIDARI and HAMIDREZA INANLU

*Department of Chemistry, Faculty of Sciences, University of Guilan, P. O. Box 41335-1914, Iran*

(Received 29 July 2014, revised 24 February, accepted 26 February 2015)

*Abstract*: Silver nanoparticles deposited on the surface of zeolite A were prepared *via* the post ion-exchange reduction and reduction–deposition methods. The formation of silver nanoparticles on the surface of zeolite A was verified by surface plasmon spectra using diffuse reflectance spectroscopy and ultraviolet–visible spectroscopy. The morphology of the prepared samples was characterized by X-ray diffraction and scanning electron microscopy. Furthermore, silver nanoparticles deposited on the zeolite A after fixation of rhodamine B dye molecules on them were successful in the selective detection of $Hg^{2+}$. After treatment with the so-obtained sensor, a colour change from colourless to pink was visible to the naked eye for concentrations of the $Hg^{2+}$ solution down to $1.0\times10^{-8}$ mol $L^{-1}$. Antibacterial tests demonstrated the multifunctional application of the silver nanoparticles deposited on zeolite A.

*Keywords*: sensor; zeolite A; silver; nanoparticle; rhodamine B; mercury.

## INTRODUCTION

Fascinating chemical and physical properties of noble metal nanostructures and their applications, for example, in catalysis,[1] optics[2] and sensing,[3] have attracted extensive attention in recent years. Of the hitherto studied metallic nanoparticles, silver is the most attractive because of its intense nano size related colorimetric effects. The performance of silver nanoparticles in most applications could be significantly enhanced by control of the dimensions and uniformity. Therefore, many approaches have been invented to fabricate silver nanoparticles.[4] One of the most significant aspects of silver nanoparticles is their localized surface plasmon resonance (LSPR), which is derived from interaction of light and metal nanoparticles when the conduction electrons oscillate locally around the nanoparticles at a certain frequency. This optical feature gives rise to captivating colours and is related to particle shape,[5,6] size[7] and environment.[8,9]

* Corresponding author. E-mail: Khorshidi@guilan.ac.ir
doi: 10.2298/JSC140729020K

A number of strategies have been devised to control the morphologies of silver nanoparticles.[10–14] Anisotropic silver nanoparticles deposited on various supports have also found application in recent years, for example in the coloration of fabrics.[15,16]

The detection and quantification of heavy metal ions, on the other hand, has been a subject of interest due to its importance in waste management, environmental monitoring and clinical toxicology. Among heavy and transition metals, mercury is a well-known chemical pollutant that can cause serious threats to human health. For the successive detection of $Hg^{2+}$, sensitive optical sensors based on fluoresce were reported, which depend on the change of fluorescence of small organic molecules[17–19] to indicate the concentration of $Hg^{2+}$ and usually function in organic media.[20,21] Hence, the development of new and practical chemosensors that offer a promising approach for mercury ion detection is still a great challenge.

Furthermore, zeolite A is one of the most important zeolites that have been used as water softeners in detergents, additives in poly(vinyl chloride) (PVC) plastics, gas drying and separation of linear and branched hydrocarbons. Ongoing interest in the study of transition metals chemistry and ion-exchanged zeolites,[22–24] together with a recent report on rhodamine 6G absorbed on the surface of silver nanoparticles as a probe for the detection of $Cu^{2+}$,[25] prompted the present evaluation of the sensory response of silver nanoparticles deposited on the surface of zeolite A, as a stable solid support for rhodamine B (RhB) dye molecules, toward the detection of heavy metal ions.

## EXPERIMENTAL

### *Materials*

Zeolite A with the composition $2.3Na_2O:1.0Al_2O_3:2SiO_2:300H_2O$ was synthesized according to Salma *et al.*[26] All other chemicals were purchased from Merck and used without further purification.

### *Preparation of silver nanoparticles deposited on the surface of zeolite A: Reduction–deposition method*

Anisotropic silver nanoparticles were prepared according to the Mirkin method.[27] Briefly, aqueous solutions of $AgNO_3$ (0.1 mM, 200 mL), trisodium citrate (100 mM, 3.6 mL), PVP (poly(vinyl pyrrolidone), 0.24g), and hydrogen peroxide (30 wt. %, 0.48 mL) were mixed and vigorously stirred under ambient condition. A freshly prepared aqueous $NaBH_4$ solution (0.65 mL, 100 mM) was then rapidly injected into the mixture. After approximately 30 min, a yellow silver colloid was obtained. To this colloid, 500 mg of zeolite A was added and the mixture was stirred. After 15 min, the zeolite was colorized to pale yellow. Eventually, the treated zeolite was centrifuged at 1000 rpm, rinsed with deionised water and dried at 373 K.

### *Preparation of silver nanoparticles deposited on the surface of zeolite A: Post ion-exchange reduction*

Zeolite A (500 mg) was ion-exchanged with $AgNO_3$ solution (0.1 mM, 200 mL) overnight under stirring at room temperature. The resulting solid was filtered and rinsed with

deionised water (three times), then suspended in 200 mL of deionised water. To this suspension, trisodium citrate (100 mM, 3.6 mL), PVP (0.24 g) and hydrogen peroxide (30 wt. %, 0.48 mL) were added and the mixture stirred vigorously. $NaBH_4$ solution (0.65 mL, 100 mM) was then rapidly injected into the mixture. After approximately 45 min, the colour of zeolite had changed to yellow. This product was separated by centrifuge at 1000 rpm, rinsed with deionised water and dried at 373 K.

*Sensor studies*

5 mL of rhodamine B dye (RhB, $1\times10^{-6}$ mol.L$^{-1}$) was gradually added to a 5 mL aqueous suspension of 500 mg of the product obtained by post ion-exchange reduction., and magnetically stirred. After 30 min, colour of the solution had faded and the mixture was centrifuged at 1000 rpm. The yellow product (RhB–Ag–ZeoA) was rinsed with deionised water (three times) and dried at 373 K. To 100 mg of this sample, 3 mL of the test solution containing metallic ions, such as $Fe^{2+}/Cu^{2+}/Zn^{2+}/Hg^{2+}/Mg^{2+}$ of concentration $1\times10^{-6}$ mol.L$^{-1}$ was added and stirred for 30 min. The best response, however, was obtained for $Hg^{2+}$, and the pink colour of RhB developed into the solution during 20 min. To investigate the sensitivity effect of the RhB–Ag–ZeoA toward $Hg^{2+}$, various concentrations of $Hg^{2+}$ ($10^{-5}/10^{-6}/10^{-7}/10^{-8}/10^{-9}$ mol L$^{-1}$) was studied by recording UV–Vis spectra of the supernatant liquid obtained after filtration of the mixture.

*Characterizations*

UV-Vis spectra were recorded on a Perkin Elmer LAMBDA 25 spectrophotometer. The diffuse reflectance spectra were recorded at room temperature using a Shimadzu UV-2100 spectrophotometer in the reflectance mode by investigating the evolution of the absorbance. X-Ray powder diffraction (XRD) measurements were performed using a Philips diffractometer with mono chromatized $CuK_\alpha$ radiation at 40 kV and 20 mA (Ni filter, $2\theta$ 10 to 70° with a step size of 0.05° and a count time of 1 s). Morphology of the synthesized samples was characterized using a Philips XL30 ESEM scanning electron microscope (SEM).

*Antibacterial activity of extracts*

*Bacteria and culture.* The bacteria *Staphylococcus aureus* (PTCC 1764) and *Pseudomonas aeruginosa* (PTCC 1074*)* were purchased from the Persian Type Culture Collection (PTCC, Tehran, Iran) and used as test microorganisms. The strains were cultured on Nutrient Broth medium and incubated at 37 °C for 24 h.

*Preparations of extracts.* 5 ml of distilled deionised water were added to 15 mg of zeolite A, $Ag^+$ ion-exchanged zeolite A ($Ag^+$A), silver nanoparticles deposited on the zeolite A *via* the reduction–deposition method (AgA–RD) and silver nanoparticles deposited on the zeolite A *via* the post ion-exchange method (AgA–PX), and stirred for 3 h at 150 rpm. Then, after centrifuging at 4000 rpm for 10 min, the supernatants were collected. Finally, 112, 225 and 450 µL volumes, each in triplicate, were chosen for antibacterial assessment.

*Antibacterial test.* Antibacterial activities of each extraction were assessed by the well diffusion method.[28] The prepared extracts were separately transferred into the wells punched in the inoculated plates using a 0.5-cm sterile cork borer and incubated at 37 °C for 24 h. The antibacterial activities were determined by measuring the diameter of the inhibition zone (mm). Drug references, *i.e.*, tetracycline (30 µg disc$^{-1}$), chloramphenicol (30 µg disc$^{-1}$) and cefotaxime (30 µg disc$^{-1}$), were used as positive controls.

*Statistical analysis*

Data were analyzed using SPSS version 19 in Windows 7. The differences between the various treatments were assessed using one-way ANOVA followed by the Duncan test at a confidence level of 95 %. There were three triplicates in all the experiments. All data are presented as the mean ± *SD*.

## RESULTS AND DISCUSSION

Formation of anisotropic silver nanoparticles is associated with a colour change of the solution to light yellow. The in-plane dipole LSPR band of the silver nanoparticles is responsible for this color,[14] and in the present experiments, it occurred at 490 nm, as is obvious from UV–Vis spectra of the solution (Fig. 1, curve a). These anisotropic silver nanoparticles were deposited on the surface of zeolite A *via* the reduction–deposition method, resulting in a pale yellow powder. The same characteristic band of the silver nanoparticles at 490 nm was observed in the diffuse reflectance spectra (DRS) of this powder (Fig. 1, curve b).

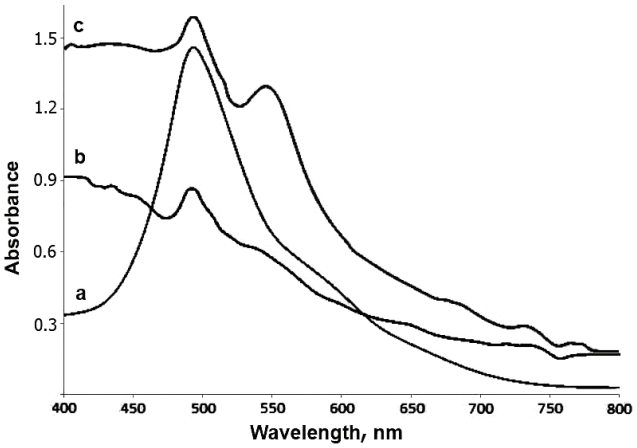


Fig. 1. a) UV-Vis spectra of silver nanoparticles, b) DRS spectra of Ag–ZeoA and c) DRS spectra of RhB–Ag–ZeoA.

The SEM technique was used to clarify the evolution of silver nanoparticles and their deposition on the surface of the zeolite. As shown in Fig. 2a, silver nanoparticles with different sizes and shapes were formed along with some aggregates. The post ion-exchange reduction method, however, resulted in more uniform semi spherical particles (Fig. 2b) with a narrower size distribution. A closer observation by TEM further confirmed this result, as could be seen in Fig. 2c.

The crystalline character of the prepared samples was analyzed by X-ray diffraction (XRD). The XRD patterns of the dried samples obtained *via* the reduction–deposition method and *via* the post ion-exchange reduction method are shown in Fig. 3, curves a and b, respectively. Both patterns, showed three index peaks at 37.9, 44.0 and 64.4°, associated with the (111), (200) and (220) reflect-

ions of fcc silver, based on the standard values given in the JCPDS card (file No. 04-783). The XRD patterns also showed that the crystal structure of the zeolite A (JCPDS card No. 73-2340) was retained after deposition of the silver nanoparticles.

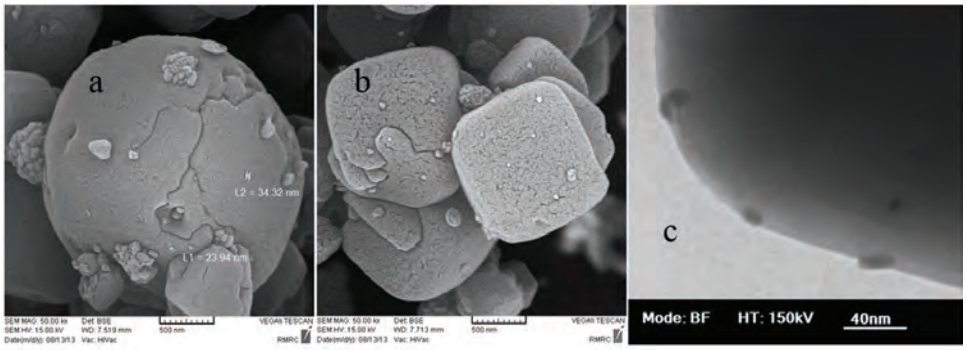


Fig. 2. SEM image of the silver nanoparticles deposited on the surface of zeolite A *via*: a) the reduction–deposition method and b) the post ion-exchange reduction method and c) a TEM image of the latter.

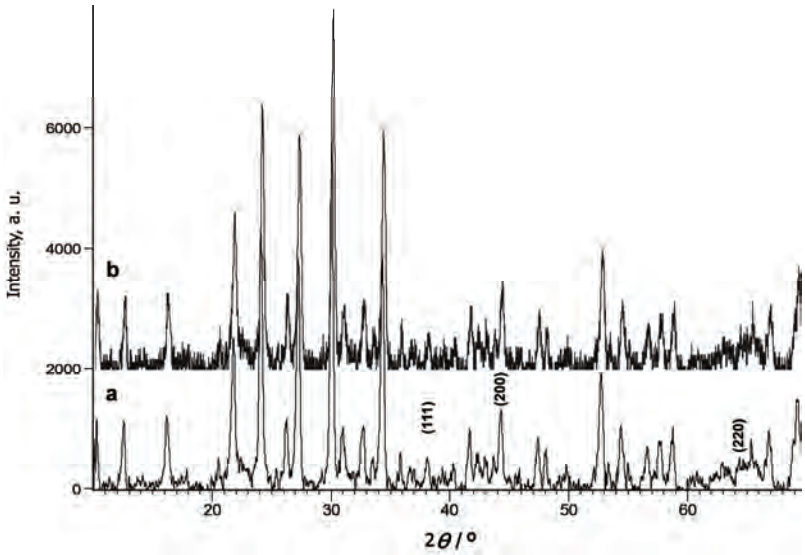


Fig. 3. XRD pattern of Ag–ZeoA obtained *via* a) the reduction deposition method and b) the post ion-exchange reduction method.

*Sensor studies*

Based on the morphological properties, the silver nanoparticles deposited on the surface of zeolite A *via* the post ion-exchange reduction method were chosen for sensor studies. Fixation of the RhB dye molecules over the surface of silver

nanoparticles deposited on zeolite A (RhB–Ag–ZeoA) was evident from the DRS spectra of the product. As shown in Fig. 1, curve c, the characteristic band of the silver nanoparticles at 490 nm and that of RhB at 550 nm are present simultaneously. Heavy metal sensing could be attributed to the replacement of dye moieties by metallic ions, according to Kirubaharan *et al.*[25] Among the different cations tested ($Fe^{2+}$/$Cu^{2+}$/$Zn^{2+}$/$Hg^{2+}$/$Mg^{2+}$), only $Hg^{2+}$ resulted in the release of dye moiety as a visual colorimetric sensor. A dilute solution of RhB dye in water is pink and this colour develops into the solution upon addition of $Hg^{2+}$ solution to the RhB–Ag–ZeoA, as $Hg^{2+}$ start to adhere to the surface of the silver nanoparticles by replacing RhB dye molecules. A colour change from colourless to pink was visible to the naked eye for concentrations of $Hg^{2+}$ in the solution down to $1.0\times10^{-8}$ mol $L^{-1}$. The proposed sensing mechanism is given in Fig. 4.

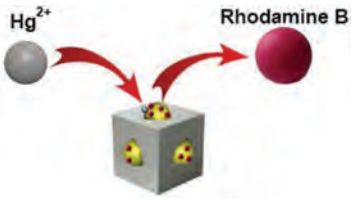


Fig. 4. The mechanism of sensing $Hg^{2+}$ ions by RhB–Ag–ZeoA.

The limit of detection, however, was determined by recording the UV–Vis spectrum of the supernatant liquid obtained after filtration of the mixture. The spectroscopic responses of 100 mg of RhB–Ag–ZeoA against 5 mL of $Hg^{2+}$ solutions of concentrations $10^{-5}/10^{-6}/10^{-7}/10^{-8}/10^{-9}$ mol $L^{-1}$ are shown in Fig. 5a. The absorbance intensity is dependent upon the concentration of $Hg^{2+}$ and

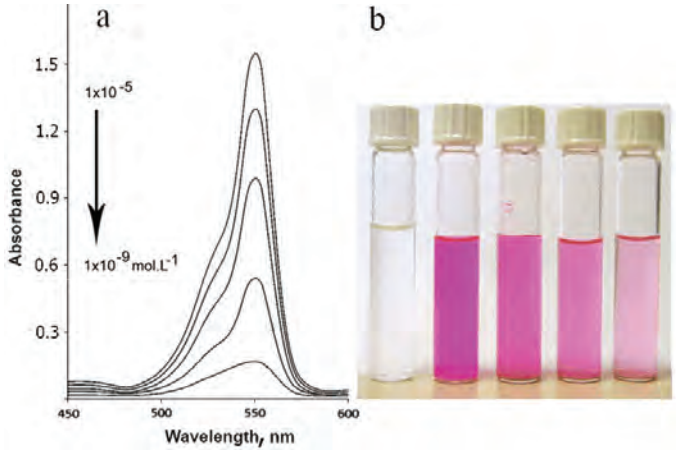


Fig. 5. a) Spectroscopic response of RhB–Ag–ZeoA upon the addition of $1.0\times10^{-5}/10^{-6}/10^{-7}/10^{-8}/10^{-9}$ mol $L^{-1}$ of $Hg^{2+}$ and b) the corresponding colour changes in solutions containing four concentrations ($1.0\times10^{-5}/10^{-6}/10^{-7}/10^{-8}$ mol $L^{-1}$) against $Hg^{2+}$ solution ($1.0\times10^{-5}$ mol $L^{-1}$) as blank (from right to left).

minimal concentration of mercuric ions ($1.0\times10^{-9}$ mol $L^{-1}$) was detectable. The corresponding colour changes of solutions containing the four upper concentrations of $Hg^{2+}$ are presented in Fig. 5b.

*The results of the antibacterial test*

Assessment of antibacterial test of the extracts using well diffusion method showed significantly different inhibitory effects on the growth of *S. aureus* and *P. aeruginosa*. Since the extract volume of 112 μL $well^{-1}$ had no effect on the growth of the bacteria, it is not mentioned in the results.

*Effects of the extracts on* S. aureus. Similar inhibitory effects were observed for the extracts with extract volumes of 225 and 450 μL $well^{-1}$ (Figs. S-1 and S--2, given in the Supplementary material to this paper). Zeolite A had no effect on *S. aureus* while the other extracts showed significant inhibitory effects on the bacteria ($p < 0.05$). The diameter of inhibition zone of $Ag^+A$ and AgA–RD were significantly higher than that of AgA–PX ($p < 0.05$, Fig. S-1). The maximum diameter of inhibition zone was measured in AgA–RD in both extract volumes.

*Effects of the extracts on* P. aeruginosa. Significant differences in the growth of *P. aeruginosa* ($p < 0.05$) were observed between the extracts with extract volumes of 225 and 450 μL $well^{-1}$ (Figs. S-3 and S-4 of the Supplementary material).

With an extract volume of 225 μL $well^{-1}$, zeolite A, $Ag^+A$ and AgA–PX had no inhibition effects but AgA–RD showed an inhibitory effect on the growth of the bacteria with an inhibition zone diameter of 8.33±1.15 mm (Fig. S-3). With an extract volume of 450 μL $well^{-1}$, $Ag^+A$ had the largest diameter of the inhibition zone (14±0 mm) in relation to AgA–PX (12±0 mm) and AgA–RD (8±1.73 mm, $p < 0.05$), while zeolite A had no effect (Fig. S-4).

*The drug references test*. The results of inhibitory effects of the drug references, *i.e.*, Tetracycline (30 μg $disc^{-1}$), Chloramphenicol (30 μg $disc^{-1}$) and Cefotaxime (30 μg $disc^{-1}$), as positive controls on the growth of the bacteria, are given in Table I. Although the results showed that all antibiotics had larger inhibitory effects compared to those of the extracts, some extracts gave comparable values for bacterial inhibition as the antibiotics (data in Fig. S-4).

TABLE I. Antibacterial tests (diameter of inhibition zone, mm) of the extracts and positive controls on *S. aureus* (*S. a.*) and *P. aeruginosa* (*P. a.*); mean values bearing different superscripts in each column are significantly different ($p < 0.05$)

| Extract | Extract volume, μL $well^{-1}$ | | | | | | 30 μg/disc | |
|---|---|---|---|---|---|---|---|---|
| | 112 | | 225 | | 450 | | | |
| | Bacterium | | | | | | | |
| | *S. a.* | *P. a.* | *S. a.* | *P. a.* | *S. a.* | *P. a.* | *S. a.* | *P. a.* |
| Zeolite A | 0 | 0 | $0^c$ | $0^b$ | $0^c$ | $0^d$ | – | – |
| $Ag^+A$ | 0 | 0 | $9\pm1^a$ | $0^b$ | $10\pm2^a$ | $14\pm0^a$ | | |

TABLE I. Continued

| Extracts | Extract volume, µL well$^{-1}$ | | | | | | 30 µg/disc | |
|---|---|---|---|---|---|---|---|---|
| | 112 | | 225 | | 450 | | | |
| | Bacterium | | | | | | | |
| | *S. a.* | *P. a.* | *S. a.* | *P. a.* | *S. a.* | *P. a.* | *S. a.* | *P. a.* |
| AgA–RD | 0 | 0 | 9.66±2.08$^{a}$ | 8.33±1.15$^{a}$ | 11±2$^{a}$ | 8±1.7$^{c}$ | – | – |
| AgA–PX | 0 | 0 | 7±2$^{b}$ | 0$^{b}$ | 9.33±2.33$^{b}$ | 12±0$^{b}$ | | |
| Antibiotics | | | | | | | | |
| Tetracycline | – | – | – | | – | – | 12±0.1 | 12±0.2 |
| Chloramphenicol | – | – | – | | – | – | 13±0.2 | 13±0.1 |
| Cefotaxime | – | – | – | | – | – | 14±0.1 | 14±0.2 |

## CONCLUSIONS

In conclusion, an easy to preserve, stable and reliable colorimetric chemosensor for the successful detection of $Hg^{2+}$ ions in solution was developed. Antibacterial activity of silver nanoparticles deposited on zeolite A, also, promises multifunctional usage of this type of material.

## SUPPLEMENTARY MATERIAL

The effects of extracts at different concentrations on the bacteria, Figs. S-1–S-4, are available electronically from http://www.shd.org.rs/JSCS/, or from the corresponding author on request.

*Acknowledgment*. Partial support of this study by the Research Council of the University of Guilan is gratefully acknowledged.

## ИЗВОД

## ИСПИТИВАЊЕ СЕЛЕКТИВНЕ КОЛОРИМЕТРИЈСКЕ ДЕТЕКЦИЈЕ $Hg^{2+}$ И АНТИБАКТЕРИЈСКОГ ДЕЈСТВА АНИЗОТРОПНИХ НАНОЧЕСТИЦА СРЕБРА НАНЕТИХ НА ЗЕОЛИТ

ALIREZA KHORSHIDI, BEHROOZ HEIDARI и HAMIDREZA INANLU

*Department of Chemistry, Faculty of Sciences, University of Guilan, P. O. Box 41335-1914, Iran*

Наночестице сребра нанете на површину зеолита А припремљене су редукцијом након јонске измене и редукционо–депозиционом методама. Формирање наночестица сребра на површини зеолита А је потврђено спектрима површинских плазмона применом дифузне рефлексионе спектроскопије и UV–Vis спектроскопије. Морфологија припремљених узорака је одређена дифракцијом X-зрачења и скенирајућом електронском микроскопијом. Наночестице сребра нанете на зеолит А на којима су фиксирани молекули родамин Б боје су успешно примењене за селективну детекцију $Hg^{2+}$. Након третмана са сензором добијем на наведени начин, промена боје од безбојне до розе била је видљива оком за концентрације раствора $Hg^{2+}$ до $1{,}0\times10^{-8}$ mol $L^{-1}$. Антибактеријски тестови су показали мултифункционалну примену наночестица сребра нанетих на зеолит А.

(Примљено 29. јула 2014, ревидирано 24. фебруара, прихваћено 26. фебруара 2015)

REFERENCES


1. F. Zhang, G. B. Braun, Y. F. Shi, Y. C. Zhang, X. H. Sun, N. O. Reich, D. Y. Zhao, G. Stucky, *J. Am. Chem. Soc*. **132** (2010) 2850
2. K. Gude, R. Narayanan, *J. Phys. Chem., C* **114** (2010) 6356
3. A. Saha, S. K. Basiruddin, R. Sarkar, N. Pradhan, N. R. Jana, *J. Phys. Chem., C* **113** (2009) 18492
4. D. P. Perez, *Silver nanoparticles*, In-Teh, Vukovar, 2010, p. 35
5. L. J. Sherry, R. C. Jin, C. A. Mirkin, G. C. Schatz, R. P. van Duyne, *NanoLett*. **6** (2006) 2060
6. L. J. Sherry, S. H. Chang, G. C. Schatz, R. P. van Duyne, B. J. Wiley, Y. N. Xia, *NanoLett*. **5** (2005) 2034.
7. C. L. Haynes, R. P. van Duyne, *J. Phys. Chem., B* **105** (2001) 5599
8. J. J. Mock, D. R. Smith, S. Schultz, *NanoLett*. **3** (2003) 485
9. M. Hu, J. Chen, M. Marquez, Y. Xia, G. Hartland, *J. Phys. Chem., C* **111** (2007) 12558
10. R. C. Jin, Y. W. Cao, C. A. Mirkin, K. L. Kelly, G. C. Schatz, J. G. Zheng, *Science* **294** (2001) 1901
11. C. J. Murphy, T. K. Sau, A. M. Gole, C. J. Orendorff, J. Gao, L. Gou, S. E. Hunyadi, T. Li, *J. Phys. Chem., B* **109** (2005) 13857
12. Y. Xia, Y. Xiong, B. Lim, S. E. Skrabalak, *Angew. Chem. Int. Ed*. **48** (2008) 60
13. E. Hao, K. L. Kelly, J. T. Hupp, G. C. Schatz, *J. Am. Chem. Soc*. **124** (2002) 15182
14. B. Tang, S. Xu, J. An, B. Zhao, W. Xu, *J. Phys. Chem., C* **113** (2009) 7025
15. B. Tang, M. Zhang, X. Hou, J. Li, L. Sun, X. Wang, *Ind. Eng. Chem. Res*. **51** (2012) 12807
16. F. M. Kelly, J. H. Johnston, *ACS Appl. Mater. Interfaces* **3** (2011) 1083
17. G. Hennrich, H. Sonnenschein, U. Resch-Genger, *J. Am. Chem. Soc*. **121** (1999) 5073
18. E. M. Nolan, S. J. Lippard, *J. Am. Chem. Soc*. **125** (2003) 14270
19. A. G. Lista, M. E. Palomeque, B. S. Fernàndez Band, *Talanta* **50** (1999) 881
20. K. Rurack, U. Resch-Genger, J. L. Bricks, M. Spiele, *Chem. Commun*. **21** (2000) 2103
21. D. S. McClure, *J. Chem. Phys*. **20** (1952) 682
22. A. Khorshidi, *Chin. Chem. Lett*. **23** (2012) 903
23. A. Khorshidi, *Ultrason. Sonochem*. **19** (2012) 570
24. A. Khorshidi, K. Tabatabaeian, *J. Mol. Cat., A: Chem*. **344** (2011) 128
25. C. J. Kirubaharan, D. Kalpana, Y. S. Lee, A. R. Kim, D. J. Yoo, K. S. Nahm, G. Kumar, *Ind. Eng. Chem. Res*. **51** (2012) 7441
26. M. Tarek Salama, O. Ibraheem Ali, I. Ahmed Hanafy, M. Waffa Al-Meligy, *Mat. Chem. Phys*. **113** (2009) 159.
27. G. S. Metraux, C. A. Mirkin, *Adv. Mater*. **17** (2005) 412
28. N. Kiani, B. Heidari, M. Rassa, M. Kadkhodazadeh, B. Heidari, *J. Basic Clin. Physiol. Pharmacol*. **25** (2014) 367.

Journal of the Serbian Chemical Society
JSCS@tmf.bg.ac.rs • www.shd.org.rs/JSCS
*J. Serb. Chem. Soc. 80* (6) S215–S217 (2015) *Supplementary material*

SUPPLEMENTARY MATERIAL TO

# Anisotropic silver nanoparticles deposited on zeolite A for selective $Hg^{2+}$ colorimetric sensing and antibacterial studies

ALIREZA KHORSHIDI*, BEHROOZ HEIDARI and HAMIDREZA INANLU

*Department of Chemistry, Faculty of Sciences, University of Guilan, P. O. Box 41335-1914, Iran*

*J. Serb. Chem. Soc.* 80 (6) (2015) 779–787

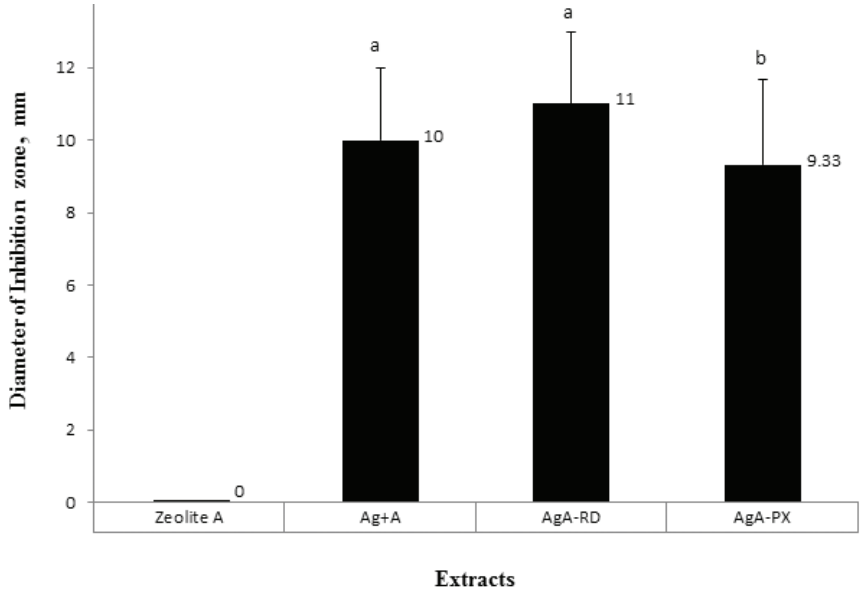


Fig. S-1. The effects of extracts with extract volume of 450 µL $well^{-1}$ on the growth of *S. aureus*. Mean values bearing different superscripts are significantly different ($p < 0.05$).

* Corresponding author. E-mail: Khorshidi@guilan.ac.ir

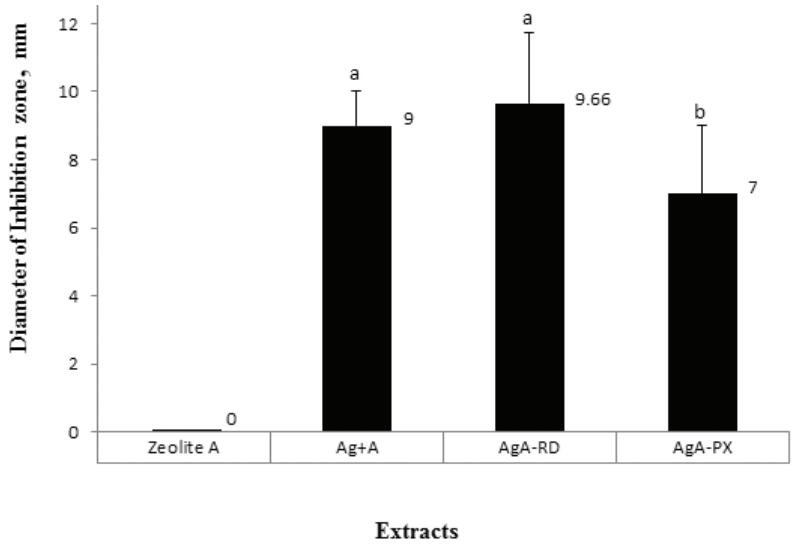


Fig. S-2. The effects of extracts with an extract volume of 225 µL well$^{-1}$ on the growth of *S. aureus*. Mean values bearing different superscripts are significantly different ($p < 0.05$).

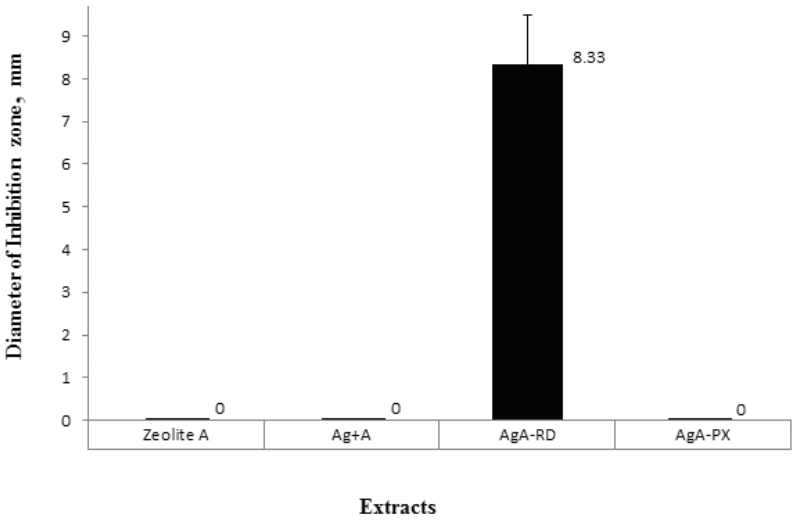


Fig. S-3. The effects of treatments with extract volume of 225 µL well$^{-1}$ on the growth of *P. aeruginosa*. Mean values bearing different superscripts are significantly different ($p < 0.05$).

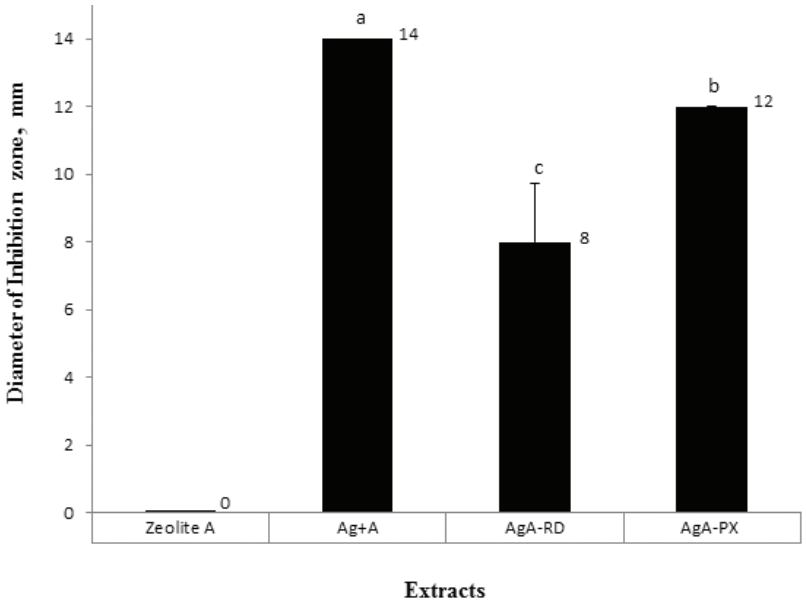


Fig. S-4. The effects of treatments with extract volume of 450 µL well$^{-1}$ on the growth of *P. aeruginosa.* Mean values bearing different superscripts are significantly different ($p < 0.05$).

Journal of the Serbian Chemical Society
JSCS-info@shd.org.rs • www.shd.org.rs/JSCS
*J. Serb. Chem. Soc. 80* (6) 789–799 (2015) UDC 577.164.1+544.6.076.32–039.26:543.552
*JSCS–4758* *Original scientific paper*

# Voltammetric determination of carbidopa and folic acid using a modified carbon nanotubes paste electrode

NASRIN KESHTKAR[1,2], MOHAMMAD ALI TAHER[1] and HADI BEITOLLAHI[3]*

[1]*Department of Chemistry, Shahid Bahonar University of Kerman, P. O. Box 76175-133, Kerman, Iran,* [2]*Young Researchers Society, Shahid Bahonar University of Kerman, P. O. Box 76175-133, Kerman, Iran and* [3]*Environment Department, Institute of Science and High Technology and Environmental Sciences, Graduate University of Advanced Technology, Kerman, Iran*

(Received 26 December 2013, revised 11 April, accepted 17 April 2014)

*Abstract*: A novel electrochemical sensor for the selective and sensitive detection of carbidopa in the presence of a large excess of folic acid at physiological pH was developed by the bulk modification of a carbon paste electrode (CPE) with carbon nanotubes (CNTs) and vinylferrocene. Large peak separation, good sensitivity and stability allow this modified electrode to be used for the analysis of carbidopa individually and simultaneously along with folic acid. Applying square wave voltammetry (SWV), a linear dynamic range of $1.0\times10^{-6}$–$7.0\times10^{-4}$ M with a detection limit of $2.0\times10^{-7}$ M was obtained for carbidopa. Finally, the proposed method was applied to the determination of carbidopa and folic acid in a urine sample.

*Keywords*: carbidopa; folic acid; carbon nanotubes; modified electrodes.

## INTRODUCTION

Carbon nanotubes (CNTs) have received enormous attention in the last years due to their unique structural, mechanical, geometric and chemical properties.[1] Their closed topology and tubular structure have made them very attractive materials.[2,3] CNTs have demonstrated themselves to be extremely useful for the development of new electrode materials. Their electrocatalytic properties have been widely demonstrated in connection with several compounds of clinical, biological and environmental interest.[4–17]

In addition, the application of chemically modified electrodes (CMEs) in electroanalysis offers several advantages. They can lower the overpotential, increase the reaction rate and sensitivity and improve selectivity.[18–27]

* Corresponding author. E-mail: h.beitollahi@yahoo.com
doi: 10.2298/JSC131216046K

Carbidopa (lodosyn) is a drug used in the treatment of Parkinson's disease by inhibiting the peripheral metabolism of levodopa.[28] A combination of carbidopa/levodopa carries the brand names sinemet, parcopa and atamet; while stalevo is a combination with entacapone, which enhances the bioavailability of carbidopa and levodopa. Therefore, determination of this drug is very important in biological sample such as urine. Different techniques have been employed for the determination of carbidopa, including spectrophotometry, capillary zone electrophoresis, high performance liquid chromatography (HPLC) and liquid chromatography (LC). Long analysis times, the use of organic solvents and high costs are some of the drawbacks associated with these techniques. Voltammetry is considered as an important electrochemical technique utilized in electroanalytical chemistry because it provides low cost, sensitivity, precision, accuracy, simplicity and rapidity.[29–35]

Folic acid, often regarded as a part of the vitamin B complex, possesses considerable biological importance for human health, especially during periods of rapid cell division and growth.[36] A deficiency of general folic acid may cause serious illness, notably for women planning pregnancy, which can result in malformations of the spine, skull, and brain.[37] Therefore, the determination of folic acid has drawn significant attention, and a reliable and sensitive detection method is widely anticipated. At present, some techniques, such as spectrophotometry, fluorometry, HPLC, and flow injection chemiluminescence have been used to detect folic acid.[38] However, these techniques are complex, time-consuming, and require expensive instruments. Electrochemical methods have also been used and have attracted enormous interest due to their advantages of simplicity, rapid response, excellent reproducibility, good stability, low cost, low detection limit, *etc*.[39–42]

In the present study, a new electrode composed of a carbon nanotube paste electrode (CNPE) modified with vinylferrocene (VFCNPE) was prepared and its performance for the electrocatalytic determination of carbidopa in aqueous solutions investigated. The analytical performance of the modified electrode for quantification of carbidopa in the presence of folic acid was also evaluated.

## EXPERIMENTAL

### *Apparatus and chemicals*

The electrochemical measurements were performed with an Autolab potentiostat/galvanostat (PGSTAT 302 N, Eco Chemie, the Netherlands). The experimental conditions were controlled with General Purpose Electrochemical System (GPES) software. A conventional three-electrode cell was used at 25±1 °C. An Ag/AgCl/KCl (3.0 M) electrode, a platinum wire, and the VFCNPE were used as the reference, auxiliary and working electrodes, respectively. A Metrohm 827 pH/ion meter was used for pH measurements.

All solutions were freshly prepared with double distilled water. Carbidopa, folic acid and all other reagents were of analytical grade from Merck (Darmstadt, Germany). Graphite powder (particle diameter = 0.1 mm) and paraffin oil (DC 350, density = 0.88 g $cm^{-3}$) as the

binding agent (both from Merck) were used for preparing the pastes. Multiwalled carbon nanotubes (purity more than 95 %) with o. d. between 10 and 20 nm, i. d. between 5 and 10 nm, and tube length from 0.5 to 200 μm were prepared by Nanostructured & Amorphous Materials, Inc. The buffer solutions were prepared from orthophosphoric acid and its salts in the pH range of 2.0–11.0. Vinylferrocene (VF) was purchased from Sigma Aldrich.

*Preparation of the electrode*

The VFCNPEs were prepared by hand mixing 0.01 g of VF with 0.89 g graphite powder and 0.1 g CNTs with a pestle and mortar. Then, *ca*. 0.7 mL of paraffin oil was added to this mixture and mixed for 20 min until a uniformly wetted paste was obtained. The paste was then packed into the end of a glass tube (*ca.* 3.4 mm i. d. and 15 cm long). A copper wire inserted into the carbon paste provided the electrical contact. When necessary, a new surface was obtained by pushing an excess of the paste out of the tube and polishing with a weighing paper.

For comparison, a VF modified CPE electrode (VFCPE) without CNTs, a CNTs paste electrode (CNPE) without VF, and an unmodified CPE in the absence of both VF and CNTs were also prepared in the same way.

## RESULTS AND DISCUSSION

### *Electrochemical properties of VFCNPE*

A VFCNPE was constructed and its electrochemical properties were studied in a 0.1 M phosphate buffer solution (PBS, pH 7.0) using cyclic voltammetry (CV). The experimental results showed well defined and reproducible anodic and cathodic peaks related to the vinylferrocene/vinylferricenium ion redox system, with $E_{pa}$, $E_{pc}$ and $E°'$ of 0.41, 0.3 and 0.355 V *vs.* Ag/AgCl/KCl (3.0 M), respectively. The observed peak separation potential, $\Delta E_p = (E_{pa} - E_{pc})$ of 110 mV, was greater than the value of $59/n$ mV expected for a reversible system,[43] suggesting that the redox couple of VF in the VFCNPE had a quasi-reversible behavior in aqueous medium.

### *Influence of pH*

The electrochemical behavior of carbidopa was dependent on the pH value of the aqueous solution, whereas the electrochemical properties of the $Fc/Fc^+$ redox couple were independent of pH. Therefore, pH optimization of the solution was necessary in order to obtain the electrocatalytic oxidation of carbidopa. Thus the electrochemical behavior of carbidopa was studied in 0.1 M PBS at different pH values ($2.0 < pH < 11.0$) at the surface of VFCNPE by CV. It was found that the electrocatalytic oxidation of carbidopa at the surface of VFCNPE was more favored under neutral conditions than in acidic or basic medium. This appears as a gradual growth in the anodic peak current and a simultaneous decrease in the cathodic peak current in the CVs of VFCNPE. Thus, the pH 7.0 was chosen as the optimum pH for electrochemical oxidation of carbidopa at the surface of a VFCNPE.

In addition, pH optimization of the solution was necessary in order to obtain the best peak resolution for carbidopa and folic acid. Thus, the electrochemical behavior of carbidopa and folic acid was studied in 0.1 M PBS at different pH values (2.0 < pH < 11.0) at the surface of VFCNPE by square wave voltammetry (SWV). It was found that the best condition to separate oxidation peaks of carbidopa and folic acid was pH 7.0. Thus, the pH 7.0 was chosen as the optimum pH for simultaneous determination of carbidopa and folic acid.

*Electrocatalytic oxidation of carbidopa at a VFCNPE*

The CV responses for the electrochemical oxidation of 0.4 mM carbidopa at an unmodified CPE (curve b), a CNPE (curve d), a VFCPE (curve e) and a VFCNPE (curve f) are depicted in Fig. 1. As can be seen, while the anodic peak potentials for carbidopa oxidation at the CNPE, and unmodified CPE were 700 and 750 mV, respectively, the corresponding potentials at the VFCNPE and VFBCPE were ≈410 mV. These results indicate that the peak potential for carbidopa oxidation at the VFCNPE and VFCPE is shifted by ≈290 and 340 mV toward negative values compared to the peak potentials at the CNPE and unmodified CPE, respectively. However, the VFCNPE showed a much higher anodic peak current for the oxidation of carbidopa compared to the VFCPE, indicating that the combination of CNTs and the mediator (VF) significantly improved the performance of the electrode toward carbidopa oxidation. In fact, VFCNPE in the absence of carbidopa exhibited a well-behaved redox reaction (Fig. 1, curve c) in 0.1 M PBS (pH 7.0). However, there was a drastic increase in the anodic peak current in the presence of 0.4 mM carbidopa (curve f), which could be related to the strong electrocatalytic effect of the VFCNPE towards this compound.[43]

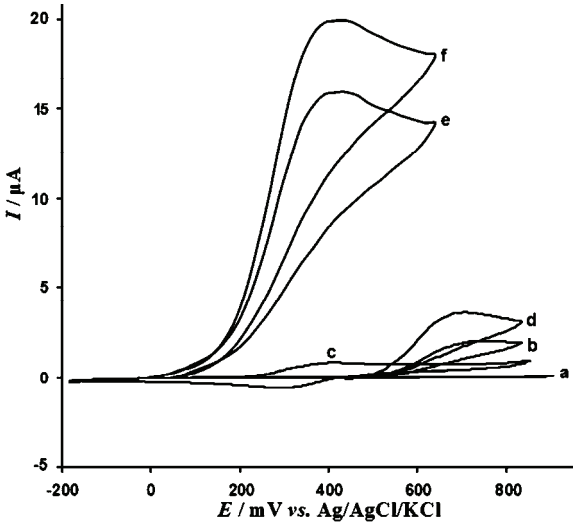


Fig. 1. CVs of: a) unmodified CPE in 0.1 M PBS (pH 7.0), b) unmodified CPE in 0.4 mM carbidopa, c) VFCNPE in 0.1 M PBS, d) CNPE in 0.4 mM carbidopa, e) VFCPE in 0.4 mM carbidopa and f) VFCNPE in 0.4 mM carbidopa. In all cases, the scan rate was 10 mV $s^{-1}$.

The effect of scan rate on the electrocatalytic oxidation of carbidopa at the VFCNPE was investigated by CV (Fig. 2). As could be observed in Fig. 2, the oxidation peak potential shifted to more positive potentials with increasing scan rate, confirming kinetic limitation in the electrochemical reaction. Furthermore, a plot of peak height ($I_p$) *vs*. the square root of the scan rate ($v^{1/2}$) was found to be linear in the range of 6–16 mV $s^{-1}$, suggesting that, at sufficient overpotential, the process is diffusion rather than surface controlled (Fig. 2A).

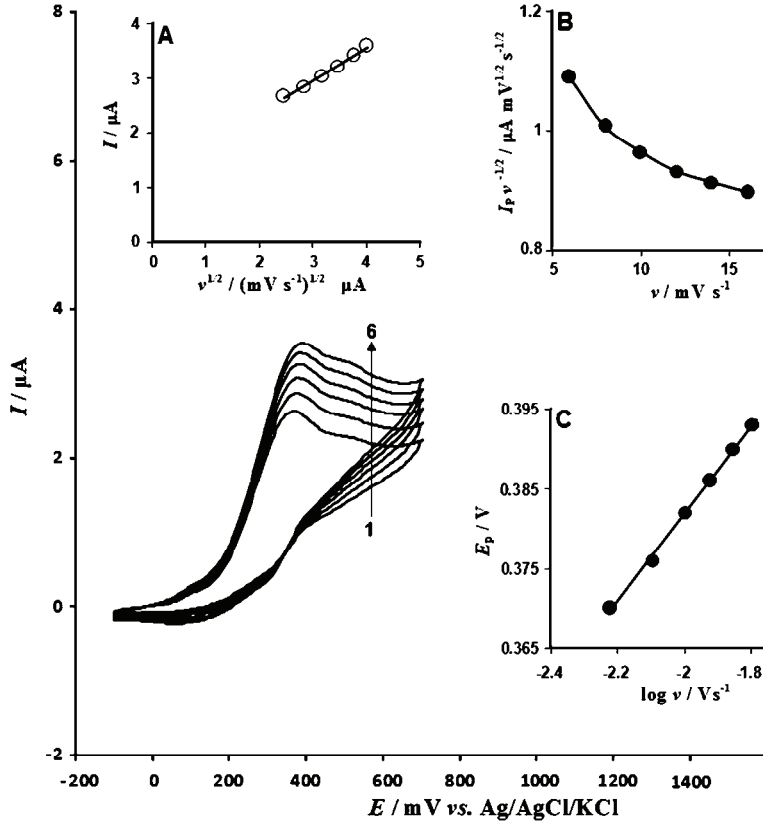


Fig. 2. CVs at the VFCNPE in 0.1 M PBS (pH 7.0) containing 100.0 μM carbidopa at various scan rates; Numbers 1–6 correspond to of 6, 8, 10, 12, 14 and 16 mV $s^{-1}$, respectively. Insets: variation of: A) anodic peak current *vs*. $v^{1/2}$, B) normalized current ($I_p/v^{1/2}$) *vs*. *v* and C) anodic peak potential *vs*. log *v*.

A plot of the scan rate-normalized current (($I_p/v^{1/2}$)) *vs*. scan rate (Fig. 2B) exhibited the characteristic shape typical of an EC′ process.[43]

The Tafel slope (*b*) could be obtained from the slope of $E_p$ *vs*. log *v* using Eq. (1):[43]

$$E_p = \frac{b}{2}\log v + \text{constant} \quad (1)$$

The Tafel slope was found to be 0.109 V (Fig. 2C), which indicates that a one-electron transfer process is the rate limiting step assuming a transfer coefficient ($\alpha$) of 0.46.

*Chronoamperometric measurements*

Chronoamperometric measurements of carbidopa at the VFCNPE were performed by setting the working electrode potential at 0.5 V *vs*. Ag/AgCl/KCl (3.0 M) for various concentration of carbidopa in PBS (pH 7.0), Fig. 3. For an electroactive material (carbidopa in this case) with a diffusion coefficient of *D*, the current observed for the electrochemical reaction under mass transport limited conditions is described by the Cottrell equation.[43] Experimental plots of *I vs.* $t^{-1/2}$ were employed, with the best fits for different concentrations of carbidopa (Fig. 3A). The slopes of the resulting straight lines were then plotted *vs*. the carbidopa concentration (Fig. 3B). From the resulting slope and the Cottrell equation, the mean value of the *D* was found to be $1.7\times10^{-6}$ cm$^2$ s$^{-1}$.

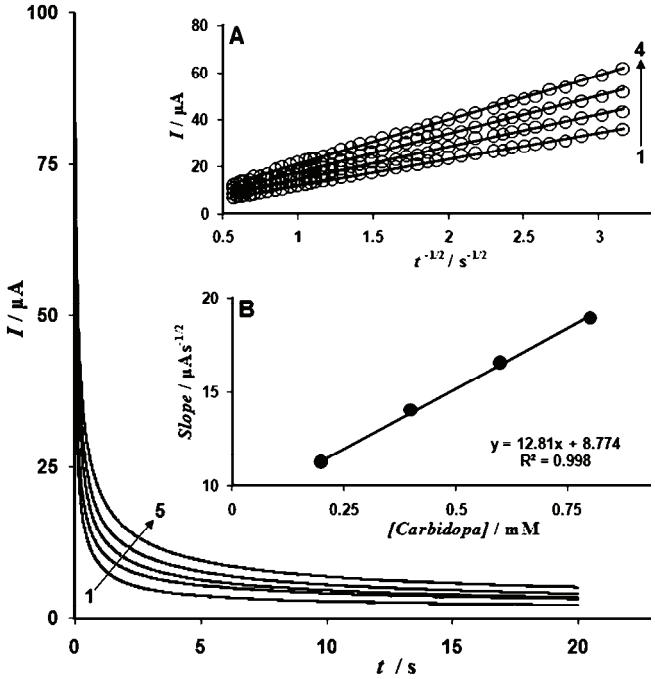


Fig. 3. Chronoamperograms obtained at the VFCNPE in 0.1 M PBS (pH 7.0) for different concentration of carbidopa. The numbers 1–5 correspond to 0.0, 0.2, 0.4, 0.6 and 0.8 mM of carbidopa. Insets: A) plots of *I vs.* $t^{-1/2}$ obtained from the chronoamperograms 2–5 and B) plot of the slope of the straight lines against the carbidopa concentration.

*Calibration plot and limit of detection*

The SWV method was used to determine the concentration of carbidopa (Fig. 4; initial potential = 0.05 V, end potential = 0.7 V, step potential = 0.001 V, amplitude = 0.02 V, frequency = 10 Hz). The plot of peak current *vs.* carbidopa concentration consisted of two linear segments with slopes of 0.220 and 0.021 μA $\mu M^{-1}$ in the concentration ranges of 1.0–10.0 μM and 10.0–700.0 μM, respectively. The decrease in sensitivity (slope) of the second linear segment is likely due to kinetic limitations.[43] The detection limit ($3\sigma$) of carbidopa was found to be 0.2 μM.

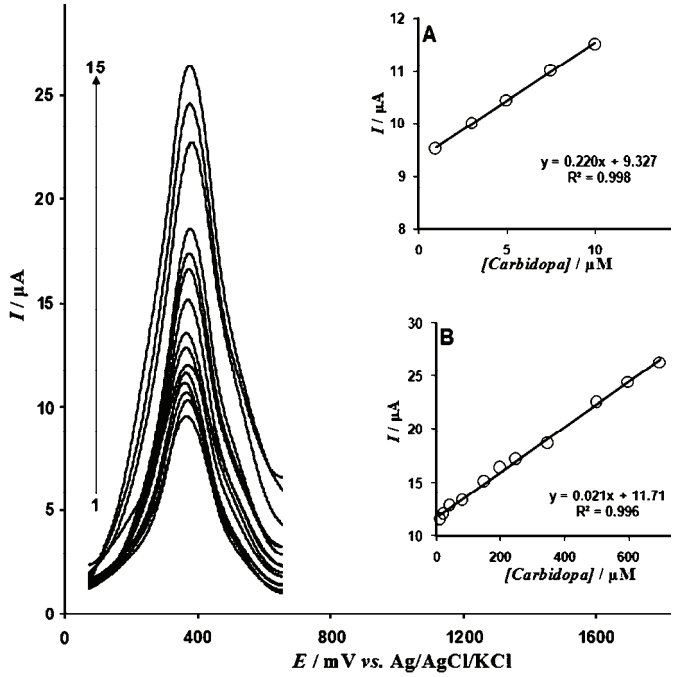


Fig. 4. SWVs of the VFCNPE in 0.1 M PBS (pH 7.0) containing different concentrations of carbidopa. Numbers 1–15 correspond to 1.0, 3.0, 5.0, 7.5, 10.0, 20.0, 40.0, 80.0, 150.0, 200.0, 250.0, 350.0, 500.0, 600.0 and 700.0 μM of carbidopa. Insets: plots of the electrocatalytic peak current as a function of carbidopa concentration in the range of 1.0–10.0 μM (A) and 10.0–700.0 μM (B).

*Simultaneous determination of carbidopa and folic acid*

One of the main objectives of this study was to detect carbidopa and folic acid simultaneously using the VFCNPE. The determination of carbidopa and folic acid in mixtures was performed at the VFCNPE using SWV. The concentration of folic acid was varied, while keeping the carbidopa concentration constant. The results are shown in Fig. 5 (initial potential = –0.1 V, end potential =

= 1.1 V, step potential = 0.001 V, amplitude = 0.02 V, frequency = 10 Hz). When the concentration of carbidopa was kept constant at 500.0 μM, the peak current of folic acid was proportional to its concentration from 100.0 μM –1200.0 μM. No changes in the peak current and potential of carbidopa could be observed.

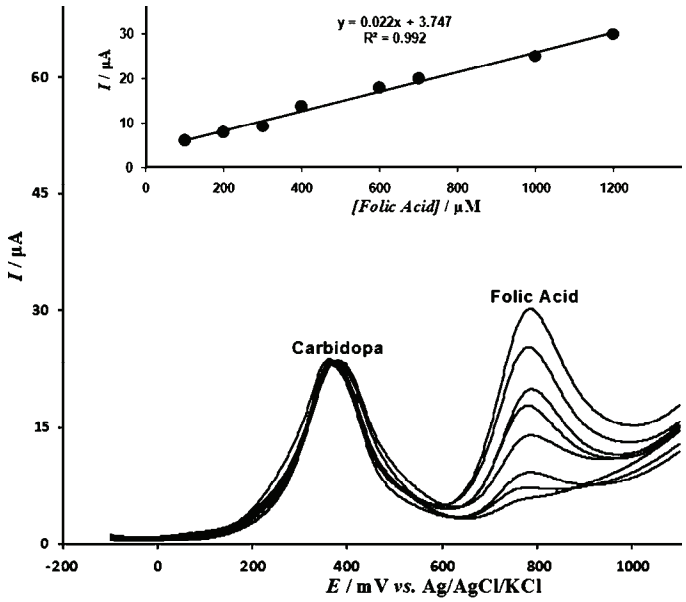


Fig. 5. SWVs at the VFCNPE in 0.1M PBS (pH 7.0) containing 500.0 μM carbidopa and different concentrations of folic acid (from inner to outer): 100.0, 200.0, 300.0, 400.0, 600.0, 700.0, 1000.0 and 1200.0 μM. Inset: plot of the electrocatalytic peak current as a function of folic acid concentration.

Furthermore, experiments were performed in which the concentrations of carbidopa and folic acid were simultaneously changed, and the SWVs recorded (initial potential = 0.02 V, end potential = 0.93 V, step potential = 0.001 V, amplitude = 0.02 V, frequency = 10 Hz). The voltammetric results showed well-defined anodic peaks at potentials of 390 and 780 mV, corresponding to the oxidation of carbidopa and folic acid, respectively, indicating that the simultaneous determination of these compounds at the VFCNPE is feasible, as shown in Fig. 6.

The sensitivity of the modified electrode towards the oxidation of carbidopa was found to be 0.022 μA $\mu M^{-1}$. This is equal to the value obtained in the absence of folic acid, indicating that the oxidation processes of these compounds at the VFCNPE are independent and therefore, the simultaneous determination of their mixtures is possible without significant interferences.

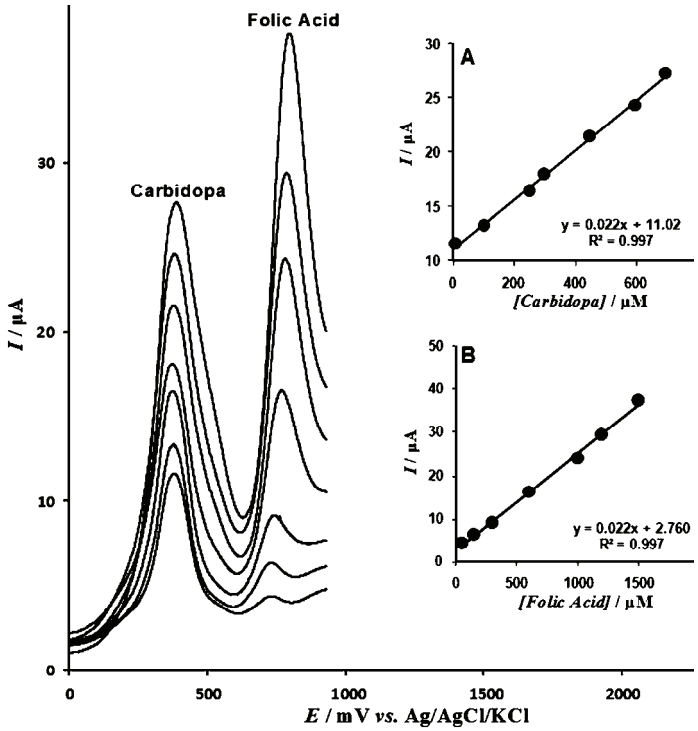


Fig.6. SWVs at the VFCNPE in 0.1 M PBS (pH 7.0) containing different concentrations of carbidopa+folic acid in µM, from inner to outer: 10.0+50.0, 100.0+150.0, 250.0+300.0, 300.0+600.0, 450.0+1000.0, 600.0+1200.0 and 700.0+1500.0, respectively. Insets: plots of $I_p$ *vs*. carbidopa (A) and folic acid concentration (B).

*Determination of carbidopa and folic acid in urine sample*

In order to evaluate the analytical applicability of the proposed method, it was also applied to the determination of carbidopa and folic acid in urine samples. The results for the determination of the carbidopa and folic acid in the urine samples are given in Table I. Satisfactory recovery was found for carbidopa

TABLE I. Determination of carbidopa and folic acid in urine samples. All the concentrations are given in µM ($n$ = 5)

| Carbidopa added, µM | Folic acid added µM | Carbidopa | | | Folic acid | | |
|---|---|---|---|---|---|---|---|
| | | Found µM | Recovery % | *RSD* % | Found µM | Recovery % | *RSD* % |
| 0 | 0 | ND | – | – | ND | – | – |
| 15.0 | 5.0 | 15.3 | 102.0 | 2.9 | 5.3 | 106.0 | 2.4 |
| 25.0 | 10.0 | 24.6 | 98.4 | 1.8 | 9.9 | 99.0 | 3.1 |
| 35.0 | 15.0 | 34.1 | 97.4 | 1.9 | 15.1 | 100.7 | 2.2 |
| 45.0 | 20.0 | 45.1 | 100.2 | 2.3 | 20.2 | 101.0 | 2.8 |
| 55.0 | 25.0 | 54.8 | 99.6 | 2.6 | 25.6 | 102.4 | 1.7 |

and folic acid. The reproducibility of the method was demonstrated by the mean relative standard deviation (*RSD*).

## CONCLUSIONS

A novel modified carbon nanotube paste electrode was fabricated and applied to the determination of carbidopa and folic acid. The modified electrode showed excellent electrocatalytic activity for the oxidation of carbidopa and folic acid. Moreover, the modified electrode presented wide linear ranges, low detection limits and high stability for the simultaneous determination carbidopa and folic acid, suggesting this electrode as a good and attractive candidate for practical applications.

## ИЗВОД

## ВОЛТАМЕТРИЈСКО ОДРЕЂИВАЊЕ КАРБИДОПЕ И ФОЛНЕ КИСЕЛИНЕ КОРИШЋЕЊЕМ МОДИФИКОВАНЕ ЕЛЕКТРОДЕ ОД УГЉЕНИЧНЕ ПАСТЕ

NASRIN KESHTKAR[1,2], MOHAMMAD ALI TAHER[1] и HADI BEITOLLAHI[3]

[1]*Department of Chemistry, Shahid Bahonar University of Kerman, P. O. Box 76175-133, Kerman, Iran,* [2]*Young Researchers Society, Shahid Bahonar University of Kerman, P. O. Box 76175-133, Kerman, Iran и* [3]*Environment Department, Institute of Science and High Technology and Environmental Sciences, Graduate University of Advanced Technology, Kerman, Iran*

Развијен је нови електрохемијски сензор на бази угљеничне пасте модификоване угљеничним наноцевима и винил-фероценом са циљем селективне и осетљиве детекције карбидопе у присуству великог вишка фолне киселине у раствору физиолошке вредности pH. Велика сепарација струјних пикова, добра осетљивост и стабилност омогућавају да се помоћу ове електроде одреди концентрација карбидопе индивидуално и у присуству фолне киселине. Примењујући волтаметрију са правоугаоним сигналом, за карбидопу је добијен линеарни динамички опсег од $1{,}0\times10^{-6}$–$7{,}0\times10^{-4}$ M уз границу детекције $2{,}0\times10^{-7}$ M. Предложена метода примењена је и за одређивање карбидопе и фолне киселине у узорку урина.

(Примљено 26 децембра 2013, ревидирано 11. априла, прихваћено 17. априла 2014)

## REFERENCES

1. S. Tajik, M. A. Taher, H. Beitollahi, *Sens. Actuators, B* **188** (2013) 923
2. J. U. Yan, L. Y. Feng, R. W. Zhong, *J. Serb. Chem. Soc.* **70** (2005) 277
3. M. Coates, T. Nyokong, *Electrochim. Acta* **91** (2013) 158
4. A. Mokhtari, H. Karimi-Maleh, A. A. Ensafi, H. Beitollahi, *Sens. Actuators, B* **169** (2012) 96
5. H. Beitollahi, J. B. Raoof, R. Hosseinzadeh, *Electroanalysis* **23** (2011) 1934
6. R. García-González, A. Fernández-La Villa, A. Costa-García, M. T. Fernández-Abedul, *Sens. Actuators, B* **181** (2013) 353
7. H. Beitollahi, J. B. Raoof, R. Hosseinzadeh, *Anal. Sci.* **27** (2011) 991
8. R. Emamali Sabzi, K. Rezapour, N. Samadi, *J. Serb. Chem. Soc.* **75** (2010) 537
9. S. Mohammadi, H. Beitollahi, A. Mohadesi, *Sensor Lett.* **11** (2013) 388
10. K. E. Moore, B. S. Flavel, J. Yu, A. D. Abell, J. G. Shapter. *Electrochim. Acta* **89** (2013) 206
11. H. Beitollahi, M. A. Taher, M. Ahmadipour, R. Hosseinzadeh, *Measurement* **47** (2014) 770

12. M. Mazloum-Ardakani, H. Beitollahi, Z. Taleat, M. Salavati-Niasari, *J. Serb. Chem. Soc.* **76** (2011) 575
13. S. Sheng, L. Zhang, G. Chen, *Food Chem.* **145** (2014) 555
14. R. Olivé-Monllau, F. Xavier Muñoz-Pascual, E. Baldrich, *Sens. Actuators, B* **185** (2013) 685
15. W. Zhang, X. Zhang, L. Zhang, G. Chen, *Sens. Actuators* **192** (2014) 459
16. B. Dogan-Topal, B. Bozal-Palabıyık, B. Uslu, S. A. Ozkan, *Sens. Actuators, B* **177** (2013) 841
17. L. Zhang, L. Xu, J. He, J. Zhang, *Electrochim. Acta* **117** (2014) 192
18. K. Addisu Shimeles, A. Desalegn Birhanu, S. Refera Tesfaye, J. *Serb. Chem. Soc.* **78** (2013) 701
19. L. Fernández, I. Ledezma, C. Borrás, L. Alfredo Martínez, H. Carrero, *Sens. Actuators, B* **182** (2013) 625
20. J. B. Raoof, R. Ojani, H. Beitollahi, R. Hosseinzadeh, *Anal. Sci.* **22** (2006) 1213
21. Z. Taleat, M. Mazloum Ardakani, H. Naeimi, H. Beitollahi, M. Nejati, H. R. Zare, *Anal. Sci.* **24** (2008) 1039
22. R. Zhang, S. Liu, L. Wang, G. Yang, *Measurement* **46** (2013) 1089
23. J. B. Raoof, R. Ojani, H. Beitollahi, *Electroanalysis* **19** (2007) 1822
24. A. Vulcu, C. Grosan, L. Maria Muresan, S. Pruneanu, L. Olenic, *Electrochim. Acta* **88** (2013) 839
25. J. B. Raoof, R. Ojani, H. Beitollahi, R. Hossienzadeh, *Electroanalysis* **18** (2006) 1193
26. J. B. Raoof, R. Ojani, M. Baghayeri, *Chin. J. Catal.* **32** (2011) 1685
27. M. Mazloum-Ardakani, H. Beitollahi, M. K. Amini, F. Mirkhalaf, M. Abdollahi-Alibeik, *Sens. Actuators, B* **151** (2010) 243
28. Q. Wang, M. R. Das, M. Li, R. Boukherroub, S. Szunerits, *Bioelectrochemistry* **93** (2013) 15
29. N. Rastakhiz, H. Beitollahi, A. Kariminik, F. Karimi, *J. Mol. Liq.* **172** (2012) 66
30. P. C. Damiani, A. C. Moschetti, A. J. Rovetto, F. Benavente, A. C. Olivieri, *Anal. Chim. Acta* **543** (2005) 192
31. H. Mahmoudi Moghaddam, *Int. J. Electrochem. Sci.* **6** (2011) 6557
32. H. Beitollah, M. Goodarzian, M. A. Khalilzadeh, H. Karimi-Maleh, M. Hassanzadeh, M. Tajbakhsh, *J. Mol. Liq.* **173** (2012) 137
33. M. Chamsaz, A. Safavi, J. Fadaee, *Anal. Chim. Acta* **603** (2007)140
34. M. Mazloum-Ardakani, Z. Taleat, A. Khoshroo, H. Beitollahi, H. Dehghani, *Biosens. Bioelectron.* **35** (2012) 75
35. H. Yaghoubian, H. Karimi-Maleh, M. A. Khalilizadeh, F. Karimi, *J. Serb. Chem. Soc.* **74** (2009) 1443
36. H. X. Guo, Y. Q. Li, L. F. Fan, X. Q. Wu, M. D. Guo, *Electrochim. Acta* **51** (2006) 6230
37. G. M. Shaw, D. Schaffer, E. M. Velie, K. Morland, J. A. Harris, *Epidemiology* **6** (1995) 219
38. C. Wang, C. Li, L. Ting, X. Xu, C. Wang, *Microchim. Acta* **152** *(*2006) 233
39. L. Bandžuchová, R. Šelešovská, T. Navrátil, J. Chýlkov, *Electrochim. Acta* **56** (2011) 2411
40. K. Tyszczuk, *Electrochim. Acta* **56** (2011) 3975
41. H. Yang, B. Lu, B. Qi, L. Guo, *J. Electroanal. Chem.* **660** (2011) 2
42. M. Korolczuk, K. Tyszczuk, *Electroanalysis* **19** (2007)1959
43. A. J. Bard, L. R., Faulkner, *Electrochemical Methods Fundamentals and Applications*, 2nd ed., Wiley, New York, 2001.

Journal of the Serbian Chemical Society
JSCS-info@shd.org.rs • www.shd.org.rs/JSCS
*J. Serb. Chem. Soc. 80* (6) 801–804 (2015)
*JSCS–4759*
UDC 546.34+546.33+546.3–71+
544.6.076.2–145.2
*Extended abstract*

EXTENDED ABSTRACT

# Comparison of lithium and sodium intercalation materials•

MILICA VUJKOVIĆ*

*Faculty of Physical Chemistry, University in Belgrade, Studentski trg 12, 11000 Belgrade, Serbia*

(Received 19 November, revised 14 December, accepted 25 December 2014)

*Abstract*: The low abundance of lithium in the Earth's crust and its high participation in overall cost of lithium-ion batteries incited intensive investigation of sodium-ion batteries, in the hope that they may become similar in their basic characteristics: specific energy and specific power. Furthermore, over the last years, research has been focused on the replacement of the organic electrolytes of Li- and Na-ion batteries by aqueous electrolytes, in order to simplify the production and improve safety of use. In this lecture, some recent results on selected intercalation materials are presented: layered structure vanadium oxides, olivine and nasicon phosphates, potentially usable in both Li and Na aqueous rechargeable batteries. After their characterization by X-ray diffraction and electron microscopy, the electrochemical behavior was studied by both cyclic voltammetry and chronopotentiometry. By comparing the intercalation kinetics and coulombic capacity of these materials in $LiNO_3$ and $NaNO_3$ solutions, it was shown that the following ones: $Na_{1.2}V_3O_8$, $Na_2V_6O_{16}$/C, $NaFePO_4$/C and $NaTi_2(PO_4)_3$/C may be used as electrode materials in aqueous alkali-ion batteries.

*Keywords*: sodium and lithium storage capacity; metal-ion aqueous batteries.

Thanks to their excellent electrochemical performance, such as high voltage (3–5 V) and high specific energy density (150–200 Wh $kg^{-1}$), Li-ion batteries with organic electrolytes are widely used as power sources in portable electronic devices (mobile phones, laptops, digital cameras, *etc*.) and are regarded as one of the best alternative to fossil fuels in electric vehicles. They were commercialized in the early 90-ties. The first Li-ion battery was produced by the Sony Company in 1991 and consisted of a graphitic carbon anode, a $LiCoO_2$ cathode, and $LiPF_6$ dissolved in an organic solvent (mixture of ethylene carbonate and dimethyl car-

* E-mail: milicavuj5@yahoo.com

• Lecture at the Meeting of Electrochemical Section of the Serbian Chemical Society held on 10 November 2014, Belgrade, Serbia.

doi: 10.2298/JSC141119127V

bonate) as electrolyte. This battery type is used in the majority of modern portable electronic devices.[1] Recently, Na-ion batteries have attracted increasing attention of researchers, expressed through the rising number of publications on sodium intercalation materials and sodium ion batteries, but a commercial model has not yet appeared on the market. Na-ion batteries are identical in their working principle to Li-ion batteries. Namely, in both, conductive electrolyte shuttles ions ($Li^+$ or $Na^+$) between the positive and negative electrode materials during charging and discharging. The main reasons for using sodium instead of lithium are higher abundance, lower price and comparable energy density. Although the ionic radius of $Na^+$ is somewhat higher than that of $Li^+$, this is not always a substantial obstacle for efficient intercalation ability. It was evidenced in the literature that many lithium intercalation materials (V-, Mn- and Ti-based oxides, olivine $LiFePO_4$, nasicon structures, sulfate compounds, etc.) are also able to intercalate sodium. Contemporary research is also directed to the development of Li-ion and Na-ion batteries with aqueous electrolytes. The reasons are higher environmental friendliness and easier production of batteries with aqueous electrolytes.[2]

The presented lecture delivers an overview of the electrochemical behavior of several materials types synthesized in various ways (layered Na-vanadium oxides, olivine and nasicon phosphate), in Li- and Na-containing, aqueous electrolytic solutions.[3–5] The intercalation kinetics and intercalation capacity of these materials were evaluated and compared with respect to their applicability in lithium-ion or sodium-ion aqueous rechargeable batteries. It was shown that structure, morphology and chemical composition determine the electrochemical performance of materials in aqueous electrolytic solution, and lead to some difference in the coulombic capacities.

Unlike $Li_{1.2}V_3O_8$, which is one of the most investigated materials for Li-ion aqueous rechargeable batteries, the electrochemical behavior of $Na_{1.2}V_3O_8$ in aqueous electrolyte was practically unknown. $Na_{1.2}V_3O_8$ has a larger interlayer distance and higher chemical diffusion coefficient than $Li_{1.2}V_3O_8$. Recently, a paper regarding the electrochemical behavior of one-dimensional $Na_{1.2}V_3O_8$ micro/nano belts synthesized by sol–gel method, in aqueous solutions of $LiNO_3$, $NaNO_3$ and $Mg(NO_3)_2$ was published.[4] The capability to intercalate ions of different radii makes this material promising for Li, Na and Mg aqueous rechargeable batteries. Apart from $Na_{1.2}V_3O_8$, a hydrothermally synthesized $Na_2V_6O_{16}$/C composite was also found to be an excellent bifunctional material for Na and Li aqueous rechargeable batteries. The micro/nano belt-like morphology of $Na_2V_6O_{16}$/C was also obtained but spherical particles (≈50 nm), caused by the presence of the carbon nanoparticles, were also observed. The presence of a few anodic and cathodic redox peaks in the CVs of both layered oxides $Na_{1.2}V_3O_8$ and $Na_2V_6O_{16}$/C measured in $LiNO_3$ and $NaNO_3$, indicated successful intercal-

ation of $Na^+$ and $Li^+$ into energetically non-equivalent tetrahedral positions. Higher Li *vs*. Na capacity was measured for both layered oxides. There is some theoretical prediction that an open-layered structure can easier accommodate larger $Na^+$, but this was not the case with these belt-like morphologies. Here, the ionic radius is the key factor that determines the diffusion rate through the layered structure and thus, the intercalation ability.

Contrary to the vanadate-layered structure, it was found that olivine and nasicon structures may be synthesized in a way to exhibit higher Na *vs*. Li storage capacity in an aqueous electrolyte, in spite of the unfavorable differences in ionic radii. Such behavior makes these materials very promising for use in aqueous Na-ion batteries. Olivine $LiFePO_4$/C and nasicon $NaTi_2(PO_4)_3$/C, synthesized by a gel-combustion procedure, exhibited the same morphology, consisting of agglomerated spherical particles with an average particle size of 75 nm. $LiFePO_4$ incorporated in a carbon matrix[3] showed very fast kinetics of lithiation/ /delithiation in aqueous $LiNO_3$ solution. This composite was successfully transformed into $NaFePO_4$/C by electrochemical replacement Li by Na ions in a saturated aqueous solution of $NaNO_3$. The delitihiated $FePO_4$/C composite demonstrated the very high storage capacity of 118 mAh $g^{-1}$ at 10 mV $s^{-1}$ in $NaNO_3$, *i.e*., two times higher than the corresponding storage capacity in $LiNO_3$.[3,5] One of the reasons for this is the weaker $Na^+$–$PO_4^{3-}$ bond when compared to the $Li^+$–$PO_4^{3-}$ bond. Cyclic voltammetry, in the combination with X-ray analysis, showed that the sodiation/desodiation reaction of $NaFePO_4$/C in $NaNO_3$ goes through the formation of the intermediate phase $Na_{0.7}FePO_4$[6] and its efficiency strongly depends on the applied current.

An aqueous type of sodium rechargeable battery consisting of $Na_{1.2}V_3O_8$ as the anode material[4] and olivine $LiFePO_4$/C[3] as the cathode material was fabricated and tested. The battery delivered very high currents with a quite good cyclic stability (80 % of the initial capacity) after 1000 charging/discharging cycles. The main problem of this battery for commercial purpose was its low average voltage, which is a general problem with aqueous batteries. In order to enhance the voltage, the employment of another anode material, such as nasicon $NaTi_2(PO_4)_3$, could be a good choice, thanks to the low redox potential of this material (–0.6 V *vs*. NHE). This compound is well known as a Na superionic conductor, and its theoretical capacity is 133 mAh $g^{-1}$. Both cyclic voltammetric and chronopotentiometric measurements of gel-combustion synthesized $NaTi_2(PO_4)_3$/C displayed faster diffusion of $Na^+$ ions *vs*. $Li^+$, which is advantageous for the purposes of sodium aqueous rechargeable batteries.

ИЗВОД

## ПОРЕЂЕЊЕ МАТЕРИЈАЛА ЗА ИНТЕРКАЛАЦИЈУ ЛИТИЈУМА И НАТРИЈУМА

МИЛИЦА ВУЈКОВИЋ

*Факултет за Физичку хемију, Универзитет у Београду, Студентски трг 12, 11000 Београд*

Ниска заступљеност литијума у Земљиној кори и његово високо учешће у укупној цени литијум-јонских батерија подстиче истраживаче да интезивно истражују натријум-јонске батерије, у нади да оне могу бити сличне у основним карактеристикама: специфична енергија и специфична снага. Последњих година истраживачи се фокусирају на замену органских електролита литијум и натријум јонских батерија, са воденим електролитичким раствором, са циљем да поједноставе производњу и побољшају безбедност батерије. У овом предавању, приказани су резултати неколико интеркалатних материјала: слојевити оксиди ванадијума, оливин- и насикон-фосфати, који могу да се користе и у литијум и у натријум јонским секундарним батеријима. После њихове карактеризације рендгеноструктурном анализом и електронском микроскопијом, електрохемијско понашање испитано је цикличном волтаметријом и хронопотенциометријом. Поредећи кинетику интеркалације/деинтеркалације и кулонски капацитет ових материјала у $LiNO_3$ и $NaNO_3$, показано је да следећи материјали $Na_{1.2}V_3O_8$, $Na_2V_6O_{16}$/C, $NaFePO_4$/C и $NaTi_2(PO_4)_3$/C могу да се користе као електродни материјали у воденим алкал-јонским батеријама.

(Примљено 19. новембра, ревидирано 14. децембра, прихваћено 25. децембра 2014)

## REFERENCES

1. B. Scrosati, J. Garche, *J. Power Sources* **195** (2010) 2419
2. H. Pan, Y.-S. Hu, L. Chen, *Energy. Environ. Sci*. **6** (2013) 2338
3. M. Vujković, I. Stojković, N. Cvjetićanin, S. Mentus, *Electrochim. Acta* **92** (2013) 248
4. M. Vujković, B. Sljukić, I. Stojković-Simatović, M. Mitrić, C. Sequeira, S. Mentus, *Electrochim. Acta* **147** (2014) 167
5. M. Vujković, S. Mentus, *J. Power Sources* **247** (2014) 184
6. P. Moreau, D. Guyomard, J. Gaubicher, F. Boucher, *Chem. Mater*. **22** (2010) 4126.

Journal of the Serbian Chemical Society
JSCS-info@shd.org.rs • www.shd.org.rs/JSCS
*J. Serb. Chem. Soc. 80* (6) 805–817 (2015)
*JSCS–4760*
UDC 27–526.62:7.023.1–037.1+
547.97–035.67:543.4+543.424.2
*Original scientific paper*

# Spectroscopic investigation of two Serbian icons painted on canvas

LJILJANA DAMJANOVIĆ[1]*, OLGICA MARJANOVIĆ[1], MILICA MARIĆ STOJANOVIĆ[2], VELIBOR ANDRIĆ[3] and UBAVKA B. MIOČ[1]

[1]*University of Belgrade-Faculty of Physical Chemistry, Studentski trg 12–16, 11000 Belgrade, Serbia,* [2]*National Museum Belgrade, Trg Republike 1a, 11000 Belgrade, Serbia and* [3]*University of Belgrade-Vinča Institute of Nuclear Sciences, P. O. Box 522, 11000 Belgrade, Serbia*

(Received 22 July, revised 6 October, accepted 8 October 2014)

*Abstract*: A multianalytical study of two Serbian icons, "The Virgin and Child" and "St. Petka", painted on canvas by unknown authors was performed in order to identify the materials used as pigments, binders and the ground layer. The investigated icons belong to the Museum of the Serbian Orthodox Church in Belgrade. Samples, collected from different parts of the icons, were analysed by: optical microscopy (OM), energy dispersive X-Ray fluorescence (EDXRF), Fourier transform infrared (FTIR) and micro-Raman spectroscopy. The obtained results revealed the presence of the following pigments: Prussian Blue, ultramarine, Green Earth, iron oxides, Lead White and Zinc White. Linseed oil was used as the binder. The materials used for the ground layers were gypsum, calcite, baryte and Lead White. The gilded surface of the icon "The Virgin and Child" was made of gold. The gilded surface on the frame of this icon was made of imitation of gold, *i.e.*, Schlagmetal, since EDXRF spectroscopy showed the presence of copper and zinc, while gold was not detected. Based on the style and the consideration of an art historian, as well as on the obtained results for the corresponding pigments and binder, both icons were most probably made at the end of 19$^{th}$ or the beginning of the 20$^{th}$ century.

*Keywords*: pigments; EDXRF; FTIR spectroscopy; micro-Raman spectroscopy.

## INTRODUCTION

Preservation of cultural heritage is traditionally a task for conservators, restorers and art historians. Scientific investigation of cultural heritage started at the beginning of 20$^{th}$ century.[1] Nowadays, the application of different analytical methods is essential for the identification of the materials of which artworks are made and of the techniques employed by the artists. These analyses aid art histo-

* Corresponding author. E-mail: ljiljana@ffh.bg.ac.rs
doi: 10.2298/JSC140722099D

rians to better understand the history of an object since many of the choices made by the artist were influenced by the current state of technology, economics, politics and many other factors.[2] They provide important information not only for the determination of the provenience and authenticity of works of art, but also can help conservators and restorers to choose the most appropriate procedure for restoration, conservation and display.[3]

Scientific investigation of paintings or icons is a demanding task due to the small amounts of the samples, usually in the micro or sub-micro range (when available), and the presence of different organic and inorganic compounds in the sample. In order to obtain complete characterization of these complex mixtures, the application of different analytical techniques is required.[4] When possible, samples are taken from damaged regions or from the edges of the painting, and they should be representative of the area under study. The technological procedure followed by painters and iconographers usually means that the ground layer is applied first to prepare the surface of a canvas or a panel, followed by application of a painting layer, which is a mixture of pigments and binding media and their composition gives the colour quality. Finally, varnish, which is mainly based on natural resins, is applied as a protective coating but also for particular visual effects.[5] Pigments can be organic or inorganic compounds and chronological use of most pigments is known today.[6,7] Hence, identification of pigments enables indirect dating of painted art objects.

In this work, a multianalytical study of two icons, "The Virgin and Child" (dimensions: 57 cm×90 cm) and "St. Petka" (dimensions: 55 cm×69 cm), painted on canvas by unknown authors was performed. The investigated icons are the property of the Museum of the Serbian Orthodox Church in Belgrade. Art historians classified the icons "The Virgin and Child" and "St. Petka" as Serbian icons made under the influence of West European baroque. The investigated icons represent two iconographic types: one depicts the Virgin Hodegetria, which is an often used motive, while other shows an individual Saint. Based on the style and art historian considerations, both icons were most probably made at the end of the 19$^{th}$ or the beginning of the 20$^{th}$ century. The icons were brought for restoration at the Academy of the Serbian Orthodox Church for Art and Conservation and a scientific investigation was performed during the restoration procedure. The aim of this study was to identify the materials used as pigments, binders and the ground layer on two icons by application of the physicochemical methods optical microscopy (OM), energy dispersive X-Ray fluorescence (EDXRF), Fourier transform infrared (FTIR) and micro-Raman spectroscopy. The obtained results contributed to the selection of an appropriate restoration procedure.

It is important to note that icons are usually studied from the historical, theological, iconographic and stylistic point of view. Only in the past decade was the materials aspect of icons considered.[8] Therefore, the results of this study

together with art historical research will contribute to a better understanding of the painting techniques of Serbian icons.

## EXPERIMENTAL

### *Samples*

Samples were collected during the restoration procedure. Paint chips, approximately 1 $mm^2$ or even smaller, were removed by a clean and sharp scalpel from the edges of existing damaged regions on the icons (Fig. 1). All samples contained small pieces of ground layer attached to the paint layer. A description of all the investigated samples and used analytical techniques are given in Table I.


Fig. 1. Icons painted on canvas: A) “The Virgin and Child” and B) “St. Petka”. Samples were taken from the marked areas.

TABLE I. Description of investigated samples and used analytical methods

| Icon | Sample ID | Description | Analytical methods |
|---|---|---|---|
| A | A1 | Virgin’s mantle, Blue | OM, EDXRF, FTIR |
| The Virgin and Child | A2 | Gilded area on the icon | OM, EDXRF, FTIR |
| | A3 | Gilded area on the frame | OM, EDXRF, FTIR |
| B | B1 | Grass, Green | OM, EDXRF, FTIR |
| St. Petka | B2 | St. Petka’s mantle, Blue–Brownish | OM, EDXRF, FTIR, $\mu$Raman |
| | B3 | Sky, Light Blue | OM, EDXRF, FTIR |

### *Analytical methods*

Optical microscopy provides information about the sequence and the thickness of the layers in the paint chips samples and allows a preliminary characterisation of the materials in the paint layer and the ground layer. Cross sections of investigated samples were recorded by an Olympus BX51M optical microscope equipped with an Olympus U-RFL-T UV lamp and U-MWUS3 and U-MWBS3 filters.

EDXRF spectroscopy is an often used method for non-destructive analysis of cultural heritage objects. It is a fast and reliable analytical technique that provides information about the elemental chemical composition. Due to the penetrative nature of X-rays, characteristic fluorescence radiation is recorded not only from the surface paint layers, but also from the covered layers including even the ground layer. In this work, qualitative EDXRF spectroscopy measurements were performed on an EDXRF spectrometer with a Canberra Si(Li) semiconductor detector and MCA analyzer S35+. MicroSAMPO software was used for the spectra acquisition and measurement time was 800 s for all the samples. For the excitation, an annular radioisotope source $^{109}$Cd (manufactured by Isotope Products) with nominal activity of 740 MBq was used.

FTIR spectroscopy was used in order to reveal the molecular composition of organic and inorganic compounds in the investigated samples. FTIR spectra of all samples were recorded on a Nicolet 6700 spectrophotometer, using the KBr pellets technique in the wavenumber range from 4000 to 400 cm$^{-1}$.

Micro-Raman spectroscopy as non-destructive and micro-probe method is very convenient for investigation of samples from painted objects. Micro-Raman spectra were recorded on a DXR Raman Microscope (Thermo Scientific). The 532 nm line of a diode-pumped solid-state high brightness laser was used as the exciting radiation and the power of illumination at the sample surface was 0.5 mW. Collection of the scattered light was made through an Olympus microscope with infinity-corrected confocal optics, 25 μm pinhole aperture, standard working distance objective 50×, and grating of 900 lines mm$^{-1}$. The acquisition time was 10 s, with 10 scans. The laser spot diameter on the sample was 1 μm. Thermo Scientific OMNIC software was used for spectra collection and manipulation.

## RESULTS AND DISCUSSION

### *Icon A: "The Virgin and Child"*

Representative optical micrographs of samples taken from the icon "The Virgin and Child" are shown in Fig. 2. The obtained optical micrographs, which are diversely coloured and show a multilayered structure, will be discussed later combined with the results of the EDXRF and FTIR spectroscopic analyses.

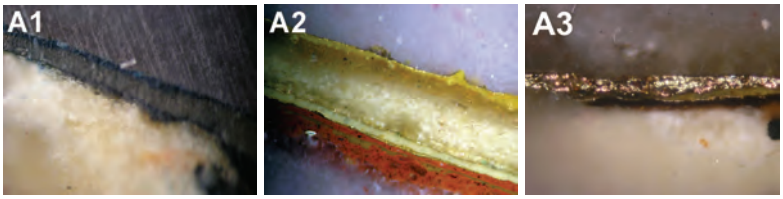


Fig. 2. Representative optical micrographs of samples taken from the icon "The Virgin and Child"; magnification 200×.

Samples of paint chips taken from the icon "The Virgin and Child" (Table I) were investigated by qualitative EDXRF spectroscopic analysis on both sides: the side with the surface paint layer and the side with the ground layer. The results obtained by EDXRF spectroscopy measurements are given in Table II.

TABLE II. Results obtained by EDXRF spectroscopy of samples taken from the icons “The Virgin and Child” (A) and “St. Petka” (B)

| Sample ID | Detected elements |
|---|---|
| A1 | Ca, Fe, Pb, Sr |
| A2 | Ca, Fe, Cu, Zn, Pb, Au |
| A3 | Ca, Fe, Cu, Zn |
| B1 | Ca, Ba, Fe, Zn, Pb, Sr |
| B2 | Ca, Ba, Fe, Zn, Pb, Sr |
| B3 | Ca, Ba, Fe, Zn, Pb, Sr |

EDXRF spectroscopy is an elemental analysis and the results obtained by this method could be inconclusive. Therefore, it was important to combine this method with other techniques for the identification of the compounds present in the investigated samples. The results obtained by FTIR spectroscopy for the samples taken from the icon “The Virgin and Child” are shown in Fig. 3. The investigated samples were mixtures of inorganic and organic compounds, which resulted in a broadening of the FTIR adsorption bands due to the overlapping of different vibrational modes.

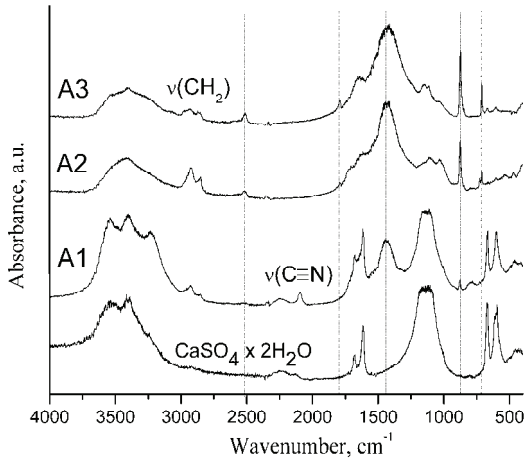


Fig. 3. FTIR spectra of samples taken from the icon “The Virgin and Child” and reference spectrum of gypsum; vertical lines represent the positions of the characteristic bands of calcite.

In the case of the blue sample, A1, the characteristic band in the FTIR spectrum, Fig. 3, at 2094 $cm^{-1}$ was assigned to the ν(C≡N) stretching vibration, which is highly specific for the pigment Prussian Blue, $Fe_4[Fe(CN)_6]_3$.[9] This result combined with the presence of Fe determined by EDXRF spectroscopy (Table II) confirmed that Prussian Blue was used as the blue pigment. FTIR spectrum of sample A1 (Fig. 3) showed bands at 1143, 670 and 600 $cm^{-1}$, which were attributed to the stretching modes of the sulphate group, $\nu(SO_4^{2-})$, while the bands at 3545, 3405, 1686, 1617 $cm^{-1}$ were attributed to $OH^-$ stretching and bending vibrations.[10] These bands originate from gypsum, dehydrated calcium

sulphate ($CaSO_4 \cdot 2H_2O$), as can been seen by comparison of FTIR spectra of sample A1 and gypsum (Fig. 3). Gypsum was traditionally used for the ground layer of icons[11–13] and it was often naturally occurring mixed with celestine, strontium sulphate ($SrSO_4$), which explains the presence of Sr detected by EDXRF spectroscopy. The bands around 1450–1400 $cm^{-1}$ originate from the vibrational mode of the carbonate group $\nu(CO_3^{2-})$.[14] Weak bands at 2514, 1796, 873 and 713 $cm^{-1}$ in the FTIR spectrum of sample A1 (Fig. 3) together with a broad band at 1430 $cm^{-1}$ confirmed the presence of calcite ($CaCO_3$).[10] The EDXRF spectra of the ground and paint layer of sample A1 are shown in Fig. 4. The intensity of the peak for Ca in the EDXRF spectra of sample A1 was higher for the ground layer than for the paint layer. Therefore, the ground layer was made of gypsum and calcite. Since Pb was detected by EDXRF spectroscopy, the carbonate bands in the FTIR spectrum of sample A1 could also originate from Lead White, basic lead carbonate ($2PbCO_2 \cdot Pb(OH)_2$). The intensities of the peaks originating from Pb in the EDXRF spectra were higher for the side with the paint layer than for the side with the ground layer (Fig. 4). This finding indicates that Lead White was used as the pigment to obtain an appropriate hue of blue, which is in accordance with the presence of white grains in the blue paint layer of sample A1, observed in the optical micrographs (Fig. 2).

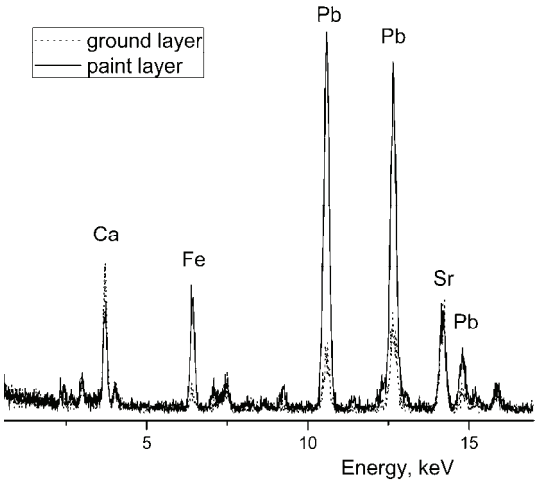


Fig. 4. EDXRF spectra of the ground layer and paint layer of sample A1.

In all the FTIR spectra, characteristic bands originating from $CH_2$ and $CH_3$ stretching vibrations appeared at 2925 and 2850 $cm^{-1}$, revealing the presence of organic matter[15] that originates from a binder, but the particular compound could not be unambiguously determined based solely on this finding. Considering the detected pigments and style of the icon, most probably linseed oil was used.

In the cross section of sample A2, taken from the gilded area of the icon, several different layers could be seen (Fig. 2). The multilayered structure indicates that gilding was performed on several occasions.

There are two well-known gilding procedures: water gilding and oil gilding.[5,16] Gold is usually applied in a form of thin leaves for decorative purposes on different materials. For water gilding, the ground layer was traditionally made of Red Earth pigment - Red Ochre (often called Red Bole). Application of gold on Red Ochre (composed of $Fe_2O_3$, clay and silica) results in warmer colours.[5,16] The red–orange ground layer could be seen on the cross section of sample A2 (Fig. 2). The EDXRF spectrum of the red–orange ground layer of sample A2 is shown in Fig. 5.

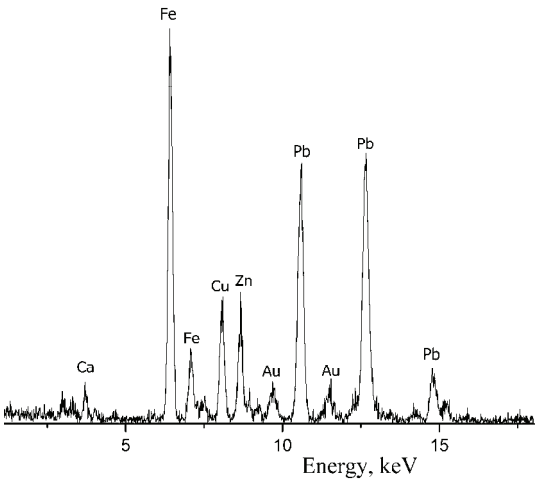


Fig. 5. EDXRF spectra of the ground layer of sample A2.

The high intensity of the Fe peaks in the EDXRF spectrum of the ground layer (Fig. 5) and the characteristic bands at 1107 and 1030 $cm^{-1}$ in the FTIR spectrum of sample A2 (Fig. 3), originating from Si–O stretching vibrations of aluminosilicates,[14] confirm the presence of the earth pigment ochre. In the case of ochres, the colouring agent is some non-clay pigment, *e.g.*, iron oxides.[5] Depending on the iron oxide as well as on size of the grains, the ochres have different colours. In this particular case, careful examination of the optical micrograph (Fig. 2) revealed the presence of red and yellow pigment grains, which led to the conclusion that the Red Ochre was mixed with Yellow Ochre ($Fe_2O_3 \cdot H_2O$ or FeOOH, clay and silica),[17] often called Yellow Bole, for obtaining a particular visual effect. As can be seen in Fig. 5, the presence of Au was confirmed by EDXRF spectroscopy. The optical micrograph of sample A2 (Fig. 2) revealed the presence of three thin layers of gold. The first thin layer of gold was originally applied on a mixture of Red and Yellow Ochre. During previous restoration procedures, additional ground layer and gold layer were added twice on the same area.

EDXRF spectroscopy also showed the presence of Ca, Zn and Pb in this sample. The FTIR spectrum of sample A2 (Fig. 3) confirmed the presence of calcite by the presence of characteristic bands. However, a broad band at 1430 $cm^{-1}$ attributed to vibrational mode of carbonate group $\nu(CO_3^{2-})$ could be the result of overlapping of signals originating from both calcite and Lead White. Moreover, the fluorescence of Zinc White was detected under UV light in the layer between the gold leaf applied on the mixture of Red and Yellow Bole and the next gold leaf. These findings indicate that the additional two ground layers were made of Lead White, Zinc White (ZnO) and calcite.

In addition, Cu was identified in the sample A2 by EDXRF spectroscopy. An alloy made of gold and copper is often used for gilding.[16] Amount of gold in the alloy is usually higher than 70 %. The relative intensities of the Cu and Au signals did not correspond to the expected values in the case of a gold and copper alloy, showing a higher amount of Cu (Fig. 5). The optical micrographs revealed the presence of blue pigment grains in the top ground layer. Therefore, copper in the investigated sample could originate from an alloy with gold used for gilding as well as from a copper-based blue pigment in the top ground layer.

The EDXRF spectra of the surface layer and ground layer of sample A3 are shown in Fig. 6. Cu and Zn were detected in the surface layer of sample A3, but not Au. An alloy of Cu and Zn in which the amount of Cu is 80 % or higher is known as Schlagmetal. It has the visual effect of gold and is used for gilding. The relative intensities of the Cu and Zn peaks in the EDXRF spectrum confirmed that Schlagmetal was used for the surface gilding layer on the frame.

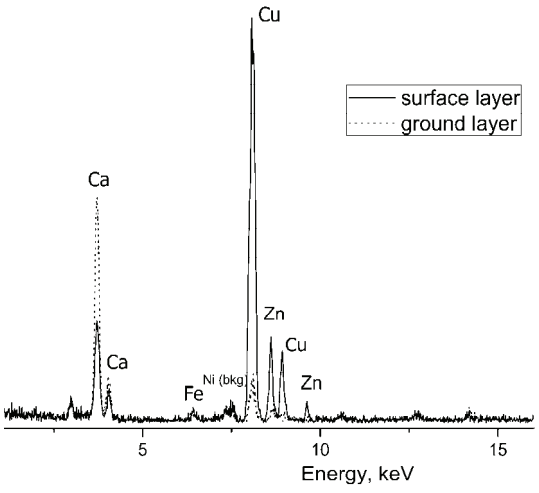


Fig. 6. EDXRF spectra of the ground layer and surface layer of sample A3; bkg – background signal.

On the cross section of sample A3 (Fig. 2), a yellow layer below the gilding could be seen. Iron present in sample A3 (Fig. 6) and the bands in the FTIR

spectrum at 1111 and 1030 $cm^{-1}$, originating from Si–O stretching vibrations (Fig. 3), indicate the presence of the Yellow Earth pigment – Yellow Ochre. The presence of calcite, identified in the FTIR spectrum of sample A3 (Fig. 3), indicated that a mixture of calcite and Yellow Bole was used as the ground layer for the gilding on the frame.

*Icon B: "St. Petka"*

Representative optical micrographs and fluorescence photographs under UV light of samples taken from the icon "St. Petka" are shown in Fig. 7.

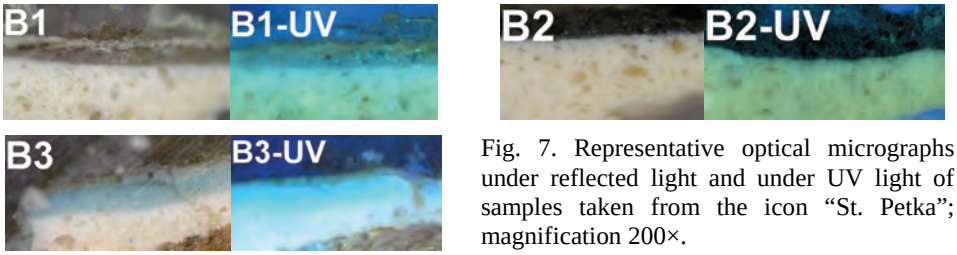


Fig. 7. Representative optical micrographs under reflected light and under UV light of samples taken from the icon "St. Petka"; magnification 200×.

The fluorescence photographs of the green B1 and blue B3 samples (Table I), presented in Fig. 7, show the intensive fluorescence of white pigment in the paint layer. The fluorescence was more intense for sample B3 compared to sample B1, Fig. 7, revealing that the blue paint layer of sample B3 contained a higher amount of white pigment than the green paint layer of sample B1.

EDXRF spectroscopy analysis showed for all three samples the presence of the same elements, regardless of the sample colour (see Table II). The EDXRF spectra of the paint layers of samples B1, B2 and B3 are shown in Fig. 8. The peak originating from Zn had the highest intensity in all three EDXRF spectra.

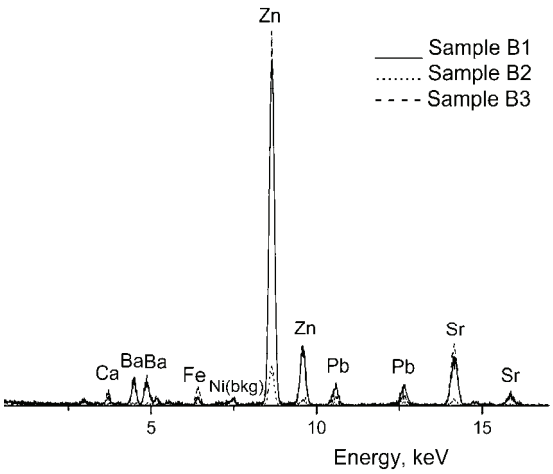


Fig. 8. EDXRF spectra of the paint layers of samples B1, B2 and B3; bkg – background signal.

The fluorescence detected under UV light in combination with the Zn identified in paint layer by EDXRF spectroscopy confirmed the use of Zinc White as the white pigment to achieve a particular hue. Application of ZnO as a white pigment started in the first half of the 19th century[7] and by the end of the 19th century, it was considered the best quality white pigment.

The FTIR spectra of the investigated samples taken from the icon "St. Petka" are shown in Fig. 9. The bands at 1174, 1120, 1077, 643 and 608 $cm^{-1}$ in FTIR spectra of all three samples originated from barium sulphate ($BaSO_4$).[18] This is in agreement with the Ba detected in the EDXRF spectra. The presence of Sr, identified by EDXRF spectroscopy, indicated that natural baryte ore was used for the ground layer.[11]

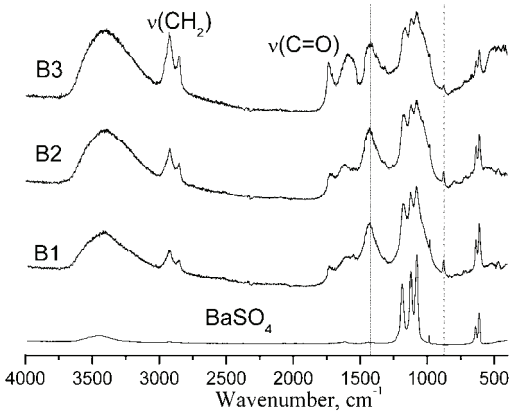


Fig. 9. FTIR spectra of samples taken from the icon "St. Petka" and the reference spectrum of barium sulphate; vertical lines represent the positions of the characteristic bands of calcite.

A broad, medium intensity band of $\nu(CO_3^{2-})$ was detected at 1430 $cm^{-1}$. Since Ca and Pb are present in all three samples, both calcite and Lead White could contribute to this band.

Ground layer appeared as a single, thick and consistent layer in all the investigated samples. As no fluorescence was detected in the ground layer, it can be concluded that ZnO was used as a pigment, while baryte, Lead White and calcite were used for the ground layer.

Iron detected in the paint layer of sample B1 was the only indication of which pigment was used for the green colour. Most probably it was the pigment Green Earth, the colour of which originates from the specific ratio of divalent and trivalent iron incorporated in the structure of the clay minerals glauconite and celadonite.[5,7] FTIR bands characteristic for Si–O stretching vibrations, between 1200–900 $cm^{-1}$,[19] were detected as a shoulder at about 990 $cm^{-1}$ probably due to overlapping with the bands of barium sulphate. In addition, the employed EDXRF experimental setup cannot analyse elements such as Si, Al, Na and Mg. However, green pigments, other than Green Earth, contain some of the following elements: Co, Cu or Cr, but none of them were detected in the sample B1.

In the case of sample B2 and B3, EDXRF and FTIR spectroscopic analyses did not give conclusive answers about the used pigments. For this reason, micro-Raman spectroscopic analysis was performed. For sample B2 blue pigments Prussian Blue and ultramarine ($Na_{8–10}[Al_6Si_6O_{24}]S_{2–4}$) were identified in the paint layer by characteristic Raman shifts,[20] as can be seen in Fig. 10.

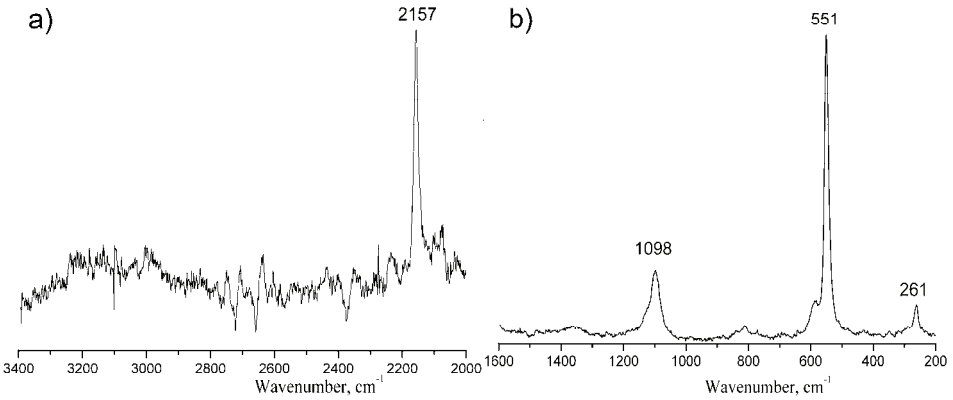


Fig. 10. Raman spectra of the blue pigments in the paint layer of sample B2: a) Prussian Blue and b) ultramarine.

Sample B3 showed intensive fluorescence during micro-Raman analysis and no definite answer about the used blue pigment was obtained. Considering presence of Fe detected in this sample by EDXRF spectroscopy, most probably Prussian Blue was used as the blue pigment.

In all FTIR spectra, characteristic bands originating from $CH_2$ and $CH_3$ stretching vibrations appeared at 2925 and 2850 cm$^{-1}$ and carbonyl (C=O) stretching vibrations at 1740 cm$^{-1}$ were present, confirming the use of linseed oil as binder.[15]

## CONCLUSIONS

Two Serbian icons painted on canvas, “The Virgin and Child” and “St. Petka”, by unknown authors were investigated by optical microscopy, EDXRF, FTIR and micro-Raman spectroscopy. The following pigments were identified: Prussian Blue, ultramarine, Green Earth, iron oxides, Lead White and Zinc White. The binder on both icons was linseed oil. The ground layers were made of gypsum, Lead White, calcite and baryte. The gilded surface of the icon “The Virgin and Child” was made of gold, while the gilded surface on the frame of this icon was made of imitation of gold, *i.e.*, Schlagmetal, since EDXRF spectroscopy showed the presence of copper and zinc, while gold was not detected.

The materials identified as pigments, binders and ground layer in both investigated icons were widely in use during the 19$^{th}$ century and at the beginning of

the 20th century. This finding confirms the initial assumption of the ages of these icon made by art historians and restorers.

*Acknowledgments*. The authors gratefully acknowledge the financial support provided by Ministry of Education, Science and Technological Development of the Republic of Serbia within the framework of Project No. 177021. The authors would like to thank Dr Danica Bajuk-Bogdanović for performing the micro-Raman spectroscopy experiments and the art historian Mrs. Radmila Petronijević, curator of the Museum of the Serbian Orthodox Church in Belgrade, for useful discussions.

ИЗВОД

## СПЕКТРОСКОПСКО ИСПИТИВАЊЕ ДВЕ СРПСКЕ ИКОНЕ СЛИКАНЕ НА ПЛАТНУ

ЉИЉАНА ДАМЈАНОВИЋ[1], ОЛГИЦА МАРЈАНОВИЋ[1], МИЛИЦА МАРИЋ СТОЈАНОВИЋ[2], ВЕЛИБОР АНДРИЋ[3] и УБАВКА МИОЧ[1]

*[1]Универзитет у Београду – Факултет за физичку хемију, Студентски трг 12–16, 11000 Београд, [2]Народни Музеј, Трг Републике 1а, 11000 Београд и [3]Универзитет у Београду – Институт за нуклеарне науке "Винча", п. пр. 522, 11000 Београд*

Мултианалитичко испитивање две српске иконе сликане на платну (Богородица са Христом и Света Петка) које су радови непознатих аутора извршено је са циљем да се идентификују материјали коришћени као пигменти, везива и подлога. Испитиване иконе су власништво Музеја Српске православне цркве у Београду. Узорци, узети са различитих делова икона, су анализирани: оптичком микроскопијом, енергетски дисперзивном рендгенском флуоресцентном анализом, инфрацрвеном спектроскопијом са Фуријe трансформацијом и микро-Раманском спектроскопијом. Идентификовани су следећи пигменати: пруско плаво, ултрамарин, зелена земља, оксиди гвожђа, олово бело и цинк бело. Ланено уље је коришћено као везиво. Материјали коришћени за подлогу су гипс, калцит, барит и олово бело. Позлаћене површине иконе Богородица са Христом су рађене од злата, док је за позлату рама исте иконе коришћена имитација злата тзв. шлагметал јер су EDXRF спектроскопијом идентификовани бакар и цинк, док злато није детектовано. Стил израде икона има карактеристике западно-европског барока. Идентификовани пигменти и везиво одговарају онима који су били у широкој употреби у XIX веку и почетком XX века.

(Примљено 22 јула, ревидирано 6. октобра, прихваћено 8. октобра 2014)

## REFERENCES

1. F. Casadio, L. Toniolo, *J. Cult. Herit.* **2** (2001) 71
2. W. S. Taft Jr., J. W. Mayer, *The Science of Paintings*, Springer, New York, 2000
3. S. Daniilia, D. Bikiaris, L. Burgio, P. Gavala, R. J. H. Clark, Y. Chryssoulakis, *J. Raman Spectrosc.* **33** (2002) 807
4. M. T. Doménech-Carbó, M. J. Casas-Catalán, A. Doménech-Carbó, R. Mateo-Castro, J. V. Gimeno-Adelantado, F. Bosch-Reig, *Fresenius J. Anal. Chem.* **369** (2001) 571
5. D. Hradil, T. Grygar, J. Hradilova, P. Bezdička, *Appl. Clay Sci.* **22** (2003) 223
6. N. Eastaugh, V. Walsh, T. Chaplin, R. Siddall, *Pigment Compendium: A Dictionary and Optical Microscopy of Historical Pigments*, Butterworth-Heinemann as an imprint of Elsevier, Waltham, MA, 2008
7. R. J. H. Clark, *C. R. Chim.* **5** (2002) 7
8. S. Sotiropoulou, S. Daniilia, *Acc. Chem. Res.* **43** (2010) 877

9. M. Ortega-Avilés, P. Vandenabeele, D. Tenorio, G. Murillo, M. Jiménez-Reyes, N. Gutiérrez, *Anal. Chim. Acta* **550** (2005) 164
10. E. Pavlidou, M. Arapi, T. Zorba, M. Anastasiou, N. Civici, F. Stamati, K. M. Paraskevopoulos, *Appl. Phys., A* **83** (2006) 709
11. D. Korolija-Crkvenjakov, V. Andrić, M. Marić-Stojanović, M. Gajić-Kvaščev, J. Gulan, N. Marković, *The Iconostasis of the Krušedol Monastery Church*, The Gallery of Matica srpska, Novi Sad and Vinča Institute of Nuclear Sciences, Belgrade, 2012
12. I. C. A. Sandu, S. Bracci, I. Sandu, M. Lobefaro, *Micros. Res. Tech.* **72** (2009) 755
13. L. Burgio, R. J. H. Clark, K. Theodoraki, *Spectrochim. Acta, A* **59** (2003) 2371
14. S. Akyuz, T. Akyuz, G. Emre, A. Gules, S. Basaran, *Spectrochim. Acta, A* **89** (2012) 74
15. M. R. Derrick, D. Stulik, J. M. Landry, *Infrared Spectroscopy in Conservation Science*, The Getty Conservation Institute, Los Angeles, CA, 1999
16. I. Crina Anca Sandu, M. Helena de Sá, M. Costa Pereira, *Surf. Interface Anal.* **43** (2011) 1134
17. D. Bikiaris, S. Daniilia, S. Sotiropoulou, O. Katsimbiri, E. Pavlidou, A. P. Moutsatsou, *Spectrochim. Acta, A* **56** (1999) 3
18. R. A. Nyquist, R. O. Kagel, *Infrared spectra of inorganic compounds*, Academic Press, New York, 1971
19. M. F. La Russa, S. Ruffolo, C. M. Belifore, V. Comite, A. Casoli, M. Berzoli, G. Nava, *Appl. Phys., A* **144** (2014) 733
20. I. M. Bell, R. J. H. Clark, P. J. Gibbs, *Spectrochim. Acta, A* **53** (1993) 2159.

Journal of the Serbian Chemical Society
JSCS-info@shd.org.rs • www.shd.org.rs/JSCS
*J. Serb. Chem. Soc. 80* (6) 819–826 (2015) UDC 549.67+547.466+678.743:615.281–188
*JSCS–4761* *Original scientific paper*

# Antibacterial activity of copper-containing clinoptilolite/PVC composites toward clinical isolate of *Acinetobacter baumannii*

JELENA K. MILENKOVIĆ[1]*, JASNA J. HRENOVIĆ[2], IVANA S. GOIĆ-BARIŠIĆ[3], MILOŠ D. TOMIĆ[1#] and NEVENKA Z. RAJIĆ[4]

*[1]Innovation Centre of the Faculty of Technology and Metallurgy, University of Belgrade, 11000 Belgrade, Serbia, [2]Faculty of Science, Division of Biology, University of Zagreb, 10000 Zagreb, Croatia, [3]Split University Hospital and School of Medicine, Department of Clinical Microbiology, University of Split, 21000 Split, Croatia and [4]Faculty of Technology and Metallurgy, University of Belgrade, 11000 Belgrade, Serbia*

(Received 25 December 2014, revised 13 February, accepted 18 February 2015)

*Abstract*: The multidrug-resistant bacteria *Acinetobacter baumannii* cause serious hospital infections. Commercial poly(vinyl chloride) (PVC) used for endotracheal tubes was modified in order to obtain a composite with an antibacterial effect towards a clinical isolate of *A. baumannii* ST145. The composites were prepared by addition of different amounts of copper-containing zeolite tuff (CuZ) and by successive impregnation with D-tyrosine (D-Tyr) solution. The composites that were obtained by addition of CuZ (CuZ–PVC) only did not exhibit an antibacterial effect. The impregnation of the CuZ–PVC by D-Tyr resulted in an antibacterial effect which was explained by a synergistic effect of CuZ and D-Tyr. Rheological tests confirmed that the modification of PVC by CuZ does not affect its processability and reformability.

*Keywords*: natural zeolite; multidrug resistance; polymers; poly(vinyl chloride); amino acids.

## INTRODUCTION

Worldwide, there has been a growing demand for the design of novel antimicrobial materials for biomedical applications. Most of the reported materials exerting antimicrobial activity were based on a suitable matrix in which metals, metal oxides, or novel engineered nanoparticles were incorporated.[1–3] These antimicrobial agents interact with microbial cells through variety of mechanisms. The interactions include protein dysfunction and loss of enzyme activity, production of reactive oxygen species, influence on membrane function, interfere with nutrient transport or exert genotoxicity.[4]

* Corresponding author. E-mail: jmilenkovic@tmf.bg.ac.rs
# Serbian Chemical Society member.
doi: 10.2298/JSC141225017M

Recently, naturally occurring minerals, such as clays and zeolites, have attracted great attention considering their possible use as antimicrobial agents in a variety of applications.[5–8] The negatively charged aluminosilicate lattice of zeolites has a unique possibility to host different metal cations, allowing their controlled release into the environment and, accordingly, preventing the metal ions from causing a concentration-dependent toxicity in the environment.[9]

Bacterial infections in hospitals are frequently caused by pathogenic bacteria species hosted in the ventilation systems and on the surfaces of medical devices.[10] *Acinetobacter baumannii* usually cause nosocomial infections in intensive care units.[11,12] These Gram-negative bacteria show resistance to most common antimicrobial agents and survive for a long period in the environment.[13,14] *Acinetobacter* spp. colonizes medical devices for mechanical ventilation (endotracheal tubes)[15] commonly produced from thermoplastic polymers. Accordingly, great effort has been expended in the modification of polymers to inhibit bacterial attachment. Composites based on different polymers were prepared mainly with Ag particles,[16] but also with various metal oxides.[3,17] It should be noted that although the antimicrobial effect of Ag is the most applicable and efficient, the main advantages of metals such as copper or zinc over silver is in their physicochemical stability and cost benefits. Recently, the antimicrobial effects of copper and zinc were investigated and both the metals and their oxides were found to be promising candidates for disinfectants. The metal ions and their oxides exhibited antibacterial efficacy towards *Escherichia coli* and *Staphylococcus aureus*.[6,18]

Furthermore, it was recently reported that some amino acids, in particular D-tyrosine (D-Tyr), can prevent the formation of the biofilm formed by some pathogenic bacteria.[5,19]

Considering these facts, two types of poly(vinyl chloride) (PVC) composites were prepared and their antibacterial activity towards a clinical isolate of *A. baumannii* ST145 investigated. The first composite, denoted as CuZ–PVC, was prepared by adding different amounts of copper-containing zeolite tuff (CuZ) into the PVC matrix and the second type, denoted as D-Tyr–CuZ–PVC, was obtained by impregnation of the CuZ–PVC composite with D-Tyr. Dynamic and mechanical analyses were performed on the CuZ–PVC composite in order to test the reformability of the PVC matrix.

## EXPERIMENTAL

### *Preparation of the composites*

Natural zeolite tuff (Z) obtained from the Zlatokop Mine, Vranjska Banja deposit, containing 73 wt. % of clinoptilolite, was enriched by copper according to a previously reported procedure.[6] The copper-loaded zeolite (containing 1.54 wt. % Cu) was added into a solution containing 1 g of PVC in 20 $cm^3$ tetrahydrofuran (THF). CuZ was added in different amounts (5–15 wt. %). The suspensions were firstly homogenized with magnetic shaker (RTC

standard, IKA for 2 h at 500 rpm) and then intensively by an Ultra Turrax mixer (IKA T18 Basic at 8000 rpm for 10 minutes). The composites CuZ5–PVC, CuZ10–PVC and CuZ15––PVC (number denotes CuZ percentage in the composite) were obtained by drying for 72 h at 25°C, than in vacuum oven (0.4 kPa, 25 °C) for 6 h and finally cut into small squares (1 $cm^2$, thickness around 350 μm). The composites were submerged in 70 wt. % ethanol for 10 min and dried at 37 °C until the ethanol had evaporated completely.

Impregnation of the composites with D-Tyr was performed by immersing the CuZ–PVC into a solution of D-Tyr (100 mg $dm^{-3}$), following the incubation in a temperature programmed water bath at 37 °C for 16 h with shaking at 150 rpm. The composites D-Tyr–CuZ5––PVC, D-Tyr–CuZ10–PVC and D-Tyr–CuZ15–PVC were washed with phosphate buffer solution (PBS, pH 7.2). The sterility of both types of composites was checked by placing the composites into nutrient agar followed by incubation at 37 °C for 24 h. No microbial contamination of the composites was observed.

*Antibacterial activity test*

The antibacterial activity was examined toward a clinical isolate of *A. baumannii* ST145 deposited at the University Hospital Centre, Split, Croatia. *A. baumannii* was first pre-grown on a blood agar for 16 h at 37.0±0.1 °C to obtain the culture in the log phase of growth. The bacterial biomass was then suspended in PBS (initial concentration of the suspension was around $10^8$ CFU $cm^{-3}$ (colony forming units per $cm^3$)). The tubes were left to incubate in the dark for 24 h at 37.0±0.1 °C without stirring. The number of planktonic bacteria was determined at beginning of the experiment and after 24 h of contact. 0.1 $cm^3$ of the original sample or serially diluted sample ($10^{-1}$–$10^{-8}$) was inoculated (by the spread plate method) onto the nutrient agar. The plates were incubated for 24 h at 37.0±0.1 °C. The number of immobilized *A. baumannii* cells was determined after 24 h of contact. The immobilized cells were separated from the composites by vortex treatment (45 Hz/5 min). The number of bacteria was determined and presented as CFU $cm^{-3}$ or CFU $cm^{-2}$.

In order to check antibacterial activity of D-Tyr itself, an experiment with D-Tyr at a concentration of 100 mg $dm^{-3}$ was performed. The statistical analysis was realised using Statistica Software 10.0 (StatSoft, Tulsa, OK, USA). The number of planktonic and immobilized cells was logarithmically presented in order to equalize the variances of the measured parameters. The comparisons between composites were performed using one-way analysis of variance (ANOVA) and subsequently the *post hoc* Duncan test was performed for the calculation of pair-wise comparisons. Statistical decisions were made at a significance level of $p < 0.05$. Leaching of copper ions from CuZ15–PVC in PBS solution was tested after 24 h of the experiment by measuring the Cu concentration in filtrate by atomic absorption spectroscopy (SpectrAA 55B, Varian).

*Mechanical and rheological testing*

Dynamic rheological data, *i.e.*, the dynamic storage modulus ($G'$), the loss modulus ($G''$), the phase angle (tan $\delta$) and the complex dynamic viscosity ($\eta^*$) of PVC and the CuZ–PVC samples were obtained using a Discovery Hybrid rheometer HR2 (TA Instruments, New Castle, DE, USA). The rheological properties of molten samples were analysed on pastilles in the dynamic shear mode between two parallel plates (diameter 25 mm; gap 1.5 mm) at three different temperatures: 180, 190 and 200 °C. Frequency sweep scans were conducted from 0.1 to 100 rad $s^{-1}$ and at a strain of 0.5 %. The complex dynamic viscosity of the sample melts obtained at different temperatures were used to calculate the activation energy of flow ($E_a$),

which was calculated using the relation between viscosity and temperature (Arrhenius equation).

## RESULTS AND DISCUSSION

The antibacterial activities of the CuZ–PVC composites are given in Fig. 1. The data on the activity of the composites with Z and D-Tyr–Z are not shown here. In a previous work,[5] it was found that these materials do not exhibit antibacterial activity towards *A. baumannii* ST145.

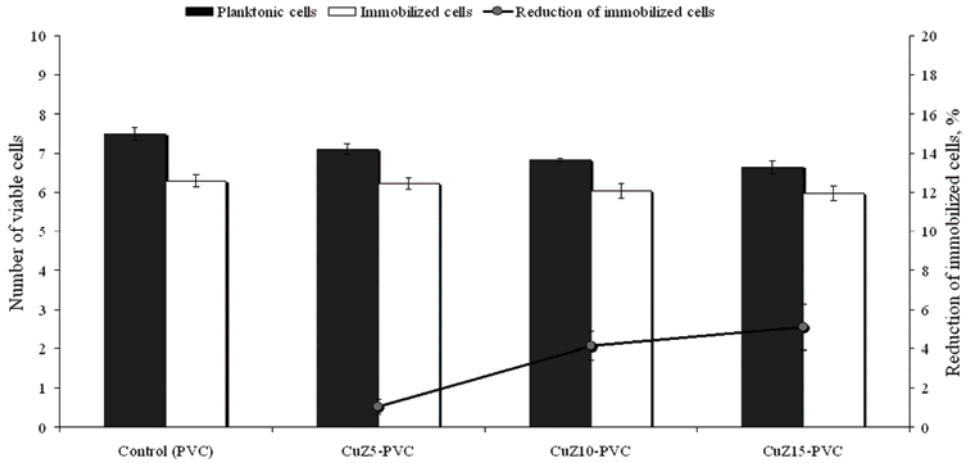


Fig. 1. Antibacterial activity of the control material (PVC) and CuZ–PVC composites after 24 h contact (number of viable cells is expressed as log (*CFU* $cm^{-3}$) or log (*CFU* $cm^{-2}$) for planktonic and immobilized cells, respectively). $t_0$ *A. baumannii* (log *CFU* $cm^{-3}$) = 7.79±0.20.

The composites containing CuZ in all examined amounts did not exhibit antibacterial activity towards either immobilized or planktonic cells (antibacterial activity was only 5 % reduction of immobilized cells for the CuZ15–PVC composite). This could be explained by the fact that the *A. baumannii* produces a high amount of biofilm which protect the cells of *A. baumannii* from antibacterial agents. The explanation is supported by the antibacterial effect found for D-Tyr––CuZ–PVC (Fig. 2).

The reduction of planktonic cells was not significant, but the reduction of immobilized cells on the D-Tyr–CuZ–PVC composites was evident. There was a slight increasing trend with increasing amount of CuZ in the composites. The reduction of the immobilized cells varies from 10 % (D-Tyr–CuZ5–PVC) to 14 % (D-Tyr–CuZ15–PVC). A one log CFU reduction in the immobilised *A. baumannii* cells on D-Tyr–CuZ15–PVC was achieved in comparison to the control (a commercial endotracheal tube).

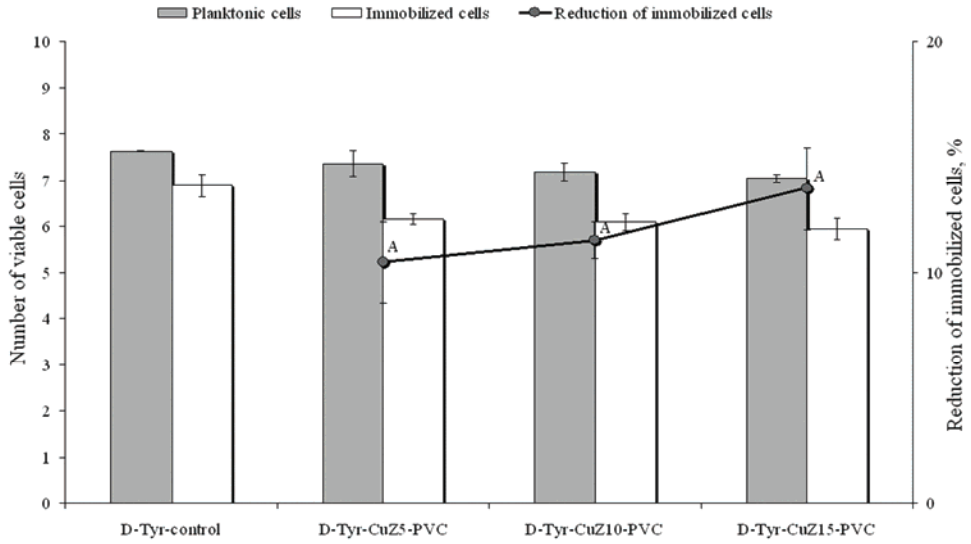


Fig. 2. Antibacterial activity of D-Tyr–PVC (control) and D-Tyr–CuZ–PVC composites after 24 h of contact (number of viable cells is expressed as log (*CFU* $cm^{-3}$) or log (*CFU* $cm^{-2}$) for planktonic and immobilized cells, respectively) $t_0$ *A. baumannii* (log *CFU* $cm^{-3}$) = 7.72±0.13; A – significant reduction as compared to the control.

D-Tyr showed a repellent activity towards microbial aggregates, including *Amaricoccus macauensis* strain, *Leifsonia* sp., *Microbacterium* sp., *Mesorhizobium* sp., *Burkholderia cepacia*, *Alicycliphilus* sp. and *Acidovorax* sp.,[19] *Staphylococcus aureus*[20] and *Pseudomonas aeruginosa*.[21] In this study, it was found that the antibacterial activity of CuZ15–PVC towards *A. baumannii* develops only in a presence of D-Tyr. Moreover, pH value did not change significantly during the experiments. It increased from 6.70 to 7.20, which is the optimal pH range for growth of *Acinetobacter* spp.[22] This supports the fact that antibacterial effect cannot be ascribed to differences in the pH.

Since antibacterial activity of various metal-containing antibacterial materials has been attributed to leaching of metal ions,[23] the possibility of Cu leaching from the composite with the highest amount of CuZ (CuZ15–PVC) was examined. It was found that less than 1 % of the total amount of Cu present in the CuZ had leached into PBS after 24 h of contact. This indicates that free Cu ions are not responsible for the antibacterial activity. In addition, antibacterial effect of a D-Tyr solution at the concentration used for the impregnation of the composite was examined. No activity of the D-Tyr towards *A. baumannii* ST145 was found. The results obtained in this study show that the mechanism of the antibacterial activity of the prepared composites towards *A. baumannii* includes a synergetic activity of CuZ and D-Tyr. Further work will be directed towards detailed investigations on the mechanism itself.

Finally, in order to check whether the addition of CuZ influences the dynamic mechanical properties of the PVC matrix, the dynamic mechanical properties of the CuZ15–PVC composite and neat PVC in the molten and solid states were compared (Fig. 3).

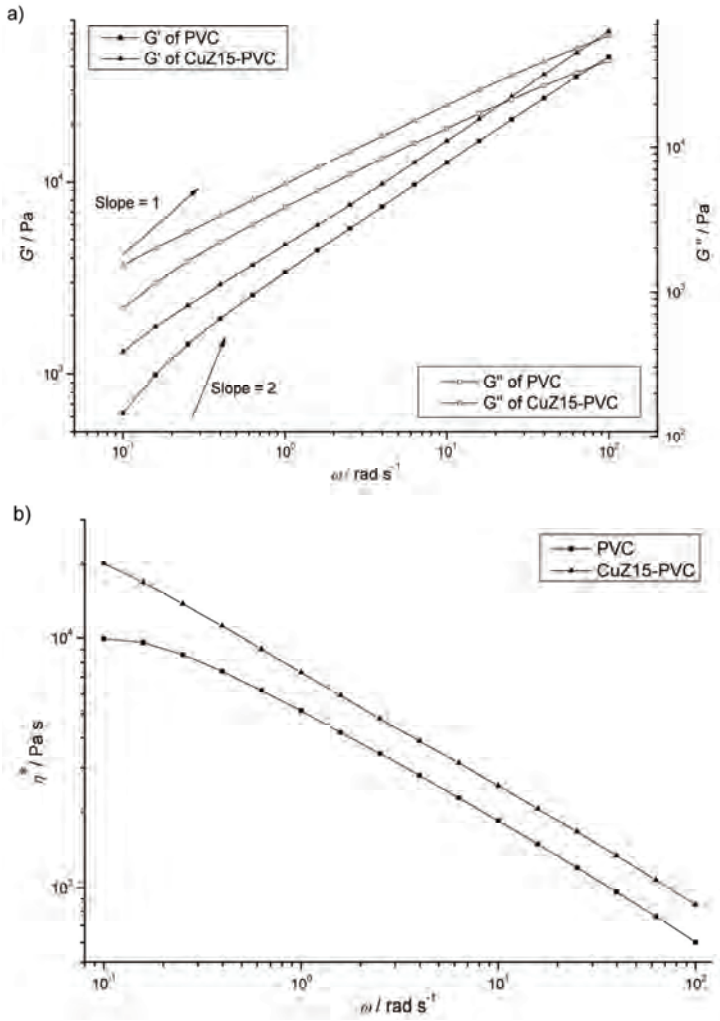


Fig. 3. a) Frequency dependences of the storage and loss modulus and b) the complex viscosity of PVC (control) and CuZ15–PVC at 200 °C.

Considering the higher values of rheological parameters, activation energy of flow ($E_a$) and reduced slopes of $G'$, $G''$ and $\eta^*$ at 0.1 rad $s^{-1}$ ($\eta^*_{0.1}$) and the frequency dependences ($\omega$) at low frequencies (Table I), it could be concluded that the addition of CuZ into PVC improved its rheological behaviour.

TABLE I. Results of dynamic–mechanical analysis

| Sample | $\eta^*_{0.1}$ / kPa s | Melts | | | | Solid | |
|---|---|---|---|---|---|---|---|
| | | $\eta^* \approx \omega^p$ | $G' \approx \omega^m$ | $G'' \approx \omega^n$ | $E_a$ kJ mol$^{-1}$ | $G'$ at 25 °C MPa | $G'$ at 100 °C MPa |
| PVC | 9.9 | –0.077 | 0.889 | 0.808 | 38.5 | 24 | 4.14 |
| CuZ15–PVC | 20.1 | –0.415 | 0.603 | 0.575 | 75.5 | 75 | 8.4 |

The addition of CuZ improved $G'$ in the rubbery state ($T$ > 60 °C), as well as at 25 °C, and enhanced the elastic behaviour of PVC. The improved rheological and mechanical properties of the PVC composite indicated that CuZ could play the role of physical crosslinker due to the possibility of the formation dipole––dipole interactions between the electronegative chlorine atoms on the PVC chains and the polar zeolite particles.[24]

## CONCLUSIONS

The study showed that commercial PVC could be modified by a simple procedure to achieve an antibacterial effect towards the multidrug resistant *A. baumannii*. The rheological results showed that the addition of natural zeolite (15 wt. %) did not affect the processability and formability of the PVC. On the contrary, the addition of the zeolite to PVC improved its rheological behaviour.

Preliminary results indicated that D-Tyr and copper-containing zeolite are promising candidates for the modification of thermoplastic polymers that are used in biomedical devices. Further research will be directed towards a study of the antibacterial mechanism as well as to optimisation of the modification process.

*Acknowledgments*. This work was supported by the Ministry of Education, Science and Technological Development of the Republic of Serbia (Project No. 172018) and the Ministry of Science, Education and Sports of the Republic of Croatia (Project No. 1191155-1203). The authors are very grateful to Prof. Juraj Sipusic (Faculty of Chemical Engineering and Technology, University of Zagreb) for micronization of the zeolite samples.

И З В О Д

## АНТИБАКТЕРИЈСКА АКТИВНОСТ КОМПОЗИТА НА БАЗИ БАКРОМ ОБОГАЋЕНОГ ЗЕОЛИТА/ПОЛИ(ВИНИЛ-ХЛОРИДА) ПРЕМА КЛИНИЧКОМ ИЗОЛАТУ *Acinetobacter baumannii*

ЈЕЛЕНА К. МИЛЕНКОВИЋ[1], JASNA J. HRENOVIĆ[2], IVANA S. GOIĆ-BARIŠIĆ[3], МИЛОШ Д. ТОМИЋ[1] и НЕВЕНКА З. РАЈИЋ[4]

*[1]Иновациони центар Технолошко–металуршког факултета, Универзитет у Београду, Карнегијева 4, 11000 Београд, [2]Faculty of Science, Division of Biology, University of Zagreb, 10000 Zagreb, Croatia, [3]Split University Hospital and School of Medicine, Department of Clinical Microbiology, University of Split, 21000 Split, Croatia и [4]Технолошко–металуршки факултет, Универзитет у Београду, Карнегијева 4, 11000 Београд*

Мултирезистентна бактерија *Acinetobacter baumannii* изазива озбиљне болничке инфекције. У овом раду комерцијални поли(винил-хлорид), који се користи за производњу ендотрахијалних тубуса, модификован је бакром обогаћеним зеолитом у циљу добијања композита који показују антибактеријску активност према клиничком изолату

*Acinetobacter baumannii* ST145. Композити су припремани додавањем различите количине бакром обогаћеног зеолитног туфа (CuZ), а затим су импрегнисани раствором D--тирозина (D-Tyr). Композити са CuZ (CuZ–PVC) нису показали антибактеријску активност. Композити CuZ–PVC који су импрегнисани раствором D-Tyr показали су антибактеријску активност. Активност је објашњена синергистичким деловањем CuZ и D-Tyr. Реолошким мерењима показано је да модификација поли(винил-хлорида) бакром обогаћеним зеолитом не утиче на процесибилност овог полимера као ни на његову поновну обраду.

(Примљено 25. децембра 2014, ревидирано 13. фебруара, прихваћено 18. фебруара 2015)

REFERENCES

1. P. Kaali, E. Stromberg, R. E. Aune, G. Czel, D. Momcilovic, S. Karlsson, *Polym. Degrad. Stabil.* **95** (2010) 1456
2. D. Zampino, T. Ferreri, C. Puglisi, M. Mancusi, R. Zaccone, R. Scaffaro, D. Bennardo, *J. Mater. Sci.* **46** (2011) 6734
3. J. T. Seil, T. J. Webster, *Acta Biomater.* **7** (2011) 2579
4. J. A. Lemire, J. J. Harrison, R. J. Turner, *Microbiology* **11** (2013) 371
5. J. Milenkovic, J. Hrenovic, I. Goic-Barisic, M. Tomic, J. Djonolagic, N. Rajic, *Biofouling* **30** (2014) 965
6. J. Hrenovic, J. Milenkovic, T. Ivankovic, N. Rajic, *J. Hazard. Mater.* **201**–**202** (2012) 260
7. J. Hrenovic, J. Milenkovic, N. Daneu, R. Matonickin Kepcija, N. Rajic, *Chemosphere* **88** (2012) 1103
8. J. Hrenovic, J. Milenkovic, I. Goic-Barisic, N. Rajic, *Micropor. Mesopor. Mater.* **169** (2013) 148
9. J. Wang, Z. Wang, S. Guo, J. Zhang, Y. Song, X. Dong, X. Wang, J. Yu, *Micropor. Mesopor. Mater.* **146** (2011) 216
10. A. Hidron, J. Edward, J. Patel, T. Horan, D. Sievert, D. Pollock. S. Fridkin, *Infect. Cont. Hosp. Ep.* **29** (2008) 996
11. A. Levin, A. Barone, J. Penso, M. Samtos, I. Marinho, E. Arruda, E. Manqrique, S. Costa, *Clin. Infect. Dis.* **28** (1999) 1008
12. I. Goic-Barisic, V. Kaliterna, *Med. Glas.* **8** (2011) 312
13. J. A. Gaddy, L. Actis, *Future Microbiol.* **4** (2009) 273
14. P. Espinal, S. Martı, J. Vila, *J. Hosp. Infect.* **80** (2012) 56
15. S. Gil-Perotin, P. Ramirez, V. Marti, J. M. Sahuquillo, E. Gonzalez, I. Calleja, R. Menendez, J. Bonastre, *Crit. Care* **16** (2012) R93
16. S. H. Jeong, S. Y. Yeo, S. C. Yi, *J. Mater. Sci.* **40** (2005) 5407
17. A. Ananth, S. Dharaneedharan, M. S. Heo, Y. S. Mok, *Chem. Eng. J.* **262** (2015) 179
18. Dj. Stojakovic, J. Hrenovic, M. Mazaj, N. Rajic, *J. Hazard. Mater.* **185** (2011) 408
19. X. Si, X. Quana, Q. Li, Y. Wua, *Water Res.* **54** (2014) 247
20. A. I. Hochbaum, I. Kolodkin-Gal, L. Foulston, R. Kolter, J. Aizenberg, R. Losick, *J. Bacteriol.* **193** (2011) 5616
21. H. Xu, Y. Lui, *J. Membrane Sci.* **376** (2011) 266
22. G. M. Garrity, D. J. Brenner, N. R. Krieg, J. T. Stale, *Bergey's Manual of Systematic Bacteriology, Part B*, Vol. 2, Springer, New York, 2005, p. 425
23. B. Kwakye-Awuah, C. Williams, M. A. Kenward, I. Radecka, *J. Appl. Microbiol.* **104** (2008) 1516
24. G. Sodeifian, H. Z. Nikooamal, A. A. Yousefi, *J. Polym. Res.* **19** (2012) 9897.

Journal of the Serbian Chemical Society
JSCS-info@shd.org.rs • www.shd.org.rs/JSCS
*J. Serb. Chem. Soc. 80* (6) 827–838 (2015)
*JSCS–4762*
UDC 628.336+546.47/.49'56'815:
504.054:628.515/.516
*Original scientific paper*

# Heavy metals in Neogene sedimentary rocks as a potential geogenic hazard for sediment, soil, and surface and groundwater contamination (eastern Posavina and the Lopare Basin, Bosnia and Herzegovina)

NENAD GRBA[1,2], FRANZ NEUBAUER[2], ALEKSANDRA ŠAJNOVIĆ[3]*[#], KSENIJA STOJANOVIĆ[1#] and BRANIMIR JOVANČIĆEVIĆ[1#]

[1]*University of Belgrade, Faculty of Chemistry, Studentski trg 12–16, 11000 Belgrade, Serbia* [2]*Paris Lodron University of Salzburg, Department of Geography and Geology, Hellbrunnerstrasse 34,5020 Salzburg, Austria and* [3]*University of Belgrade, Center of Chemistry, ICTM, Njegoševa 12, 11000 Belgrade, Serbia*

(Received 17 March, revised 28 April, accepted 29 April 2014)

*Abstract*: The influence of geochemical processes (weathering, erosion and dilution) of the Internal Dinarides to the Posavina Neogene Basin and their implication to the pollution of the Sava River sediments at four sampling sites in the Eastern Posavina (Županja, Brčko, Bosanska Rača and Sremska Mitrovica) was studied. For this purpose, comparison of contents of heavy metals (Pb, Zn, Cu, Ni, Cr, Cd, As and Hg) of the Eastern Posavina sediments with local background values was performed. Sediments from two boreholes of the Lopare Basin considered as non-polluted and representative for specific geologic and hydrogeologic system were used for the calculation of local background values. The aim was to assess whether the observed heavy metals concentrations at four sampling sites along the Sava River represent background/natural or anthropogenic contamination. This task was performed using the geo-accumulation index and total enrichment factor. According to values of the total enrichment factor (0.25–0.71), the anthropogenic impact on the investigated area was quite low. The heavy metals contents in river sediments, soil and groundwater were mainly controlled by geochemical processes, particularly weathering (chemical proxy of alteration value ≈ 60). The results also offer novel insights into the elevated geogenic levels of Cr and Ni in the Eastern Posavina region.

*Keywords:* pollution; river sediments; geo-accumulation index; total enrichment factor; weathering.

* Corresponding author. E-mail: sajnovica@bg.ac.rs
[#] Serbian Chemical Society member.
doi: 10.2298/JSC140317047G

## INTRODUCTION

The assessment of heavy metal pollution in fluvial sediments is a complex process, in which physical, chemical and biological data are required. Since in many areas the necessary biological data are not available, in environmental geochemistry, the assessment of the contamination status is normally based on Sediment Quality Guidelines (SQGs) or quantitative indexes such as the enrichment factor with respect to reference values, such as regional/local background values or average concentrations of shale, average continental crust or upper continental crust, *etc*.[1]

The key environmental problem in the Sava River Basin is often directed to the release of contaminated untreated effluents from municipalities and industrial facilities. However, recent investigations showed that the sedimentary rocks from the Lopare Basin contain relatively high heavy metal concentrations.[2] Since, erosion activity weather these rocks to soils, the high heavy metal contents represent a significant geogenic hazard and could potentially represent a hazard for surface and groundwater, as well.[2] It is known that the majority of the clastic material was transported to the Eastern Posavina region by rivers and streams from the Bosnian Mountains.[3] This was confirmed by the mineral composition of fluvial sediments, which originated from the serpentinite zone in Bosnia.[3] The main direction of transport from south to north correlates with reducing proportions of coarse-grained clasts and a decreasing grain size in the same direction.[4] In this way, in the southern part, along the Sava River, gravels are predominantly deposited, and sands in the northern sections.[5]

The catchments of Drina and Bosna Rivers are much larger than the catchments of rivers from the Papuk Mountains in the north of the Posavina Basin (Fig. S-1 of the Supplementary material to this paper). Consequently, sediments from the south should dominate sediments in this part of the Sava River, respectively the Posavina region. In this paper, the influence of geochemical processes of sediments from the Lopare Basin, which is drained by the Drina and Bosna Rivers, on the eastern part of the Neogene Posavina Basin (Eastern Posavina region) was studied. The contents of eight heavy metals (Pb, Zn, Cu, Ni, Cr, Cd, As and Hg) of the Eastern Posavina region (Županja, Brčko, Bosanska Rača and Sremska Mitrovica) were taken from published data.[6] For local background values, the average concentration of the eight heavy metals (Zn, Cu, Cd, Pb, Cr, Ni, As and Hg) from two sediment boreholes, POT 1 (depth from 18.5 to 193 m) and POT 3 (depth from 27.8 to 344 m), of the Neogene Lopare Basin (Fig. S-1; Table S-I of the Supplementary material) were used. These sediments are considered as non-polluted and representative for this specific and unique geologic and hydrogeologic system.

In the investigated Neogene basins, a significant influence of regional and local hydrogeological relations as part of the system of groundwater circulation

was observed. The most important aquifers within the alluvial formations are in the terrains of northern Bosnia. Given the thickness of the gravel–sand formations and spatial position in relation to rivers, the conclusion may be drawn that the presence of aquifers is almost regularly found in direct hydraulic contact with renewable quantities of groundwater. The water quality is directly dependent on the lithologic composition of the hinterland.[9] According to the aquifer characteristics, the first and partly the second hydrogeological groups are present in the investigated region. Group I (in the northern region) represents a high water-rich aquifer with a high transmissibility coefficient (more than $10^{-3}$ $m^2$ $s^{-1}$). Group II, in the southern part (the region of Majevica; Fig. S-1) is a medium water-rich aquifer and it is characterized by an intermediate transmissibility coefficient ($10^{-3}$ $m^2$ $s^{-1}$). This is a very important factor in regard to processes such as dilution by tributaries and hill slope erosion from the Bosnian Mountains in the upper part of sediments of the tributaries of the Sava River, namely from the Majevica Mountains, and the Bosna and Drina Rivers in the eastern Posavina region. Therefore, the aspect of weathering processes to soils as a potential hazard for surface and groundwater contamination in this region was also investigated.

## MATERIALS AND METHODS

The investigated region included the eastern part of the Posavina Basin (sampling sites Županja, Brčko, Bosanska Rača and Sremska Mitrovica), the Lopare Basin and the Drina and Bosna River catchment (Fig. S-1). This unique region represents a part of the Internal Dinarides, which are formed between the Dinaric Ophiolite belt and the Sava–Vardar Zone. From geologic and hydro-geologic points of view, it belongs to the unique Sava–Vardar nappe and terrain with aquifers of intergranular porosity.[9] It was formed during a late stage of orogeny in the Dinarides by extensional tectonic processes and it is considered to be a part of the wider Pannonian Basin and trapped sediments from the surrounding Alpine–Carpathian–Dinarian source area.

The Lopare Basin is a depression between the main Majevica ridge to the south, which divides the Lopare and Tuzla Basins, and the northern Majevica ridge, which is a natural border to the Posavina Basin (Fig. S-1).

The investigated sampling sites (along the Sava River), Brčko and Bosanska Rača are situated in the northeastern (NE) part of Bosnia and Herzegovina; Županja is located in the NE part of Croatia; and Sremska Mitrovica, is located in the northwestern part of Serbia (Fig. S-1).

From a total of 46 sediment samples from two boreholes POT-1 (depth to 193 m) and POT-3 (depth to 344 m) (Table S-I), a quarter of the core for analysis was taken using the “dot method”. Firstly, the sediment samples were dried at 105 °C. In the next step, the samples were successively ground in three stages to a grain size less than 2.36 mm. The samples were first grinded by a jaw crusher, than by cone crusher and finally by a roller crusher. After this stage, the samples were homogenized. The rough mill fragmented samples were subsequently finely pulverized and sieved into a grain size fraction < 63 μm.

The contents of heavy metals were determined by inductively coupled plasma atomic emission spectrometry (ICP-AES). The ICP-AES measurements were performed using a Thermo Scientific iCAP 6500 Duo ICP (Thermo Fisher Scientific, Cambridge, UK) spectrometer equipped with RACID86 Charge Injector Device (CID) detector, pneumatic cross-flow

type nebulizer, quartz torch, and alumina injector, which enabled the detection of samples containing HF in a small amount. Nitric acid ($HNO_3$, 65 %), hydrochloric acid (HCl, 37 %), orthophosphoric acid ($H_3PO_4$, 85 %) and hydrofluoric acid (HF, 50 %) were used for digestion. The experimental procedure was explained in detail in a previous paper.[10]

## RESULTS AND DISCUSSION

### *Heavy metal content in background sediments*

The background levels of heavy metals were uniformly distributed with depth of the sediment within the boreholes POT 1 and POT 3 (Table S-I). The content of almost all heavy metals were generally high compared to standard values (Tables S-I and I). According to their lithologically homogeneous composition and the uniform distribution of metals (Table S-I), it can be concluded that they were derived predominantly from homogeneous natural sediment sources and could, therefore, be used as background levels for surface sediments of the Sava River in the eastern Posavina Basin to determine the difference between the geogenic and anthropogenic sources. For background levels of heavy metals in the Lopare Basin sediments, the average reduced value in relation to the amount of diluted calcium carbonate[11] of the two boreholes POT 1 and POT 3 (Table I) was used. The amount of diluted calcium carbonate was calculated from the CaO contents in the sediments.[2,10] The shallowest sample from borehole POT 1, which had a sandy clay composition as the result of weathering, (sample at a depth of 11.85 m; Table S-I) was excluded from the calculation of the background levels.

TABLE I. Values of the total element concentrations (mg $kg^{-1}$) in sediments of the Sava River (up to 15 cm),[6] values of the local background and reference standards

| Sampling site | Pb | Zn | Cu | Ni | Cr | Cd | As | Hg |
|---|---|---|---|---|---|---|---|---|
| Županja | 33.9 | 134.0 | 31.1 | 212.0 | 381.0 | 0.47 | 19.8 | 0.27 |
| Brčko | 52.0 | 165.0 | 43.4 | 185.0 | 312.0 | 0.62 | 16.7 | 0.30 |
| Bosanska Rača | 122.0 | 184.0 | 47.1 | 186.0 | 273.0 | 0.66 | 17.9 | 0.37 |
| Sremska Mitrovica | 79.0 | 275.0 | 44.9 | 177.0 | 276.0 | 0.84 | 23.6 | 0.44 |
| Local background values[a] | 136.8 | 49.4 | 26.2 | 135.8 | 159.4 | 1.02 | 20.6 | 0.53 |
| ISQG[b] | 30.2 | 124.0 | 18.7 | – | 52.3 | 0.70 | 7.2 | 0.17 |
| ÖNORM S 2088-2[c] | 100.0 | 300.0 | 100.0 | 60.0 | 100.0 | 1.00 | 20.0 | 1.00 |
| FBiH 72/09[d] | 125.0 | 250.0 | 100.0 | 62.5 | 125 | 1.88 | 25.0 | 1.88 |
| PEL[e] | 112.0 | 271.0 | 108.0 | – | 160.0 | 4.20 | 41.6 | 0.49 |

[a]The average reduced value in relation to the amount of diluted calcium carbonate of two boreholes POT 1 and POT 3.[11] The shallowest sample from POT 1 with a sandy clay composition was excluded because of weathering processes; [b]interim sediment quality guideline (ISQG) values correspond to the threshold level effects below which diverse biological effects are not expected (Canadian Sediment Quality Guidelines for the Protection of Aquatic Life);[12] [c]Austrian Standards on Contaminated Land Management general protocol and generic criteria (trigger values) for risk assessment regarding human exposure and plant uptake (ÖNORM S 2088-2) for soil samples from 0 to 20 cm in depth;[13] [d]guideline for the determination of permitted quantities of harmful and hazardous substances in soil and methods of their investigation (published in an Official Gazette of the Federation of Bosnia and Herzegovina, No. 72/09);[14] [e]probable effect level (PEL) characterizes the concentrations of pollutants that may affect aquatic life (Canadian Sediment Quality Guidelines for the Protection of Aquatic Life)[12,15]

*Distribution of heavy metals in the eastern Posavina region*

Most of concentrations in the sediments at the sampling sites exceeded the Interim Sediment Quality Guideline (ISQG)[12] values, but they were notably lower in comparison to the Austrian Standard, ÖNORM S 2088-2,[13] and the Bosnian and Herzegovinian Guideline for the determination of the permitted quantities of harmful and hazardous substances in the soil and the methods of their investigation, FBiH 72/09[14] values (Table I). The contamination gradation increased from Županja to Sremska Mitrovica, with the exception of Ni and Cr. At all sampling locations, the concentrations of Cr were higher than the probable effect level, PEL[12,15] (160.0 mg $kg^{-1}$ of Cr), ISQG[12] (52.3 mg $kg^{-1}$ of Cr), ÖNORM S 2088-2[13] (100.0 mg $kg^{-1}$ of Cr) and FBiH 72/09[14] (125.0 mg $kg^{-1}$ of Cr) values. However, interestingly, the local background values of 159.4 mg $kg^{-1}$ for Cr were also much higher than ISQG,[12] but very similar to PEL[12,15] and closer to the ÖNORM S 2088-2[13] and FBiH 72/09[14] values (Table I). A similar observation found for the Ni and Pb contents. The contents of Cr and Ni were much higher than those for average continental mudstones.[16] It is also evident, that compared to the standards ÖNORM S 2088-2[13] and FBiH 72/09,[14] the most representative comparative results were obtained in this study, because their values were the most similar ones to the element concentrations in the Sava River sediments and the local background values. Elevated Ni and Cr contents may result from ophiolites (ocean floor on land that is usually rich in some heavy metals, such as Cr and Ni) occurring in the neighborhood (Dinaric Ophiolite Belt).[17] Alluvial flooding by the Bosna River, which drains the Central Dinaric Ophiolite Belt (CDOB) of Central Bosnia, resulted in abnormally high concentration of Cr (502 mg $kg^{-1}$) in the easternmost part of the Posavina area. The highest content of Cr in the sample of the site Županja (381.0 mg $kg^{-1}$ of Cr; Table I) also corroborates this hypothesis. In the absence of industrial pollutants in the wider area, all the elevated concentrations of Cr in the Pannonian region are assumed to be of geogenic origin.[18]

The Bosanska Rača and Sremska Mitrovica samples had on average higher concentrations of heavy metals than the samples from Županja and Brčko (Table I), consistent with the quantity of material that flows close to these sites from the Drina River, which is a confluent of the Sava River. During geological time, the Drina River changed its flow into the Mačva lowlands from east to west and formed the spacious terrace plane. The Sava River flow has a direct influence in the draining and inundation of the alluvial plane and the fuelling of minor flows and ground-water aquifers below the average river level during maximum water level events.[19]

*Calculation of background/natural and anthropogenic contaminated levels*

The use of the total concentrations as a criterion to assess the potential effects of a sediment concentration implies that all forms of a given metal have an equal impact on the environment; such an assumption is clearly untenable.[20] In this study, the geo-accumulation index ($I_{geo}$) and the total enrichment factor ($R$) were used as tools for understanding the geogenic *versus* anthropogenic hazards.

The geo-accumulation index ($I_{geo}$) was originally defined by Müller (1979)[7] for metal concentrations in pulverized sediment fractions (<2 μm). A previous expression on sediment fractions (less than 63–65 μm) combined with regional backgrounds was also established.[21] The same approach was performed in this study.

The $I_{geo}$ was developed for global standard scale values, which is expressed as follows:

$$I_{geo} = \log_2\left(\frac{C_n}{1.5B_n}\right) \quad (1)$$

where $C_n$ is the measured concentration of metal n in the sediment, which was taken from a published study,[6] $B_n$ is the geochemical background value for the metal n (heavy metal concentration in background sediment, Table I), and the factor 1.5 is incorporated in the relationship to account for possible variation in the background data due to lithologic effects.

The geo-accumulation index ($I_{geo}$) scale consists of seven grades (0 to 6) ranging from unpolluted to very strongly polluted (Table II).[7] The $I_{geo}$ values of the investigated sediments are given in Table III.

TABLE II. The geo-accumulation index ($I_{geo}$) scale (after Müller, 1979)[7]

| $I_{geo}$ | Class | Pollution intensity |
|---|---|---|
| >5 | 6 | Very strongly polluted |
| 4–5 | 5 | Strongly to very strongly polluted |
| 3–4 | 4 | Strongly polluted |
| 2–3 | 3 | Moderately to strongly polluted |
| 1–2 | 2 | Moderately polluted |
| 0–1 | 1 | Unpolluted to moderately polluted |
| 0 | 0 | Unpolluted |

The analytical data corresponding to each sampling site can be used for the calculation of an enrichment factor ($r$), defined as the ratio:[8]

$$r = \frac{(C_{sed} - C_{back})}{C_{back}} \quad (2)$$

where $C_{sed}$ is the content of a metal in each sample site (the value was taken from a published study[6]), while $C_{back}$ is the mean concentration of the same metal for all the background sediment levels (Table I). The $r$ values for the Sava River sediments sampling sites are given in Table III. The metals with $r > 1.0$ could be considered as indicators of anthropogenic metal pollution and used for evaluating the degree of pollution of the surface sediments by calculation of a total enrichment factor ($R$), for each site, by averaging the $r$ values of all ($n$) indicator-metals as follow:

$$R = \frac{\sum r}{n} \tag{3}$$

$R$ values exceeding 1.5 indicate high pollution. $R$ values between 1.5 and 1 imply moderately pollution, whereas samples with $R$ values below unity are considered as unpolluted or exposed to low pollution.[8] As a synthetic multi-parameter indicator, $R$ can be assumed as an integrated index of the local metal pollution pattern for sample sites: Županja, Brčko, Bosanska Rača and Sremska Mitrovica (Table III).

TABLE III. Values of the geo-accumulation index ($I_{geo}$), enrichment factor ($r$) and total enrichment factor ($R$) for the sampling sites of the Sava River sediments

| Sampling site | Pb | Zn | Cu | Ni | Cr | Cd | As | Hg |
|---|---|---|---|---|---|---|---|---|
| | | | $I_{geo}$ | | | | | |
| Županja | –2.60 | **0.86** | –0.34 | 0.06 | **0.67** | –1.70 | –0.64 | –1.56 |
| Brčko | –1.98 | **1.16** | 0.14 | –0.14 | **0.38** | –1.30 | –0.89 | –1.41 |
| Bosanska Rača | –0.75 | **1.31** | 0.26 | –0.13 | **0.19** | –1.21 | –0.79 | –1.11 |
| Sremska Mitrovica | –1.38 | **1.89** | 0.19 | –0.20 | **0.21** | –0.87 | –0.39 | –0.86 |
| Mean values | –1.68 | 1.30 | 0.07 | –0.10 | 0.36 | –1.27 | –0.68 | –1.23 |
| | | | $r$ | | | | | |
| Županja | –0.75 | **1.71** | 0.19 | 0.56 | **1.39** | –0.54 | –0.04 | –0.49 |
| Brčko | –0.62 | **2.34** | 0.66 | 0.36 | **0.96** | –0.39 | –0.19 | –0.44 |
| Bosanska Rača | –0.11 | **2.73** | 0.80 | 0.37 | 0.71 | –0.35 | –0.13 | –0.30 |
| Sremska Mitrovica | –0.42 | **4.57** | 0.71 | 0.30 | 0.73 | –0.18 | 0.14 | –0.17 |
| Mean values | –0.48 | 2.84 | 0.59 | 0.40 | 0.95 | –0.37 | –0.05 | –0.35 |
| | | | $R$ | | | | | |
| Županja | | | | 0.25 | | | | |
| Brčko | | | | 0.33 | | | | |
| Bosanska Rača | | | | 0.46 | | | | |
| Sremska Mitrovica | | | | 0.71 | | | | |

In general, according to the $R$ values below unity, the target area could be considered as exposed to low pollution. However, taking $r = 1.0$ as an operational threshold value, Zn at all sites and Cr at Županja could be considered as synthetic indicators of a local pattern of anthropogenic metal pollution, and furthermore, could be used for evaluating the degree of pollution of surface sediments. Based

on the mean value of *r*, the sediments are enriched in metals in the following order: Zn > Cr > Cu > Ni > As > Hg > Cd > Pb. In contrast to Zn and Cr, the other elements have values below unity. Elevated values for Zn and Cr most likely resulted from anthropogenic activities, considering that these metals have content at least two times higher than the background sediment (Table I). Moreover, the obtained results clearly show that Ni is not related to an anthropogenic source of pollution in any of the investigated sediments of the Sava River (Table III).

A gradient increase of the mean $I_{geo}$ value in the following order: Zn > Cr > Cu > Ni > As > Hg > Cd > Pb was observed. The $I_{geo}$ index for Zn implies unpolluted to moderately polluted classification of the Županja site and moderately pollution for the other sites. The increase in this parameter for Zn values follows the course of the Sava River and because of the influence of its tributary Drina River, reaches the highest level of 1.89 in the Sremska Mitrovica sediments (Table III). In the group of the unpolluted to moderately polluted sites, the $I_{geo}$ for Cr varies from 0.19 to 0.67, but in the opposite direction to the gradient of the Zn values. Higher values of *r* and $I_{geo}$ indexes for Zn and Cr could be explained as being the result of geochemical processes, which will be discussed in the following paragraph.

*Geochemical association significant for carbonate rock weathering and river transport*

Weathering and erosion processes express themselves in the chemical composition of the so-called “Critical Zone” extending from the unweathered bedrock through soils to the atmosphere.[22]

The chemical proxy of alteration, $CPA = [Al_2O_3/(Al_2O_3 + Na_2O)]\times100$[23] is a geochemical proxy for measuring the weathering intensity. It does not involve silicate CaO that is difficult to estimate in calcareous sediments or potassium because of its inconsistent behavior during chemical weathering. The index was proposed as a geochemical proxy of silicate weathering for loess and paleo-soils. As a proxy of the intensity of silicate weathering for the upper part of borehole POT 1 (sample 1 at a depth of 11.85 m; Table S-I, with values of 18.8 % for $Al_2O_3$ and 7.7 % for $Na_2O$), the *CPA* has a value of 60, indicating a relatively high intensity of alteration.[23]

On larger spatial scales, rivers are natural integrators of these weathering and erosion products and fluxes over their drainage areas.[24] The hydrological differentiation processes that operate on river sediments combined with source rock composition and chemical weathering tend to produce sediment suites with different chemical compositions.[25,26] As discussed above, the elevated Cr values are of geogenic origin and also the consequence of anomalies registered in the easternmost part of the Posavina area due to alluvial flooding by the Bosna River, which drains the Central Dinaric Ophiolite Belt. In the area of an active con-

tinental margin, an indented relief with several rises and troughs existed facilitating the emplacement of the olistostromes and the deposition of first overstep sequences, in which ophiolitic material was re-deposited. Sedimentation occurred in some areas in shallow-water environments and some of the rises emerged and the ophiolites underwent weathering according to models of the geodynamic evolution of the Central Dinarides.[27] This is likely one of several reasons for the elevated metal contents in the Posavina region. Considering the total enrichment factor ($R$), which is very low, there was no anthropogenic pollution following the Sava River flow from Županja to Sremska Mitrovica. When discussing river transport of heavy metals, it is interesting to mention that more than 97 percent of the mass transport of heavy metals to the oceans is associated with river sediments.[28] It is most likely that the geological weathering and river transport (Bosna and Drina Rivers) are the factors responsible for the increase in the concentration of the given heavy metals.

Zn represents a chemical element that was introduced mainly into the environment by the natural weathering of ore deposits. In the Pannonian region, the transport of fine fractions still occurs and results in the concentration of this group of elements being higher in the topsoil. In addition, the topographic depressions occurring in these evaporite karst areas are frequently prone to flooding either by the concentration of surface runoff or by groundwater flooding when the water table rises above the ground level,[29] thereby intensifying the process of diluting the sediment.

By reviewing the data from the flood hydrograph, it could be asserted that intensive floods occurred over a limited space. The most flood-prone area is the region called Donje Posavlje, downstream of Županja. The flood duration depends on the flood volume (measured by a hydrograph) and the size of the catchment. The flood duration of the Sava River near the Sremska Mitrovica sampling site is 40 to 70 days.[30]

In historically or periodically flooded areas of the Pannonian region, the average concentrations of Cd (1.7 mg $kg^{-1}$ topsoil, 1.2 mg $kg^{-1}$ subsoil), Pb (170 mg $kg^{-1}$ topsoil; 130 mg $kg^{-1}$ subsoil) and Zn (470 mg $kg^{-1}$ topsoil, 390 mg $kg^{-1}$ subsoil)[31] are similar to those observed in this study (Table II).

## CONCLUSIONS

This study proves that the local background values of heavy metals in the sedimentary rocks play an important role in the interpretation of the level of geochemical hazard of the investigated region.

The geo-accumulation indexes ($I_{geo}$)[7] and the total enrichment factors ($R$)[8] were calculated to assess whether the observed concentrations represent background/natural or anthropogenic contamination.

Analyzing the significance of $I_{geo}$, *R* and chemical proxy of alteration (*CPA*) leads to the conclusion that weathering, erosion and dilution during aquatic transport are the major factors regarding their effects on the various environmental media (sediments, soil, surface and groundwater). The aspect of the weathering process to soils is a potential hazard for surface and groundwater in the Eastern Posavina region. Based on the geologic processes associated with sediment transfer from source to sink, geochemical principles play a major role in defining the origin of the heavy metal pollution levels in the region.

A geogenic hazard is generated by primary enrichment in rocks, processes of weathering and hill slope erosion as factors that determine the source of pollution in the investigated region. In this paper, based on European (Austrian) ÖNORM S 2088-2 and Bosnian and Herzegovinian FBiH 72/09 values, it was clearly shown that the high local geogenic background values exclude a dominant anthropogenic influence on the high heavy metal contents (*e.g.*, Cr and Ni) in the river sediments.

## SUPPLEMENTARY MATERIAL

Figure S-1 and Table S-I are available electronically from http://www.shd.org.rs/JSCS/, or from the corresponding author on request.

*Acknowledgements.* Investigations within this study were realized in cooperation with the Department of Geography and Geology, Paris Lodron University Salzburg, Salzburg, Austria within the European Commission Project Erasmus Mundus Action 2 SIGMA and the company Rio Tinto – Rio Sava Exploration from Serbia. The study was partly funded by the Ministry of Education, Science and Technological Development of the Republic of Serbia (Project No. 176006). We are also grateful to Ass. Prof. Dr. Bernhard Salcher for preparing the map in Figure 1 and the anonymous reviewers.

## ИЗВОД

## САДРЖАЈ ТЕШКИХ МЕТАЛА У НЕОГЕНИМ СЕДИМЕНТНИМ СТЕНАМА – МОГУЋИ РИЗИК ОД НАТИВНОГ ЗАГАЂЕЊА СЕДИМЕНАТА, ЗЕМЉИШТА, ПОВРШИНСКИХ И ПОДЗЕМНИХ ВОДА (ИСТОЧНА ПОСАВИНА И ЛОПАРСКИ БАСЕН, СЕВЕРОИСТОЧНА БОСНА И ХЕРЦЕГОВИНА)

НЕНАД ГРБА[1,2], FRANZ NEUBAUER[2], АЛЕКСАНДРА ШАЈНОВИЋ[3], КСЕНИЈА СТОЈАНОВИЋ[1] и БРАНИМИР ЈОВАНЧИЋЕВИЋ[1]

*[1]Универзитет у Београду, Хемијски факултет, Студентски трг 12–16, 11000 Београд, [2]Paris Lodron University of Salzburg, Department of Geography and Geology, Hellbrunnerstrasse 34,5020 Salzburg, Austria и [3]Универзитет у Београду, Центар за хемију, ИХТМ, Његошева 12, 11000 Београд*

Испитиван је утицај геохемијских процеса (атмосферског деловања на стене, ерозије и разблаживања) унутрашњих Динарида на Посавски неогени басен и њихове импликације на загађивање седимената реке Саве са 4 локације у источној Посавини (Жупања, Брчко, Босанска Рача и Сремска Митровица). У том циљу изведено је поређење садржаја тешких метала (Pb, Zn, Cu, Ni, Cr, Cd, As и Hg) у седиментима са наведених локација са просечним локалним садржајима ових елемената у нативним незагађеним седиментима. Просечни локални садржај тешких метала израчунат је на основу њиховог садржаја у незагађеним седиментима из две бушотине лопарског басена који је репре-

зентативан за овај специфичан геолошко-хидрогеолошки систем. Циљ рада је био да се процени да ли је повећан садржај тешких метала на 4 локалитета дуж реке Саве последица природног или антропогеног загађења. У ту сврху примењени су индекс геоакумулације и укупни фактор обогаћења. На основу вредности укупног фактора обогаћења (0,25–0,71) утврђено је да је утицај антропогеног загађења у испитиваном региону веома низак. Садржај тешких метала у седиментима, земљишту и подземним водама претежно је контролисан геохемијским процесима, посебно атмосферским деловањем на стене (хемијски индекс промене ~60). Резултати овог испитивања такође су омогућили нови начин сагледавања нативно повишених концентрација Cr и Ni у региону источне Посавине.

(Примљено 17. марта, ревидирано 28. априла, прихваћено 29. априла 2014)

REFERENCES

1. H. Ho, R. Swennen, A. Van Damme, *Geol. Belg.* **13** (2010) 37
2. N. Grba, F. Neubauer, A. Šajnović, B. Jovančićević, in *Geophysical Research Abstracts of the European Geosciences Union – General Assembly*, Vienna, Austria, 2014, [EGU2014-10850] (in press)
3. R. Mutić, *Acta Geol.* **23** (1993) 1
4. K. Urumović, Z. Hernitz, J. Šimon, *Geol. Vjesnik* **30** (1978) 297 (in Serbo-Croatian)
5. P. Miletić, A. Bačani, D. Mayer, A. Capar, *Geol. Vjesnik* **39** (1986) 137 (in Serbo--Croatian)
6. R. Milačić, J. Ščančar, S. Murko, D. Kocman, M. Horvat, *Environ. Monit. Assess.* **163** (2010) 263
7. G. Müller, *Umschan* **79** (1979) 778
8. G. Adami, P. Barbieri, E. Reisenhofer, *Toxicol. Environ. Chem.* **77** (2000) 189
9. http://aoa.ew.eea.europa.eu/tools/virtual_library/bibliography-details-each-assessment/ /answer_0519986588/w_assessment-upload/index_html?as_attachment:int=1 (last accessed April 26, 2014)
10. N. Grba, A. Šajnović, K. Stojanović, V. Simić, B. Jovančićević, G. Roglić, V. Erić, *Chem. Erde-Geochem.* **74** (2014) 107
11. R. Wehausen, H.-J. Brumsack, in *Proceedings of the Ocean Drilling Program, Scientific Results*, A. H. F. Robertson, K.-C. Emeis, C. Richter, A. Camerlenghi, Eds., Texas A&M University, College Station, TX, 1998, p. 207
12. https://www.elaw.org/system/files/sediment_summary_table.pdf (last accessed April 26, 2014)
13. ÖNORM S 2088-2: *Austrian Standards on Contaminated Land Management: Risk assessment for polluted soil concerning impacts on surface environments*, 2000
14. http://www.uip-zzh.com/files/zakoni/poljoprivreda/72-09.pdf (last accessed April 26, 2014)
15. Environment Canada and Ministère du Développement durable, de l'Environnement et des Parcs du Québec, *Criteria for the Assessment of Sediment Quality in Quebec and Application Frameworks:Prevention, Dredging and Remediation*, 2007, p. 7
16. M. Brown, T. Rushmer, *Evolution and Differentiation of the Continental Crust*, Cambridge University Press, New York, USA, 2008, p. 92
17. K. Ustaszewski, S. M. Schmid, B. Lugović, R. Schuster, U. Schaltegger, D. Bernoulli, L. Hottinger, A. Kounov, B. Fügenschuh, S. Schefer, *Lithos* **108** (2009) 106
18. J. Halamić, Z. Peh, S. Miko, L. Galović, A. Šorša, *J. Geochem. Explor.* **115** (2012) 36

19. M. Gajić, S. Vujadinović, *Glasnik srpskog geografskog društva* **89** (2009) 115 (in Serbian)
20. A. Tessier, P. G. C. Campbell, M. Bisson, *Anal. Chem.* **51** (1979) 844
21. B. Rubio, M. A. Nombela, F. Vilas, *Mar. Pollut. Bull.* **40** (2000) 968
22. S. L. Brantley, M. Lebedeva, *Annu. Rev. Earth Planet. Sci.* **39** (2011) 387
23. B. Buggle, B. Glaser, U. Hambach, N. Gerasimenko, S. Marković, *Quatern. Int.* **240** (2011) 12
24. B. A. McKee, R. C. Aller, M. A. Allison, T. S. Bianchi, G. C. Kineke, *Cont. Shelf Res.* **24** (2004) 899
25. H. W. Nesbitt, G. M. Young, *J. Geol.* **97** (1989) 129
26. P. W. Fralick, B. I. Kronberg, *Sediment. Geol.* **113** (1997) 111
27. J. Pamić, I. Gušić, V. Jelaska, *Tectonophysics* **297** (1998) 251
28. C. K. Jain, C. K. Sharma, *J. Hydrol.* **253** (2001) 81
29. F. Gutiérrez, A. H. Cooper, K. S. Johnson, *Environ. Geol.* **53** (2008) 1007
30. http://www.savacommission.org/dms/docs/dokumenti/srbmp_micro_web/backgroundpapers_final/no_9_background_paper_integration_of_water_protection_in_developments_in_the_sava_rb.pdf (last accessed April 26, 2014)
31. R. Šajn, J. Halamić, Z. Peh, L. Galović, J. Alijagić, *J. Geochem. Explor.* **110** (2011) 278.

Journal of the Serbian Chemical Society
JSCS@tmf.bg.ac.rs • www.shd.org.rs/JSCS
*J. Serb. Chem. Soc. 80* (6) S218–S220 (2015) *Supplementary material*

SUPPLEMENTARY MATERIAL TO

# Heavy metals in Neogene sedimentary rocks as a potential geogenic hazard for sediment, soil, and surface and groundwater contamination (eastern Posavina and the Lopare Basin, Bosnia and Herzegovina)

NENAD GRBA[1,2], FRANZ NEUBAUER[2], ALEKSANDRA ŠAJNOVIĆ[3*#], KSENIJA STOJANOVIĆ[1#] and BRANIMIR JOVANČIĆEVIĆ[1#]

[1]*University of Belgrade, Faculty of Chemistry, Studentski trg 12–16, 11000 Belgrade, Serbia* [2]*Paris Lodron University of Salzburg, Department of Geography and Geology, Hellbrunnerstrasse 34,5020 Salzburg, Austria and* [3]*University of Belgrade, Center of Chemistry, ICTM, Njegoševa 12, 11000 Belgrade, Serbia*

*J. Serb. Chem. Soc.* 80 (6) (2015) 827–838

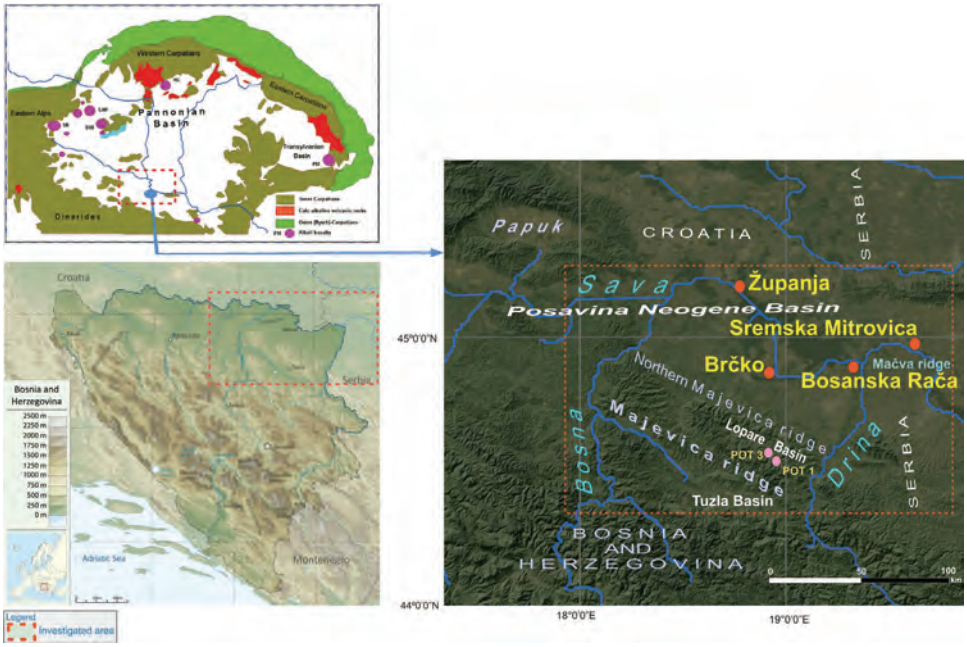


Fig. S-1. Map of Bosnia and Herzegovina and locations of the Lopare Basin and four sampling sites along the Sava River (Županja, Brčko, Bosanska Rača and Sremska Mitrovica).

* Corresponding author. E-mail: sajnovica@bg.ac.rs

TABLE S-I. List of sediment samples from the Lopare Basin with contents of heavy metals (mg kg$^{-1}$)

| Borehole | Sample No. | Depth m | Lithology | Pb | Zn | Cu | Ni | Cr | Cd | As | Hg |
|---|---|---|---|---|---|---|---|---|---|---|---|
| POT 1 | 1[a] | 11.85 | Sandy clay | 200.8 | 96.3 | 30.7 | 151.3 | 207.7 | 1.86 | 18.2 | 0.00 |
| | 2 | 18.55 | Marlstone | 186.9 | 70.0 | 38.5 | 149.8 | 198.6 | 1.17 | 0.8 | 0.00 |
| | 3 | 23.85 | Marlstone | 140.5 | 63.3 | 32.8 | 188.8 | 211.5 | 0.98 | 3.5 | 0.00 |
| | 4 | 31.45 | Marlstone | 165.9 | 64.5 | 34.1 | 225.3 | 234.7 | 0.87 | 1.7 | 0.00 |
| | 5 | 43.65 | Marlstone | 178.5 | 69.1 | 41.0 | 151.0 | 199.2 | 0.47 | 0.0 | 0.00 |
| | 6 | 49.65 | Marlstone | 192.6 | 59.5 | 31.4 | 143.9 | 179.4 | 6.08 | 183.1 | 0.00 |
| | 7 | 52.45 | Marlstone | 117.8 | 20.3 | 13.8 | 39.5 | 51.2 | 1.46 | 3.2 | 2.52 |
| | 8 | 62.55 | Marlstone | 158.3 | 52.4 | 35.6 | 164.8 | 186.0 | 0.91 | 6.8 | 0.92 |
| | 9 | 68.55 | Marlstone | 169.8 | 44.7 | 33.5 | 175.5 | 182.3 | 1.04 | 18.9 | 0.48 |
| | 10 | 76.75 | Marlstone | 144.7 | 40.0 | 37.2 | 140.0 | 162.5 | 0.87 | 2.1 | 0.28 |
| | 11 | 90.35 | Marlstone | 120.7 | 33.4 | 33.4 | 134.4 | 141.9 | 0.80 | 3.7 | 0.46 |
| | 12 | 99.65 | Marlstone | 166.5 | 38.6 | 36.1 | 179.6 | 177.9 | 1.22 | 8.4 | 0.58 |
| | 13 | 113.45 | Marlstone | 161.3 | 39.0 | 34.4 | 183.0 | 198.4 | 1.23 | 12.3 | 0.37 |
| | 14 | 119.4 | Marlstone | 146.9 | 37.5 | 29.5 | 90.8 | 121.2 | 2.30 | 95.6 | 0.45 |
| | 15 | 132.55 | Marlstone | 234.8 | 50.6 | 22.4 | 158.0 | 176.0 | 1.48 | 44.3 | 0.19 |
| | 16 | 141.55 | Marlstone | 145.1 | 32.3 | 34.0 | 163.6 | 172.6 | 0.99 | 8.8 | 0.39 |
| | 17 | 150.9 | Marlstone | 105.5 | 21.8 | 20.8 | 88.3 | 98.8 | 0.74 | 8.2 | 0.69 |
| | 18 | 171.5 | Marly sandstone | 108.1 | 24.7 | 27.1 | 69.5 | 93.1 | 0.50 | 19.5 | 0.49 |
| | 19 | 193.1 | Marly sandstone | 116.3 | 9.6 | 10.8 | 21.3 | 68.9 | 1.32 | 45.9 | 0.44 |
| POT 1 mean values | | | | 153.3 | 42.9 | 30.4 | 137.1 | 158.6 | 1.36 | 25.9 | 0.46 |
| POT 3 | 20 | 27.8 | Marlstone | 255.0 | 107.8 | 27.5 | 173.6 | 261.3 | 1.62 | 103.3 | 1.12 |
| | 21 | 43.25 | Marlstone | 77.4 | 94.1 | 30.2 | 147.6 | 247.1 | 0.01 | 6.0 | 1.02 |
| | 22 | 59.35 | Marlstone | 262.6 | 85.5 | 30.2 | 170.5 | 258.6 | 0.17 | 12.9 | 0.96 |
| | 23 | 73.4 | Marlstone | 129.3 | 46.4 | 24.5 | 125.0 | 141.8 | 0.25 | 5.7 | 0.03 |
| | 24 | 85.15 | Marlstone | 161.4 | 78.2 | 37.9 | 161.5 | 210.9 | 0.00 | 1.8 | 0.00 |
| | 25 | 92.15 | Marlstone | 162.0 | 67.5 | 38.7 | 153.3 | 190.3 | 0.07 | 7.3 | 0.33 |
| | 26 | 106.65 | Marlstone | 211.7 | 89.1 | 36.8 | 243.9 | 280.2 | 0.00 | 5.5 | 0.23 |
| | 27 | 119.5 | Marlstone | 211.3 | 95.9 | 28.3 | 170.7 | 222.9 | 0.11 | 28.0 | 0.42 |
| | 28 | 130.85 | Marlstone | 177.3 | 73.1 | 34.8 | 156.6 | 193.8 | 0.10 | 10.9 | 0.00 |
| | 29 | 139.65 | Marlstone | 168.3 | 58.7 | 28.8 | 263.2 | 219.5 | 0.14 | 16.8 | 0.00 |
| | 30 | 149.75 | Dolomitic marlstone | 207.4 | 75.3 | 39.2 | 197.3 | 200.0 | 0.13 | 0.0 | 0.14 |
| | 31 | 160.5 | Marlstone | 205.5 | 83.0 | 37.4 | 160.3 | 219.6 | 0.01 | 29.5 | 0.48 |
| | 32 | 164.6 | Marlstone | 141.3 | 60.7 | 33.8 | 154.4 | 176.5 | 0.00 | 2.3 | 1.71 |
| | 33 | 177.75 | Marlstone | 125.7 | 58.9 | 30.1 | 198.5 | 175.5 | 0.00 | 3.3 | 2.03 |
| | 34 | 186.75 | Marlstone | 157.1 | 67.1 | 31.1 | 182.2 | 221.5 | 0.41 | 0.1 | 2.66 |
| | 35 | 196.35 | Marlstone | 141.6 | 57.0 | 37.9 | 140.6 | 205.9 | 1.55 | 10.6 | 5.65 |
| | 36 | 208.95 | Marlstone | 189.5 | 72.6 | 44.5 | 198.7 | 231.5 | 1.37 | 0.0 | 2.03 |
| | 37 | 224.5 | Marlstone | 162.1 | 63.5 | 35.0 | 181.0 | 215.9 | 1.44 | 0.0 | 1.27 |
| | 38 | 228.65 | Marlstone | 171.8 | 63.6 | 35.8 | 223.4 | 238.0 | 1.59 | 7.4 | 0.36 |
| | 39 | 253.25 | Marlstone | 160.3 | 50.7 | 21.2 | 132.3 | 163.9 | 2.33 | 27.8 | 0.23 |
| | 40 | 273.5 | Siltstone | 238.5 | 92.8 | 39.6 | 232.1 | 276.2 | 4.94 | 111.2 | 0.00 |
| | 41 | 274.55 | Marlstone | 224.6 | 84.5 | 29.3 | 219.9 | 245.6 | 5.16 | 116.2 | 0.00 |
| | 42 | 290.5 | Marlstone | 146.6 | 57.1 | 27.2 | 158.6 | 173.6 | 2.81 | 43.5 | 0.00 |

TABLE S-I. Continued

| Borehole | Sample No. | Depth m | Lithology | Pb | Zn | Cu | Ni | Cr | Cd | As | Hg |
|---|---|---|---|---|---|---|---|---|---|---|---|
| | 43 | 304.95 | Marlstone | 141.3 | 54.1 | 29.4 | 175.1 | 192.8 | 1.04 | 2.6 | 0.00 |
| POT 3 | 44 | 318.45 | Marlstone | 150.4 | 49.8 | 28.8 | 241.5 | 233.7 | 1.19 | 9.0 | 0.00 |
| | 45 | 331.65 | Marlstone | 138.1 | 55.5 | 30.2 | 172.1 | 189.4 | 2.53 | 39.9 | 0.00 |
| | 43 | 343.75 | Siltstone/Marlstone | 143.2 | 52.4 | 35.9 | 199.3 | 205.7 | 1.62 | 15.5 | 0.51 |
| POT 3 mean values | | | | 172.6 | 70.2 | 32.7 | 182.7 | 214.5 | 1.13 | 22.9 | 0.78 |

[a]Sample was used for the calculation of the Chemical Proxy of Alteration, *CPA*, value